Mycelial compatibility in *Amylostereum areolatum*

Magrieta Aletta

van der Nest

Mycelial compatibility in *Amylostereum areolatum*

by

Magrieta Aletta van der Nest

Promotor: Prof. B.D. Wingfield

Co-promotor: Prof. M.J. Wingfield

Prof. B. Slippers

Prof. J. Stenlid

Submitted in partial fulfilment of the requirements for the degree of Philosophiae Doctor in the Faculty of Natural and Agricultural Sciences, Department of Genetics at the University of Pretoria.

September 2010

DECLARATION

I, Magrieta Aletta van der Nest, declare that this thesis, which I hereby submit for the degree Philosophiae Doctor at the University of Pretoria, is my own work and has not been submitted by me at this or any other tertiary institution.

SIGNATURE:

DATE:

TABLE OF CONTENTS

Acknowledgments

I want to thank the following people and institutions:

My study leaders Professors Brenda Wingfield, Mike Wingfield, Bernard Slippers and Jan Stenlid for their encouragement, guidance and patience.

My mother (Trisce Jane van der Nest), my grandparents (Grieta and Lambert van der Nest), Emma Steenkamp, Tuan Duong, Karlien van Zyl and Markus Wilken for their help and support.

The Fabians for their advice, help and support, especially the people in the Shaw laboratory.

FABI support staff Helen Doman, Eva Muller, Jenny Hale, Rose Louw and Martha Mahlangu, Valentina Nkosi, Maretha van der Merwe and Lydia Twala, as well as the staff at the DNA sequence facility Renate Zipfel and Gladys Mthembu for technical assistance.

The National Research Foundation (NRF), members of the Tree Protection Co-operative Programme (TPCP) and the THRIP initiative of the Department of Trade and Industry (DTI), South Africa for financial support.

The Department of Genetics at the University of Pretoria for the use of their facilities.

Preface

Amylostereum areolatum is a basidiomycete fungus that lives in symbiotic relationship with Siricid woodwasps. Like other fungi, *A. areolatum* utilizes a range of mechanisms to recognize individuals of its own and other species. Our current knowledge of the processes underlying these recognition mechanisms are based almost exclusively on the recognition systems of the model fungi. Even less is known for the recognition systems of fungi involved in symbiotic relationships with other eukaryotes and specifically insects. The research in this thesis focuses specifically on interactions among *A. areolatum* individuals, as well as how its biology and evolution could have been influenced by the association of woodwasps. The thesis is presented as six chapters, each of which is written as independent units (two of which have already been published). Thus there has been some obvious repetition of certain aspects among the chapters.

Two independent systems regulate interactions among *A. areolatum* individuals. The one system (referred to as sexual compatibility) regulates mycelial compatibility between homokaryons and is controlled by the genes encoded at the mating type (*mat*) loci, while the second system (referred to as vegetative compatibility) regulates mycelial compatibility between heterokaryons and is controlled by the genes encoded at the heterokaryon incompatibility (*het*) loci. Sexual recognition in fungi has been well-studied and is thoroughly documented in the literature. The existing literature also addresses specific key issues regarding sexual recognition, including literature about the origins and evolution of the *mat* genes and molecular processes involved in sexual recognition. Although good reviews regarding fungal vegetative compatibility are available, the current literature has a gap regarding the processes and pathways involved in vegetative incompatibility. The first chapter of this thesis, therefore, presents a critical review of literature on the molecular mechanisms underlying vegetative incompatibility in fungi. The focus is on Basidiomycetes and a discussion of the possible processes and pathways associated with this phenomenon is included.

The second chapter of this thesis provides a brief review on the research that has broadened our knowledge regarding the phylogenetics, population genetics and biology of *Amylostereum* spp. and in particular *A. areolatum*. Much of the existing literature on these issues was generated due the fact that *A. areolatum* and its symbiont, the *Sirex noctilio* woodwasp, threaten pine forestry in countries where they have been introduced. Despite

considerable efforts to control the wasp, the *Amylostereum-Sirex* complex continues to kill significant numbers of trees. In this chapter, research that increased our understanding of the biology of *Amylostereum* spp., as well as their taxonomy and evolution, are considered. The diversity of these fungi and their interactions with the wasp and host plant are also discussed.

Characterization of the sexual mating systems of Basidiomycetes has almost exclusively been limited to the model fungi. Almost no information is available about the *het* genes of Basidiomycetes. The aim of Chapter 3 of the thesis was, therefore, to characterize the *mat* and *het* loci in the non-model homobasidiomycete *A. areolatum*. We were able to determine the number of *het* loci in *A. areolatum*, as well as obtain portions of a putative pheromone receptor encoded at the *mat-B* locus and a gene (mitochondrial intermediate peptidase) linked to the *mat-A* locus of this fungus. Findings from this chapter provided some insight into the structure, organization, function and evolution of the recognition loci in Basidiomycetes, as well as the role these loci play in the development and evolution of these and other fungi.

Genetic linkage maps have been used to study the recognition loci of eukaryotes. In a similar way, the aim of Chapter 4 of this thesis was to position the recognition loci (*mat* and *het*) of *A. areolatum* on a genetic linkage map. For this purpose amplified fragment length polymorphisms (AFLPs) were used for map construction, and AFLP-based bulked segregant analysis (BSA) was used to identify markers closely linked to the recognition loci. As has been shown previously for other eukaryotes, the recognition loci of *A. areolatum* are subject to evolutionary forces that are markedly different from those acting on the rest of the genome. The findings were analysed in terms of the *in vitro* growth rate of the fungus, which showed a possible association between the recognition loci and the genes involved in fitness.

A possible explanation for the association between fitness and the recognition loci could be attributed to the evolutionary forces acting on these loci that keep them highly diverse. The aim of the study presented in Chapter 5 was to explore the evolutionary forces acting on the genes governing sexual recognition in *A. areolatum*. For this purpose, DNA sequence information was obtained from the pheromone receptor gene (*RAB1*) encoded at the *mat-B* locus and two nuclear regions (*i.e.* the eukaryotic translation elongation factor 1α gene and the ribosomal RNA internal transcribed spacer region). For comparative purposes, *A. chailletii* was included in this study. The findings suggest that balancing selection, but not positive selection, is keeping the *mat* genes of these fungi diverse.

The aim of the study presented in Chapter 6 was to increase our understanding of the molecular mechanisms underlying vegetative incompatibility in *A. areolatum*. For this purpose, genes selectively expressed during incompatibility were identified using suppression

subtractive hybridization, 454-based pyrosequencing and quantitative reverse transcription PCR. To infer the possible pathways and processes underlying vegetative incompatibility, all selectively expressed transcripts were assigned putative functions and used to reconstruct the possible the chain of events occurring during vegetative incompatibility in *A. areolatum*. Apart from increasing our knowledge regarding the molecular basis of vegetative incompatibility in fungi, the findings of this study could also have potential applications in terms of management of the *Amylostereum-Sirex* complex.

CHAPTER 1

Literature Review: The molecular basis of vegetative incompatibility in fungi, with specific reference to Basidiomycetes

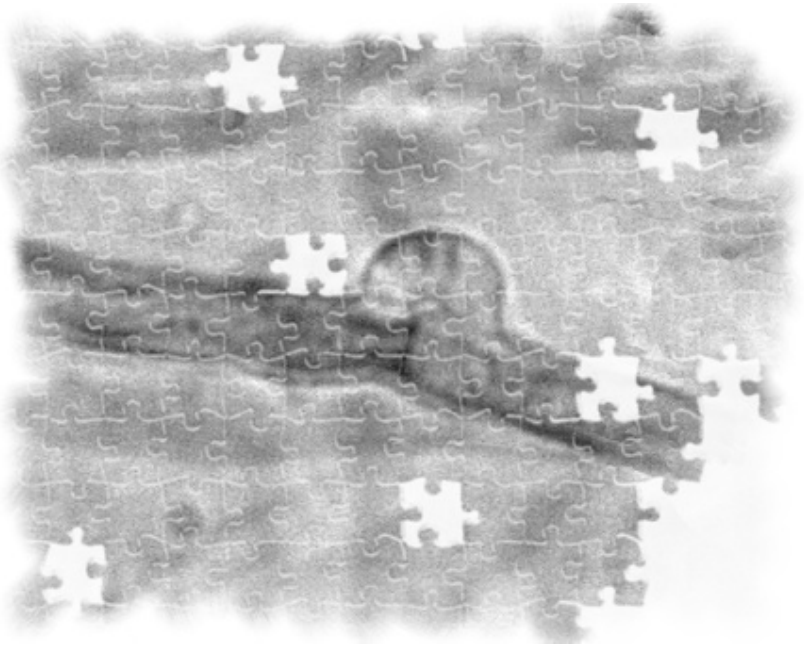

TABLE OF CONTENTS

INTRODUCTION

A typical basidiomycete life-cycle consists of a short homokaryotic phase (*i.e.*, hyphae that contain a single type of nucleus), which is followed by a predominant fertile heterokaryotic phase (*i.e.*, hyphae that contain more than one type nucleus) (Fig. 1) (Kothe et al., 2003). The heterokaryotic phase arises when the hyphae of different homokaryons fuse or mate to form a heterokaryon. Only genetically dissimilar homokaryons with different allelic specificities at their mating type (*mat*) loci are sexually compatible and able to fuse and form a heterokaryon (Fig. 2) (Kronstad and Staben, 1997; Casselton and Olesnicky, 1998; Casselton, 2002). Subsequent vegetative hyphal fusion is important for intra-hyphal communication, translocation of water and nutrients and homoeostasis within a colony (Glass et al., 2004). Vegetative hyphal fusion also occurs between different heterokaryons and is controlled by a vegetative incompatibility system (Biella et al., 2002; Pinan-Lucarré et al., 2007). Even though, the biological function of vegetative incompatibility is still unclear, it is proposed to help maintain genetic identity, inhibit the spread of harmful elements, prevent exploitation by aggressive genotypes or that it is involved in pathogen recognition (Biella et al., 2002; Pinan-Lucarré et al., 2007; Paoletti and Saupe, 2009).

Vegetative incompatibility in filamentous fungi is controlled by the genes encoded at the heterokaryon or vegetative incompatibility (*het* or *vic*) loci. If genetically similar individuals that share the same allelic specificities at all of their *het* loci meet in nature, their hyphae will fuse and they will form a single entity (e.g., Worrall, 1997; Glass and Kaneko, 2003; Pinan-Lucarré et al., 2007). When two interacting individuals are genetically dissimilar with different allelic specificities at some or all of their *het* loci, cell death of the interacting hyphae prevent hyphal fusion to persist and the heterokaryons remain separate entities (e.g., Worrall, 1997; Glass and Kaneko, 2003; Pinan-Lucarré et al., 2007). Although cell death associated with vegetative incompatibility is normally limited to the fusion cells, it sometimes extends to immediately neighbouring cells (Pinan-Lucarre et al., 2007). Vegetatively incompatible reactions are generally associated with growth inhibition, repression of asexual sporulation, hyphal compartmentalization, vacuolization of the cytoplasm, organelle degradation, shrinkage of the plasma membrane from the cell wall, and finally death of the interacting cells (Jacobson et al., 1998; Glass et al., 2000; Fedorova et al., 2005). Because vegetative incompatibility is characterized by similar morphological properties in different fungal species (despite not necessarily sharing similar sets of *het* loci),

it is believed that the mechanism of cell death is the same for all fungi (Jacobson et al., 1998). However, the exact mechanism of how cell death by incompatibility is activated remains unclear, even though this system represents one of the best studied forms of programmed cell death (PCD) in fungi (Fedorova et al., 2005).

The aim of this review is to critically summarize the existing knowledge regarding vegetative incompatibility and the activation of cell death by incompatibility in filamentous fungi. The review is focussed mainly on the model ascomycetes *Podospora anserina* and *Neurospora crassa* as the majority of the information on this topic has been generated for these species (e.g., Bérgueret et al., 1994; Saupe et al., 1996; Kubisiak and Milgroom 2006). Where possible, reference is also be made to the vegetative incompatibility system in other less well studied fungi. A brief summary of the *het* genes and the mechanisms of how their products are thought to control vegetative incompatibility is presented. Furthermore, the steps involved in the activation of PCD associated with vegetative incompatibility (*i.e.*, hyphal fusion, the activation of PCD and PCD) are considered. Finally, possible signalling pathways that may be involved in this phenomenon are briefly discussed.

THE *HET* LOCI

Fungal vegetative incompatibility has been studied for decades (e.g., Labarère et al., 1974, 1979), yet, only a few *het* loci have been characterized at the DNA level and this has been for model ascomycetes (Table 1) (e.g., Bérgueret et al., 1994; Saupe et al., 1996; Kubisiak and Milgroom, 2006). Even less is known regarding the *het* loci of basidiomycetes, except that they apparently harbour fewer *het* loci than their ascomycete counterparts (Worral, 1997). Ascomycetes generally have around 10 *het* loci that are biallelic (Perkins, 1988; Bérgueret et al., 1994; Muirhead et al., 2002), while basidiomycetes generally have less than five multiallelic *het* loci (Hansen et al., 1994; Stenlid and Vasiliauskas, 1998; Kauserud et al., 2006; van der Nest et al., 2008).

The exact biological role of the vegetative incompatibility system of fungi is not yet clear. Following one school of thought, vegetative incompatibility represents an evolutionary adaptation that functions in self/nonself recognition (Rayner, 1991; Saupe, 2000; Biella et al., 2002). This hypothesis is strengthened by the fact that some of the known *het* gene products function in self/nonself recognition only (e.g., the *het-c* gene in *N. crassa*) (Table 1). Also

consistent with this idea, the evolution of the *het* loci has been shown to be subject to strong selective forces (Glass et al., 2000). For example, transpecific polymorphism (*i.e.*, the sharing of allelic lineages across species) that is considered a strong criterion of positive Darwinian selection is present at these loci (Glass et al., 2000; Saupe, 2000). In addition, the *het-c* alleles in *N. crassa* and the *het-s* and *het-c* alleles in *P. anserina* show an excess of non-synonymous substitutions over synonymous substitutions, which is another characteristic of balancing selection (Glass et al., 2000; Saupe, 2000). Selection is also thought to allow for the maintenance of the highly polymorphic, evenly distributed and long persistence of alleles in populations at these loci (Glass et al., 2000; Saupe, 2000; Meyer and Thomson, 2001).

A second school of thought suggests that vegetative incompatibility does not have any function in natural populations (Saupe, 2000). Instead, it represents an evolutionary accident where a fraction of neutral polymorphism in a given population is detrimental when reunited in the same cytoplasm in a heterokaryon (Saupe, 2000). The fact that some of the *het* gene products (e.g., *un-24* and *het-c* in *P. anserina*) are involved in cellular functions other than self/nonself recognition (Saupe et al., 1995; Loubradou and Turcq, 2000; Saupe 2000; Smith et al., 2000), supports this hypothesis. Recently, it has also been shown that vegetative incompatibility and growth rate are closely associated in *A. areolatum*, which further supports the evolutionary accident hypothesis, because it suggests that the *het* gene products are involved in secondary cellular processes other than self/nonself recognition and that the limitation of heterokaryosis is not their sole function (van der Nest et al., 2009). However, because both the self/nonself recognition and evolutionary accident hypotheses are supported by convincing experimental evidence, both factors might play a role. For example, it is possible that vegetative incompatibility may be the product of an evolutionary accident, but that polymorphism associated with vegetative incompatibility has been maintained as an evolutionary adaptation.

MECHANISMS INVOLVED IN HETEROKARYON INCOMPATIBILITY

The exact mechanisms of how *het* genes and their products may lead to vegetative incompatibility are still unknown (e.g., Glass et al., 2000; Sarkar et al., 2002; Glass and Dementhon, 2006). However, it is known that physical interactions between alternative *het* gene products result in the activation of PCD by incompatibility (Glass and Dementhon,

2006). These interactions may be viewed as allelic or non-allelic in nature. Allelic interactions occur between gene products from the same *het* locus (e.g., the *het-s* gene products of *P. anserina*), while non-allelic interactions occur between the *het* gene products from different loci (e.g., the *het-c*/*pin-c* gene products in *N. crassa*) (Glass and Dementhon, 2006). Nevertheless, the heterocomplexes that form between the *het* gene products somehow triggers PCD by incompatibility. One possibility is that the heterocomplex acts as a poison that results directly in cell death (Bégueret et al., 1994; Glass et al., 2000), although molecular evidence suggests that *het* gene products are not directly involved in cell death (Leslie and Zeller, 1996). An alternative view is that heterocomplex formation acts as a signal to activate pathways that mediate the biochemical and morphological aspects of vegetative incompatibility (Leslie and Zeller, 1996; Glass et al., 2000; Sarkar et al., 2002).

Various lines of evidence support the hypothesis that heterocomplex formation triggers one or more signalling cascades, which in turn activate the pathways that mediate incompatibility. For example, the *het-c* gene in *P. anserina* encodes a glycolipid transfer protein that accelerates the transfer of glycosphingolipids between membranes in the cell. It was thus demonstrated that *ACD11* (the *het-c* ortholog in *Arabidopsis thaliana*) is part of the sphingolipid signaling pathway (see below) that is known to induce PCD (Pinan-Lucarré et al., 2006; West et al., 2008). The nature of the genes encoded at some of the *het* loci has also strengthened the view that PCD is associated with the activation of signalling pathways. The *het-e* and *het-d* genes in *P. anserina* and the *het-6*, *pin-c* and *tol* genes in *N. crassa*, all encode proteins with a so-called HET domain that could initiate the signalling cascade that triggers PCD by incompatibility (Fig. 3) (Paoletti et al., 2007; Paoletti and Clavé, 2007). The NACHT domain present in *het-d*, *het-e* and *het-r* might also be essential for the activation of PCD, because proteins harbouring a NACHT domain belong to the STAND class of NTPases (nucleoside triphosphate hydrolyses) that are known to activate PCD in other eukaryotes (Paoletti et al., 2007; Chevanne et al., 2009). The WD (tryptophan-aspartic acid) repeat domain present in these *het* genes that is made up of a variable number of WD40 sequence units, probably defines allele specificity (Paoletti and Clavé, 2007; Pinan-Lucarré et al., 2007; Chevanne et al., 2010). The fact that similar domains are present in fungal *het* genes and other eukaryotic PCD-associated genes, suggests that PCD by incompatibility and PCD in higher eukaryotes could, to some extent, be related (Pinan-Lucarré et al., 2007).

It has been suggested that heterocomplex formation between alternative *het* gene products disturbs the equilibrium of critical regulatory or maintenance processes of the cell, which

then indirectly triggers the cell death response (Leslie and Zeller, 1996). For example, a range of genes that are not encoded at *het* loci have been shown to be involved in vegetative incompatibility. This suggests that downstream genes are involved in the activation of PCD associated with incompatibility (Table 2). These include the *vib-1* (vegetative incompatibility block) and *Tol* (tolerant mutations) genes in *N. crassa* (Shiu and Glass, 1998; Glass et al., 2003; Xiang and Glass 2004; Dementhon et al., 2006), as well as the *mod* (modifier) and *idi* (induced during incompatibility genes) in *P. anserina* (Bourges et al., 1998; Loubradou et al., 1997, 1999; Loubradou and Turcq, 2000; Dementhon et al., 2004; Pinan-Lucarré et al., 2007). Furthermore, the NACHT family of NTPases present in some *het* genes are known to function as key integrators of stress and nutrient availability signals (Federovo et al., 2005).

PROCESSES ASSOCIATED WITH HETEROKARYON INCOMPATIBILITY

When two heterokaryons meet in nature, several different steps determine the outcome of the interaction (Fig. 4) (Leslie and Zeller, 1996; Glass et al., 2000; Pal et al., 2007). During the first or pre-fusion step the hyphae can either grow away from or towards each other (Pal et al., 2007). If the hyphae grow towards each other, irrespective of whether they are vegetatively compatible or not, their hyphae will fuse or anastomose (Leslie and Zeller, 1996; Pal et al., 2007). If they are vegetatively compatible, a stable heterokaryon will form. But, where they are vegetatively incompatible, various processes are initiated that ultimately activate the death machinery resulting in PCD (Pal et al., 2007).

Hyphal fusion

The fungal cell wall (Fig. 5) contains numerous cell wall-associated enzymes (WAEs) and structural cell wall proteins whose functions are necessary for successful hyphal fusion (Fukazawa and Kagaya, 1997; Glass et al., 2000; Bowman and Free, 2006). Some of the WAEs are involved in the breakdown (e.g., peptidases, chitinases and glucanases) and synthesis (e.g., glycosyltransferase and UTP-glucose-1-phosphate uridylyltransferase) of the cell wall to form a new cell wall bridge between the two hyphae (Glass et al., 2000; Bowman and Free, 2006). Also, the cell wall degrading enzymes (e.g., glucanases, chitinase) that attack the main constituents of the cell wall of the opponent, are considered to be a vital part of the defence response during vegetative incompatibility (Fukazawa and Kagaya, 1997).

Structural proteins in the cell wall and proteins associated with the outermost surface of the cell are important for vegetative incompatibility (Boucherie and Bernet, 1977; Boucherie et al., 1981; Leslie and Zeller, 1996), because they influence the outcome of cell-cell adhesion necessary for hyphal fusion (Gardiner et al., 1981; Fukazawa and Kagaya, 1997; Celerin and Day, 1998). For example, it was demonstrated that lectins present in the cell wall and the outermost surface of the cell, can mediate contact and recognition of the host fungus during mycoparasitism (Boddy, 2000). In *Saccharomyces cerevisiae*, the mannan moiety of mannoproteins is involved in lectin-mediated cell-cell adhesion during mating, but they do not confer mating-type specificity (Gardiner et al., 1981; Fukazawa and Kagaya, 1997; Celerin and Day, 1998). In fungi, the protein moieties of mannoproteins can apparently also function in cell-cell adhesion (Castle et al., 1996; Fukazawa and Kagaya, 1997). For example, in *Candida albicans,* one group of mannoproteins are lectin-like proteins that interact in a lectin manner with a glycoside receptor (glycoprotein or glycolipid) on the other cell. A second group of mannoproteins are analogous to animal integrins in that they facilitate cell-cell adhesion by binding to arginine-glycine-aspartic acid (RGD) containing ligands (Fukazawa and Kagaya, 1997).

Flocculins represent another group of structural glycoproteins in the cell wall that may be involved in lectin-mediated cell-cell adhesion (Fichtner et al., 2007; Douglas et al., 2007; Dranginis et al., 2007). Flocculins in *S. cerevisiae*, which are encoded by genes that belong to the FLO family, can compensate for one another in regulating diverse morphogenic events such as mating, flocculation, haploid invasion and filamentation (Guo et al., 2000; Bayly et al., 2005; Dranginis et al., 2007). All of the *Flo* gene products function in lectin-mediated cell-cell adhesion, as flocculins can bind to cell surface carbohydrates (e.g., the mannose moiety of mannoproteins) that are present on other cells, and their expression is central to regulating all adherence events in *S. cerevisiae* (Bayly et al., 2005; Fichtner et al., 2007; Douglas et al., 2007; Dranginis et al., 2007). Thus far, the only fungus in which flocculins have been implicated in vegetative incompatibility is *A. areolatum* (Chapter 6 of this thesis). However, it is possible that flocculins may not only play a role in adhesion, but also in anti-adhesion during vegetative incompatibility. This is because it was demonstrated that mucins, orthologs of flocculins in animals, appear to mediate anti-adhesion, as they prevent the interaction with ligands or receptors on the other cell (Wesseling et al., 1995, 1996; McDermott et al., 2001; Swanson et al., 2007). It is also possible that flocculins may play a

role in the regulation of PCD, as mucins appear to function in the cellular response to immunity and tumour formation (Mall, 2008).

Programmed cell death associated with vegetative incompatibility

Initially it was believed that fungal PCD by incompatibility is similar to Type I PCD or apoptosis (Jacobson et al., 1998; Marek et al., 2003; Pinan-Lucarré et al., 2003). The word apoptosis is derived from the Greek words *apo* (from) and *ptosis* (falling), thus "falling off" which refers to the type of natural death that occurs in plant cells when leaves senesce. This initial link between fungal PCD by incompatibility and apoptosis arose from the shared features, including cytoplasmic shrinkage/plasmolysis and eventually the progressive shrinkage and fragmentation of the cytoplasm results in the formation of discrete remnants resembling 'apoptotic bodies' seen in PCD associated with apoptosis (Bursch, 2001; Marek et al., 2003). However, the results of several studies suggest that PCD by incompatibility is unlikely to be equivalent to typical apoptosis that occurs in other eukaryotes. Not only do both *N. crassa* and *S. cerevisiae* lack important apoptosis-associated genes (e.g., caspases, Bcl-2/Bax and TNR receptor family proteins), but nuclear DNA fragmentation that occurs during Type I PCD is also absent during cell death by vegetative incompatibility (Marek et al., 2003).

Another hypothesis suggests that PCD by vegetative incompatibility represents Type II (non-apoptotic) PCD or autophagy (Pinan-Lucarré et al., 2003). The word autophagy is also derived from Greek meaning "self consumption", which refers to the intracellular process involved in removal of damaged or misfolded proteins or organelles. Autophagy is characterized by the packaging and vacuolar degradation of cell components, the dilation of mitochondria and the endoplasmic reticulum (ER), a slight enlargement of the Golgi and inward blebbing of the plasma membrane (Marek et al., 2003; Bras et al., 2005; Hamacher-Brady et al., 2006). PCD by incompatibility has been demonstrated to involve vacuolization and cell lysis and the eventual plasmolysis of the cytoplasm, all characteristic of autophagy (Marek et al., 2003; Pinan-Lucarré et al., 2003; Bras et al., 2005; Pinan-Lucarré et al., 2007). Furthermore, cytological evidence also supports the notion that cell death associated with incompatibility represents Type II PCD/autophagy. For example, *pspA/idi-6* (similar to vacuolar proteases B) and *idi-7* (homolog of the *S. cerevisiae* ATG8 and human LC-3 autophagy proteins involved in autophagosome formation) in *P. anserina* have been shown to

be up-regulated during cell death by incompatibility (Bourges et al., 1998; Paoletti et al., 2001; Pinan-Lucarré et al., 2003).

It appears that the two modes of cell death are not mutually exclusive, because some forms of apoptosis require an initial autophagic phase for successful PCD (Marek et al., 2003; Hamacher-Brady et al., 2006). It is possible that this is also true for PCD by incompatibility, as this fungal phenomenon shares certain hallmarks of cell death that resemble both apoptosis (e.g., cytoplasmic shrinkage) and autophagy (e.g., vacuolization) (Bursch 2001; Marek et al., 2003). However, it has been suggested that autophagy only accompanies cell death by incompatibility and that it does not represent a mechanism of PCD, since PCD by incompatibility still occurs in *P. anserina* autophagy mutants (Pinan-Lucarré et al., 2005). Also, autophagy appears not to be part of the dramatic vacuolar enlargement observed during cell death by incompatibility. This is because the presence of enlarged vacuoles and their collapse with the release of hydrolic enzymes that attack organelles, represent an important part of cell death associated with PCD by incompatibility in these autophagy mutants (Pinan-Lucarré et al., 2005). It is thus possible that autophagy is not part of PCD during incompatibility, but rather that it is a strategy for protecting cells against stress and apoptosis (Hamacher-Brady et al., 2006). Autophagy during incompatibility may, therefore, function to eliminate a "pro-death" signal(s) such as the toxic complexes formed between incompatible *het* genes or damaged organelles.

Cellular stresses associated with vegetative incompatibility and PCD

Interactions between the *het* gene products of vegetatively incompatible individuals may cause cellular defects that can disrupt the equilibrium of the cell, thus inducing the cell death response. In the following section, various stress conditions that are potentially associated with incompatibility are discussed. These include nitrogen starvation, DNA damage, and the production of reactive oxygen species (ROS).

Nitrogen starvation

Vegetative incompatibility illicit a similar response to that observed during nitrogen depletion, because both processes activate a stress response (Federovo et al., 2005; Pinan-Lucarré et al., 2003, 2007). This arises from the fact that similar genes are involved in the transcriptional regulation of nitrogen starvation and vegetative incompatibility in *Aspergillus nidulans* (Katz et al., 2006). For example, it has been demonstrated that the ortholog of the

transcriptional regulater *vib-1* of *A. nidulans* influences protease production (*i.e.*, factors that influence the outcome of the interaction) in response to nutrient limitation (Katz et al., 2006). It was further suggested that vegetative incompatibility and nitrogen starvation utilize similar pathways and processes. For example, mutations in the *mod* genes in *P. anserina* associated with vegetative incompatibility showed developmental defects in protoperithecial development that are regulated by the starvation pathway (Boucherie and Bernet, 1974; Durrens et al., 1979, 1984; Barreau et al., 1998; Loubradou and Turcq, 2000).

The notion that these two processes share similar pathways is supported by the fact that both vegetative incompatibility and nitrogen starvation trigger autophagy. In *S. cerevisiae*, genes essential for autophagy have been shown to be involved in vegetative incompatibility. These include the *idi-6/pspA* gene that encodes a serine protease (an ortholog of the vacuolar protease B of *S. cerevisiae*), which is involved in both vegetative incompatibility and autophagy (Pinan-Lucarre et al., 2003; Bras et al., 2005; Ma et al., 2007). In this respect, it is thought that autophagy functions to recycle cell content during nutrient stress, while it protects the cell against stresses associated with incompatibility. However, it was also demonstrated that alterations in nutrient signalling pathways might mediate the commitment of hyphae to enter the apoptotic phase (Glass and Dementhon, 2006). Finally, it is also important to recognise that the STAND NTPases encoded by some of the *het* genes function as key integrators of stress and nutrient availability signalling (Fedorovo et al., 2005).

DNA damage

Nuclear DNA fragmentation, which is a hallmark of apoptosis, is absent during PCD by incompatibility. However, DNA degradation, that is also characteristic of apoptotis, occurs during vegetative incompatibility (Glass et al., 2000; Marek et al., 2003; Glass and Dementhon, 2006). In *N. crassa*, direct evidence for DNA degradation came from experiments with deoxynucleotidyltransferase-mediated dUTP nick end labelling or TUNEL (Marek et al., 2003). Iakovlev (2001) also suggested that DNA damage may occur during inter-specific interactions in *Heterobasidion annosum*. It has also been suggested that DNA damage may be caused by the stresses (e.g., change in pH and redox potential and the presence of ROS, see below) that accompanies PCD by incompatibility (Leslie and Zeller, 1996; Allen et al., 2003; Kültz, 2005).

Cell wall damage

The secretion of cell wall degrading enzymes that attack the main constituents (*i.e*., glucans, chitin and mannoproteins) of the opposing individual's cell wall (Fig. 5) is an important aspect of fungus-fungus interactions (Fukazawa and Kagaya, 1997). Fungal cells respond to the stresses associated with cell wall and membrane damage by activating the cell wall integrity (CWI) pathway (see Levin, 2005 for a review). This pathway, which has been well documented in *S. cerevisiae*, maintains CWI during growth, morphogenesis and external challenges that can cause stress to the cell wall (Levin, 2005; Rodríguez-Peňa et al., 2005). In *S. cerevisiae*, the CWI pathway leads to the alteration of membrane tension and permeability, lipid rearrangements, membrane protein rearrangements, changes in trans-membrane potential and formation of lipid peroxidases and lipids (Kültz, 2005). It is likely that vegetatively incompatible reactions are accompanied by cell wall stresses and that this pathway plays an important role in limiting the damage. For example, it has been suggested that the presence of lipid in adducts in the cell during PCD by incompatibility in *P. anserina* can activate the CWI pathway and that the abnormal deposition of cell wall material during incompatibility in this fungus may be a response to the CWI pathway (Dementhon et al., 2003).

Production of reactive oxygen species (ROS)

Increased ROS levels are typical of fungal-fungal interactions (e.g., Williamson, 1997; Iakovlev, 2001; Glass and Dementhon, 2006). For example, it was shown in *H. annosum* that the outcome of interspecific reactions is linked to increased ROS levels (Iakovlev, 2001). Also, the ability of a fungus to protect itself against oxidative attack influences the outcome of fungal-fungal interactions (Score et al., 1997; Williamson, 1997; Iakovlev, 2001; De Groot et al., 2005; Kim et al., 2005). It was demonstrated that increased phenoloxidase activity, which increases melanin production and has antioxidant properties, also influences the outcome of fungal-fungal interactions in *H. annosum* (Iakovlev, 2001). Increased levels of ROS and phenoloxidase activity may also occur during vegetative incompatibility (Glass and Dementhon, 2006; Scherz-Shouval and Elazer, 2007; Paoletti and Saupe, 2009).

ROS produced during vegetative incompatibility could be crucial in the interplay between autophagic and apoptotic pathways, as well as determining the initiation point of PCD (Hamacher-Brady et al., 2006). For example, ROS may play a role in relaying signals from the initial *het* interaction to the cell's response because intracellular ROS are signalling

molecules essential for the induction of autophagy (Bras et al., 2005; Nyathi and Baker, 2006; Scherz-Shouval and Elazer, 2007). This is evident from the fact that ATG4, which is a critical protease in the autophagic pathway (Fig. 6), is a direct target for oxidation by ROS (Scherz-Shouval and Elazer, 2007). However, even though the activation of autophagy may protect the cell against major harm (Paul et al., 1992; Kiffin, 2006), prolonged ROS signalling will change the outcome of autophagy from survival to cell death (Scherz-Shouval and Elazer, 2007). This is because ROS represents an important switch between autophagy and apoptosis, as increased ROS levels influence the permeability of the mitochondrial outer membrane (referred to as the mitochondrial outer membrane permeability transition, MPT) (Lemasters et al., 1998; Hamacher-Brady et al., 2006; Pereira et al., 2007; Bosch et al., 2008). MPT triggers autophagy when MPT causes mitochondrial functional failure, which is accompanied by depolarization of the mitochondrial membrane and it is the depolarized mitochondria that are targeted for autophagy (Fig. 7) (Rodríguez-Enriquez et al., 2004; Kim et al., 2007). However, when oxidative stress increases and MPT affects greater numbers of mitochondria, autophagy becomes inadequate and cell death is activated (Lemasters et al., 1998, Rodríguez-Enriquez et al., 2004; Kiffin et al., 2006; Kim et al., 2007; Scherz-Shouval and Elazer, 2007). As has previously been mentioned, PCD associated with vegetative incompatibility appears to be similar to PCD associated with other processes (e.g., hypersensitive response during a pathogen/host interaction) (Pinan-Lucarré et al., 2007). It is, therefore, possible that MPT could also regulate the switch between apoptosis and autophagy during vegetative incompatibility.

Free radicals produced during fungus-fungus interactions may influence the redox potential of the cell (Iakovlev, 2001). Changes in redox status might cause ER stress, which arises from disturbance of the environment in the ER lumen, which impairs ER functions that are detrimental to the cell (Kültz, 2005; Schröder et al., 2005). PCD by incompatibility is activated when the cell cannot successfully deal with the ER stress (Lefranc et al., 2007). The UPR (unfolded protein response) stress response pathway protects cells against ER stress as it is involved in reducing the overall cellular protein synthesis at the transcriptional and translational levels. In this way, it assists in protein folding via the up-regulation of chaperons and foldases, repairing damaged proteins by enzymes that reverse oxidative damage, and enhancing degradation of misfolded proteins via the up-regulation of molecules involved in ER-associated degradation pathway (Ding et al., 2007). It is possible that this pathway may play a role as a protective mechanism to protect the cell against ER stress caused by the *het*

gene product interactions, as the mammalian homologue of Mod-E/HSP90 mediate the UPR stress response to ER stress (Szent-Gyorgyi, 1995; Patil and Walter, 2001).

SIGNALLING PATHWAYS AND VEGETATIVE INCOMPATIBILITY

Cell signaling plays a central role in hyphal fusion (Simonin et al., 2010), which represents a key aspects of vegetatively compatible and incompatible interactions. Fungus-fungus interactions are accompanied by the production of toxic compounds (e.g., proteinases, ROS, etc.) to attack the opponent (Iakovlev and Stenlid, 2000). It is thus also necessary that the interacting cells must be able to sense environmental changes and activate signalling cascades to respond to these changes. For this purpose, signal transducing proteins (e.g., histidine protein kinases) can allow for detection of other cells and/or sense changes associated with vegetative incompatibility (e.g., redox potential and ROS). They might also allow activation or repression of the expression of genes to deal with these changes (Kronstad and Kaiser, 2000; Wolanin et al., 2002). Several signalling pathways may be involved in regulating and coordinating processes associated with vegetative incompatibility. These include the TOR (target of rapamycin), cAMP (cyclic adenosine monophosphate)-PKA (protein kinase A), the MAPK (mitogen-activated protein kinase) and the sphingomyelin-ceramide signalling pathways.

TOR

Although the TOR signalling pathway has been conclusively linked to vegetative incompatibility (Dementhon et al., 2003; Pinan-Lucarré et al., 2006), its exact role in PCD by incompatibility is not yet clear. One hypothesis is that the interactions between the *het* gene products may affect the general cellular integrity that is sensed by the TOR pathway (Cutler et al., 2001; Meijer and Codogno, 2004; Pinan-Lucarré et al., 2006). This is a plausible explanation, because the TOR pathway senses cellular signals such as nutrient availability, mitochondrial integrity, stress signals, and changes in the levels of amino acids and ATP (Cutler et al., 2001; Meijer and Codogno, 2004; Paglin et al., 2005; Pinan-Lucarré et al., 2006). Furthermore, TOR signalling leads to the activation of autophagy (Pinan-Lucarré et al. 2003; Budovshaya et al., 2004; Pinan-Lucarré et al., 2006; Wullschleger and Hall, 2006). TOR signalling is also involved in other processes associated with incompatibility, for

example regulating vacuolization and septation (Pinan-Lucarré et al., 2005; Pinan-Lucarré et al., 2006).

The TOR signalling pathway influences important cellular processes in the cell through two complexes, the TOR complex I (TOR1) that is affected by rapamycin treatment and the TOR complex II (TOR2), not affected by rapamycin treatment (Meijer and Codogno, 2004; Pinan-Lucarré et al., 2006). TOR1 is known to be involved in PCD by incompatibility, as cells treated with rapamycin display features (e.g., vacuolization, septal deposition and lipid droplets accumulation) that are characteristic of PCD by incompatibility (Cutler et al., 2001; Pinan-Lucarré et al., 2003; Pinan-Lucarré et al., 2006). Interestingly, it has been demonstrated that rapamycin-dependent TOR negatively regulate cellular adhesion in *C. albicans* (Bastidas et al., 2009).

Although a link has not been shown between TOR2 and vegetative incompatibility, this protein complex may influence several processes involved in this phenomenon. For example, it is possible that TOR2 is involved in the modulation of the cell's response to vegetative incompatibility associated stresses (e.g., remodelling of the cell wall). This is because TOR2 is part of the CWI pathway (see above) that influences actin cytoskeleton polarization (Matsuo et al., 2007). Actin cytoskeleton polarization is likewise involved in membrane and protein trafficking events that are important for cellular response to stresses, including starvation that have previously been linked to vegetative incompatibility (Cutler et al., 2001; Verstrepen and Klis, 2006; Chen and Thorner, 2007; Vinod et al., 2008). Because the CWI pathway maintains cell wall integrity during morphogenesis (Levin, 2005; Meyer et al., 2009), the TOR2 could also influence other events, such cell-cell adhesion necessary for hyphal anastomoses occurring during vegetative incompatibility (Pinan-Lucarré et al., 2007). It has also recently been discovered that TOR2 is an upstream regulator of TOR1 in mammals (Jacinto and Lorberg, 2008), that has been linked with vegetative incompatibility (Cutler et al., 2001; Pinan-Lucarré et al., 2003; Pinan-Lucarré et al., 2006).

MAPK

Various authors have suggested that the MAPK pathway composed of sequentially acting kinases may play a role in vegetative incompatibility (e.g., Leslie and Zeller, 1996; Roux and Blenis, 2004). For example, Leslie and Zeller (1996) suggested that the G-protein signalling pathway involving MAPK, which is required for many important biological processes such as mating and sensing environmental cues (Hoffman, 2005; Shang et al., 2008), may also be

required for controlling the processes associated with vegetative incompatibility. This view is supported by the fact that the *mod-D* gene that is known to influence vegetative incompatibility, encodes an α-subunit of heterotrimeric G protein (Loubradou and Turcq, 2000). This association between the MAPK pathway and vegetative incompatibility makes sense, as the MAPK pathway is known to regulate related processes such as hyphal fusion and autophagy (Codogno and Meijer, 2005; Lam et al., 2006; Thaiville et al., 2008; Fleissner et al., 2009).

It remains unclear which members of the different MAPK families (Pearson et al., 2001) that have been characterized are involved in vegetative incompatibility. However, those involved in hyphal anastomosis mostly form part of the *S. cerevisiae* ERK MAP kinase family (Fig. 9) (e.g., Robinson and Cobb, 1997; Roca et al., 2005; Zeilinger and Omann, 2007; Villar-Tajadura et al., 2008). Members of this MAPK family include Kss1 in *S. cerevisiae*, Fus3p/Kss1p MAPK (MAK-2) in *N. crassa*, Pmk1 from *Magnaporthe grisea*, Fmk1 from *Fusarium oxysporum*, Bmp1 from *Botrytis cinerea*, as well as *tmkA* and *tvk1* from *Trichoderma*, each of which have different cellular functions (Zeilinger and Omann, 2007). For example, Kss1 in *S. cerevisiae* is part of the MAPK pathway that activates FLO genes, which are known to trigger major changes in gene expression and cellular architecture, necessary for the mating process, including cytoskeleton reorganization (Robinson et al., 1997; Stone et al., 2000; Vinod et al., 2008; Dranginis et al., 2007; Sengupta et al., 2007).

The MAPK cascade also plays a role in the defence and stress reactions during self/ nonself recognition in fungi (Silar, 2005). For example, it was demonstrated in *N. crassa* that MAK-2 and the WW (tryptophan-tryptophan) domain protein SO (referring to the pleiotropic or "soft" phenotypes displayed by SO mutants) involved in signaling during vegetative hyphal fusion (Gough, 2010), also play a role in septal pore plugging (Fleissner and Glass, 2007). Pmk1 in *Schizophyllum commune* that is involved in cell wall construction and morphogenesis as part of the CWI pathway is also activated under stress conditions (e.g., oxidative stress) (Madrid et al., 2006; Villar-Tajadura et al., 2008). The MAPK pathway also influence the outcome of fungal-fungal interactions, as the MAP kinase TmkA affects the mycoparasitism ability of *Trichoderma* species by regulating key processes (e.g., expression of hydrolytic and cell wall degradation enzymes) that influence the mycoparasitism ability of the fungus (Cho et al., 2007; Zeilinger and Omann, 2007). In addition, a Fus3/Kss1 homolog in *Cochliobolus heterostrophus* controls melanin biosynthesis at the transcriptional level, which potentially influences the outcome of fungal-fungal interactions (Eliahu et al., 2007).

Mating pheromones can activate MAPK cascades to induce death of cells that fail to mate and that are in contact with cells of the opposite mating type (referred to as pheromone-induced PCD) (for a review see Pozniakovsky et al., 2005; Severin and Hyman, 2002). The exact biological significance of this type of PCD is unknown, but it is possible that it may improve the genetic fund of the community by eliminating the weak individuals. It was proposed that the mating pheromones can induce PCD, as they act through their G-protein-coupled receptors that are physiological sensors (Zhang et al., 2006). Similar to what was proposed to occur during vegetative incompatibility (Leslie and Zeller, 1996), pheromone-induced PCD also shares hallmarks associated with vegetative incompatibility, including ROS accumulation (Madeo et al., 1999; Severin and Hyman, 2002). Furthermore, pheromone-induced PCD displays several traits (e.g., generation of reactive oxygen species in centre of the respiratory chain complex III, and cytochrome *c* release from mitochondria) that are typical for mitochondria-dependent apoptosis of animal cells, which are believed to be involved in the activation of PCD by incompatibility (Severin and Hyman, 2002; Pozniakovsky et al., 2005). It thus appears that more than one of the MAPK superfamilies may be involved in incompatibility, controlling different processes, including hyphal anastomosis, stress response and PCD.

RAS/cAMP-PKA

The RAS/cAMP-PKA pathway may regulate several key processes that determine the outcome of fungal-fungal interactions (Hoffman, 2005). For example, it was demonstrated that cAMP regulates virulence in *Cryphonectria parasitica* and melanin production in *Cryptococcus neoformans* (Hicks et al., 2005; Shang et al., 2008). The RAS/cAMP pathway also regulates key processes occurring during vegetative incompatibility, as increased levels of cAMP suppress the defects in vegetative growth in *P. anserina* carrying a mutation in *mod-D* that encodes an α-subunit of a heterotrimeric G-protein (Labradou et al., 1999; Loubradou and Turcq, 2000). In addition, the RAS/cAMP pathway, which is a TOR effector pathway, also shares the same response as TOR-depleted or rapamycin treated cells, such as G1 (Gap1, the first phase of the interphase, *i.e.*, the growth phase at the end of mitosis) cell cycle arrest, accumulation of storage carbohydrates (e.g., glycogen ad trehalose) and specific changes in transcription (Shinohara et al., 2002; Budovshaya et al., 2004; Schmelzle et al., 2004).

It is still unclear what the exact role of the RAS/cAMP pathway may be in regulating processes associated with vegetative incompatibility, as this pathway influences several

processes in the cell (e.g., actin cytoskeleton integrity, proliferation, differentiation, cell adhesion and septum formation) (Goldfinger, 2008; Justa-Schuch et al., 2010). It regulates and plays a central role in the cell's response to nutrients and carbon availability (Cutler et al., 2001; Budovskaya et al., 2004; Meijer and Codogno, 2004; Schubert et al., 2007) and it is thus possible that it regulates the cell's response to stresses (that is similar to nutrient stress response) associated with vegetative incompatibility. A link was also demonstrated between the RAS/cAMP pathway and the sensing of stresses, changes in the actin cytoskeleton and the stimulation of PCD (Leadsham et al., 2009). Apparently the RAS/cAMP pathway also regulates mitochondrial function and ROS production that are part of the PCD response (Phillips et al., 2006; Gourlay and Ayscough, 2006).

Sphingomyelin-ceramide

Sphingomyelin-ceramide signalling is thought to be fundamental to vegetative incompatibility. This arises from the fact that the interaction between *het-e* and *het-c* that triggers incompatibility in *P. anserina,* apparently activates the ceramide stress response pathway (Fedorovo et al., 2005). The *het-c* gene in *P. anserina* encodes a glycolipid transfer protein that accelerates the transfer of glycosphingolipids between membranes in the cell and it was demonstrated that *ACD11* (the *het-c* ortholog in *Arabidopsis thaliana*) is part of the sphingolipid signalling pathway that is known to induce PCD (Pinan-Lucarré et al., 2006; West et al., 2008). This signalling pathway plays an important role in the activation of PCD via two independent, and perhaps co-regulated, mechanisms (Andrieu-Abadie et al., 2001). The one mechanism involves transcriptional changes through SAPK/JNK (stress-activated protein kinase/c-Jun-NH_2-terminal kinase), because ceramide, like other stress stimuli, markedly activates the stress activated kinases or SAPK/JNK pathway (Kolesnick and Krönke, 1998). The other mechanism for ceramide to activate PCD is by directly affecting mitochondrial homeostasis, where mitochondrial perturbation represents a committed step in ceramide signalling of apoptosis (Kolesnick and Krönke, 1998; Stiban et al., 2008). Ceramide can also serve as a precursor for all major sphingolipids that are known to function in cell death activation (He et al., 2006; West et al., 2008).

FUTURE PROSPECTS

Vegetative incompatibility in fungi represents an intriguing phenomenon that has been studied for more than a century (e.g., Bérgueret et al., 1994; Saupe et al., 1996; Kubisiak and Milgroom 2006). The *het* genes have been studied in depth in model Ascomycetes such as *P.*

anserina and *N. crassa*, and their evolution, as well as their mechanisms of interaction with one another are well understood. Yet, many unanswered questions regarding vegetative incompatibility remain. Some of the most intriguing of these are:

* What is the role of stress in PCD associated with vegetative incompatibility?
* How exactly is cell death by incompatibility activated and executed?
* How is PCD by incompatibility related to cell death in other eukaryotes?
* What is the role of autophagy during the activation of PCD by incompatibility?

To answer these questions and to achieve a comprehensive understanding of vegetative incompatibility in fungi, these systems need to be studied further in model and non-model fungi. While studies on the model fungi have many advantages (e.g., extensive literature on vegetative incompatibility, full genome sequence information, well-developed experimental systems), the paucity of knowledge regarding other fungi leaves many questions to be answered. An example of this problem is that the model fungi used to study vegetative incompatibility are all Ascomycetes and little is known regarding this system in Basidiomycetes.

Few studies regarding vegetative incompatibility have considered the processes and pathways underlying the phenomenon. Of the studies that have been conducted, most employ morphological and physiological data to derive conclusions regarding the timing of PCD, organelle changes, membrane changes, etc. (e.g., Jacobson et al., 1998). Very few studies have utilized strains harbouring mutations in specific genes to address hypotheses regarding vegetative incompatibility. For example, this approach was used in *P. anserina* to show that the *mod* and *idi* genes encode vital proteins involved in signalling, protein damage, etc. during vegetative incompatibility (e.g., Loubradou and Turcq, 2000; Dementhon et al., 2004; Pinan-Lucarré et al., 2007). Nevertheless, the processes and pathways that underlie vegetative incompatibility still remain vague, at best.

The numbers of fungi for which whole genome sequences are available is increasing rapidly. It will, therefore, become progressively easier to identify genes associated with vegetative incompatibility in non-model fungi in the future. However, understanding the actual biological role of these putative *het* gene products will be dependent on experimental analyses, such as targeted gene disruption or expression profiling based on microarray or pyrosequencing technology. In the future, the identification of such genes in a wider suite of fungi than is presently the case, will allow for the development of more strongly supported

hypothesis regarding the pathways and processes underlying vegetative incompatibility. This will also lead to a better understanding of the mechanism of PCD associated with vegetative incompatibility and how it compares with PCD in other eukaryotes.

REFERENCES

Allen, T.D., Dawe, A.L., Nuss, D.L., 2003. Use of cDNA microarrays to monitor transcriptional responses of the chestnut blight fungus *Cryphonectria parasitica* to infection by virulence-attenuating hypovirus. Euk. Cell. 2, 1253-1265.

Andrieu-Abadie, N., Gouazė, V., Salvayre, R., Levade, T., 2001. Ceramide in apoptosis signaling: relationship with oxidative stress. Free Radical Biol. Med. 3, 717-728.

Barreau, C., Iskandar, M., Loubradou, G., Levallois, V., Bégueret, J., 1998. The *mod-A* suppressor of nonallelic heterokaryon incompatibility in *Podospora anserina* encodes a proline-rich polypeptide involved in female organ formation. Genetics. 149, 915-926.

Bastidas, R.J., Heitman, H., Cardenas, M.E., 2009. The protein kinase TOR1 regulates adhesin gene expression in *Candida albicans*. PLoS Path. 5, e1000294.

Bayly, J.C., Douglas, L.M., Pretorius, I.S., Bauer, F.F., Dranginis, A.M., 2005. Characteristics of Flo11-dependent flocculation in *Saccharomyces cerevisiae*. FEMS Yeast Res. 5, 1151-1156.

Bégueret, J., Turcq, B., Clavé, C., 1994. Vegetative incompatibility in filamentous fungi: *Het* genes begin to talk. Trends Genet. 10, 441-446.

Biella, S., Smith, M.L., Aist, J.R., Cortesi, P., Milgroom, M.G., 2002. Programmed cell death correlates with virus transmission in a filamentous fungus. Proc. R. Soc. Lond. 269, 2269-2276.

Boddy, L., 2000. Interspecific combative interactions between wood-decaying basidiomycetes. FEMS Microbiol. Ecol. 31, 185-194.

Bosch, M., Poulter, N.S., Vatovec, S., Franklin-Tong, V.E., 2008. Initiation of programmed cell death in self-incompatibility: Role for cytoskeleton modifications and several caspase-like activities. Mol. Plant. 1, 879-887.

Boucherie, H., Bernet, J., 1974. Protoplasmic incompatibility and female organ formation in *Podospora anserina*: Properties of mutations abolishing both processes. Mol. Gen. Genet. 135, 163-174.

Boucherie, H., Bernet, J., 1977. Protoplasmic incompatibility and self-lysis in *Podospora anserina*: Enzyme activities involved with cell destruction. Can. J. Bot. 56, 2171-2176.

Boucherie, H., Dupont, C.H., Bernet, J., 1981. Polypeptide synthesis during protoplasmic incompatibility in the fungus *Podospora anserina*. Biochim. Biophys. Acta. 653, 18-26.

Bourges, N.G., Groppi, A., Barreau, C., Clave, C., Bégueret, J., 1998. Regulation of gene expression during the vegetative incompatibility reaction in *Podospora anserina:* Characterization of three induced genes. Genetics. 150, 633-641.

Bowman, S.M., Free, S.J., 2006. The structure and synthesis of the fungal cell wall. BioEssays. 28, 799-808.

Bras, M., Queenan, B., Susin, S.A., 2005. Programmed cell death via mitochondria: Different modes of dying. Biochem. 70, 231-239.

Budovskaya, Y.V., Stephan, J.S., Reggiori, F., Klionsky, D.J., Herman, P.K., 2004. The ras/camp-dependent protein kinase signaling pathway regulates an early step of the autophagy process in *Saccharomyces cerevisiae*. J. Biol. Chem. 279, 20663-20671.

Bursch, W., 2001. The autophagosomal-lysosomal compartment in programmed cell death. Cell Death Diff. 8, 569-581.

Casselton, L., Zolan M., 2002. The art and design of genetic screens: Filamentous fungi. Nature Rev. Genetics. 3, 683-697.

Casselton, L.A., 2002. Mate recognition in fungi. Heredity. 88, 142-147.

Casselton, L.A., Olesnicky, N.S., 1998. Molecular genetics of mating recognition in basidiomycete fungi. Microbiol. Mol. Biol. Rev. 62, 55-70.

Castle, A.J., Stocco, N., Boulianne, R., 1996. Fimbrial-dependent mating in *Microbotryum violaceum* involves a mannose-lectin interaction. Can. J. Microbiol. 42, 461-466.

Celerin, M., Day, A. W., 1998. Sex, Smut, and RNA: The complexity of fungal fimbriae. Int. J. Plant Sci. 159, 175-184.

Chen, R.E., Thorner, J., 2007. Function and regulation in MAPK signaling pathways: Lessons learned from the yeast the *Saccharomyces cereviciae*. Biochim. Biophys. Acta. 177, 1311-1340.

Chevanne, D., Bastiaans, E., Debets, A., Saupe, S.J., Clavé, C., Paoletti, M., 2009. Identification of the *het-r* vegetative incompatibility gene of *Podospora anserina* as a member of the fast evolving *HNWD* gene family. Curr. Genet. 55, 93-102.

Chevanne, D., Saupe, S.J., Clavé, C., Paoletti, M., 2010. WD-repeat instability and diversification of the *Podospora anserina hnwd* non-self recognition gene family. BMC Evol. Biol. 10, 134.

Cho, Y., Cramer, R.A., Kim, K-H., Davis, J., Mitchell, T.K., Figuli, P., Pryor, B.M., Lemasters, E., Lawrence, C.B., 2007. The *Fus3/Kss1* MAP kinase homolog *Amk1* regulates the expression of genes encoding hydrolytic enzymes in *Alternaria brassicicola*. Fungal Genet. Biol. 44, 543-553.

Codogno, P., Meijer, A.J., 2005. Autophagy and signaling: Their role in cell survival and cell death. Cell Death Diff. 12, 1509-1518.

Cutler, N.S., Pan, X., Heitman, J., Cardenas, M.E., 2001. The TOR signal transduction cascade controls cellular differentiation in response to nutrients. Mol. Biol. 12, 4103-4113.

De Groot, P.W.J., Ram, A.F., Klis, F.M., 2005. Features and functions of covalently linked proteins in fungal cell walls. Fungal Genet. Biol. 42, 657-675.

Dementhon, K., Iyer, G., Glass, N.L., 2006. VIB-1 is required for expression of genes necessary for programmed cell death in *Neurospora crassa*. Euk. Cell. 5, 2161-2173.

Dementhon, K., Paoletti, M., Pinan-Lucarré, B., Loubradou-Bourges, N., Sabourin, M., Saupe, S.J., 2003. Rapamycin mimics the incompatibility reaction in the fungus *Podospora anserina*. Euk. Cell. 2, 238-46.

Dementhon, K., Saupe, S.J., Clavé, C., 2004. Characterization of IDI-4, a bZIP transcription factor inducing autophagy and cell death in the fungus *Podospora anserine*. Mol. Microbiol. 53, 1625-1640.

Ding, W.X., Ni, H.M., Gao, W., Hou, Y.F., Melan, M.A., Chen, X., Stolz, D.B., Shao, Z.M., Yin, X.M., 2007. Differential effects of endoplasmic reticulum stress-induced autophagy on cell survival. J. Biol. Chem. 282, 4702-4710.

Douglas, L.M., Li., L., Yang, Y., Dranginis, A.M., 2007. Expression and characterization of the flocculin Flo11/Muc1, a *Saccharomyces cerevisiae* mannoprotein with homotypic properties of adhesion. Euk. Cell. 6, 2214-2221.

Dranginis, A.M., Rauceo, J.M., Coronado, J.E., Lipke, P.N., 2007. Biochemical guide to yeast adhesins: Glycoproteins for social and antisocial occasions. Microbiol. Mol. Biol. Rev. 71, 282-294.

Durrens P., Laigret F., Labarère J., Bernet J., 1979. *Podospora anserina* mutant defective in protoperithecium formation, ascospore germination, and cell regeneration. J. Bacteriol. 140, 835-842.

Durrens, P., 1984. *Podospora anserina* mutation reducing cell survival under glucose starvation. Exp. Mycol. 8, 342-348.

Eliahu, N., Igbaria, A., Rose, M.S., Horwitz, B.A., Lev, S., 2007. Melanin biosynthesis in the maize pathogen *Cochliobolus heterostrophus* depends on two MAP kinases, Chk1 and Mps1, and the transcriptional factor Cmr1. Euk. Cell. 6, 421-429.

Espagne, E., Balhadère, P., Penin, M.-L., Barreau, C., Turcq, B., 2002. *Het-e* and *het-d* belong to a new subfamily of WD40 Proteins involved in vegetative incompatibility specificity in the fungus *Podospora anserine*. Genetics. 161, 71-81.

Fedorova, N.D., Badger, J.H., Robson, G.D., Wortman, J.R., Nierman, W.C., 2005. Comparative analysis of programmed cell death pathways in filamentous fungi. BMC Genomics. 6, 1-14.

Fichtner, L., Schulze, F., Braus, G.H., 2007. Differential Flo8p-dependent regulation of FLO1 and FLO11 for cell-cell and cell-substrate adherence of *S. cerevisiae* S288c. Mol. Microbiol. 66, 1276-1289.

Fleissner, A., Glass, N.L., 2007. SO, a protein involved in hyphal fusion in *Neurospora crassa*, localizes to septal plugs. Euk. Cell. 6, 84-94.

Fleissner, A., Leeder, A.C., Roca, M.G., Read, N.D., Glass, N.L., 2009. Oscillatory recruitment of signalling proteins to cell tips promotes coordinated behavior during cell fusion. Proc. Natl. Acad. Sci. USA. 106, 19387-19392.

Fukazawa, Y., Kagaya, K., 1997. Molecular bases of adhesion of *Candida albicans.* J. Med. Vet. Mycol. 35, 87-99.

Gardiner, R.B., Canton, M., Day, A.W., 1981. Fimbrial variation in smuts and heterobasidiomycete fungi source. Bot. Gazette. 142, 147-150.

Glass, N.L., Dementhon, K., 2006. Non-self recognition and programmed cell death in filamentous fungi. Curr. Opin. Microbiol. 9, 553-558.

Glass, N.L., Jacobson, D.J., Shiu, K.T., 2000. The genetics of hyphal fusion and vegetative incompatibility in filamentous ascomycetes fungi. Annu. Rev. Genet. 34, 165-186.

Glass, N.L., Kaneko, I., 2003. Fatal attraction: Nonself-recognition and heterokaryon incompatibility in filamentous fungi. Euk. Cell. 2, 1-8.

Glass, N.L., Rasmussen, C., Roca, M.G., Read, N.D., 2004. Hyphal homing, fusion and mycelial interconnectedness. Trends Microbiol. 12, 135-141.

Goldfinger, L.E., 2008. Choose your own path: Specificity in Ras GTPase signaling. Mol. BioSyst. 4, 293-299.

Gough, N.R., 2009. Taking turns sending and receiving. Sci. Signal. 2, ec379.

Gourlay, C.W., Ayscough, K.R., 2006. Actin-induced hyperactivation of the Ras signaling pathway leads to apoptosis in *Saccharomyces cerevisiae*. Mol. Cell. Biol. 26, 6487-6501.

Guo, B., Styles, C.A., Feng, Q., Fink, G.R., 2000. A *Saccharomyces* gene family involved in invasive growth, cell- cell adhesion, and mating. Proc. Natl. Acad. Sci. Usa. 97, 12158-12163.

Hamacher-Brady, A., Brady, N.R., Gottlieb, R.A., 2006. The interplay between pro-death and pro-survival signaling pathways in myocardial ischemia/reperfusion injury: Apoptosis meets autophagy. Cardiovasc. Drugs Ther. 20, 445-462.

Hansen, E.M., Stenlid, J., Johansson, M., 1994. Somatic incompatibility in *Heterobasidion annosum* and *Phellinus weirii*. In: Johansson M, Stenlid J (eds) Proceedings of the eight IUOFRO Root and Butt Rot Conference. Swedish University of Agricultural Sciences, Uppsala, pp 323-333.

He, Q., Suzuki, H., Sharma, N., Sharma, R.P., 2006. Ceramide synthase inhibition by fumonisin B_1 treatment activmarkates sphingolipid-metabolizing systems in mouse liver. Toxicol. Spec. 94, 388-397.

Hicks, J.K., Bahn, Y.-S., Heitman, J., 2005. Pde1 phosphodiesterase modulates cyclic AMP levels through a protein kinase A-mediated negative feedback loop in *Cryptococcus neoformans*. Euk. Cell. 4, 1971-1981.

Hoffman, C.S., 2005. Except in every detail: Comparing and contrasting G-protein signaling in *Saccharomyces cerevisiae* and *Schizosaccharomyces pombe*. Euk. Cell. 4, 495-503.

Iakovlev, A., 2001. Molecular responses of mycelia to fungus-fungus interactions. Doctoral thesis. Swedish University of Agricultural Sciences, Uppsala.

Iakovlev, A., Stenlid, J., 2000. Spatiotemporal patterns of laccase activity in interacting mycelia of wood-decaying basidiomycete fungi. Microb Ecol. 39, 236-245.

Jacinto, E., Lorberg, A., 2008. TOR regulation of AGC kinases in yeast and mammals. Biochem. J. 410, 19–37.

Jacobson, D.J., Beurkens, K., Klomparens, K.L., 1998. Microscopic and ultrastructural examination of vegetative incompatibility in partial diploids heterozygous at *het* loci in *Neurospora crassa*. Fungal Genet. Biol. 23, 45-56.

Justa-Schuch, D., Heilig, Y., Richthammer, C., Seiler, S., 2010. Septum formation is regulated by the RHO4-specific exchange factors BUD3 and RGF3 and by the landmark protein BUD4 in *Neuropora crassa*. Mol. Micro. 76, 220-235.

Katz, M.E., Gray, K.-A., Cheetham, B.F., 2006. The *Aspergillus nidulans xprG* (*phoG*) gene encodes a putative transcriptional activator involved in the response to nutrient limitation. Fungal Genet. Biol. 43, 190-199.

Kauserud, H., Saetre, G.-P., Schmidt, O., Decock, C., Schumacher, T., 2006. Genetics of self/nonself-recognition in *Serpula lacrymans*. Fungal Genet. Biol. 43, 503-510.

Kiffin, R., Bandyopadhyay, U., Cuervo, A.M., 2006. Oxidative stress and autophagy. Antioxid. Redox Signal. 8, 152-162.

Kim, J.-E., Han, K.-H., Jin, J., Kim, H., Kim, J.-C., Yun, S.-H., Lee, Y.-W., 2005. Putative polyketide synthase and laccase genes for biosynthesis of aurofusarin in *Gibberella zeae*. Appl. Environ. Microbiol. 71, 1701-1708.

Kim, K.-Y., Truman, A.W., Levin, D.E., 2007. Yeast Mpk1 mitogen-activated protein kinase activates transcription through Swi4/Swi6 by a noncatalytic mechanism that requires upstream signal. Mol. Cell. Biol. 28, 2579-2589.

Kolesnick, R.N., Krönke, M., 1998. Regulation of ceramide production and apoptotis. Annu. Rev. Physiol. 60, 643-665.

Kothe, E., Gola, S., Wendland, J., 2003. Evolution of multispecific mating-type alleles for pheromone perception in the homobasidiomycete fungi. Curr. Genet. 42, 268-275.

Kronstad, J.W., Kaiser, D., 2000. Growth and development signals and their transduction. Curr. Opin. Microbiol. 3, 549-552.

Kronstad, J.W., Staben, C., 1997. Mating type in filamentous fungi. Annu. Rev. Genet. 31, 245-76.

Kubisiak, T.L., Milgroom, M.G., 2006. Markers linked to vegetative incompatibility (*vic*) genes and a region of height heterogeneity and reduced recombination near the mating type locus (*MAT*) in *Cryphonectria parasitica*. Fungal Genet. Biol. 43, 453-463.

Kültz, D., 2005. Molecular and evolutionary basis of the cellular stress response. Annu. Rev. Physiol. 2005. 67, 225-57.

Labarère, J., Bégueret, J., 1979. Protoplasmic incompatibility and cell lysis in *Podospora anserina*. I. Genetic investigation on mutations of a novel modifier gene that suppresses cell destruction. Genetics. 87, 249-257.

Labarère, J., Bégueret, J., Bernet, J., 1974. Incompatibility in *Podospora anserina*: Comparative properties of the antagonistic cytoplasmic factors of a non-allelic system. Bacteriology. 120, 854-860.

Labradou, G., Bégueret, J., Turcq, B., 1999. Mod-D, a Gα subunit of the fungus *Podospora anserina*, is involved in both regulation of development and vegetative incompatibility. Genetics. 152, 519-528.

Lam, H.-M., Chiao, Y.A., Li, M.-W., Yung, Y.-K., Ji, S., 2006. Putative nitrogen sensing systems in higher plants. J. Integrative Plant Biol. 48, 873-888.

Leadsham, J.E., Miller, K., Ayscough, K.R., Colombo, S., Martegani, E., Sudbery, P., Gourlay, C.W., 2009. *Whi2p* links nutritional sensing to actin-dependent Ras-cAMP-PKA regulation and apoptosis in yeast. J. Cell Sci. 122, 706-715.

Lefranc, F., Facchini, V., Kiss, R., 2007. Proautophagic drugs: A novel means to combat apoptosis-resistant cancers, with a special emphasis on Glioblastomas. Oncologist. 12, 1395-1403.

Lemasters, J.J., Nieminen, A.-L., Qian, T., Trost, L.C., Elmore, S.P., Nishimura, Y., Crowe, R.A., Cascio, W.E., Bradham, C.A., Brenner, D.A., Herman, B., 1998. The mitochondrial permeability transition in cell death: A common mechanism in necrosis, apoptosis and autophagy. Biochim. Et. Biophys. 1366, 177-196.

Leslie, J.F., Zeller, K.A., 1996. Heterokaryon incompatibility in fungi - more than just another way to die. J. Genet. 75, 415-424.

Levin, D.E., 2005. Cell wall integrity signaling in *Saccharomyces cerevisiae*. Microbiol. Mol. Biol. Rev. 69, 262-291.

Loubradou, G., Bégueret, J., Turcq, B., 1997. A mutation in an *HSP90* gene affects the sexual cycle and suppresses vegetative incompatibility in the fungus *Podospora anserina.* Genetics.

147, 581-588.

Loubradou, G., Bégueret, J., Turcq, B., 1999. MOD-D, a Gα subunit of the fungus *Podospora anserina*, is involved in both regulation of development and vegetative incompatibility. Genetics. 152, 519-528.

Loubradou, G., Turcq, B., 2000. Vegetative incompatibility in filamentous fungi: A roundabout way of understanding the phenomenon. Res. Microbiol. 151, 239-245.

Ma, J., Jin, R., Jia, X., Dobry, C.J., Wang, L., Reggiori, F., Zhu, J., Kumar, A., 2007. An interrelationship between autophagy and filamentous growth in budding yeast. Genetics. 177, 205-214.

Madeo, F., Frohlich, E., Ligr, M., Grey, M., Sigrist, S.J., Wolf, D.H., Frohlich, K.U., 1999. Oxygen stress: A regulator of apoptosis in yeast. J. Cell Biol. 145, 757-767.

Madrid, M., Soto, T., Khong, H.K., Franco, A., Vicente, J., Pėrez, P., Gacto, M., Cansado, J., 2006. Stress-induced response, localization, and regulation of the Pmk1 cell integrity pathway in *Schizosaccharomyces pombe*. J. Biol. Chem. 281, 2033-2043.

Mall, A.S., 2008. Analysis of mucins: Role in laboratory diagnosis. J. Clin. Pathol. 61, 1018-1024.

Marek, S.M., Wu, J., Glass, N.L., Gilchrist, D.G., Bostock, R.M., 2003. Nuclear DNA degradation during heterokaryon incompatibility in *Neurospora crassa*. Fungal Genet. Biol. 40, 126-137.

Matsuo, T., Otsubo, Y., Urano, J., Tamanoi, F., Yamamoto, M., 2007. Loss of the TOR kinase Tor2 mimics nitrogen starvation and activates the sexual development pathway in fission yeast. Mol. Cell. Biol. 27:3154–3164.

McDermott, K.M., Crocker, P.R., Harris, A., 2001. Overexpression of MUC1 reconfigures the binding properties of tumor cells. Int. J. Cancer. 94, 783-91.

Meijer, A.J., Codogno, P., 2004. Regulation and role of autophagy in mammalian cells. Int. J. Biochem. Cell Biol. 36, 2445-2462.

Meyer, V., Arentshorst, M., Flitter, S.J., Nitsche, B.M., Kwon, M.J., Reynaga-Peña, C.G., Bartnicki-Garcia, S., van den Hondel, C.A.M.J.J., Ram, A.F.J., 2009. Reconstruction of signaling networks regulating fungal morphogenesis by transcriptomics. Euk. Cell. 8, 1677-1691.

Muirhead, C.A., Glass, N.L., Slatkin, M., 2002. Multilocus self-recognition systems in fungi as a cause of trans-species polymorphism. Genet. 161, 633-641.

Nyathi, Y., Baker, A., 2006. Plant peroxisomes as a source of signalling molecules. Biochim Biophys Acta. 1763, 1478-1495.

Paglin, S., Lee, N.-Y., Nakar, C., Fitzgerald, M., Plotkin, J., Deuel, B., Hackett, N., McMahill, M., Sphicas, E., Lampen, N., Yahalomi, J., 2005. Rapamycin-sensitive pathway regulates mitochondrial membrane potential, autophagy, and survival in irradiated MCF-7 cells. Cancer Res. 65, 11061-11070.

Pál, K., van Diepeningen, A.D., Varga, J., Hoekstra, R.F., Dyer, P.S., Debets, A.J.M., 2007. Sexual and vegetative compatibility genes in the aspergilli. Stud. Mycol. 59, 19-30.

Pandey, A., Roca, M.G., Read, N.D., Glass, N.L., 2004. Role of a mitogen-activated protein kinase pathway during conidial germination and hyphal fusion in *Neurospora crassa*. Euk. Cell. 3, 348-358.

Paoletti, M., Castroviejo, M., Bégueret, J., Clavé, C., 2001. Identification and characterization of a gene encoding a subtilisin-like serine protease induced during vegetative incompatibility reaction in *Podospora anserina*. Curr. Genet. 39, 244-252.

Paoletti, M., Castroviejo, M., Bégueret, J., Clavé, C., 2007. Identification and characterization of a gene encoding a subtilisin-like serine protease induced during the vegetative the vegetative incompatibility reaction in *Podospora anserina*. Curr. Genet. 39, 244-252.

Paoletti, M., Clavé, C., 2007. The Fungus-Specific HET domain mediates programmed cell death in *Podospora anserina*. Euk. Cell. 6, 2001-2008.

Paoletti, M., Saupe, S.J., 2009. Fungal incompatibility: Evolutionary origin in pathogen defense? BioEssays. 31, 1201-1210.

Paoletti, M., Saupe, S.J., Clavé, C., 2007. Genesis of a fungal non-self recognition repertoire. Plos One. 3: e283.

Patil, C., Walter, P., 2001. Intracellular signaling from the endoplasmic reticulum to the nucleus: The unfolded protein response in yeast and mammals. Curr. Opin. Cell Biol. 13, 349-355.

Paul, M.F., Guerin, B., Velours, J., 1992. The C-terminal region of subunit 4 (subunit B) is essentail for assembly of the F_o portion of yeast mitochondrial ATP synthase. Eur. J. Biochem. 205, 163-172.

Pearson, G., Robinson, F., Gibson, T.B., Xu, B.-E., Karandika, R.M., Berman, K., Cobb, M.H., 2001. Mitogen-activated protein (MAP) kinase pathways: Regulation and physiological functions. Endocrine Rev. 22, 153-183.

Pereira, C., Camougrand, N., Manon, S., Sousa, M.J., Córte-Real, M., 2007. ADP/ATP carrier is required for mitochondrial outer membrane permeabilization and cytochrome c release in yeast apoptosis. Mol. Microbiol. 66, 571-582.

Perkins, D.D., 1988. Main features of vegetative incompatibility in *Neurospora*. Fungal Genet. Newsl. 35, 44-46.

Phillips, A. J., Crowe, J.D., Ramsdale, M., 2006. Ras pathway signaling accelerates programmed cell death in the pathogenic fungus Candida albicans. Proc. Natl. Acad. Sci. USA. 103, 726-731.

Pinan-Lucarré, B., Balguerie, A., Clavé, C., 2005 Accelerated cell death in *Podospora* autophagy mutants. Euk. Cell. 4, 1765-1774.

Pinan-Lucarré, B., Iraqui I., Clave, C., 2006. *Podospora anserina* target of rapamycin. Curr. Genet. 50, 23-31.

Pinan-Lucarré, B., Paoletti, M., Clavé, C., 2007. Cell death by incompatibility in the fungus *Podospora*. Sem. Cancer Biol. 17, 101-111.

Pinan-Lucarré, B., Paoletti, M., Dementhon, K., Coulary-Salin, B., Clave, C., 2003. Autophagy is induced during cell death by incompatibility and is essential for differentiation in the filamentous fungus *Podospora anserina.* Mol. Microbiol. 47, 321-333.

Pozniakovsky, A.I., Knorre, D.A., Markova. O.V., Hyman, A.A., Skulachev, V.P., Severin, F.F., 2005. Role of mitochondria in the pheromone- and amiodarone-induced programmed death of yeast. J. Cell Biol. 168, 257-269.

Rayner, A.D.M., 1991. The phytopathological significance of mycelial individualism Ann.Rev. Phytopath. 29, 305-323.

Robinson, M.J., Cobb, M.H., 1997. Mitogen-activated protein kinase pathways. Curr. Opin. Cell Biol. 9, 180-186.

Roca, M.G., Read, N.D., Wheals, A.E., 2005. Conidial anastomosis tubes in filamentous fungi. FEMS Microbiol. Lett. 249, 191-198.

Rodríguez-Enriquez, S., He, L., Lemasters, J., 2004. Role of mitochondrial permeability transition pores in mitochondrial autophagy. Int. J. Biochem. Cell Biol. 36, 2463-2472.

Rodríguez-Peňa, J.M., Pérez-Díaz, R.M., Alvarez, S., Bermejo, C., García, R., Santiago, C., Nombela, C., Arroyo, J., 2005. The 'yeast cell wall chip,' a tool to analyse the regulation of cell wall biogenesis in *Saccharomyces cerevisiae.* Microbiol. 151, 2241-2249.

Roux, P.P., Blenis, J., 2004. ERK and p38 MAPK-activated protein kinases: A family of protein kinases with diverse biological functions. Microbiol. Mol. Biol. Rev. 68, 320-344.

Sarkar, S., Iyer, G., Wu, J., Glass, N.L., 2002. Nonself recognition is mediated by *het-C* heterocomplex formation during vegetative incompatibility. EMBO J. 21, 4841-4850.

Saupe, S.J., 2000. Molecular genetics of heterokaryon incompatibility in filamentous ascomycetes. Microbiol. Mol. Biol Rev. 64, 489-502.

Saupe, S.J., Kuldau, G.A., Smith, M.L., Glass, N.L., 1996. The product of the *het-C* incompatibility gene of *Neurospora crassa* has characteristics of a glycine-rich cell wall protein. Genetics. 143, 1589-1600.

Saupe, S.J., Turcq, B., Bégueret, J., 1995. A gene responsible for vegetative incompatibility in the fungus *Podospora anserina* encodes a protein with a GTP-binding motif and Gβ homologous domain. Gene. 162,135-139.

Scherz-Shouval, R., Elazar, Z., 2007. ROS, mitochondria and the regulation of autophagy. Trends Cell Biol.17, 422 427.

Schmelzle, T., Beck, T., Martin, D.E., Hall, M.N., 2004. Activation of the RAS/Cyclic AMP pathway suppresses a TOR deficiency in yeast. Mol. Cell. Biol. 24, 338-351.

Schröder, M., Kaufman, R.J., 2005. ER stress and the unfolded protein response. Mutation Res. 569, 29-63.

Schubert, D., Raudaskoski, M., Knabe, N., Kothe, E., 2006. Ras GTPase-activating protein GAP1 of the homobasidiomycete *Schizophyllum commune* regulates hyphal growth orientation and sexual development. Euk. Cell. 5. 683-695.

Score, A.J., Palfreyman, J.W., White, N.A., 1997. Extracellular phenoloxidase and peroxidase enzyme production during interspecific fungal interactions. Internat. Biodeter. Biodegrad. 39, 225-233.

Sengupta, N., Vinod, P.K., Venkatesh, K.V., 2007. Crosstalk between cAMP-PKA and MAP kinase pathways is a key regulatory design necessary to regulate FLO11 expression. Biophys. Chem. 125, 59-71.

Severin, F.F., Hyman, A.A., 2002. Pheromone induces programmed cell death in *S. cerevisiae*. Curr. Biol. 12, R233-R235.

Shang, J., Wu, X., Lan, X., Fan, Y., Dong, H., Deng, Y., Nuss, D.L., Chen, B., 2008. Large-scale expressed sequence tag analysis for the chestnut blight fungus *Cryphonectria parasitica*. Fungal Genet. Biol. 45, 319-327.

Shinohara, M.L., Correa, A., Bell-Pedersen, D., Dunlap, J.C., Loros, J.J., 2002. *Neurospora* clock-controlled gene 9 (ccg-9) encodes trehalose synthase: Circadian regulation of stress responses and development. Euk. Cell. 1, 33-43.

Shiu, P.K.T., Glass, N.L., 1998. Molecular characterization of tol, a mediator of mating-type-associated vegetative incompatibility in *Neurospora crassa*. Genetics. 151, 545-555.

Silar, P., 2005. Peroxide accumulation and cell death in filamentous fungi induced by contact with a contestant. Mycol. Res. 109, 137-149.

Simonin, A.R., Rasmussen, C.G., Yang, M., Glass, N.L., 2010. Genes encoding a striatin-like protein (*ham*-3) and a forkhead associated protein (ham-4) are required for hyphal fusion in *Neurospora crassa*. Fungal Genet. Biol. 47, 855-868.

Smith, M.L., Micalli, O.C., Hubbard, S.P., Mir-Rashed, N., Jacobson, D.J., Glass, N.L., 2000. Vegetative incompatibility in the *het-6* region of *Neurospora crassa* is mediated by two linked genes. Genetics. 155, 1095-1104.

Stenlid, J., Vasiliauskas, R., 1998. Genetic diversity within and among vegetative compatibility groups of *Stereum sanguinolentum* determined by arbitrary primed PCR. Mol. Ecol. 7, 1265-1274.

Stiban, J., Caputo, L., Colombini, M., 2008. Ceramide synthesis in the endoplasmic reticulum can permeabilize mitochondria to proapoptotic proteins. J. Lipid Res. 49, 625-634.

Stone, E.M., Heun, P., Laroche, T., Pillus, L., Gasser, S.M., 2000. MAP kinase signaling induces nuclear reorganization in budding yeast. Curr. Biol. 10, 373-382.

Swanson, B.J., McDermott, K.M., Singh, P.K., Eggers, J.P., Crocker, P.R., Hollingsworth, M.A., 2007. MUC1 is a counter-receptor for myelin-associated glycoprotein (siglec-4a) and their interaction contributes to adhesion in pancreatic cancer perineural invasion. Cancer Res. 67, 10222-10229.

Szent-Gyorgyi, C., 1995. A bipartite operator interacts with a heat shock element to mediate early meiotic induction of *Saccharomyces cerevisiae* HSP82. Mol. Cell Biol. 15, 6754-6769.

Thaiville, M.M., Pan, Y.-X., Gjymishka, A., Zhong, C., Kaufman, R.J., Kilberg, M.S., 2008. MEK signalin is required for phosphorylation of eIF2α following amino acid limitation of HepG2 human hepatoma cells. J. Biol. Chem. 283, 10848-10857.

Van der Nest, M.A., Slippers, B., Steenkamp, E.T., De Vos, L., Van Zyl, K., Stenlid, J., Wingfield, M.J., Wingfield, B.D., 2009. Genetic linkage map for *Amylostereum arolatum* reveals an association between vegetative growth and sexual and self recognition. Fungal Genet. Biol. 46, 632-641.

Van der Nest, M.A., Slippers, B., Stenlid, J., Wilken, P.M., Vasaitis, R., Wingfield, M.J., Wingfield, B.D., 2008. Characterization of the systems governing sexual and self-recognition in the white rot Agaricomycete *Amylostereum areolatum*. Curr. Genet. 53, 323-336.

Verstrepen, K.J., Klis, F.M., 2006. Flocculation, adhesion and biofilm formation in yeasts. Mol. Microbiol. 60, 5-15.

Villar-Tajadura, M., Coll, P.M., Madrid, M., Cansado, J., Santos, B., Pérez, P., 2008. Rga2 is a Rho GAP that regulates morphogenesis and cell integrity in *S. pompe*. Mol. Microbiol. 70, 867-881.

Vinod, P.K., Sengupta, N., Bhat, P.J., Venkatesh, K.V., 2008. Integration of global signaling pathways, cAMP-PKA, MAPK and TOR in the regulation of FLO11. Plos One, e1663.

Wesseling, J., van der Valk, S.W., Hilkens, J., 1996. A mechanism for inhibition of E-cadherin-mediated cell-cell adhesion by the membrane-associated mucin episialin/MUC1. Mol. Biol. Cell. 7, 565-77.

Wesseling, J., van der Valk, S.W., Vos, H.L., Sonnenberg, A., Hilkens, J., 1995. Episialin (MUC1) overexpression inhibits integrin-mediated cell adhesion to extracellular matrix components. J. Cell Biol. 129, 255-265.

West, G., Viitanen, L., Alm, C., Mattjus, P., Salminen, T.A., Edqvist, J., 2008. Identification of a glycosphingolipid transfer protein GLTP1 in *Arabidopsis thaliana*. FEBS J. 275, 3421-3437.

Williamson, P.R., 1997. Laccase and melanin in the pathogenesis of *Cryptococcus neoformans*. Front. Biosci. 2, e99-107.

Wolanin, P.M., Thomason, P.A., Stock, J.B., 2002. Histidine protein kinase: Key signal transducers outside the animal kingdom. Genome Biol. 3, 3013.1.

Worral, J.J., 1997. Somatic incompatibility in basidiomycetes. Mycol. 89, 24-36.

Wullschleger, R., Hall, M. N., 2006. TOR Signaling in Growth and Metabolism. Cell 124, 471-484. Wennerberg, K., Rossman, K.L., Der, C.J., 2005. The ras superfamily at a glance. J. Cell Sci. 118, 843-846.

Xiang, Q., Glass, N.L., 2004. The control of mating type heterokaryon incompatibility by *vib-1*, a locus involved in *het-c* heterokaryon incompatibility in *Neurospora crassa*. Genetics. 162, 89-101.

Zeilinger, S., Omann, M., 2007. *Trichoderma* biocontrol: Signal transduction pathways involved in host sensing and mycoparasitism. Gene Reg. Syst. Biol. 1, 227-234.

Zhang, Q., Chieu, H.K., Low, C.P., Zhang, S., Heng, C.K., Yang, H,. 2003. *Schizosaccharomyces pombe* cells deficient in triacylglycerols synthesis undergo apoptosis upon entry into the stationary phase. J. Biol. Chem. 278, 47145-47155.

FIGURES

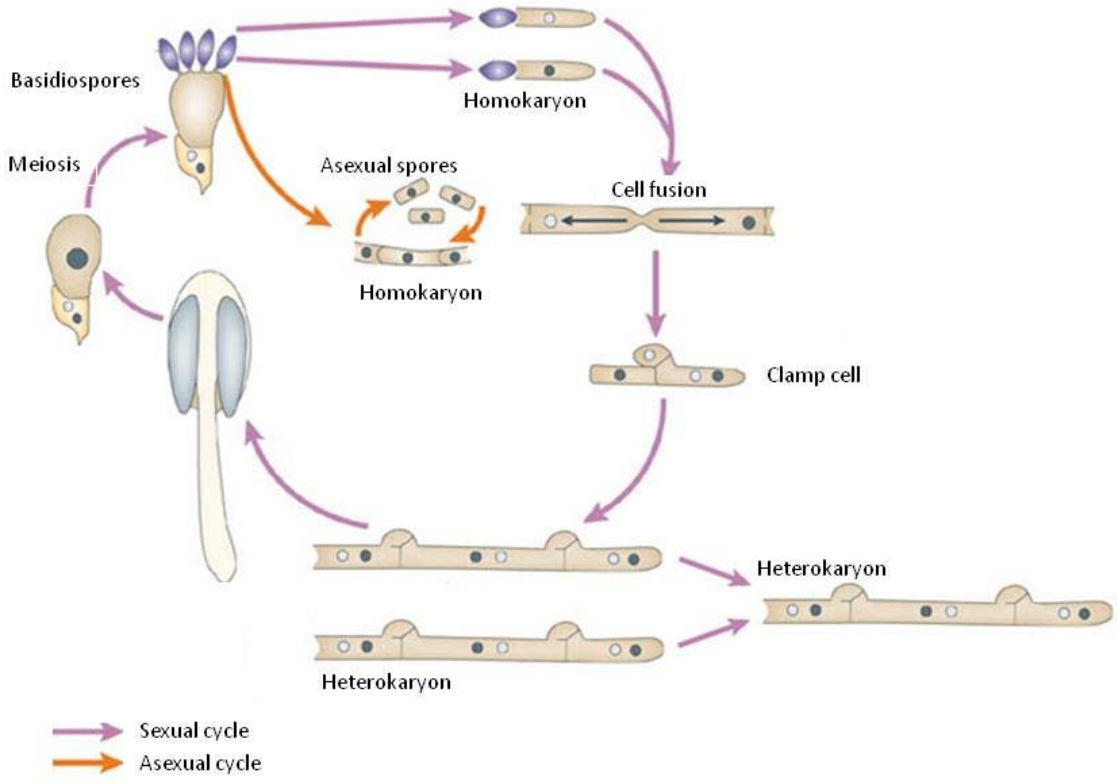

Figure 1. A typical basidiomycete life-cycle consists of a short homokaryotic phase followed by a predominant fertile heterokaryotic phase (Kothe et al., 2003). Figure adapted from Casselton and Zolan (2002).

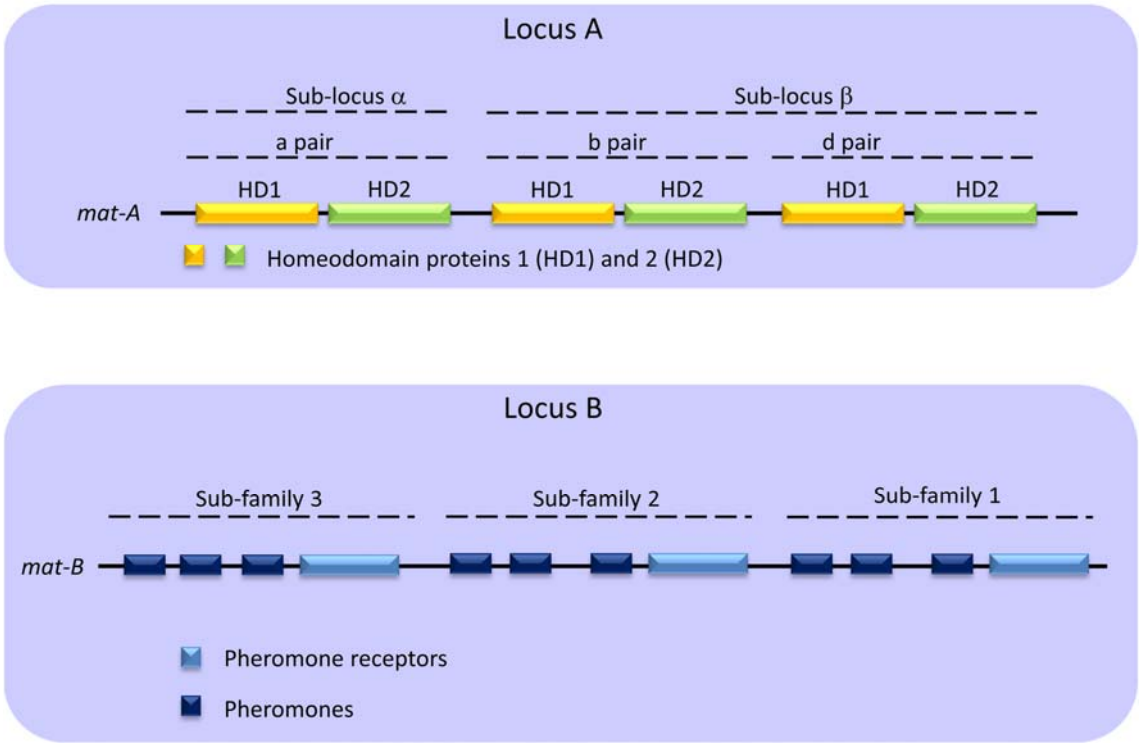

Figure 2. The genes located at the *mat-A* locus of basidiomycetes encode homeodomain proteins, while the genes present at the *mat-B* locus encode pheromones and pheromone receptors (Kronstad and Staben, 1997; Casselton and Olesnicky, 1998; Casselton, 2002).

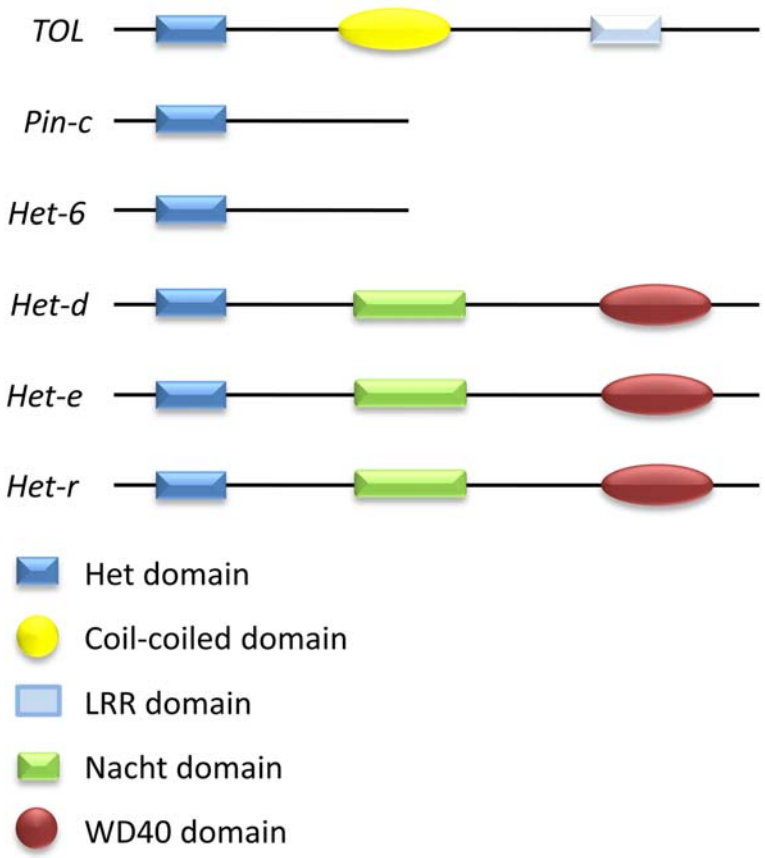

Figure 3. The *het* domain is found in *N. crassa het-6*, *pin-C* and *TOL* and in *P. anserina het-d* and *het-e*, and so appears to be critical for the activation of PCD. The HET domains in the case of *het-d* and *het-e* are followed by a NACHT domain and multiple WD repeats, while *TOR* contains a coiled-coil domain and LRR repeats. The *het-D* and *het-E* genes are paralogues and belong to the *NWD* gene familythat share a central NACHT domain and a C-terminal WD repeat domain. Within this family, five members, including *het-D* and *het-E*, also encode an N-terminal HET domain and are named *HNWD* genes (Glass and Dementhon, 2006; Pinan-Lucarré et al., 2007; Paoletti et al., 2007).

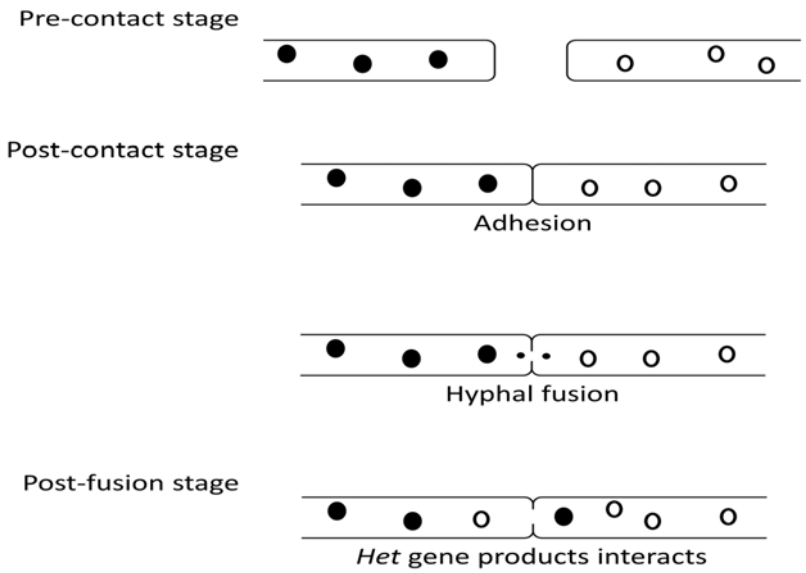

Figure 4. Flow diagram of the major steps in vegetative hyphal fusion taken from (Figure is adapted from Glass et al., 2000, 2004).

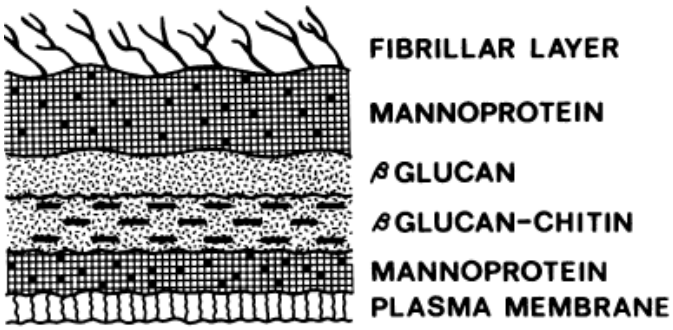

Figure 5. A schematic representation of a fungal cell wall taken from Fukazawa and Kagaya (1997). The hyphal the cell wall represents a complex macromolecule that generally consist of polysaccharides that include glucans, chitin and mannans, as well as various proteins and lipids (Fukazawa and Kagaya, 1997; Smits et al., 2001; Lesage et al., 2004; Coronado et al., 2007).

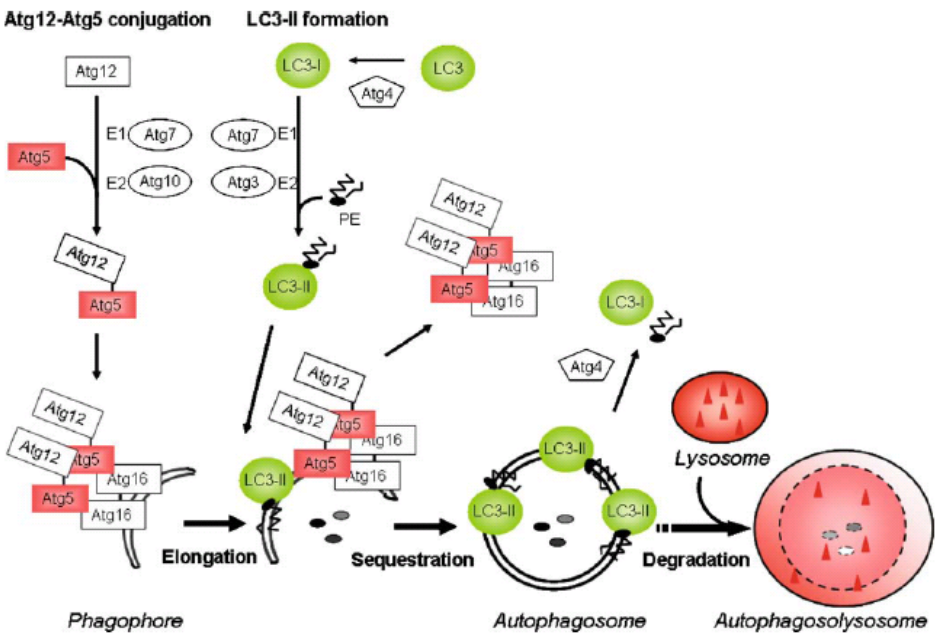

Figure 6. Schematic representation of autophagosome formation. In yeast autophagosome formation involved the function of several proteins refered to ATG proteins. Figure taken from Hamacher-Brady et al. (2006).

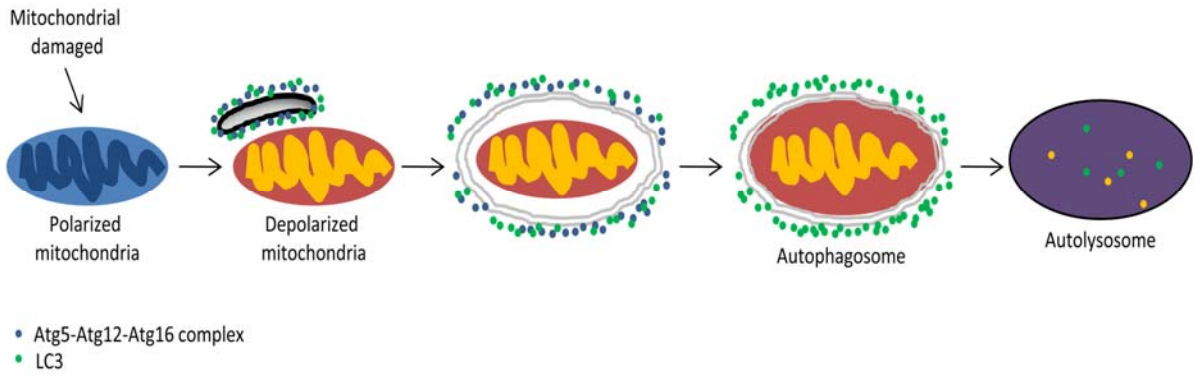

Figure 7. MPT (mitochondrial outer membrane permeability transition) can trigger autophagy as MPT causes mitochondrial functional failure that is accompanied by depolarization of the mitochondrial membrane and it is depolarized mitochondria that are targeted for autophagy (Rodríguez-Enriquez et al., 2004; Kim et al., 2007).

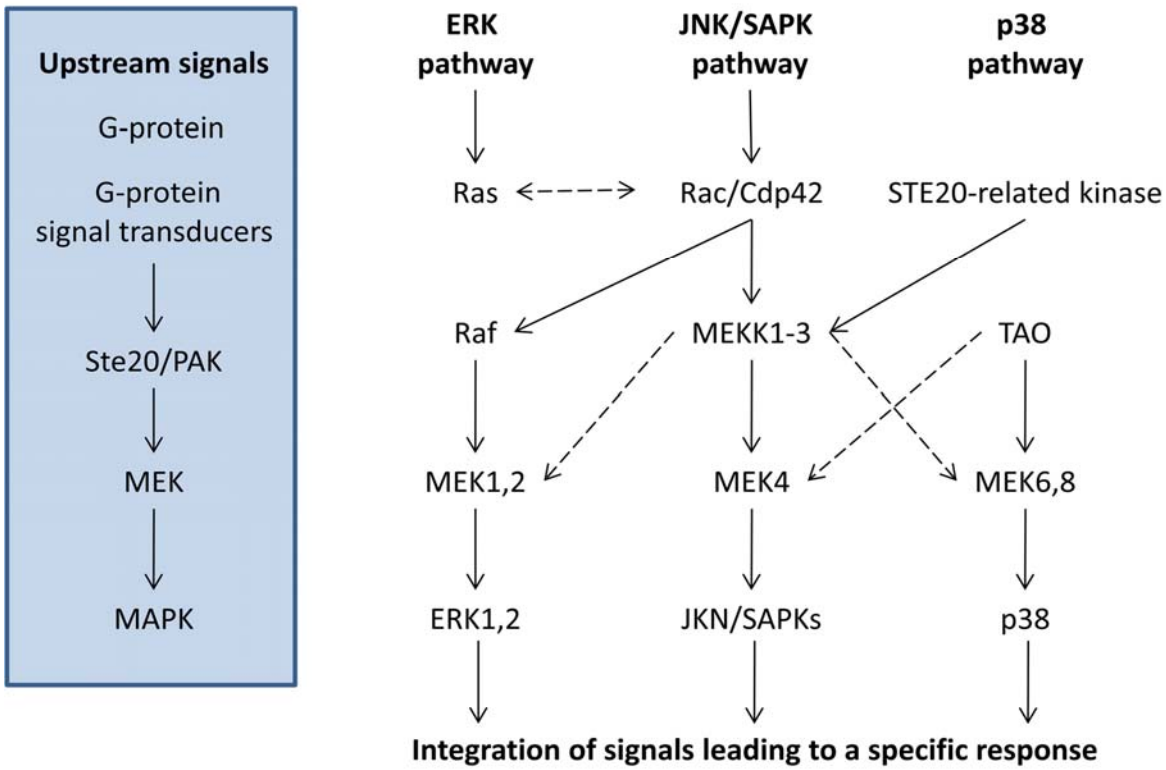

Figure 8. Schematic diagram of the currently known mammalian MAPK pathways, Dotted arrows represent connections between pathways that are known to exist but for which not enough supporting data are available (Cui et al., 2007).

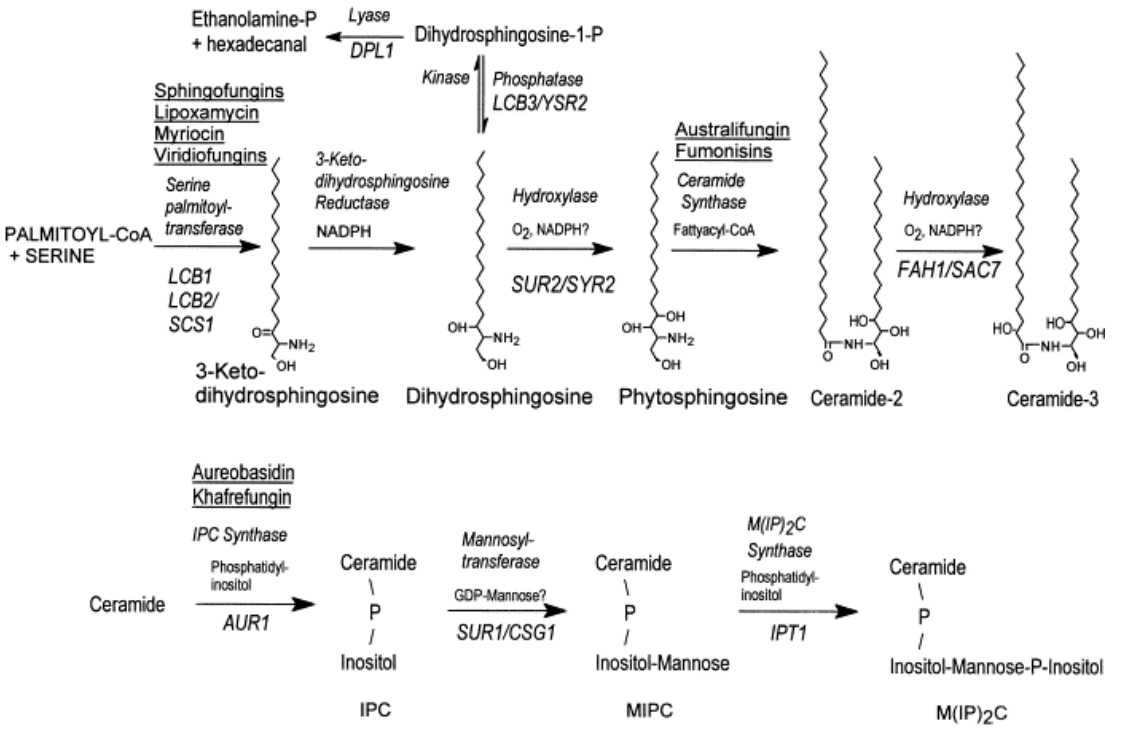

Figure 9. Sphingolipid biosynthetic pathway in *Saccharomyces cerevisiae* (Dickson and Lester, 1999).

TABLES

Table 1. The *Neuropora crassa* and *P. anserina het* genes characterized at the DNA level.

Gene	Class of gene	Nature of the protein and its functional motifs	Other cellular function	References
Neurospora crassa:				
***mat* A-1**	Allelic *het* gene	Mating-type transcriptional regulator; α-domain	Mating	Glass et al., 1990
***mat* a-1**	Allelic *het* gene	Mating-type transcriptional regulator; HMG box	Mating	Staben and Yanofsky, 1990
het-c	Allelic *het* gene	Signal peptide, variable domain, glycine-rich region	None	Saupe et al., 1996, Saupe et al., 1997
un-24	Nonallelic *het* gene	Ribonucleotide reductase, allosteric activity site, variable domain	DNA synthesis	Smith et al., 2000
het-6	Nonallelic *het* gene	Region with similarity to TOL and HET-E	None	Smith et al., 2000
Podospora anserina:				
het-s	Allelic *het* gene	Prion analog; single amino acid differences alters allelic specificity	None	Coustou et al., 1997, Turcq et al., 1991
het-e	Nonallelic *het* gene	GTP-binding domain, WD repeat, region with similarity to TOL and HET-6	None	Saupe et al., 1995
het-d	Nonallelic *het* gene	GTP-binding domain, WD repeat, region with similarity to TOL and HET-6	None	Espagne et al., 2002
het-c	Nonallelic het gene	Glycolipid transfer protein; amphipathic α-helix, single amino acid differences alters allelic specificity	Ascospore formation	Saupe et al., 1994
het-r	Nonallelic het gene	GTP-binding domain, WD repeat, region with similarity to TOL and HET-6	None	Chevanne et al., 2009

Table 2. Temperature-sensitive lethality of the SI strains in *Podospora anserina* has been used to identify *i*nduced *d*uring *i*ncompatibility (*idi*) genes and the *mod* (for *mod*ifier) genes.

Type	Gene	Connection with incompatibility	Protein Feature	References
Neurospora crassa:				
Suppressor	*tol*	Suppress mating-type-associated incompatibility	Leucine-rich repeats	Shiu and Glass, 1998
	vib-1	Suppression of *het-C*. Partial suppression of *het-e* and *het-8*	Transcriptional regulator	Xiang and Glass, 2004
Podospora anserine:				
Suppressor	*Mod-A*	Suppress all non-allelic incompatibility	SH3-binding domain	Barreau et al., 1998
	Mod-B	With *Mod-A* Suppress all non-allelic incompatibility	Paralogous to *Mod-A*	Labarère and Bégueret, 1974
	Mod-C	Suppression of *het-R* and *het-V*	Unknown	Labarère and Bégueret, 1979
	Mod-D	Partial suppression of *het-C* and *het-E*	Gα-subunit	Loubradou et al., 1999
	Mod-E	Partial suppression of *het-R* and *het-V*	HSP90	Loubradou et al., 1997
	Mod-F	Suppression of *het-R* and *het-V*	Unknown	Durrens, 1984
Inducer				
	idi-1	Induced by nonallelic incompatibility	Cell wall proteins	Bourges et al., 1998
	idi-2	Induced by *het-R*/*het-V*	Cell wall proteins	Bourges et al., 1998
	idi-3	Induced by nonallelic incompatibility	Cell wall proteins	Bourges et al., 1998
	idi-4	Induced by *het-R*/*het-V*	bZIP transcription factor	Dementhon et al., 2004
	idi-6	Induced by nonallelic incompatibility	Serine protease	Paoletti et al., 2001
	idi-7	Induced by *het-c*/*het-e* and induced by *het-R*/*het-V*	PSPA protease	Pinan-Lucarré et al., 2003

CHAPTER 2

Genetics of *Amylostereum* species associated with Siricidae woodwasps

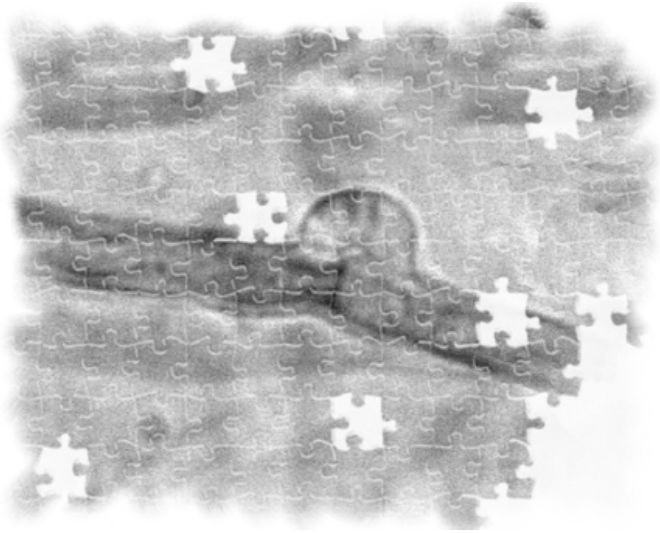

TABLE OF CONTENTS

Field Code Changed

INTRODUCTION

Amylostereum areolatum (Basidiomycotina) lives in an obligate mutualistic symbiosis with various Siricidae woodwasps, including *Sirex noctilio* (Hymenoptera: Siricidae) (Morgan, 1968; Slippers et al., 1998, 2003). The *A. areolatum* - *S. noctilio* complex is native to Eurasia and North Africa (Morgan, 1968; Spradbery and Kirk, 1978). During the last 100 years it has been introduced into New Zealand (1900) (Miller and Clarke, 1935), Australia (1952) (Gilbert and Miller, 1952), Uruguay (1980) (Maderni, 1998), Argentina (1985) (Klasmer et al., 1998), Brazil (1988) (Iede et al., 1998), South Africa (1994) (Tribe, 1995), Chile (2000) (Ahumada, 2002) and most recently into the North America (2004) (Hoebeke et al., 2005; Wilson et al., 2009). The wasp/fungus complex poses no substantial economic threat in native environments, but it represents one of the most serious sources of damage to pine-based forestry in countries where it has been introduced (Carnegie et al., 2005, Hurley et al., 2007). For example, losses due to this pest complex in South Africa have been estimated to amount to approximately R300 million ($45 million) in one region of the country during an outbreak year (Hurley et al., 2007).

Amylostereum areolatum is considered a weak pathogen of many of *Pinus* spp., but the action of the fungus and the woodwasp collectively, can kill the host tree (Coutts and Dolezal, 1969; Fong and Crowden, 1973; Madden, 1981). Female wasps actively seek weakened and stressed trees to lay their eggs. Together with *A. areolatum* spores, the wasps produce mucus that further reduces the resistance of the host tree, enabling the fungus to establish and eventually cause a dry white rot in the wood, which disrupts the vascular system of the host. The larvae of the wasp spend 1 to 3 years in the tree boring tunnels as they feed, but this damage is limited and does not contribute markedly to tree death.

In countries were *S. noctilio* and its fungal symbiont have been introduced the nematode *Deladenus* (= *Beddingia*) *siricidicola* is used as the primary control agent (Bedding, 1995; Haugen, 1990; Hurley et al., 2007). The nematode sterilizes the female wasps during a parasitic phase of its life cycle when its juveniles enter the eggs of the wasp. During a second, mycetophagous phase of the *D. siricidicola* life cycle it feeds on *A. areolatum*. This latter phase of the life-cycle is exploited to mass-rear the fungus for biocontrol purposes (Bedding, 1995). The fungus is consequently a critical factor in understanding the biology of the nematode, and in control programs to reduce the impact of the wasp.

The success of biological control programs vary significantly in different regions (Bedding, 1995; Hurley et al., 2008). Despite years of research, the reasons for the variable levels of success in control programs are poorly understood (Hurley et al. 2007, 2008). As a consequence, the pest complex continues to spread to previously unaffected areas and still kills significant numbers of trees in many areas (Hoebeke et al., 2005, Hurley et al., 2007).

A thorough understanding of the biology of *A. areolatum* is required in order to understand the factors that affect the mutualism as a whole, as well as from the perspective of developing control strategies. In recent years, various molecular tools have been applied to study the phylogeny, population genetics and genomics of *Amylostereum* spp., and in particular for *A. areolatum*. The aim of this chapter is to review these recent studies and consider how they have influenced the understanding of the systematic, ecology and evolution as well as control of the fungus and its woodwasp host.

SYSTEMATICS AND IDENTIFICATION

Based on morphological similarities of the sexual fruiting structures and vegetative mycelia *Amylostereum* has historically been linked to *Stereum* and later *Peniophora* (Boidin and Lanquetin, 1984, Slippers et al., 2003). However, phylogenetic studies have revealed a relationship between *Amylostereum* spp. and *Echinodontium, Russula, Heterobasidion* and *Bondarzewia* in addition to *Peniophora* and *Stereum* spp. (Hsiau, 1996; Hibbett et al., 1997; Slippers et al., 2002; Maijala et al., 2003). Subsequent phylogenetic studies based on sequence data for the nuclear and mitochondrial ribosomal RNA internal transcribed spacer (nuc-ITS) and 16S small subunit gene (mtSSU) demonstrated that the genus *Amylostereum* is more closely related to *Echinodontium tinctorium* than to other fungi (Tabata et al., 2000; Maijala et al., 2003; Miller et al., 2006). *Amylostereum* and *Echinodontium* species also share micro-morphological characteristics, such as their amyloid basidiospores and thick-walled and heavily encrusted cystidia. These genera are currently both accommodated in the family Echinodontiaceae (Slippers et al., 2003). However, the exact phylogenetic relationship of *Amylostereum* spp. and their relatives are still largely unresolved (Miller et al., 2006).

The genus *Amylostereum* includes four species, namely the type species *A. chailletii* (Pers.:Fr.) Boid. (= *Stereum chailletii*), *A. areolatum* (Fr.) Boid. (= *S. areolatum*), *A. laevigatum* (Fr.) Boid (=*Peniophora laevigata*) and *A. ferreum* (Berk. & Curt.) Boid. & Lanq. (= *S. ferreum*). All of these species have smooth amyloid basidiospores, hyaline-encrusted

cystidia, and resupinate to effuso-reflexed fruiting bodies (Boidin, 1958). These species can be distinguished based on morphology of the sexual fruiting structures, using characters such asthe spore size and the colour and texture of the basidiocarps (Thomsen, 1998). However, an important limitation of this approach is that basidiocarps of these fungi are rarely found in nature and in some areas, such as in the southern hemisphere, they have never been observed (Slippers et al., 2003, Slippers, personal communication). For this reason, the identification of *Amylostereum* spp. has in the past also been done based on morphology in culture (e.g., mono- or dimyctic hyphae and the formation of arthrospores) or asexual spores found in the mycangia of the woodwasp (Thomsen, 1996; Slippers et al., 2003). These characters, however, have limited variation and substantial experience is required to apply them accurately.

The phylogenetic relationship amongst species of *Amylostereum* was first determined using mating experiments and the Buller phenomenon (Boidin and Lanquetin, 1984). *Amylostereum areolatum* was not compatible with any of the other species, and was thus considered to be the most divergent species in the genus, despite its similarity to *A. chailletii*. *Amylostereum laevigatum* and *A. chailletii* were considered to be both more closely related to *A. ferreum* than to each other, as *A. chailletii* and *A. laevigatum* were completely incompatible while they were both partially compatible with *A. ferreum*. These relationships were later confirmed using comparisons of sequence data for the nuclear ribosomal ITS and intergenic spacer (IGS) regions, mtSSU and the partial manganese-dependent peroxidase gene. These studies also showed that *A. ferreum* and *A. laevigatum* were more closely related to each other, than to *A. chailletii* and *A. areolatum* (Vasiliauskas et al., 1999; Slippers et al., 2000, 2002; Tabata et al., 2000; Nielsen et al., 2009). Sequence data for the IGS region could consequently be used to develop a rapid and accurate PCR-RFLP method to distinguish between the species of *Amylostereum* (Slippers et al., 2002).

SYMBIOTIC SPECIFICITY

The results of DNA sequence comparisons have confirmed previous reports that specific Siricid species always carry the same *Amylostereum* species, *i.e.*, the association between the fungus and woodwasp appear to be specific for the wasp host (Tabata and Abe, 1997, 1999; Slippers et al., 2003; Slippers et al., unpublished). Recent work on the Xyphydridae, a genus of woodwasps closely related to *S. noctilio* that infests hardwoods, has shown that a species

of these wasps can be associated with more than one *Daldinia* spp. (Paźoutavá et al., 2010). For example, while a single *Daldinia* spp. normally dominated the association with a specific *Xyphidria* spp. (e.g., *X. longicollis* associated with *D. childiae*), a small number of isolates associated with different symbiont species (e.g., *X. camelus* associated with *D. decipiens* and *D. petriniae*). This was observed in a study of fungal associates of a large number of wasps (n = 1389), using molecular identification (using Inter Simple Sequence Repeats, ISSRs). Such large scale studies have not been done for Siricidae and this begs the question as to whether the current views regarding the symbiont specificity in the Siricidae group are not based on inordinately few samples and incorrect identifications. Also, studies of smaller numbers of wasps would possibly have overlooked these rare cases of symbiont switching.

It is believed that transmission of *Amylostereum* is uniparental and vertical between host generations, *i.e.*, offspring obtain the fungal mutualist directly from the female parent. Strict vertical transmission of the symbiont would, however, predict a tight pattern of co-evolution of species of the fungus and wasp. On the contrary, however, one *Amylostereum* species can be carried by more than one wasp species and even different wasp genera. For example, *A. areolatum* is the symbiont of *S. noctilio*, *S. juvencus* Linn., *S. nitobei* Mats., while *A. chailletii* is carried by *S. cyaneus* Fabr., *S. imperialis* Kirby., *S. areolatus* Cress., *S. californicus* Nort., *Urocerus gigas* Linn., *U. augur augur* Klug. and *U. augur sah* Mocs. (Gaut, 1969, 1970; Tabata, 2000; Slippers et al., 2003). These patters suggest that there is not a strict co-evolution of species. Rather that historically, species of *Amyostereum* have been exchanged horizontally between the different species and genera of the Siricidae.

Nielsen et al (2009) found identical genotypes of *A. areolatum* associated with *S. noctilio* and *S. edwardsii*, which was thought to carry *A. chailletii*, when they emerged from the same logs. Identical genotypes of *A. areolatum* have also been shown to be associated with *S. juvencus* and *S. noctilio* (Slippers, Stenlid and Vasaitis, unpublished). The latter authors have also found identical genotypes of *A. chailletii* to occur between *U. augar* and *U. gigas*. These results suggest that horizontal transmission of fungal genotypes between wasp generations, and even species, might occur fairly commonly, given that none of the studies considered particularly large numbers of specimens. Larger sample sizes from local populations containing different wasp species are needed to clarify the question of how frequently horizontal transmission of fungal genotypes occur between different wasp generations and different species.

Amylostereum laevigatum occurs throughout Europe, but is not known to be associated with woodwasps in this region. In Japan, *A. laevigatum* has, however, been shown to be associated with *U. japonicas* and *U. antennatus* (Tabata and Abe, 1997, 1999). *Amylostereum ferreum* is not known to be associated with any woodwasps.

MODE OF REPRODUCTION

Typical of a basidiomycete fungus, *Amylostereum* spp. has a life cycle consisting of a short homokaryotic phase (*i.e.*, that contain hyphae with a single genetically distinct nucleus per cell), followed by a predominant heterokaryotic phase (*i.e.*, that contain hyphae with more than one genetically distinct nucleus per cell) (Kües, 2000). The fertile heterokaryotic phase arises when the hyphae of two sexually compatible homokaryons fuse (mate). Karyogamy (nuclear fusion) and meiosis only occurs later within specialized cells of the basidiocarp. This temporal and spatial separation of hyphal fusion and karyogamy is unique to *A. areolatum* and other Basidiomycetes.

Amylostereum basidiocarps are typically resupinate and smooth macroscopically (Boidin, 1958; Thomsen, 1996). The fruiting structures appear infrequently and in unique distribution patterns for each of the species. Basidiocarps of *A. chailletii* are, for example, more common than *A. laevigatum* and *A. areolatum* in Europe (Vasiliauskas and Stenlid 1999; Slippers et al. 2003; Slippers, Vasaitis and Stenlid, personal observation). Fruiting bodies of *A. areolatum* are much rarer and geographically restricted, occurring most frequently in central parts of Europe (Thomsen, 1996; Solheim 2006; Slippers, Vasaitis and Stenlid, personal observation). The fruiting structures of the latter species have never been reported from North America, the Southern Hemisphere or Asia, where it is known to occur (Slippers et al. 2003; Nielsen et al. 2009). This is despite the fact that *A. areolatum* isolates from the Southern Hemisphere has been shown to be able to fruit in the laboratory (Talbot, 1977). The patterns of fruiting of *A. laevigatum* are less well documented, but are known to be rare.

Amylostereum areolatum is a heterothallic basidiomycete that has a tetrapolar mating system. In this mating system the alleles present on two unlinked mating type (*mat*) loci (*mat-A* and *mat-B*) have to be different for two homokaryons to be sexually compatible (Boidin and Lanquetin, 1984; van der Nest et al., 2008, 2009). The *mat-A* locus harbours genes that encode homeodomain transcriptional factors, while the *mat-B* locus harbours genes that encode pheromones and pheromone receptors that controls separate but

complementary pathways involved in this process (Casselton, 2002). At present, only a gene encoding a putative pheromone receptor (*RAB1*) at the *mat-B* locus and a gene encoding a mitochondrial intermediate peptidase (*MIP*), that is closely linked to the *mat-A* locus, have been identified for *A. areolatum* (van der Nest et al., 2008). Future studies could use this information to obtain a larger portion of the *mat* loci, as well as to investigate the structure and evolution of these loci.

The *mat* loci of basidiomycete fungi that have a tetrapolar mating system are usually multiallelic (Kothe et al., 1999, 2003; Schirawski et al., 2005; James et al., 2006). This is also true for the *mat* loci of *A. areolatum* (van der Nest et al., 2008, 2009). Despite of the unique life history of the mutualistic association with the woodwasps, these latter studies have shown that the *mat* loci of this fungus appear to be subject to similar evolutionary forces than those acting on the recognition loci of other eukaryotes (van der Nest et al., 2008, 2009). These forces may include balancing selection and the selection for rare alleles, as well suppressed recombination that keep these loci polymorphic (Awadalla and Charlesworth, 1999; May et al., 1999; van der Nest et al., 2009).

Amylostereum areolatum can also reproduce asexually through vegetative mycelium that fragments into oidia or arthrospores. This mode of reproduction is associated with the symbiosis between *Amylostereum* and Siricidae woodwasps. Asexual spores of the fungus that is carried in a specialized mycangium of the female wasp (present near the base of the ovipositor) is inoculated into the wood during oviposition (Coutts, 1969; Coutts and Dolezal, 1969; Madden, 1981). This ensures that not only the same species, but the same genotype of the fungus is transmitted between generations. Such clonal, vertical transmission of a symbiont between host generations is common in mutualistic systems and is thought to help align the reproductive interests of the different partners (Herre et al., 1999). As has been shown in other mutualistic systems, and is discussed above, a certain level of horizontal acquisition of the symbiont (either from asexually or sexually produced lineages) appears to also be occurring.

VEGETATIVE INCOMPATIBILITY AND POPULATION DIVERSITY STUDIES

A self/non-self rejection mechanism known as somatic or vegetative incompatibility that distinguishes individual genotypes from one another has been widely used to differentiate

genotypes of *A. areolatum* and *A. chailletii* (Vasiliauskas et al., 1998; Thomsen and Koch, 1999; Vasiliauskas and Stenlid, 1999, Slippers et al., 2001). Fungal isolates, including *Amylostereum* spp., are considered to be vegetatively compatible if their interacting hyphae are able to merge (anastomose) and intermingle, while isolates are considered incompatible if cell death prevents hyphal anastomosis from persisting. The latter process is usually characterized by the formation of a zone of sparse growth of aerial hyphae between the interacting heterokaryons (Thomsen and Koch, 1999; Worrall, 1997, van der Nest, 2008).

Heterokaryons of basidiomycete fungi are vegetatively compatible if they are genetically similar and share identical alleles at all of their *het* loci (Table 1), while they are vegetatively incompatible if they are genetically different and have different alleles at some or all of their *het* loci (Rayner, 1991; Worrall, 1997). *Amylostereum areolatum* has a relatively low number of *het* loci (at least two) (van der Nest et al., 2008), which is similar to the number of *het* loci present in other homobasidiomycetes. For example, *Phellinus weirii* has a single *het* locus, *Serpula lacrymans* has two *het* loci and *Heterobasidion annosum* has three to four *het* loci (Hansen et al., 1994; Kauserud et al., 2006; Lind et al., 2007). The two *het* loci identified in *A. areolatum* appear to be multi-allelic, similar to the other homobasidiomycetes mentioned above (Stenlid and Vasiliauskas, 1998; Lind et al., 2007).

It was suggested and shown that the limited number of *het* loci in *Amylostereum* spp. may limit the ability of vegetative compatibility group (VCG) assays to distinguish between genetically different individuals, which would lead to an underestimation of the genetic diversity. This is despite the fact that in some cases different genets with identical DNA fingerprinting profiles have been distinguished using VCGs in the past (one case in *A. areolatum*, and two cases in *A. chailletii*) (Vasiliauskas et al., 1998; Kauserud, 2004; van der Nest et al., 2008). It is also important to remember that VCG assays are not selectively neutral and should therefore ideally be used in combination with selectively neutral genetic markers (e.g. neutral DNA based markers) (van der Nest et al., 2008). In the past this has been achieved in *A. areolatum* and *A. chailletii* by combining data from VCGs and DNA fingerprinting using the M13 core sequence as a primer, restriction fragment length polymorphism (RFLP) and DNA sequencing data (Vasiliauskas et al,. 1998; Thomsen and Koch, 1999; Vasiliauskas and Stenlid, 1999; Slippers et al., 2001).

VCGs, DNA sequencing and DNA fingerprinting studies of *A. areolatum* have shown the presence of large clonal populations that persist over time and space (Vasiliauskas et al., 1998; Thomsen and Koch, 1999; Vasiliauskas and Stenlid, 1999; Slippers et al., 2001). For

example, *A. areolatum* isolates that belong to the same VCG were isolated from Denmark, Sweden and Lithuania (Thomsen and Koch, 1999). This pattern differs from the diversity observed in central parts of Europe (Austria and the Czech Republic), where 55 isolates from wood represented 50 distinct VCGs (Slippers, Kirisits and Vasaitis, unpublished data). These patterns of diversity correlate with levels of sexual sporulation of the fungus, which is fairly common in central Europe and rare in Scandinavia (as discussed above). These results suggest that genotypic diversity is likely to be strongly influenced by the ability of the fungus to reproduce and spread sexually in an area, or predominantly asexually via the wasp in areas where it fruits less successfully.

An even more extreme example of the presence of clonal territorial lineages is that *A. areolatum* isolates from Brazil, Uruguay and South Africa belong to the same VCG, while isolates from New Zealand and Tasmania were partially vegetatively compatible (Slippers et al., 2001).The genetic similarity of these populations was confirmed as *A. areolatum* isolates from South Africa, Brazil, New Zealand and Tasmania contained the same heterogenic combination of sequences for the IGS region (Slippers et al., 2001). These data indicate that the pest complex was most likely introduced into the Southern Hemisphere only once or a limited number of times from the same origin, after which they spread between countries in the Southern Hemisphere (Slippers et al., 2001, 2002).

Clonal lineages (groups of isolates with identical VCG and DNA fingerprinting profiles) are also present in *A. chailletii*, but to a much smaller degree than in *A. areolatum* (Vasiliauskas et al., 1998). The proportion of compatible isolates of *A. chailletii* was significantly lower than those of *A. areolatum* from Sweden and Lithuania indicating that *A. chailletii* spread less frequently through asexual spores than *A. areolatum* in this region (Vasiliauskas et al., 1998). In fact, the population structure of *A. chailletii* in these regions is similar to that of natural populations of other airborne wood decaying basidiomycetes that are not associated with insects (Stenlid et al., 1994; Högberg and Stenlid, 1994; Vasiliauskas et al., 1998). Not only are there fewer clonal lineages present in *A. chailletii,* but clonal lineages are also not as widely distributed as those of *A. areolatum*. For example, in Denmark compatible isolates of *A. chailletii* were never separated by more than 75 km (Thomsen, 1996; Vasiliauskas et al., 1998). These findings are in accordance with the fact that the basidiocarps of *A. chailletii* in nature are more commonly observed in Scandinavia than those of *A. areolatum* (Thomsen, 1998).

CONCLUSIONS AND FUTURE PROSPECTS

Molecular DNA studies during the last decade have significantly informed our understanding of the relationships of *Amylostereum* spp. to each other, and to other Basidiomycetes. However, to determine the exact phylogenetic relationship of *Amylostereum* spp. and their relatives, multi-gene phylogenies that included all the representative taxa is needed. Molecular DNA studies have also given us the ability to accurately identify the different species in the genus. These studies have shown that there is at least one undescribed species of *Amylostereum* in North America.

The ability to accurately identify *Amylostereum* spp. and genotypes using DNA based studies has increased our knowledge regarding the co-evolution between the wasp and the fungus.For example, the identity of a number of Amylostereum spp. associated with specific wasp species could be accurately determined. These data confirmed that the same fungal species, and even genotype, can be carried by more than one wasp species and genus, suggesting that horizontal exchange of the fungal symbiont occurs between host species. It is thus possible that previous conclusions about the specificity of the wasp and fungus represent artefacts of restricted experimental sample sizes and incorrect identifications. Studies based on molecular identification of larger sample sizes from native areas where diverse wasp species/populationsco-exist are needed to determine the extent of the levels of specificity between the symbiont and host.

Studies based on VCGs and molecular markers have revealed the dramatic effect that the spread of asexual spores of the fungus by the wasp has on populations of this fungus to create clones that span across extensive geographic areas, and even across continents. The sexual mode of reproduction, however, clearly continues to play an important role in the ecology of *Amylostereum* spp. The interaction between sexually spread individuals and populations associated with woodwasps is, however, poorly understood. This is likely to differ between regions where sexual sporulation of the fungus occurs at different frequencies, which too is a phenomenon that begs to be characterized further.

The current project to sequence the genome of *A. areolatum* (Currie, Slippers, van der Nest and co-workers, personal communication) holds much promise to significantly inform questions about the evolution of the mutualism and its effects on the fungus. Comparative genomics with the genome of *Heterobasidion annosum*, a close relative of *A. areolatum* that has recently been sequenced (Stenlid and co-workers, unpublished), and other Basidiomycetes will provide particular power in the analysis of the genome. At the moment

the genomes of at least 9 basidiomycetes have been sequenced (these are *Cryptococcus neoformans*, *C. neoformans* var *neoformans*, *Coprinopsis cinerea*, *Schizophyllum commune*, *Moniliophthora perniciosa*, *Malassezia globosa*, *Ustilago maydis*, *Postia maydis* and *Laccaria bicolor*) completed and many are under way (98 genomes) http://www.genomesonline.org; http://www.ncbi.nlm.nih.gov). The work on the initial characterization of recognition loci (mating and vegetative), as well as the intriguing link of these regions to genes that influence growth rate, can be completed using such data. Importantly, genes regulating the interaction between the fungus and the tree host can also be studied with much greater accuracy and more completely. These data will also provide a rich source of markers to study ecological and evolutionary questions.

It is expected that the continued use of genetic resources and the increased use of genomic resources the coming decade will further increase our understanding of the ecology and evolution of *Amylostereum* spp., as well as the mutualism as a whole. It is hoped that these advances will assist to bring our understanding of the natural history of Siricidae and *Amylostereum* mutualism on a par with other better studied systems (such as leaf cutting ants and termites), which is necessary for meaningful comparisons and for addressing fundamental questions about the evolution of fungal-insect mutualism in general.

REFERENCES

Ahumada, R., 2002. Diseases in commercial eucalyptus plantations in Chile, with special reference to *Mycosphaerella* and *Botryosphaeria* Species. M.Sc. thesis, Faculty of Natural and Agricultural Science, University of Pretoria, Pretoria, South Africa.

Awadalla, P., Charlesworth, D., 1999. Recombination and selection at *Brassica* self-incompatibility loci. Genetics. 152, 413-425.

Bedding, R.A., 1995. Biological control of *Sirex noctilio* using the nematode *Deladenus siricidicola.* In: Bedding, R.A., Akhurst, R.J., Kaya, H., (eds.) nematodes and biological control of insect pests. CSIRO, Melbourne, pp. 11-20.

Boidin, J., 1998. Taxonomie moleculaire des Aphyllophorales. Mycotaxon. 66,445-491.

Boidin, J., Lanquentin, P., 1984. Le genre *Amylostereum* (Basidiomycetes) intercompatibilités partielles entre espèces allopartriques. Bull. Soc. Mycol. Fr. 100, 211-236.

Boidin, J., 1958. Heterobasidiomycetes saprophytes et Homobasidiomycetes resupines: V. - Essai sur le genre *Stereum* Pers. ex S.F. Gray. Rev. Mycol. 23, 318-346.

Buller, A.H.R., 1931. Researches on Fungi, vol. IV. Longmans, Green, London. 36.

Carnegie, A.J., Mamoru, M., Hurley, B.P., Ahumada, R., Haugen, D.A., Klasmer, P., Sun, J., Lede, E.T., 2006. Predicting the potential distribution of *Sirex noctilio* (Hymenoptera: Siricidae), a significant exotic pest of *Pinus* plantations. Ann. Forest Sci. 63, 119-128.

Casselton, L.A., 2002. Mate recognition in fungi. Heredity. 88, 142-147.

Coutts, M.P., 1969. The mechanism of pathogenicity of *Sirex noctilio* on *Pinus radiata*. I. Effects of the symbiotic fungus *Amylostereum* sp. (Thelophoraceae). Aust. J. Biol. Sci. 22, 915-924.

Coutts, M.P., Dolezal, J.E., 1969. Emplacement of fungal spores by the woodwasp, *Sirex noctilio*, during oviposition. Forest Sci. 15, 412-416.

Devier, B., Aguileta, G., Hood, M.E., Giraud, T., 2009. Ancient trans-specific polymorphism at pheromone receptor genes in Basidiomycetes. Genetics. 181, 209-223.

Donk, M.A., 1964. A conspectus of the families of Aphyllophorales. Persoonia. 3, 199-324.

Fong, L.K., Crowden, R.K., 1973. Physiological effects of mucus from the wood wasp, *Sirex noctilio* F., on the foliage of *Pinus radiata* D. Don. Aust. J. Biol. Sci. 26, 365-378.

Gaut, I.P.C., 1969. Identity of the fungal symbiont of *Sirex noctilio.* Aust. J. Biol. Sci. 22, 905-914.

Gaut, I.P.C., 1970. Studies of siricids and their fungal symbionts. Ph.D. thesis, University of Adelaide, Australia.

Gilbert, J.M., Miller, L.W., 1952. An outbreak of *Sirex noctilio* Tasmania. Aust. J. Biol. Sci. 22, 905 - 914.

Gross, H.L., 1964. The Echinodontiaceae. Mycopath. Mycol. Appl. 24, 1-26.

Hansen, E.M., Stenlid, J., Johansson, M., 1994. Somatic incompatibility in *Heterobasidion annosum* and *Phellinus weirii*. In: Johansson M, Stenlid J (eds.) Proceedings of the eight

IUOFRO Root and Butt Rot Conference. Swedish University of Agricultural Sciences, Uppsala, pp 323-333.

Haugen, D.A., 1990. Control procedures for *Sirex noctilio* in the Green Triangle: Review from detection to severe outbreak (1977-1987). Aust. Forestry. 53, 24-32.

Herre, E.A., Knowlton, N., Mueller, U.G., Rehner S.A., 1999. The evolution of mutualisms: exploring the paths between conflict and cooperation. TREE. 14, 49 -53.

Hibbett, D.S., Pine, E.M., Langer, E., Langer, G., Donoghue, M.J., .1997. Evolution of gilled mushrooms and puffballs inferred from ribosomal DNA sequences. Proc. Natl Acad. Sci. USA. 94, 12002-12006.

Hoebeke, E.R., Haugen, D.A., Haack, R.A., 2005. *Sirex noctilio*: Discovery of a Palearctic siricid woodwasp in New York. Newsletter Michigan Entomol. Soc. 50, 24 - 25.

Högberg, N., Stenlid, J., 1994. Genetic structures of rare and common wood decay fungi. In: Abstracts of Fifth International Mycological Congress, August 14-21, 1994. Vancouver, British Columbia, Canada, 92.

Hsiau, P.T.-W., 1996. The taxonomy and phylogeny of the mycangial fungi from *Dendroctonus brevicomis* and *D. frontalis* (Coleoptera: Scolytidae). D.Phil. thesis, Iowa State University. Ames.

Hurley, B.P., Slippers, B., Wingfield, M.J., 2007. A comparison of control results for the alien invasive woodwasp, *Sirex noctilio*, in the southern hemisphere. Agric. Forest Entomology. 9, 159-171.

Iede, E.T., Penteado, S.R.C., Schaitza, E.G., 1998. *Sirex noctilio* problem in Brazil - detection, evaluation and control. In: Iede, E., Shaitza, E., Penteado, S., Reardon, R., Murphy, T. (eds.) Proceedings of a conference: Training in the control of *Sirex noctilio* by use of natural enemies. FHTET 98-13. USDA Forest Service, Morgantown, MV. pp. 45 - 52.

James, T.Y., Srivilai, P., Kües, U., Vilgalys, R., 2006. Evolution of the bipolar mating system of the mushroom *Coprinellus disseminatus* from its tetrapolar ancestors involves loss of mating-type-specific pheromone receptor function. Genetics. 172, 1877-1891.

Kauserud, H., 2004. Widespread vegetative compatibility groups in the dry-rot fungus *Serpula lacrymans*. Mycologia 96:232-239

Kauserud, H., Saetre, G.-P., Schmidt, O., Decock, C., Schumacher, T., 2006. Genetics of self/nonself-recognition in *Serpula lacrymans*. Fungal. Genet. Biol. 43, 503-510.

Kim, S.Y., Jung, H.S., 2000. Phylogenetic relationships of the Aphyllophorales inferred from sequence analysis of nuclear small subunit ribosomal DNA. J. Microbiol. 38, 122-131.

Klasmer, P., Fritz, G., Corley, J., Botto, E., 1998. Current status of research on *Sirex noctilio* F. in the Andean-Patagonian region in Argentina. In: Iede, E., Shaitza, E., Penteado, S., Reardon, R., Murphy, T. (eds.) Proceedings of a conference: Training in the control of *Sirex noctilio* by use of natural enemies. FHTET 89 - 90. USDA Forest Service, Morgantown, MV. pp. 89 - 90.

Kothe, E., 1999. Review: Mating types and pheromone recognition in the homobasidiomycetes *Schizophyllum commune*. Fungal Genet. Biol. 27, 146-152.

Kothe, E., Gola, S., Wendland, J., 2003. Evolution of multispecific mating-type alleles for pheromone perception in the homobasidiomycetes fungi. Curr. Genet. 42, 268-275.

Kües, U., 2000. Life history and developmental processes in the basidiomycete *Coprinus cinereus*. Microbiol. Mol. Biol. Rev. 64, 316-353.

Lind. M., Stenlid, J., Olson, A., 2007. Genetics and QTL mapping of somatic incompatibility and intraspecific interactions in the basidiomycete *Heterobasidion annosum s.l.* Fungal Genet. Biol. 44, 1242-1251.

Madden, J.L., 1981. Egg and larval development in the woodwasp, *Sirex noctilio* F. Aust. J. Zoology. 29, 493-506.

Maderni, J.F.P., 1998. *Sirex noctilio* F. present status in Uruguay. In: Iede, E., Shaitza, E., Penteado, S., Reardon, R., Murphy, T. (eds.) Proceedings of a conference: Training in the control of *Sirex noctilio* by use of natural enemies. FHTET 98-13. USDA Forest Service, Morgantown, MV. pp. 81 - 82.

Maijala, P., Harrington, T.C., Raudaskoski, M., 2003. A peroxidase gene family and gene trees in Heterobasidion and related genera. Mycologia 95: 209–221.

Martin, M.M., 1992. The evolution of insect-fungus associations: From contract to stable symbiosis. Amer. Zoo. 32, 593-605.

May, G.S., Badrane, H., Vekemans, X., 1999. The signature of balancing selection: Fungal mating compatibility gene evolution. Proc. Natl. Acad. Sci. USA**.** 96, 9172-9177.

Miller, D., Clarke, A.F., 1935. *Sirex noctilio* (Hym.) and its parasites in New Zealand. Bull. Entomol. Res. 26, 149 - 154.

Miller, S.L., Larsson, E., Larsson, K.-H., Verbeken, A., Nuytinck, J., 2006. Perspectives in the new Russulales. Mycologia. 98, 960-970.

Morgan, F., 1968. Bionomics of Siricidae. Annu. Rev. Entomol. 13, 239-256.

Nielsen, C., Williams, D.W., Hajek, A.E., 2009. Putative source of the invasive *Sirex noctilio* fungal symbiont, *Amylostereum areolatum*, in the eastern United States and its association with native siricid woodwasps. Mycol. Res. 113, 1242-1253.

Paźoutavá, S., Šrůrk, P., Holuša, J., Chudíčkova, M., Lokařík, M., 2010. Diversity of xylariaceous symbionts in Xiphydria woodwasps: role of vector and a host tree. Fungal Ecol. 3, 392-401.

Rayner, A.D.M., 1991. The challenge of the individualistic mycelium. Mycologia, 83, 48-71.

Schirawski, J., Heinze, B., Wagenknecht, M., Kahmann, R., 2005. Mating type loci of *Sporisorium reilianum*: Novel pattern with three *a* and multiple *b* specificities. Euk. Cell. 4, 1317-1327.

Slippers, B., 1998. The *Amylostereum* symbiont of *Sirex noctilio* in South Africa. M.Sc. thesis. University of the Free State, Bloemfontein.

Slippers, B., Wingfield, B.D., Coutinho, T.A., Wingfield, M.J., 2002. DNA sequence and RFLP data reflect relationships between *Amylostereum* species and their associated wood wasp vectors. Mol. Ecol. 11, 1845-1854.

Slippers, B., Wingfield, M.J., Wingfield, B.D., Coutinho, T.A., 2000. Relationships among *Amylostereum* species associated with siricid woodwasps inferred from mitochondrial ribosomal DNA sequences. Mycologia. 92, 955-963.

Slippers, B., Wingfield, M.J., Wingfield, B.D., Coutinho, T.A. 2001. Population structure and possible origin of *Amylostereum areolatum* in South Africa. Plant Pathol. 50, 206-210.55.

Slippers, B., Coutinho, T.A., Wingfield, B.D., Wingfield, M.J., 2003. A review of the genus *Amylostereum* and its association with woodwasps. SA J. Sci. 99, 70-74.

Solheim, H., 2006. Treveps og assosierte sopper i Norge. Agarica. 26, 87–95.

Spradbery, J.P., Kirk, A.A., 1978. Aspects of the ecology of siricid woodwasps (Hymenoptera: Siricidae) in Europe, North Africa and Turkey with special reference to the biological control of *Sirex noctilio* F. in Australia. Bull. Entomol. Res. 68, 341-359.

Stenlid, J., Karlsson, J.O., Högberg, N., 1994. Intraspecific genetic variation in *Heterobasidion annosum* revealed by amplification of minisatelite DNA. Mycol. Res. 98, 57-63.

Stenlid, J., Vasiliauskas, R., 1998. Genetic diversity within and among vegetative compatibility groups of *Stereum sanguinolentum* determined by arbitrary primed PCR. Mol. Ecol. 7, 1265-1274.

Tabata, M., Abe, Y., 1997. *Amylostereum laevigatum* associated with the Japanese horntail, *Urocerus japonicus.* Mycoscience. 38, 421-427.

Tabata, M., Abe, Y., 1999. *Amylostereum laevigatum* associated with a horntail, *Urocerus antennatus.* Mycoscience. 40, 535-539.

Tabata, M., Harrington, T.C., Chen, W., Abe, Y., 2000. Molecular phylogeny of species in the genera *Amylostereum* and *Echinodontium.* Mycoscience. 41, 585-593.

Talbot, P.H.B., 1964. Taxonomy of the fungus associated with *Sirex noctilio.* Aust.J. Bot. 12, 46-52.

Talbot, P.H.B., 1977. The *Sirex-Amylostereum-Pinus* association. Annu. Rev. Phytopathol. 15, 41-54.

Thomsen, I.M., 1996. *Amylostereum areolatum* and *Amylostereum chailletii,* symbiotic fungi of woodwasps (*Sirex* sp. and *Urocerus* sp.). Ph.D. thesis, Danish Forest and Landscape Research Institute, Horsholm.

Thomsen, I.M., 1998. Fruit body characters and cultural characteristics useful for recognizing *Amylostereum areolatum* and *A. chailletii.* Mycotaxon. 69, 419-428.

Thomsen, I.M., Koch, J., 1999. Somatic compatibility in *Amylostereumareolatum* and *A. chailletii* as a consequence of symbiosis with siricidwoodwasps. Mycol. Res. 103, 817-823.

Tribe, G., 1995. The woodwasp *Sirex noctilio* Fabricius (Hymenoptera; Siricidae), a pest of *Pinus* species, now established in South Africa. Afr. Entomol. 3, 215-217.

Tribe, G.D., 1995. The woodwasp *Sirex noctilio* Fabricius (Hymenoptera: Siricidae), a pest of *Pinus* species, now established in South Africa. Afr. Entomol. 3, 216-217.

Van der Nest, M.A., Slippers, B., Stenlid, J., Wilken, P.M., Vasaitis, R., Wingfield M.J., Wingfield, B.D., 2008. Characterization of the systems governing sexual and self-recognition in the white rot homobasidiomycete *Amylostereum areolatum*. Curr. Genet. 53, 323-336.

Van der Nest, M.A., Slippers, B., Steenkamp, E.T., de Vos, L., van Zyl, K., Stenlid, J., Wingfield, M.J., Wingfield, B.D., 2009. Genetic linkage map for *Amylostereum arolatum* reveals an association between vegetative growth and sexual and self recognition. Fungal Genet. Biol. 46, 632-641.

Vasiliauskas, R., Johannesson, H., Stenlid, J., 1999. Molecular relationships within the genus *Amylostereum* as determined by internal transcribed spacer sequences of the ribosomal DNA. Mycotaxon. 71, 155-161.

Vasiliauskas, R., Johannesson, H., Stenlid, J. 1999. Molecular relationships within the genus *Amylostereum* as determined by internal transcribed spacer sequences of the ribosomal DNA. Mycotaxon. 71, 155-161.

Vasiliauskas, R., Stenlid, J., 1999. Vegetative compatibility groups of *Amylostereum areolatum* and *A. chailletii* from Sweden and Lithuania. Mycol. Res. 103, 824-829.

Vasiliauskas, R., Stenlid, J., Thomsen, I.M., 1998. Clonality and genetic variation in *Amylostereum areolatum* and *A. chailletii* from Northern Europe. New Phytol. 139, 751-758.

Vasiliauskas, R., Stenlid, J., 1999. Vegetative compatibility groups of *Amylostereum areolatum* and *A. chailletii* from Sweden and Lithuania. Mycol. Res.103, 824-829.

Wilson, A.D., Schiff, N.M., Haugen, D.A., Hoebeke, E.R., 2009. First report of *Amylostereum areolatum* in pines in the United States. Plant Disease. 93, 109.

Worrall, J.J., 1997. Somatic compatibility in Basidiomycetes. Mycologia. 89, 24-36.

CHAPTER 3

Characterization of the systems governing sexual and self-recognition in the white rot homobasidiomycete *Amylostereum areolatum*

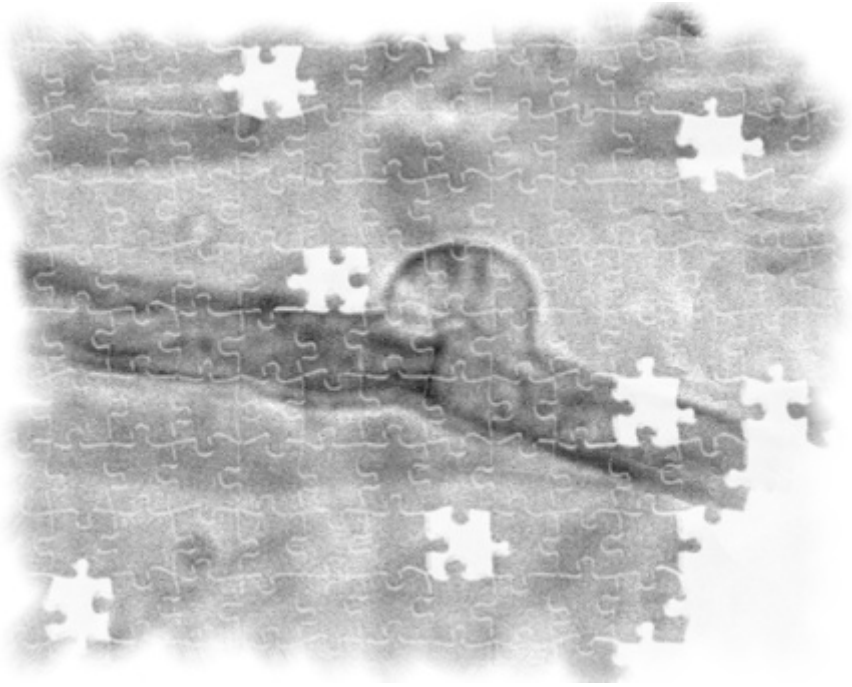

Published as: van der Nest, M.A., Slippers, B., Stenlid, J., Wilken, P.M., Vasaitis, R., Wingfield M.J., Wingfield, B.D. 2008. Characterization of the systems governing sexual and self-recognition in the white rot homobasidiomycete *Amylostereum areolatum*. *Current Genetics* 53:323-336.

TABLE OF CONTENTS

ABSTRACT

This study considered the systems controlling sexual and self-recognition in *Amylostereum areolatum*, a homobasidiomycetous symbiont of the *Sirex* woodwasp. To investigate the structure and organization of these systems in *A. areolatum*, we identified a portion of a putative homologue (RAB1) of the pheromone receptor genes of *Schizophyllum commune* and *Coprinus cinereus*, and a portion of a putative homologue of the *S. commune* mitochondrial intermediate peptidase (*mip*) gene. Diagnostic DNA-based assays for mating type were developed and their application confirmed that the fungus has a heterothallic tetrapolar mating system. Segregation analysis showed that *RAB1* is linked to mating type B, while *mip* is linked to mating type A. The results of sexual and vegetative compatibility tests suggest that sexual recognition in *A. areolatum* is controlled by two multiallelic *mat* loci, while self-recognition is controlled by at least two multiallelic *het* loci. Therefore, despite the association of *A. areolatum* with the woodwasp and the unique mixture of sexual and clonal reproduction of the fungus, both recognition systems of the fungus appear to be similar in structure and function to those of other homobasidiomycetes. This is the first report regarding the genes controlling recognition of a homobasidiomycete involved in an obligate mutualistic relationship with an insect.

INTRODUCTION

A typical homobasidiomycete life cycle consists of a short homokaryotic phase during which hyphal cells contain a single type of nucleus, followed by a predominantly fertile heterokaryotic phase during which hyphal cells harbor more than one type of nucleus. The sexual recognition system, under the control of the mating type (*mat*) loci, determines hyphal fusion or mating between homokaryotic hyphae (Kronstad and Staben, 1997, Casselton and Olesnicky, 1998). The vegetative incompatibility system, under the control of the heterokaryon incompatibility (*het*) loci, determines hyphal fusion between mostly heterokaryotic hyphae (*i.e.*, self/nonself recognition) (Worrall, 1997). So far, these systems have been characterized in a limited number of homobasidiomycetes. This study represents the first report regarding the genes controlling sexual and self/nonself recognition in *Amylostereum areolatum*, a homobasidiomycete involved in an obligate mutualistic relationship with Siricid woodwasps.

Genetic studies in homobasidiomycetes are hampered by the fact that some species are unculturable or their spores fail to germinate, while others (including *A. areolatum*) rarely fruit in nature and do not readily produce fruiting bodies in the laboratory (Martin, 1992, James et al., 2004a). Furthermore, the variable nature of the genes encoded at the *mat* loci makes their genetic identification problematic, because these genes do not cross-hybridize in Southern analyses and it is difficult to design degenerate primers (Badrane and May, 1999; Halsall et al., 2000, James et al., 2004a). At the DNA-level, characterization of mating systems have almost exclusively been limited to the model homobasidiomycetes *Schizophyllum commune* and *Coprinopsis cinerea* (Kronstad and Staben, 1997; Casselton and Olesnicky, 1998). Even less information is available for the self/nonself recognition systems, except that the homobasidiomycetes and other Basidiomycetes harbor apparently fewer *het* loci than their ascomycete relatives (Worrall, 1999). Research regarding these systems will therefore provide valuable insight into the structure, organization, function and evolution of the recognition loci, as well as the role these loci play in the development and evolution of homobasidiomycetes and other fungi.

The white rot mushroom, *A. areolatum*, lives in an obligate symbiosis with various woodwasp species, including *Sirex noctilio* (Gaut, 1969; Talbot, 1977; Slippers et al., 2003). The symbiosis is a highly evolved mutualism in which the asexual spores of the fungus are spread by the wasp, while wood decay by the fungus is necessary for the development of the larvae (Gilmour, 1965;

King, 1966; Madden and Coutts, 1979). As a result, the life cycle of *A. areolatum* involves a unique interplay between asexual and sexual reproduction (Gilmour, 1965; King, 1966; Madden and Coutts, 1979). The importance of asexual reproduction in the life cycle of this fungus is reflected in its overall low genetic diversity based on vegetative incompatibility and DNA-based studies (Vasiliauskas et al., 1998; Thomsen and Koch, 1999; Vasiliauskas and Stenlid, 1999; Slippers et al., 2001). Furthermore, *A. areolatum* fruiting bodies have never been found in the Southern Hemisphere and are only rarely found in the Northern Hemisphere, except in some areas in central Europe (Thomsen, 1998; Slippers and Vasaitis, unpublished). The close association between the fungus and the woodwasp is the inferred explanation for this low heterogeneity, because the genetic homogeneity of the fungal partner is promoted through vertical transmission of asexual spores by the *Sirex* woodwasp, as has been shown for other insect-fungus symbioses (Frank, 1996; Douglas, 1998; Korb and Aanen, 2003). This form of reproduction is thought to ensure maintenance of genotypes that are better adapted for symbiosis in *A. areolatum* (Herre et al., 1999).

The recognition loci of *A. areolatum* have not yet been characterized. It is, however, known that fusion of homokaryotic hyphae of this fungus is controlled by a tetrapolar mating system where sexual compatibility is governed by two unlinked *mat* loci (locus A and B) (Boidin and Lanquentin, 1984). Only genetically distinct homokaryons with different allelic specificities at both their *mat* loci are sexually compatible and will allow reciprocal nuclear migration to occur after cell fusion to form a heterokaryon (Kronstad and Staben, 1997; Casselton and Olesnicky, 1998). The heterokaryon can produce fruiting bodies under favorable conditions with karyogamy and meiosis occurring within specialized cells (Kües et al., 2002). This sexual process, albeit rare in *A. areolatum* (Boidin and Lanquentin, 1984; Thomsen, 1998; Slippers et al., 2001), might be important to allow adaptation to changing environments. In terms of the self/nonself recognition system it may be expected to operate the same as in other fungi, where hyphal fusion is only permitted between genetically similar heterokaryons sharing the same allele specificities at all of their *het* loci (Rayner, 1991; Worrall, 1997; Glass and Kaneko, 2003). When two interacting heterokaryons are genetically dissimilar with different allelic specificities at some or all of their *het* loci, cell death of the interacting hyphae prevents unlike individuals from anastomosing (Rayner, 1991; Worrall, 1997). As vegetative incompatibility essentially represents a self/nonself recognition system that preserves genetic identity (Worrall, 1997; Glass and Kaneko, 2003), it is

possible that it may also help to ensure maintenance of *A. areolatum* genotypes that are better adapted for symbiosis.

In this study we characterized the loci controlling sexual and self/nonself recognition in a set of *A. areolatum* homokaryons and their mated heterokaryons obtained from field-collected basidiocarps. Furthermore, a portion of a putative homologue of the pheromone receptors encoded at the *mat-B* locus of *S. commune* and *C. cinerea* were characterized and genetic linkage between this gene and mating type B was established. Similarly, a portion of a putative homologue of the mitochondrial intermediate peptidase (*mip*) gene in *A. areolatum* was characterized and linkage between the putative *mip* gene and mating type-A was demonstrated. These putative pheromone receptor and *mip* sequences were subsequently used to developed DNA-based assays for diagnosing mating type in *A. areolatum*. These data allowed us to compare the recognition systems of *A. areolatum*, a homobasidiomycete closely associated with an insect symbiont, to those of other homobasidiomycetes.

MATERIALS AND METHODS

Fungal isolates

Nineteen single-spored, homokaryotic isolates were obtained from a single basidiocarp of *A. areolatum* and a heterokaryotic culture (CMW16828) was made from the structure to serve as a genetic record of the parent. A second basidiocarp of *A. areolatum* was collected and yielded 80 single-spored, homokaryotic isolates and a culture (CMW16848) was taken from the parent structure. Both basidiocarps were collected in Austria by R. Vasaitis and B. Slippers (Table 1). The parent strains are hereafter referred to as CMW16828 and CMW16848 and their respective homokaryotic progeny are referred to as CMW16828$_{[1\text{-}19]}$ and CMW16848$_{[1\text{-}80]}$. The parent strains, CMW16828 and CMW16848, are vegetatively incompatible and represent separate genets (see below). The single-spored isolates were obtained by placing a portion of the hymenophore on the underside of a Petri dish lid over 1% malt yeast agar (MYA) (20 gL^{-1} malt extract, 2 gL^{-1} yeast extract and 15 gL^{-1} agar) (Biolab, Johannesburg, South Africa) or by placing a piece of hymenophore on a piece of wax paper. Following a spore shower onto the paper, the collected spores were suspended in sterile water and dilutions of these spore suspensions were plated onto 1% MYA and incubated for 24 h at 25 °C. Individual germinating spores were identified using a dissection microscope and transferred to separate MYA plates. For comparative purposes, representative heterokaryons from the Southern and Northern Hemisphere were also included in the study (Table 1). All of the cultures were maintained on MYA made with pine extract (PE-MYA). Pine extract was prepared by twice autoclaving 200 g pine wood chips in 1 L of distilled water and then passing the liquid through a cotton cloth. All isolates of *A. areolatum* used in this study are stored and maintained at 4 ºC in the culture collection (CMW) of the Forestry and Agricultural Biotechnology Institute (FABI), University of Pretoria, Pretoria, South Africa.

AFLP analysis

To ensure that each of the respective homokaryotic progeny used in this study originated from either CMW16828 or CMW16848, AFLP (amplified fragment length polymorphism, Vos et al., 1995) analysis was used. It was necessary to verify the origin of the homokaryons, because samples were collected from the field, and it is possible that spores from another basidiocarp

could have been sampled. Also, hyphae from the basidiocarp could have been sampled instead of germinating spores. For this purpose DNA was isolated from all of the homokaryons and the parent heterokaryons using the method described by Zhou et al. (2004) and stored at -20 °C. AFLP analyses was performed as previously described (Vos et al., 1995) using three primer combinations (E-ac + M-02, E-ac + M-04 and E-tc + M-03) where both *Eco*RI (E) and *Mse*I (M) primers included two selective nucleotides at their 3'-ends. The *Eco*RI (E) primers were 5'-end labeled with IRDye™ 700 or IRDye™ 800 (LI-COR, Lincoln, NE) and the *Mse*I (M) primers (Inqaba Biotechnologies, RSA) were unlabelled. The resulting fragments were separated using the 4200 LI-COR® automated DNA sequencer (LI-COR) and analyzed with QUANTAR Version 1.0 (KeyGene Products B.V., The Netherlands) during which fragments were scored as present or absent.

Morphological diagnosis of mating types

Hyphal morphology was used to determine the mating types of the homokaryons isolated from basidiocarps CMW16828 and CMW16848 by pairing homokaryotic isolates on PE-MYA and incubating these cultures at ± 25 ºC in darkness. Mycelial plugs (± 5 mm diam) taken from the homokaryotic isolates were placed 1 cm apart and after 4 wks an agar plug (± 5 mm diam) containing the intermingling mycelium was transferred to a new plate. After two weeks of growth, hyphal morphology was examined using a Zeiss Axiocam light microscope. The absence of clamp connections indicated incompatible mating interactions, their presence indicated compatible interactions, while the presence of curly and irregular hyphal structures and hyper branching, as well as the presence of clamp cells that are unable to fuse indicated partially successful sexual interactions. The mating types of the 19 homokaryons for family CMW16828 were determined by pairing all of the homokaryons in this family in all possible combinations and studying the hyphal morphology of the interacting individuals. To determine the mating types of the 80 homokaryons for family CMW16848, four tester strains were first identified by pairing eight homokaryons in all possible combinations. After assigning mating types to the four tester homokaryons, they were used in pairings to determine the mating types of the remaining homokaryons in family CMW16848.

PCR-based diagnoses of mating types

PCR-based diagnostic procedures were developed to determine the mating types of the homokaryons isolated from basidiocarps CMW16828 and CMW16848. For mating type A, we used segregation analysis to determine if the putative *mip* gene in *A. areolatum* is also linked to the *mat-A* locus, as was found in other homobasidiomycetes (James et al., 2004a). If the two genes are indeed linked, it will be possible to identify the alleles segregating at the *mat*-A locus based on segregation of *mip* alleles. For this purpose, a portion of *mip* was amplified from the parent heterokaryon CMW16848 using previously designed degenerate primers MIP1F and MIP2R (James et al., 2004a). PCR was performed on an Eppendorf thermocycler (Eppendorf AG, Germany) using a reaction mixture containing 1 ng/µl DNA, 0.2 mM of each of the four dNTPs, 1.5 mM $MgCl_2$, 0.5 µM of each primer and 0.05 U/µl FastStart Taq (Roche Diagnostics, Mannheim). Thermal cycling conditions included an initial denaturation step at 94 °C for 2 min followed by 30 cycles of denaturation at 94 °C for 30 s, annealing at 50 °C for 30 s, extension at 72 °C for 30 s, and a final extension at 72 °C for 10 min. DNA was separated by electrophoresis on 1 % agarose gels (wt/v) (Roche Diagnostics) (Sambrook et al., 1989). Sizes of the amplicons were determined by comparison against a 100 base pair (bp) molecular weight marker (O'RangeRuler™ 100bp DNA ladder, Fermentas Life Sciences). The resulting PCR products were purified using polyethylene glycol (PEG) precipitation (Steenkamp et al., 2006). The purified PCR products were resuspended in 20 µl sterile distilled water and cloned using pGEM-T Easy vector System I (Promega Corporation, Madison, USA) following the manufacturer's instructions.

The cloned products were amplified from individual colonies using plasmid specific primers, after which the PCR products were purified using PEG precipitation and sequenced using a Big Dye Cycle Sequencing kit version 3.1 (Applied Biosystems, Foster City, USA) and an ABI3700 DNA analyzer (Applied Biosystems). Sequence analyses were performed with Chromas Lite 2.0 (Technelysium) and BioEdit version 7.0.2.5 (Hall, 1999). The resulting DNA sequences were compared to those in the protein database of the National Centre for Biotechnology Information (www.ncbi.nih.nlm.gov) using *blastx* to confirm gene identity. From these sequences, allele-specific PCR primers MIPAro1F (5'-gtcctttcactcttcggtac-3') and MIPAro1R (5'-

caaataactggcgccatacc-3') were designed using the programme Primer 3 (v. 0.4.0) (http://frodo.wi.mit.edu/) and applied to homokaryons CMW16848[1-80].

For mating type B, we targeted the *A. areolatum* homologue of the pheromone receptor present at the *mat-B* locus of *S. commune* and *C. cinerea* (Kronstad and Staben, 1997; Casselton and Olesnicky, 1998). This gene was amplified in the heterokaryotic parental isolate CMW16848 using degenerate primers br1-F and br1-R designed by James et al. (2004b). The fragment was cloned and sequenced as described above. After confirming the identity of the sequenced portion using *blastx* as described above, PCR-based genome walking (Siebert et al., 1995) was used to obtain the upstream and downstream sequences of this fragment. Based on the resulting information, sequence-specific primers RAB1-470F (5'-tcttgggctgacttttcc-3') and RAB1-1800R (5'-ggcaggtagatcgaggttga-3') were designed using Primer 3. These primers were used to amplify a portion of the putative pheromone receptor gene in the parental heterokaryon CMW16848, as well as representative isolates from the Southern and Northern Hemisphere. The resulting fragments were purified, cloned and at least 5 clones per heterokaryotic isolate were sequenced. These sequences were compared to identify unique restriction sites to use in a PCR-RFLP (restriction fragment length polymorphism) procedure that will allow identification of different alleles of the putative pheromone receptor in the parental heterokaryon CMW16848 and its progeny. The PCR-RFLP entailed amplification of the putative *A. areolatum* pheromone receptor with primers RAB1-470F and RAB1-1800R, followed by digestion with the enzyme *Eco*RV (Roche Diagnostics) at 37 °C for 2 h. In all cases, χ^2 tests were used to evaluate the goodness of fit of observed allelic distributions to expected Mendelian segregation ratios, as well as to test co-segregation of alleles identified using microscopy and those identified using the DNA-based assays (Steel et al., 1997).

Generation of synthetic heterokaryons

Sibling heterokaryons were generated by pairing sexually compatible homokaryons originating from parental strain CMW16828, in all possible combinations. For the homokaryons derived from CMW16848, sibling heterokaryons were generated in the same way. To generate sib-related heterokaryons, homokaryons from the same basidiocarp were paired with a sexually compatible but unrelated homokaryon. The sib-related heterokaryons were thus produced by pairing the unrelated homokaryon CMW16848[57] with sexually compatible homokaryotic

progeny of strain CMW16828. Homokaryon CMW16828[1] was also paired with homokaryotic progeny of strain CMW16848, to generate a second set of sib-related heterokaryons. All the sib-related heterokaryons, therefore, had a nucleus in common (*i.e.*, that of either homokaryon CMW16848[57] or CMW16828[1]) with vegetative incompatibility being determined only by the related nucleus. Synthetic heterokaryons were generated by placing mycelial plugs (± 5 mm diam) containing homokaryotic hyphae 1 cm apart on PE-MYA, followed by incubation at ± 25 ºC in the dark. After 4 wks, agar plugs containing the intermingling heterokaryotic mycelium were transferred to new plates. Successful interaction and heterokaryon formation was verified by the presence or absence of clamp connections, observed using a Zeiss Axiocam light microscope (Carl Zeiss Ltd., München, Germany) as described before.

Vegetative compatibility

To assay compatibility all of the pairings were done by placing mycelial plugs (± 5 mm diam) 1 cm apart from each other on PE-MYA, followed by incubation at ± 25 ºC in the dark. Hyphal interactions were scored after 4 wks. Compatible reactions were scored as 0 and showed no visible reaction, with the interacting hyphae intermingling. Weakly incompatible reactions were scored as 1, with very light pigmentation of the interaction zone. Strongly incompatible reactions were scored as 2, based on relative sparseness of aerial hyphae and brown discoloration of interacting hyphae. All pairings were done in duplicate and a self-pairing was always included as a compatible control.

The vegetative compatibility groups (VCGs) for all of the *A. areolatum* isolates used in this study were determined. The parental heterokaryotic isolates (CMW16828 and CMW16848) were paired with each other to verify that the two basidiocarps, from which the respective progenies were derived, represent different VCGs. This also provided verification that a homokaryon belonging to one family could be used as an unrelated homokaryon to generate sib-related heterokaryons with the other family. The vegetative incompatibility of the sib-related heterokaryons for both the families were determined by pairing 16 selected sib-related heterokaryons from each family with each other in all possible combinations. Thus, sib-related heterokaryons derived from compatible homokaryons from one basidiocarp (CMW16828) were paired with each other and likewise, sib-related heterokaryons derived from compatible homokaryons from the other basidiocarp (CMW16848) were also paired with each other. To

confirm the presence of individual VCGs in family CMW16848, four sib-related heterokaryons that belong to the identified VCGs were paired with the rest of the sib-related heterokaryons isolated from that basidiocarp. The results of these pairings were confirmed with sibling pairings, where 25 selected sibling heterokaryons from basidiocarp CMW16828 were paired with each other in all possible combinations, and likewise, 25 sibling heterokaryons of basidiocarp CMW16848 were paired with each other in all possible combinations.

RESULTS

AFLP analysis

We confirmed the parent-progeny relationship between heterokaryons CMW16828 and CMW16848 and their respective homokaryotic offspring using AFLPs. The homokaryons in each family shared all of their AFLP fragments with the heterokaryon from which it originated. Each of the individual homokaryons also was recombinant as they displayed unique fingerprints.

Morphological diagnosis of mating type

The four possible mating types of the homokaryons isolated from basidiocarps CMW16828 and CMW16848 were determined using microscopy. Based on these findings alleles A1B1, A1B2, A2B1 and A2B2 segregating at the *mat-A* and *mat-B* loci, representing the four mating types, were identified for the progeny of parental heterokaryon CMW16848. Similarly, alleles A3B3, A3B4, A4B3 and A4B4 segregating at the *mat-A* and *mat-B* loci, representing the four mating types, were identified for the progeny of parental heterokaryon CMW16828. Sexually incompatible homokaryons were identified based on the absence of clamp connections, which indicated that homokaryons belong to the same mating type and share the same alleles at both their *mat* loci. In contrast, sexually compatible homokaryons were identified based on the presence of clamp connections, which indicated that the homokaryons belong to opposite mating types and have different alleles at both their *mat* loci (e.g., A1B1 *vs.* A2B2 and A1B2 *vs.* A2B1). Homokaryons displaying partial sexual compatibility were identified based on their inability to produce a heterokaryon with clamp connections, but displayed abnormal hyphal morphology. Interacting homokaryons that have different alleles at their *mat-B* locus, but the same allele at their *mat-A* locus (e.g. A1B1 *vs.* A1B2; A2B2 *vs.* A2B1), were identified by the presence of curly and irregular hyphal structures and hyper-branching growth. Interacting homokaryons with different alleles at their *mat-A* locus, but with the same allele at their *mat-B* locus (e.g. A1B1 *vs.* A2B1; A2B2 *vs.* A1B2), were identified by the presence of false clamp connections. Representative homokaryons of the four mating types in one family were all sexually compatible with those of the other family, while the ratio of compatible to incompatible crosses between homokaryons of the same progeny or basidiocarp was 1:3.

PCR-based diagnosis of mating types

The alleles (A1B1, A1B2, A2B1 and A2B2) assigned to the four possible mating types of the homokaryons isolated from basidiocarp CMW16848 were also identified using PCR-based assays. The *mip* gene that has been shown to co-segregate with the *mat-A* locus in other homobasidiomycetes (James et al., 2004a) was successfully amplified using MIP1F and MIP2R in the parental heterokaryon CMW16848. Based on the *blastx* analyses, the sequence (GenBank accession number EU380311) of the 415 bp fragment of *A. areolatum* was 67 % similar at the amino acid level to the *mip* gene of *S. commune* (GenBank accession number AAB01371). Specific primers that amplify the one *mip* allele of *A. areolatum* based on this sequence, generated a 332 bp PCR product in 44 of the 80 homokaryons of family CMW16848 (Fig. 1). It was thus possible to distinguish between the *mip* alleles present in the progeny with the two *mip* alleles segregating 1:1 in the progeny ($p < 0.05$). As predicted, the two *mip* alleles also co-segregated ($p < 0.05$) with the microscopically identified *mat-A* alleles (A1 and A2), confirming that the putative *mip* gene of *A. areolatum* is indeed closely linked to the *mat-A* locus.

An 884 bp fragment of a putative pheromone receptor was amplified in the parental heterokaryon of family CMW16848 using degenerate primers br1-F and br1-R (James *et al.*, 2004b). Based on the *blastx* analyses the sequence of this fragment was 62 % similar at the amino acid level to the Bbr2 pheromone receptor sequence of *S. commune* (GenBank accession number AAK58068) and 68 % similar to the rcb1 pheromone receptor sequence of *C. cinerea* (GenBank accession number AAQ96348). This putative pheromone receptor in *A. areolatum* was designated the acronym RAB1 (pheromone receptor in *Amylostereum* present at *mat* locus B; GenBank accession numbers EU380312 and EU380313). A further ~500 bp of the upstream and downstream sequence was obtained using PCR genome-walking. Specific primers (RAB1-946F and RAB1-1800R) that amplify an 845 bp fragment of *RAB1* in *A. areolatum* were designed based on this sequence. Amplification, cloning and sequencing of *RAB1* in the parental heterokaryon CMW16848 revealed that one of the *RAB1* alleles, but not the other, harbors an *Eco*RV restriction site. The undigested RAB1 fragment (845 bp) was present in 39 of the 80 homokaryons of family CMW16848 and is designated *RAB1.1* (Fig. 2). The digested fragments (652 and 193 bp) were present in the remaining homokaryons and are designated *RAB1.2* (Fig. 2). The two *RAB1* alleles segregated 1:1 in the progeny ($p < 0.05$) of CMW16848 and they also

co-segregated with the microscopically identified *mat-B* alleles (B1 and B2) in the homokaryons of family CMW16848 ($p < 0.05$). Since there is more than one pheromone receptor encoded at the *mat-B* locus of the homobasidiomycetes studied thus far (Halsall et al. 2000), it is possible that RAB1 or another pheromone receptor tightly linked to this putative pheromone receptor, may be involved in determining mating type specificity in these crosses.

Application of the RAB1-specific primers designed in this study also generated the expected 845 bp fragment in heterokaryon CMW16828 and its homokaryotic offspring, as well as the representative Southern and Northern Hemisphere heterokaryons (Table 1). Based on restriction digestion with *Eco*RV and sequence analyses of the cloned 845 bp products, heterokaryons CMW16828, and CMW28219 appeared to be homozygous for the *RAB1.1* allele while heterokaryon CMW28223 was homozygous for the *RAB1.2* allele. All of the remaining heterokayons appeared to be heterozygous, with heterokaryons CMW16848 and CMW28217 harboring *RAB1.1* and *RAB1.2*, heterokaryons CMW28225 and CMW28221 harboring *RAB1.1* and *RAB1.3*, and the Southern Hemisphere heterokaryons CMW8900, CMW8898, CMW3300 and CMW28224 harboring *RAB1.2* and *RAB1.3*. Comparison of the sequences of the three identified alleles to the corresponding region of the pheromone receptor genes of the model homobasidiomycetes revealed that *RAB1* harbors three putative introns at positions similar to those identified for Rcb3.42 of *C. cinerea* (Halsall et al., 2000). Of the 14 polymorphic sites, eight are located in the introns, while those in the putative exons represent synonymous substitutions not affecting the inferred amino acid sequences (Fig. 3). We did however, only sequence a portion of RAB1 (*i.e.,* 845 bp) and only five clones per heterokaryon. It may therefore be possible that we might have missed additional alleles for the putative pheromone receptor gene of *A. areolatum*.

Vegetative incompatibility

The heterokaryon interactions, which included the sibling, sib-related and unrelated interactions, were scored after 4 wks as 0, 1 or 2 (Fig. 4). All self-pairings included as compatible controls (0 reactions) were characterized by intermingling hyphae. Pairing of the heterokaryons CMW16828 and CMW16848 with those collected in the Southern Hemisphere (South Africa, New Zealand and Brazil) served as strongly incompatible controls (2 reactions) and interacting hyphae were relatively sparse with brown discoloration.

The proportion of strongly incompatible (2 reactions) interactions for sib-related heterokaryons for family CMW16828 (pairings CMW16828$_{[n]}$ x CMW16848$_{[57]}$) and for family CMW16848 (pairings CMW16848$_{[n]}$ x CMW16828$_{[1]}$), were both 19 % (Tables 1, 2 and 3). Fifty four percent of the pairings between the sib-related heterokaryons for family CMW16828 and 59 % for family CMW16848 were weakly incompatible (1 reaction). Segregation of the compatibility trait in both sets of sib-related heterokaryons (22 % and 27 %) did not differ significantly from the 1:3 ratio ($p < 0.05$). A segregation pattern of 50 %, 25 %, 12.5 %, or 6.25 % indicate that there are either one, two, three or four loci controlling vegetative incompatibility, respectively. Given that the percentage of compatible interactions in both sets of sib-related heterokaryons did not deviate significantly (at the 0.05 level) from 25 %, vegetative incompatibility in *A. areolatum* is probably controlled by at least two *het* loci. Furthermore, for all of the sib-related pairings, it appeared that the mating type genes do not to play a role in vegetative incompatibility, because the VCGs did not significantly (at the 0.05 level) correlate with the different mating types (Tables 3 and 4).

The proportion of strongly incompatible interactions (2 reactions) between the sibling heterokaryons for family CMW16848 (pairings CMW16848$_{[n]}$ x CMW16848$_{[n]}$) was 12 % (Tables 2 and 5) and 9% between sibling heterokaryons for family CMW16828 (pairings CMW16828$_{[n]}$ x CMW16828$_{[n]}$) (Tables 2 and 6). Fifty five percent of the pairings between the sibling heterokaryons for family CMW16828 and 66 % for family CMW16848 were weakly incompatible (1 reaction). The proportion of compatible interactions between the sibling heterokaryons for family CMW16848 was 22 % and 36% between sibling heterokaryons for family CMW16828. No obvious vegetative compatibility groupings were observed for the pairings between the siblings in either of the two families. The parental heterokaryons of the two families were vegetatively incompatible and the sibling heterokaryons of family CMW16848 were also never compatible with sibling heterokaryons of family CMW16828. It is, therefore, likely that both the parental heterokaryons are heterozygous at the two *het* loci and that the homokaryons representing the two families do not share alleles at either of these loci. An alternative hypothesis is that the parental heterokaryons are heterozygous at different *het* loci and that there are more than two *het* loci in *A. areolatum*.

Sib-related heterokaryons of families CMW16828 and CMW16848 were separated into four groups based on strong incompatibility (2 reactions) (Tables 3 and 4). For both sets of sib-related interactions, the heterokaryons in VCG 1 were strongly incompatible with sib-related heterokaryons in VCG 3, while those in VCG 2 were strongly incompatible with the heterokaryons in VCG 4. These groups may, therefore, reflect the four different alleles of the two loci controlling strong incompatibility in the isolates examined. These would thus have alleles *1a* and *1b* at the *het-1* locus and alleles *2a* and *2b* at the *het-2* locus for family CMW16848 and alleles *1c* and *1d* at the *het-1* locus and alleles *2c* and *2d* at the *het-2* locus for family CMW16828. It was, therefore, possible to assign alleles *1a2a* to VCG 1, *1a2b* to VCG 2, *1b2b* to VCG 3 and *1b2a* to VCG 4 for family CMW16848 or alleles *1c2c* to VCG 5, *1c2d* to VCG 6, *1d2d* to VCG 7 and *1d2c* to VCG 8 for family CMW16828.

The presence of the four VCGs in each family, identified with the sib-related pairings, was verified when sibling heterokaryons from homokaryons in VCG 2 were strongly incompatible with sibling heterokaryons of homokaryons in VCG 4 for family CMW16848 (Tables 2 and 5). Likewise the sibling heterokaryons of family CMW16828 (Tables 2 and 6) consisting of homokaryons in VCG 6 were strongly incompatible with sibling heterokaryons derived from homokaryons in VCG 8. The presence of the four VCGs in each family was further confirmed when four selected sib-related heterokaryons representing the four VCGs of family CMW16848 were paired with all of the other sib-related heterokaryons of this family to give the predicted outcomes of compatible (0 reactions), weakly incompatible (1 reactions) and strongly incompatible reactions (2 reactions). Different from what was expected, some of the sib-related heterokaryons in VCG 5 (with alleles *1c* and *2c*) were strongly incompatible with sib-related heterokaryons in VCG 8 (with alleles *1d* and *2c*) of family CMW16828. Furthermore, some of the sib-related heterokaryons in VCG 6 (with alleles *1c* and *2d*) were strongly incompatible with some of the sib-related heterokaryons in VCG 7 (with alleles *1d* and *2d*). These sib-related heterokaryons have different alleles at the *het-1* locus, but they share the same allele at the *het-2* locus (Table 4). Also different from what was expected, sibling heterokaryons from homokaryons in VCG 2 of family CMW16848 were not only strongly incompatible with sibling heterokaryons from homokaryons in VCG4, but also with sibling heterokaryons from VCG 1 and VCG 3 (Table 5). This indicates that vegetative incompatibility in *A. areolatum* may be more complex than an allelic interaction of the two identified *het* loci.

DISCUSSION

In this study we characterized the sexual and self-recognition systems of *A. areolatum*. Self-recognition in this fungus appears to follow the general trend identified in basidiomycetes in that it is controlled by a small number of multiallelic *het* loci. Our results also confirmed that sexual recognition among individuals are determined by a tetrapolar mating system in which two multiallelic *mat* loci are involved. The basic function and genetic make-up of these loci seem to resemble those of the model homobasidiomycetes. We identified a homologue in *A. areolatum* of a pheromone receptor (RAB1) encoded at the *mat-B* locus in *S. commune* and *C. cinerea* that was linked to mating type B. We also identified a putative *mip* gene in *A. areolatum* that co-segregated with mating type A, which has been shown to be linked to the *mat-A* locus of other homobasidiomycetes. This study represents the first report regarding the genes implicated in sexual and self-recognition in a homobasidiomycetous obligate symbiont of an insect. The observed segregation of *mat* and *het* alleles in the progenies studied will facilitate construction of a genetic linkage map and subsequent characterization of the recognition loci in their entirety in *A. areolatum* and other *Amylostereum* species. Comparison of these regions among *Amylostereum* species, some of which are not associated with insects, will allow full appreciation of how this association influences the evolution of the recognition loci.

The observed 1:3 ratio of sexually compatible to incompatible crosses between homokaryons of *A. areolatum* from the same basidiocarp is consistent with a tetrapolar mating system that consists of two *mat* loci resulting in four possible mating types (Boidin and Lanquentin, 1984). The four mating types of the homokaryons derived from two sets of progeny were identified using microscopy, following pairings, as well as through PCR-based diagnostic assays developed in this study. Our data show that, like the *mat* loci of some other homobasidiomycetes, the *mat* loci of *A. areolatum* are multiallelic (Kothe, 1996). Three alleles (*RAB1.1*, *RAB1.2* and *RAB1.3*) were present in the small number of isolates tested, confirming the observed multiallelism. This is also illustrated by the fact that all of the homokaryons from one family were compatible with the tested homokaryons of the other family. Homokaryons from different families thus all differ at both *mat* loci, allowing the formation of heterokaryons with clamp connections. However, because there is potentially additional pheromone receptors located at the *mat-B* locus of *A.*

areolatum, it may be possible that the two homokaryotic families are actually dissimilar at different pheromone receptors **(**Kothe, 1996**;** Halsall et al., 2000).

Morphology-based diagnosis of mating types in basidiomycetous fungi like *A. areolatum* is a tedious and time consuming process that does not always yield conclusive results. Mating types can only be assigned after pairings between homokaryotic individuals have been incubated for extended periods of time, and even then morphological differences associated with the presence or absence of certain *mat* alleles are not always evident. DNA-based diagnoses of mating types are therefore far less subjective, more efficient and can be used for both homo- and heterokaryotic isolates. In this study, we used published information on the *mat* locus of Basidomycetes (James et al., 2004a; James et al., 2004b) to develop DNA-based assays for identifying mating types in *A. areolatum*. For locus *mat-A*, we designed specific primers that allow amplification of a portion of the *mip* gene, closely linked to the *mat-A* locus, that enable differentiation between the alleles of this locus. For locus *mat-B*, we developed a PCR-RFLP method based on putative pheromone receptor sequences for RAB1 for differentiating the alleles of this locus. Although similar approaches have been used extensively for differentiating MAT-1 and MAT-2 (Coppin et al., 1997; Turgeon and Yoder, 2000) mating types of ascomycetes (e.g., Mara and Milgroom, 1999; Steenkamp et al., 2000; Yokoyama et al., 2004), multiallelism and the hyperdiverse nature of sequences encoded at the mating type loci of homobasidiomycetes (James et al., 2004b), limit the use of DNA-based mating type assays for non-model homobasidiomycetes. The fact that our PCR-based mating type assays did not function on close relatives (*i.e.*, *A. chialletii* and *A. laevigatum*, results not shown) of *A. areolatum* is, therefore, to be expected. Also, the DNA-based diagnostic procedures described here should be used with caution in broad population studies of the fungus as additional alleles which have as yet not been characterized might be missed.

Like other homobasidiomycetes, *A. areolatum*, has fewer *het* loci than the ascomycetes that have been studied thus far (Worrall, 1997). Our results suggest that vegetative incompatibility in *A. areolatum* is controlled by at least two *het* loci (loci A and B), since 25 % of the vegetative interactions among the sib-related heterokaryons were compatible. Examples of homobasidiomycetes with relatively few *het* loci include *Phellinus weirii* with a single *het* locus, *Serpula lacrymans* with two *het* loci and *Heterobasidion annosum* that has three to four *het* loci (Hansen et al., 1994; Kauserud et al., 2006; Lind et al., 2007). In contrast the ascomycetes, such

as *Neurospora crassa*, have at least eleven *het* loci, and *Podospora anserina* has at least nine *het* loci (Perkins, 1988; Bérgueret et al., 1994). The two *het* loci identified in *A. areolatum* appear to be multiallelic as is also the case for other homobasidiomycetes (Stenlid and Vasiliauskas, 1998; Lind et al., 2007), but different to the situation in ascomycetes that mostly have biallelic *het* loci (Cortesi and Milgroom, 1998; Muirhead et al., 2002). This is because sib-related heterokaryons of the one family were never compatible with sib-related heterokaryons of the other family. However this incompatibility between the families may be due to heterozygosity at additional *het* loci. Also, additional *het* loci may be present in *A. areolatum* that could not be detected in our study due to possible homozygosity in the parental heterokaryons tested. Nevertheless, our results conclusively show that *A. areolatum* harbors at least two *het* loci that appear to be multiallelic. It may therefore be expected that *A. areolatum* has many different VCGs, just like the multiallelic nature of *mat* loci increase the number of expected number of mating types (Kothe, 1996).

Among the vegetative compatibility pairings examined in this study, two types of incompatible interactions were observed, *i.e.,* strongly incompatible and weakly incompatible. It would be expected that sib-related dikaryons differing at both loci are strongly incompatible, whereas interacting sib-related heterokaryons differing at a single locus would display weak incompatibility. This was, however, not always the case, as some of the sib-related heterokaryons consisting of homokaryons derived from parent isolate CMW16828, presumably differing at only a single locus, were strongly incompatible. Furthermore, sibling heterokaryons consisting of homokaryons derived from parent CMW16828 differing at a single locus was also strongly incompatible. The same result was observed for sibling heterokaryons consisting of homokaryons derived from the parental isolate CMW16848. These findings suggest that in some cases, a single locus (*het-1* locus) controls strong incompatibility. This is similar to the situation in *Collybia fusipes*, where only one of the possible three *het* loci controls strong incompatibility (Marçais et al., 2000). This locus, however, clearly does not act in isolation. If a single locus exclusively determines vegetative incompatibility, as is the case for *Phellinus gilvus* (Rizzo et al., 1995), the sib-related heterokaryons of family CMW16828 should have separated into two and not four groups based on strong incompatibility. Also, not all of the sib-related heterokaryons differing at their *het-1* locus are strongly incompatible, as would be expected if the *het-1* locus alone controls strong incompatibility. It, therefore, appears that there may be

other genes present in *A. areolatum* that interfere in determining the strength of vegetative incompatibility interactions.

Additional genes potentially involved in determining the outcome of vegetative incompatibility in *A. areolatum*, may represent genes that are not encoded at the *het* loci. This has been shown for the *tol* gene of *N. crassa* and the *mod* genes for *P. anserina*. The *tol* gene appears to influence the outcome of mating type mediated vegetative incompatibility in *N. crassa*, although it is not a mating type nor a *het* gene (Leslie and Yamashiro, 1997). In *P. anserina*, the *mod* (for modifier) genes have been demonstrated to interfere with the signals mediating vegetative incompatibility, thereby repressing cell autolysis and preventing fusion of the interacting individuals (Bernet, 1992; Barraeau et al., 1998). However, these examples refer specifically to ascomycetes and non-*het* genes involved in vegetative incompatibility have not yet been identified for basidiomycetes. In addition, the *mat* loci are not implicated in self-recognition of the basidiomycetes that have been examined (Hansen et al., 1993; Marçais et al., 2000) and they also do not appear to be involved in determining vegetative incompatibility in *A. areolatum*.

The presence of *het* loci, in addition to those identified, might offer an alternative explanation for the absence of strong incompatibility in some pairings between individuals differing at the *het-1* locus. Their presence would have been masked if it is closely linked to the *het-1* locus. This is also known in other fungi. For example, in the ascomycete *N. crassa,* the closely linked *pin-c* (for partner for incompatibility) and *het-c* loci interact in a non-allelic fashion to mediate vegetative incompatibility (Kaneko et al., 2006). Although the intensity of this non-allelic interaction is also influenced by allelic interactions at the *het-c* locus, allelic interactions at the *pin-c* locus has no effect. In *P. anserina,* it has been shown that not all of the various non-allelic interactions between the *het-c* and *het-e* loci will mediate vegetative incompatibility (Saupe et al., 1995). For example, only interactions between *het-c1* with *het-e2* and *het-e3*, and interactions between *het-c2* with *het-e1* mediate vegetative incompatibility. Following these examples, it may thus be possible that multiple *het* alleles in *A. areolatum* from tightly linked genes act together through an allelic and/or non-allelic mechanism. It is also possible that not all of these allelic interactions will mediate vegetative incompatibility, because not all of the loci would contribute equally to the interaction or not all the alleles present at these loci would interact with each other to mediate vegetative incompatibility.

The low genetic diversity combined with asexual reproduction in *A. areolatum* in some populations of the fungus (Thomsen and Koch, 1999; Vasiliauskas and Stenlid, 1999; Slippers et al., 2001) may eventually result in inbreeding. This could happen as a result of sexual recombination between related individuals in specific regions where the diversity is low. Such an inbred population would be characterized by increased homozygosity, *i.e.* a reduction in the number of alleles at a specific locus (Charlesworth and Charlesworth, 1987; Stenlid and Vasiliauskas, 1998; Milgroom and Cortesi, 1999). It was demonstrated that such an increase in homozygosity only happens when a large percentage of the population reproduce asexually (Nauta and Hoekstra, 1996). The apparent lack of such an increase in homozygosity at the recognition loci in certain populations may be due to the fact that the forces governing evolution of the recognition loci differ from those acting on the rest of the genome (May et al., 1999; Takebayashi et al., 2004; Uyenoyama, 2004). It is believed that the recognition loci are kept diverse by evolutionary forces, such as balancing selection, that maintain a large number of alleles that are evenly distributed in a population (Richman, 2000; Muirhead et al., 2002; Takebayashi et al., 2004). Extensive population studies and detailed examination of the sexual and self-recognition systems and the loci governing them, will determine if the recognition loci in *A. areolatum* is also under selective pressure to remain diverse and if the frequency of asexual reproduction is indeed high enough to reduce the number of alleles present at the recognition loci.

The present study showed that vegetative incompatibility assays could not differentiate successfully between closely related *A. areolatum* individuals such as full siblings. This is clear from the fact that a large proportion of the *A. areolatum* siblings examined in this study (36 % for family CMW16828) were vegetatively compatible. This is consistent with the situation in some other basidiomycetes, where the capacity of VCG assays to differentiate between close relatives (e.g. siblings) is limited. For example, Barret and Uscuplic (1971) showed compatibility between 98 % of the *Phaeolus schweinitzii* siblings that they examined. The low levels of incompatibility observed between the *A. areolatum* siblings used in this study can be explained by the fact that only the two parental alleles at the *het* loci can segregate in the siblings. VCG assays allowed for the identification of a maximum of four VCGs among the offspring, even though their genomic AFLP fingerprints clearly showed that each individual is genetically unique. Application of VCG assays would therefore not be useful for determining the diversity

of *A. areolatum* populations with a low genetic diversity, because it would merely reflect the limited heterozygosity of the *het* loci (Matsumoto et al., 1996; Stenlid and Vasiliauskas, 1998; Kauserud, 2004). This inability of VCGs to distinguish between genetically different but closely related, individuals may result in an under-estimation of the genetic diversity as suggested by previous authors (Matsumoto et al., 1996; Stenlid and Vasiliauskas, 1998; Kauserud, 2004). However, the effectiveness of VCG assays is closely correlated with allelic diversity of the *het* loci which appears to be relatively high in *A. areolatum*, suggesting that VCG analysis remains a useful tool for population studies of this fungus on larger geographic scales. However, VCG assays are not selectively neutral and caution should therefore be taken when interpreting VCG data and should preferably be used in combination with selectively neutral genetic markers.

REFERENCES

Badrane, H., May, G., 1999. The divergence-homogenization duality in the evolution of the *b1* mating type gene of *Coprinus cinereus*. Mol. Biol. Evol. 16, 975-986.

Barraeau, C., Iskandar, M., Loubradou, G., Levallois, V., Bérgueret, J., 1998. The mod-A suppressor of nonallelic heterokaryon incompatibility in *Podospora anserina* encodes a proline-rich polypetide involved in female organ formation. Genetics. 149, 915-926.

Barret, D.K., Uscuplic, M., 1971. The field distribution of interacting strains of *Polyporus Schweinitzii* and their origin. New Phytol. 70, 581-598.

Bégueret, J., Turcq, B., Clavé, C., 1994. Vegetative incompatibility in filamentous fungi: *het* genes begin to talk. Trends Genet. 10, 441-446.

Bernet, J., 1992. In *Podospora anserina*, protoplasmic incompatibility genes are involved in cell death control via multiple gene interactions. Heredity. 68, 79-87.

Boidin, J., Lanquentin, P., 1984. Le genre *Amylostereum* (Basidiomycetes) intercompatibilités partielles entre espèces allopartriques. Bulletin de la Société Mycologique de France. 100, 211-236.

Casselton, L.A., Olesnicky, N.S. 1998. Molecular genetics of mating recognition in basidiomycete fungi. Micro. Mol. Biol. Rev. 62, 55-70.

Charlesworth, D., Charlesworth, B., 1987. Inbreeding depression and its evolutionary consequences. Ann. Rev. Ecol. Syst. 18, 237-268.

Coppin, E., Debuchy, R., Arnaise, S., Picard, M., 1997. Mating types and sexual development in filamentous ascomycetes. Microbiol. Mol. Biol. R. 61, 411-428.

Cortesi, P., Milgroom, M.G., 1998. Genetics of vegetative incompatibility in *Cryphonectria parasitica*. App. Environ. Microbiol. 64, 2988-2994.

Douglas, A.E., 1998. Host benefit and the evolution of specialization in symbiosis. Hered. 81, 599-603.

Frank, S.A., 1996. Host control of symbiont transmission: the separation of symbionts into germ and soma. Amer. Nat. 148, 1113-1124.

Gaut, I.P.C., 1969. Identity of the fungal symbiont of *Sirex noctilio*. Aust. J. Biol. Sci. 22, 905-914.

Gilmour, J.W., 1965. The life cycle of the fungal symbiont of *Sirex noctilio*. NZ. J. For. 10, 80-89.

Glass, N.L., Kaneko, I., 2003. Fatal attraction: Nonself recognition and heterokaryon incompatibility in filamentous fungi. Euk. Cell. 2, 1-8.

Hall, T.A., 1999. BioEdit: a user-friendly biological sequence alignment editor and analysis program for Windows 95/98/NT. Nucl. Acids. Symp. Ser. 41, 95-98.

Halsall, J.R., Milner, M.J., Casselton, L.A. 2000. Three subfamilies of pheromone and receptor genes generated multiple *B* mating specificities in the mushroom *Coprinus cinereus*. Genetics. 154, 1115-1123.

Hansen, E.M., Stenlid, J., Johansson, M., 1993. Genetic control of somatic incompatibility in the root-rotting basidiomycete *Heterobasidion annosum*. Mycol. Res. 97, 1229-1233.

Hansen, E.M., Stenlid, J., Johansson, M., 1994. Somatic incompatibility in *Heterobasidion annosum* and *Phellinus weirii*. In: Johansson M, Stenlid J (eds) Proceedings of the eight IUOFRO Root and Butt Rot Conference. Swedish University of Agricultural Sciences, Uppsala, pp 323-333

Herre, E.A., Knowlton, N., Mueller, U.G., Rehner, S.A., 1999. The evolution of mutualisms: exploring the paths between conflict and cooperation. Trends Ecol. Evol. 14, 49-53.

James, T.Y., Kües, U., Rehner, S.A., Vilgalys, R., 2004a. Evolution of the gene encoding mitochondrial intermediate peptidase and its cosegregation with the A mating type locus of mushroom fungi. Fungal Genet. Biol. 41, 381-390.

James, T.Y., Liou, S.-R., Vilgalys, R., 2004b. The genetic structure and diversity of the A and B mating type genes from the tropical oyster mushroom, *Pleurotus djamor*. Fungal Genet. Biol. 41, 813-825.

Kaneko, I., Dementhon, K., Xiang, Q., Glass, N.L., 2006. Nonallelic interactions between het-c and a polymorphic locus, *pin-c*, are essential for nonself-recognition and programmed cell death in *Neurospora crassa*. Genetics. 172, 1545-1555.

Kauserud, H., 2004. Widespread vegetative compatibility groups in the dry-rot fungus *Serpula lacrymans*. Mycol. 96, 232-239.

Kauserud, H., Saetre, G.-P., Schmidt, O., Decock, C., Schumacher, T., 2006. Genetics of self/nonself-recognition in *Serpula lacrymans*. Fungal Genet. Biol. 43, 503-510.

King, J.M., 1966. Same aspects of the biology of the fungal symbiont of *Sirex noctilio*. Aust. J. Bot. 14, 25-30.

Korb, J., Aanen, D.K., 2003. The evolution of uniparental transmission of fungal symbionts in fungus-growing termites (Macrotermitinae). Behav. Ecol. Sociobio. 53, 65-71.

Kothe, E., 1996. Tetrapolar fungal mating types: sexes by the thousands. FEMS Microbiol. Rev. 18, 65-87.

Kronstad, J.W., Staben, C., 1997. Mating type in filamentous fungi. Annu. Rev. Genet. 31, 245-76.

Kües, U., Walser, P.J., Klaus, M.J., Aebi, M., 2002. Influence of activated A and B mating-type pathways on developmental processes in the basidiomycete *Coprinus cinereus*. Mol. Genet. Genomics. 268, 262-271.

Lind, M., Stenlid, J., Olson, A., 2007. Genetics and QTL mapping of somatic incompatibility and intraspecific interactions in the basidiomycete *Heterobasidion annosum s.l.* Fungal Genet. Biol. 44, 1242-1251.

Leslie, J.F., Yamashiro, C.T., 1997. Effects of the tol mutation on allelic interactions at the *het* loci in *Neurospora crassa*. Genome. 40, 834-840.

Madden, J.L., Coutts, M.P., 1979. The role of fungi in the biology and ecology of woodwasps (Hymenoptera: Siricidae). In: Batra LR (eds) Insect-Fungus Symbiosis. John Wiley Press, New York, pp 165-174.

Mara, R.E., Milgroom, M.G., 1999. PCR amplification of the mating type idiomorphs in *Cryphonectria parasitica*. Mol. Ecol. 8, 1947-1950.

Marçais, B., Caël, O., Delatour, C., 2000. Genetics of somatic incompatibility in *Collybia fusipes*. Mycol. Res. 104, 304-310.

Matsumoto, N., Uchiyama, K., Tsushima, S., 1996. Genets of *Typhula ishikariensis* biotype A belonging to a vegetative compatibility group. Can. J. Bot. 74, 1695-1700.

May, G., Shaw, F., Badrane, H., Vekemans, X., 1999. The signature of balancing selection: fungal mating compatibility gene evolution. Proc. Natl. Acad. Sci. USA. 96, 9172-9177.

Martin, M.M., 1992. The evolution of insect-fungus associations: from contact to stable symbiosis. Amer. Zool. 32, 593-605.

Milgroom, M.G., Cortesi, P., 1999. Analysis of population structure of the chestnut blight fungus based on vegetative incompatibility genotypes. Proc. Natl. Acad. Sci. USA. 96, 10518-10523.

Muirhead, C.A., Glass, N.L., Slatkin, M., 2002. Multilocus self-recognition systems in fungi as a cause of trans-species polymorphism. Genetics. 161, 633-641.

Nauta, M.J., Hoekstra, R.F., 1996. Vegetative incompatibility in ascomycetes: highly polymorphic but selectively neutral. J. Theor. Biol. 183, 67-76.

Perkins, D.D., 1988. Main features of vegetative incompatibility in *Neurospora*. Fungal Genet. Newsl. 35, 44-46.

Rayner, A.D.M., 1991. The challenge of the individualistic mycelium. Mycol. 83, 48-71.

Richman, A., 2000. Evolution of balanced genetic polymorphism. Mol. Ecol. 9, 1953-1963.

Rizzo, D.M., Rentmeester, R.M., Burdsall, H.H., 1995. Sexuality and somatic incompatibility in *Phellinus gilvus*. Mycol. 87, 805-820.

Sambrook, J., Fritsch, E.F., Maniatis, T., 1989. Molecular Cloning: A laboratory manual, Cold Spring Harbour Laboratory Press. New York, USA.

Saupe, S.J., Turcq, B., Bégueret, J., 1995. A gene responsible for vegetative incompatibility in the fungus *Podospora anserina* encodes a protein with a GTP-binding motif and Gβ homologous domain. Gene. 162, 135-139.

Siebert, P.D., Chenchik, A., Kellog, D.E., Lukyanov, K.A., Lukyanov, S.A. 1995. An improved PCR method for walking in uncloned genomic DNA. Nucleic Acids Res. 23, 1087-1088.

Slippers, B., Coutinho, T.A., Wingfield, B.D., Wingfield, M.J., 2003. A review of the genus *Amylostereum* and its association with woodwasps. SA J. Sci. 99, 70-74.

Slippers, B., Wingfield, M.J., Coutinho, T.A., Winfield, B.D., 2001. Population structure and possible origin of *Amylostereum areolatum* in South Africa. Plant. Pathol. 50, 206-210.

Steel, R.G., Torrie, J.H., Dickey, D.A., 1997. Principles and procedures of statistics, A biometrical approach. McGraw-Hill, New York.

Steenkamp, E.T., Wingfield, B.D., Coutinho, T.A., Zeller, K.A., Wingfield, M.J., Marasas, W.F.O., Leslie, J.F., 2000. PCR-based identification of MAT-1 and MAT-2 in the *Gibberella fujikuroi* species complex. Appl. Environ. Microbiol. 66, 4378-4382.

Steenkamp, E.T., Wright, J., Baldauf, S.L., 2006. The protistan origins of animals and fungi. Mol. Biol. Evol. 23, 93-106.

Stenlid, J., Vasiliauskas, R., 1998. Genetic diversity within and among vegetative compatibility groups of *Stereum sanguinolentum* determined by arbitrary primed PCR. Mol. Ecol. 7, 1265-1274.

Takebayashi, N., Newbigin, E., Uyenoyama, M.K., 2004. Maximum-likelihood estimation of rates of recombination within mating type regions. Genetics. 167, 2097-2109.

Talbot, P.H.B., 1977. The *Sirex-Amylostereum-Pinus* association. Ann. Rev. Phytopathol. 15, 41-54.

Thomsen, I.M., 1998. Characters of fruitbodies, basidiospores and cultures useful for recognizing *Amylostereum areolatum* and *Amylostereum chailletii*. Mycotaxon. 69, 419-428.

Thomsen, I.M., Koch, J., 1999. Somatic incompatibility in *Amylostereum areolatum* and *A. chialletii* as a consequence of symbiosis with siricid woodwasp. Mycol. Res. 103, 817-823.

Turgeon, G., Yoder, O.C., 2000. Proposed nomenclature for mating type genes of filamentous ascomycetes. Fungal Genet. Biol. 31, 1-5.

Uyenoyama, M.K., 2004. Evolution under tight linkage to mating type. New Phytol. 165, 63-70.

Vasiliauskas, R., Stenlid, J., 1999. Vegetative compatibility groups of *Amylostereum areolatum* and *A. chialletii* from Sweden and Lithuania. Mycol. Res. 103, 824-829.

Vasiliauskas, R., Stenlid, J., Thomsen, I.M., 1998. Clonality and genetic variation in *Amylostereum areolatum* and *A. chailletii* from northern Europe. New Phytol. 139, 751-758.

Vos, P., Hogers, R., Bleeker, M., Reijans, M., van de Lee, T., Hornes, M., Friters, A., Pot, J., Paleman, J., Kuiper, M., Zabeau, M., 1995. AFLP: A new technique for DNA fingerprinting. Nucleic Acids Res. 23, 4407-4414.

Worrall, J.J., 1997. Somatic incompatibility in Basidiomycetes. Mycologia. 89, 24-36.

Yokoyama, E., Yamagishi, K., Hara, A., 2004. Development of a PCR-based mating type assay for *Clavicipitaceae*. FEMS Microbiol Letters. 237, 205-212.

Zhou, X.D., De Beer, Z.W., Ahumada, R., Wingfield, B.D., Wingfield, M.J., 2004. Ophiostomatoid fungi associated with two pine-infesting bark beetles from Chile. Fungal Div. 15, 253-266.

FIGURES

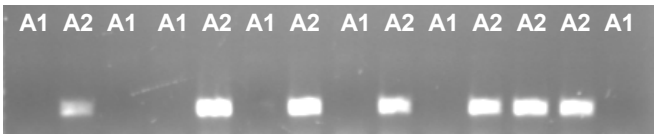

Figure 1. Segregation of the putative mitochondrial intermediate peptidase (*mip*) gene fragment among CMW16828$_{[n]}$ and CMW16848$_{[n]}$ progeny. Application of primers MIPAro1F and MIPAro1R in PCR generates ~350 bp products only in those isolates designated as harboring the A1 allele of locus *mat-A*.

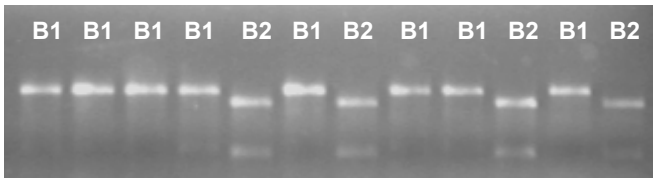

Figure 2. Segregation of the putative pheromone receptor *RAB1* PCR-RFLP fragments among CMW16828$_{[n]}$ and CMW16848$_{[n]}$ progeny. The 845 bp amplified portion of the *RAB1* allele linked to mating type B2 is digested into two fragments of sizes 652 and 193 bp, while the 845 bp amplified portion of the *RAB1* allele linked to mating type B1 is undigested.

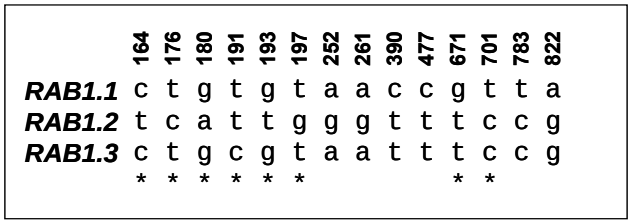

Figure 3. Polymorphic nucleotide sites associated with the 845 bp portion of the putative pheromone receptor RAB1 of *A. areolatum*. The respective *RAB1* alleles are indicated to the left of the nucleotides and their positions are indicated at the top. Eight of these polymorphisms are located in putative introns (indicated with *), while those located in the exons represent synonymous substitutions. The diagnostic *Eco*RV restriction site that distinguishes *RAB1.1* from the other two alleles is located at postion 193.

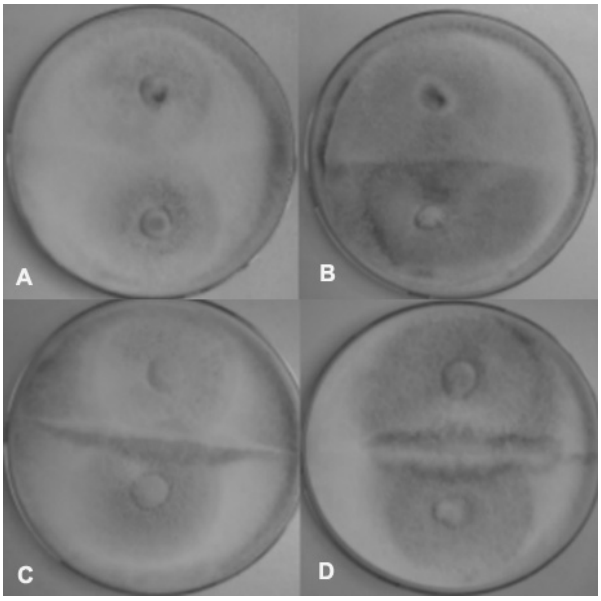

Figure 4. The outcome of vegetative compatibility interactions between sib-related heterokaryons CMW16848$_{[n]}$ x CMW16828$_{[1]}$. A: Compatible interactions was scored as 0 when the hyphae of the interacting heterokaryons behaved as one confluent mycelium. B: Weakly incompatible interactions were scored as 1 when a thin demarcation line was visible between the interacting heterokaryons. C: Strongly vegetative incompatible interactions were scored as 2 when thinning and pigmentation of the interacting mycelium occurred in either one of the heterokaryons. D: Strongly vegetative incompatible interactions were also scored as 2 when the thinning and pigmentation of mycelium occurred in both of the heterokaryons.

TABLES

Table 1. Origin of *Amylostereum areolatum* heterokaryons used in this study.

Isolate number [a]	**Geographic origin**	**Collector**	***RAB1* allele/s** [b]
CMW16828	Austria	B. Slippers	*RAB1.1*
CMW16848	Austria	B. Slippers	*RAB1.1*; *RAB1.2*
CMW8900	South Africa	B. Slippers	*RAB1.2*; *RAB1.3*
CMW8898	Brazil	B. Slippers	*RAB1.2*; *RAB1.3*
CMW3300	New Zealand	G.B. Rawlings	*RAB1.2*; *RAB1.3*
CMW28217	Lithuania	R. Vasaitis	*RAB1.1*; *RAB1.2*
CMW28219	Lithuania	R. Vasaitis	*RAB1.1*
CMW28225	Denmark	I.M. Thomsen	*RAB1.1*; *RAB1.3*
CMW28221	Norway	H. Solheim	*RAB1.1*; *RAB1.3*
CMW28223	Switzerland	O. Holdenrieder	*RAB1.2*
CMW28224	Switzerland	O. Holdenrieder	*RAB1.2*; *RAB1.3*

[a] CMW (Culture collection of the Tree Pathology Co-operative Programme, University of Pretoria, South Africa).

[b] *RAB1* alleles in each isolate was identfied using DNA-based assays (Fig. 2) and sequence analysis.

Table 2. Vegetative incompatibility between sib-related and siblings heterokaryons.

Heterokaryons paired	Number of pairings [e]	Pairings rated as % [f]		
		0	1	2
Sib-related heterokaryons				
$CMW16848_{[n]}$ x $CMW16828_{[1]}$ [a]	129	22	59	19
$CMW16828_{[n]}$ x $CMW16848_{[57]}$ [b]	132	27	54	19
Sibling heterokaryons				
$CMW16848_{[n]}$ x $CMW16848_{[n]}$ [c]	166	22	66	12
$CMW16828_{[n]}$ x $CMW16828_{[n]}$ [d]	132	36	55	9

[a] Sib-related heterokaryons obtained by pairing homokaryons obtained from fruiting body CMW16848 with unrelated homokaryon $CMW16828_{[1]}$ obtained from fruiting body CMW16828.

[b] Sib-related heterokaryons obtained by pairing homokaryons obtained from fruiting body CMW16828 with unrelated homokaryon $CMW16848_{[57]}$ obtained from fruiting body CMW16848.

[c] Sibling heterokaryons obtained by pairing two homokaryons obtained from fruiting body CMW16848.

[d] Sibling heterokaryons obtained by pairing two homokaryons obtained from fruiting body CMW16828.

[e] Excluding self pairings.

[f] 0: compatible reaction, 1: weak incompatible reaction and 2: strong incompatible reaction.

Table 3. Vegetative incompatibility between sib-related heterokaryons CMW16848$_{[n]}$[a] x CMW16828$_{[1]}$.

	Strain	*mat* alleles [b]	VCG[c]	*het* alleles [d]	1	2	3	4	5	6	7	8	9	10	11	12	13	14	15	16	17	18
1:	41	A1B1	G1	1a2a	"																	
2:	30	A1B1	G1	1a2a	0	"																
3:	55	N	G2	1a2b	0	0	"															
4:	60	A2B2	G2	1a2b	0	1	0	"														
5:	14	A2B1	G2	1a2b	0	0	1	0	"													
6:	77	A1B2	G2	1a2b	0	0	1	1	1	"												
7:	57	A1B1	G2	1a2b	0	1	1	0	1	0	"											
8:	38	A2B2	G2	1a2b	1	0	1	1	1	N	1	"										
9:	43	A2B1	G2	1a2b	N	N	1	N	1	1	1	1	"									
10:	58	A2B1	G2	1a2b	1	1	1	1	1	1	1	1	1	"								
11:	59	A2B2	G3	1b2b	2	1	1	1	1	1	1	1	1	1	"							
12:	87	A1B2	G3	1b2b	2	2	1	1	1	1	1	1	1	1	1	"						
13:	42	A2B2	G3	1b2b	2	1	1	1	0	1	0	1	1	1	1	1	"					
14:	12	A1B2	G3	1b2b	2	2	1	1	0	1	1	1	1	1	1	1	1	"				
15:	23	A1B1	G3	1b2b	2	2	1	0	1	1	1	1	1	1	1	0	1	1	"			
16:	5	A1B1	G3	1b2b	2	1	2	0	1	0	1	2	1	1	N	1	1	0	1	"		
17:	3	A2B1	G4	1b2a	0	N	2	2	2	2	1	N	1	2	1	1	1	0	0	0	"	
18:	25	A1B2	G4	1b2a	1	2	2	2	2	2	2	2	2	2	1	1	1	0	0	1	0	"

[a] Heterokaryons were obtained from a pairing between a homokaryon obtained from fruiting body of family CMW16848$_{[n]}$ with an unrelated homokaryon CMW16828$_{[1]}$ obtained from fruiting body of family CMW16828.

[b] Sib-related heterokaryons of family CMW16848 could be separated into four mating type groups based on microscopy and DNA-based assays (Fig.s 1and 2). The mating type groups represent the four different alleles of the two loci controlling mating in *A. areolatum*, with alleles A1 and A2 at locus *mat-A* and alleles B1 and B2 of locus *mat-B*. The *mat*-alleles for strain CMW16848$_{[55]}$ were not determined.

[c] Sib-related heterokaryons of family CMW16828 could be separated into four VCGs based on strong incompatibility, sib-related heterokaryons in VCG 1 were strongly incompatible with sib-related dikaryons in VCG3 while those in VCG 2 were strongly incompatible with the heterokaryons in VCG 4. Interactions that could not be clearly assigned as 0, 1 or 2 (Table 2) are indicated with "N".

[d] The four different alleles (1a and 1b at locus *het-1* and alleles 2a and 2b of locus *het-2*) present at the two *het* loci in *A. areolatum* were arbitrary assigned to the four VCGs, with alleles 1a2a assigned to VCG 1, alleles 1b2b assigned to VCG 3, alleles 1a2b assigned to VCG 2 and alleles 1b2a assigned to VCG 4.

Table 4. Vegetative incompatibility between sib-related heterokaryons CMW16828$_{[n]}$[a] x CMW16848 [57].

	Strain	*mat* alleles[b]	VCG[c]	*het* alleles[c]	1	2	3	4	5	6	7	9	8	10	11	12	13	14	15	16	17	18
1:	10	A3B4	G5	A3B3	-																	
2:	1	A4B4	G6	A3B4	1	-																
3:	16	A3B3	G6	A3B4	1	1	-															
4:	18	A3B4	G6	A3B4	N	1	1	-														
5:	2	A4B4	G6	A3B4	1	1	1	1	-													
6:	15	A4B4	G6	A3B4	1	1	1	1	1	-												
7:	6	A3B3	G6	A3B4	1	1	1	1	1	1	-											
8:	13	A4B4	G6	A3B4	0	1	0	1	1	1	1	-										
9:	19	N	G7	A4B4	1	1	0	1	0	N	0	1	-									
10:	8	A3B3	G7	A4B4	0	0	0	1	1	1	0	1	1	-								
11:	7	A4B3	G7	A4B4	2	1	1	1	N	1	1	1	1	1	-							
12:	11	A4B3	G7	A4B4	2	N	1	1	1	1	1	1	0	1	0	-						
13:	17	A4B4	G7	A4B4	2	1	1	2	0	1	1	1	0	1	1	1	-					
14:	12	A3B3	G7	A4B4	2	2	0	1	1	0	1	0	0	1	1	0	1	-				
15:	4	A3B4	G7	A4B4	2	2	2	2	1	1	0	0	1	0	0	0	1	1	-			
16:	5	N	G7	A4B4	2	2	2	2	2	1	1	1	1	1	0	1	0	1	1	-		
17:	3	A4B4	G7	A4B4	1	1	2	2	2	0	1	1	1	1	1	0	1	1	0	1	-	
18:	14	A3B3	G8	A4B3	2	2	2	2	2	2	2	1	1	0	0	0	0	0	0	0	0	-

[a] Heterokaryons were obtained from a pairing between homokaryons obtained from fruiting body of family CMW16828$_{[n]}$ with an unrelated homokaryon CMW16848 $_{[57]}$ obtained from fruiting body of family CMW16848.

[b] Sib-related heterokaryons of family CMW16848 could be separated into four mating type groups based on microscopy and DNA-based assays (Fig.s 1and 2). The mating type groups represent the four different alleles of the two loci controlling mating in *A. areolatum*, with alleles A3 and A4 at locus *mat-A* and alleles B3 and B4 of locus *mat-B*. The *mat*-alleles for strain CMW16828$_{[19]}$ and strain CMW16828$_{[5]}$ were not determined.

[c] Sib-related heterokaryons of family CMW16828 could be separated into four VCGs based on strong incompatibility, sib-related heterokaryons in VCG 5 were strongly incompatible with sib-related dikayons in VCG 7 while those in VCG 6 were strongly incompatible with the heterokaryons in VCG 8. Interactions that could not be clearly assigned as 0, 1 or 2 (Table 2) are indicated with "N".

[d] The four different alleles (1c and 1d at locus *het-1* and alleles 2c and 2d of locus *het-2*) present at the two *het* loci in *A. areolatum* were arbitrary assigned to the four VCGs, with alleles 1c2c assigned to VCG 5, alleles 1d2d assigned to VCG 7, alleles 1c2d assigned to VCG 6 and alleles 1d2c assigned to VCG 8.

Tab le 5. Vegetative incompatibility between the sibling heterokaryons of family CMW16848[a].

	Strains	Homokaryon Group [b]	1	2	3	4	5	6	7	8	9	10	11	12	13	14	15	16	17	18	19
1:	42x41	G3G1	"																		
2:	59x30	G3G1	0	"																	
3:	59x41	G3G1	0	1	"																
4:	42x30	G3G1	0	0	1	"															
5:	3x55	G4G2	1	1	1	0	"														
6:	14x25	G2G4	1	1	1	0	1	"													
7:	3x77	G4G2	1	1	1	0	0	1	"												
8:	58x25	G2G4	1	0	1	1	0	0	1	"											
9:	3x25	G4G4	1	1	1	1	1	1	1	0	"										
10:	60x30	G2G1	1	0	1	0	0	1	0	1	1	"									
11:	60x41	G2G1	1	1	0	1	1	1	1	1	1	1	"								
12:	38x41	G2G1	1	N	1	1	1	1	1	1	1	0	1	"							
13:	59x5	G2G3	0	0	1	1	1	0	1	0	1	0	0	1	"						
14:	38x5	G2G3	1	1	0	1	1	1	1	1	1	1	1	1	1	"					
15:	38x23	G2G3	1	1	1	1	1	1	0	1	1	1	1	1	1	1	"				
16:	14x55	G2G2	0	0	0	1	1	N	1	1	1	1	0	1	0	1	1	"			
17:	58x55	G2G2	0	0	0	N	2	2	1	1	2	0	1	1	1	1	1	1	"		
18:	14x77	G2G2	2	2	2	2	2	2	2	2	N	1	1	1	0	1	1	1	N	"	
19:	58x77	G2G2	2	2	2	2	2	2	2	2	2	1	1	1	1	1	1	1	1	0	"

[a] Sibling heterokaryons obtained from pairing between two homokaryons from the CMW16848 basidiocarp.

[b] Homokaryons isolated from basidiocarp CMW16848 separated into four VCGs based on strong incompatibility (Table 3). Interactions that could not be clearly assigned as 0, 1 or 2 (Table 2) are indicated with “N”.

Table 6. Vegetative incompatibility between the sibling heterokaryons of family CMW16828 [a].

	Strains	Homokaryon Group [b]	1	2	3	4	5	6	7	8	9	10	11	12	13	14	15	16	17	18
1:	1x16	G6G6	-																	
2:	2x16	G6G6	1	-																
3:	12x17	G7G7	1	1	-															
4:	3x12	G7G7	1	1	0	-														
5:	4x7	G7G7	1	1	1	0	-													
6:	16x3	G6G7	2	N	1	0	0	-												
7:	2x12	G6G7	2	1	1	0	0	0	-											
8:	2x8	G6G7	0	1	1	0	0	0	0	-										
9:	16x17	G6G7	1	1	1	0	0	0	0	0	-									
10:	8x13	G7G6	1	1	1	1	1	1	1	1	1	-								
11:	6x17	G6G7	1	1	1	1	0	1	1	0	1	0	-							
12:	1x8	G6G7	1	1	1	1	1	1	1	2	1	1	1	-						
13:	8x17	G7G7	1	1	0	N	1	1	0	1	1	0	0	0	-					
14:	3x8	G7G7	1	0	1	N	1	1	1	1	1	0	0	0	0	-				
15:	3x14	G6G7	2	2	1	0	1	1	1	1	1	1	0	0	1	0	-			
16:	14x17	G8G7	2	2	1	1	1	1	1	1	1	1	0	2	0	0	0	-		
17:	14x15	G8G7	2	2	N	1	0	1	1	1	0	0	1	1	0	0	0	0	-	
18:	2x14	G5G8	2	2	1	0	1	0	0	0	1	1	1	1	1	1	1	1	0	-

[a] Sibling heterokaryons obtained from pairing between two homokaryons from the CMW16828 basidiocarp.

[b] Homokaryons obtained from basidiocarp CMW16828 separated into four VCGs based on strong incompatibility (Table 4). Interactions that could not be clearly assigned as 0, 1 or 2 (Table 2) are indicated with "N".

CHAPTER 4

Genetic linkage map for *Amylostereum areolatum* reveals an association between vegetative growth and sexual and self recognition

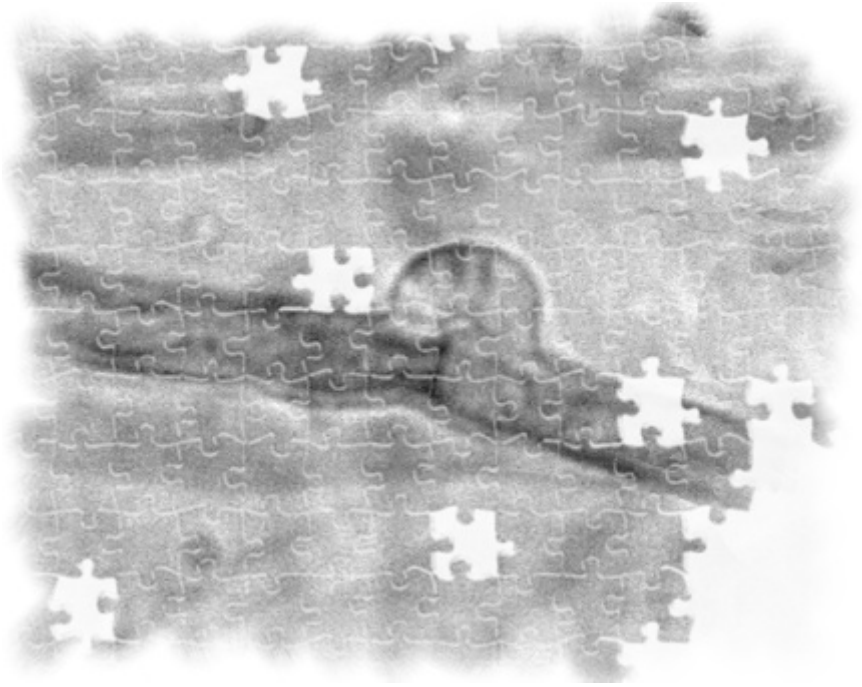

Published as: van der Nest, M.A., Slippers, B., Steenkamp, E.T., de Vos, L., van Zyl, K., Stenlid, J., Wingfield, M.J., Wingfield, B.D. 2009. Genetic linkage map for *Amylostereum arolatum* reveals an association between vegetative growth and sexual and self recognition. *Fungal Genetics and Biology* 46:632-641.

TABLE OF CONTENTS

ABSTRACT

Amylostereum areolatum is a filamentous fungus that grows through tip extension, branching and hyphal fusion. In the homokaryotic phase, the hyphae of different individuals are capable of fusing followed by heterokaryon formation, only if they have dissimilar allelic specificities at their mating type (*mat*) loci. In turn, hyphal fusion between heterokaryons persists only when they share the same alleles at all of their heterokaryon incompatibility (*het*) loci. In this study we present the first genetic linkage map for *A. areolatum*, onto which the *mat* and *het* loci, as well as quantitative trait loci (QTLs) for mycelial growth rate are mapped. The recognition loci (*mat-A* and *het-A*) are positioned near QTLs associated with mycelial growth, suggesting that the genetic determinants influencing recognition and growth rate in *A. areolatum* are closely associated. This was confirmed when isolates associated with specific *mat* and *het* loci displayed significantly different mycelial growth rates. Although the link between growth and sexual recognition has previously been observed in other fungi, this is the first time that an association between growth and self recognition has been shown.

INTRODUCTION

The sexual and self/nonself recognition systems of fungi and other eukaryotes such as animals and plants have been extensively studied (Nauta and Hoekstra, 1994). In filamentous fungi, sexual recognition is controlled by the genes encoded at the mating type (*mat*) loci (e.g., Casselton, 2002), while self/nonself recognition is controlled by the genes encoded at the heterokaryon incompatibility (*het*) loci (e.g., Worral, 1997; Glass et al., 2000). Although the recognition systems in plants and animals are well-characterized at the genomic and functional levels (Awadalla and Charlesworth, 1999; Meyer and Thomsen, 2001), the recognition systems in fungi have received less attention. Only a few *het* genes have been characterized at the DNA level and these have been limited to the model ascomycetes *Neurospora crassa* and *Podospora anserina* (e.g., Glass et al., 2000; Saupe, 2000). To date, no basidiomycete *het* genes have been identified. With respect to sexual recognition, the genomic and functional aspects of ascomycete *mat* loci are relatively well understood, while studies of the *mat* loci of basidiomycetes have been limited to the models *Schizophyllum commune*, *Coprinopsis cinerea* and *Ustilago maydis* (e.g. Casselton, 2002).

In this study we considered the sexual and self/nonself recognition systems of the white rot fungus *Amylostereum areolatum* (Homobasidiomycetes, Basidiomycotina). *Amylostereum areolatum* lives in a mutualistic association with various woodwasp species (e.g., *Sirex noctilio*) (Slippers et al., 2003). This partnership is thought to influence the reproductive mode of the fungus, because fungal asexual spores are effectively spread by the woodwasp (Slippers et al., 2003; van der Nest et al., 2008). This asexual mode of reproduction, therefore, serves to explain the overall low genetic heterogeneity of the fungus, as well as the fact that fruiting bodies for *A. areolatum* are rarely found in nature (van der Nest et al., 2008). A*mylostereum areolatum* thus represents a unique model for studying recognition systems as it has an interesting life cycle that involves a unique interplay between sexual and asexual reproduction.

Sexual recognition in *A. areolatum* is controlled by a tetrapolar mating system where two unlinked *mat* (*mat-A* and *mat-B*) loci determine the outcome of sexual interactions (van der Nest et al., 2008). Homokaryons that are genetically distinct with different allelic specificities at both of their *mat* loci are sexually compatible and will allow reciprocal nuclear migration after cell fusion to form a heterokaryon (Casselton, 2002). In the homobasidiomycete model fungi *C.*

cinerea and *S. commune*, the *mat-A* locus encodes homeodomain transcriptional factors, while the *mat-B* locus encodes pheromones and pheromone receptors that control heterokaryon formation (Casselton, 2002). Despite these similarities, the *mat* loci of *C. cinerea* and *S. commune* differ, especially in terms of the number of sub-loci and the amount of recombination between sub-loci (James et al., 2004). However, little is known for the *mat*-loci of non-model homobasidiomycetes. This is also true for *A. areolatum*, where knowledge regarding the loci determining sexual recognition is restricted to putative genes that have been identified at the *mat-B* locus and near the *mat-A* locus of the fungus (*i.e.*, *RAB1* pheromone receptor and *MIP* mitochondrial intermediate peptidase genes, respectively) (van der Nest et al., 2008).

As is the case in other homobasidiomycetes, *A. areolatum* has at least two *het* loci (van der Nest et al., 2008), which is in contrast to the multiplicity of *het* loci found in ascomycetes. For example, the homobasidiomycetes *Phellinus weiriii, Serpula lacrymans* and *Heterobasidion annosum* have one, two and three/four *het* loci, respectively (Lind et al., 2007), while *N. crassa* has at least eleven *het* loci and *P. anserina* at least nine *het* loci (Glass et al., 2000; Saupe, 2000). In general, if two heterokaryons meet in nature, their mycelia will merge, although hyphal anastomoses only persists when the interacting heterokaryons are genetically similar, sharing identical alleles at all of their *het* loci (Worrall, 1997). When the interacting heterokaryons have different alleles at some or all of their *het* loci, cell death prevents anastomosis and a zone of inhibition forms between the interacting heterokaryons. In general, it is thought that vegetative incompatibility plays a role in preserving genetic identity and preventing the spread of mycoviruses, debilitated organelles and deleterious plasmids (Worral, 1997). However, the precise biological significance of this phenomenon is still largely unclear, and a deeper understanding of how and why vegetative incompatibility evolved, will require comparative studies of the *het* loci of many diverse fungi.

The overall goal this study was to establish a genetic foundation from which to eventually study the structure, organization and evolution of the recognition loci of *A. areolatum*. This entailed construction of a genetic linkage map for *A. areolatum* and positioning of its recognition loci, as have been done for other eukaryotes (e.g., Kubisiak and Milgroom, 2006; Lind et al., 2007; Leppälä et al., 2008). For this purpose we used amplified fragment length polymorphisms (AFLPs) (Vos et al., 1995) for map construction and AFLP-based bulked segregant analysis (BSA) to identify markers closely linked to the recognition loci. We also compared marker

distribution and segregation ratio distortions associated with markers linked to the recognition loci, with those associated with the rest of the genome. This was particularly relevant because it has previously been shown that the recognition loci are subject to evolutionary forces that are markedly different from those acting on the rest of the genome (e.g., Meyer and Thomson, 2001; Takebayashi et al., 2004; Uyenoyama, 2005). A final objective was to use the map to reveal a possible association between the recognition loci and the genes involved in fitness, as has been shown for other homobasidiomycetes (e.g., Callac et al., 1997; Larraya et al., 2001; Larraya et al., 2002; Olson 2006). This was accomplished by identifying putative quantitative trait loci (QTLs) linked to mycelial growth rate as a measure of fitness (Hill and Otto, 2007) and determining whether or not they are associated with the recognition loci of *A. areolatum*.

MATERIALS AND METHODS

Isolates and growth conditions

Eighty homokaryotic isolates that were obtained from an *A. areolatum* basidiocarp (van der Nest et al., 2008) collected in Austria were used for segregation analysis. Working cultures of the parent strain (CMW16848) and homokaryons (CMW16848$_{[1\text{-}80]}$) were maintained on pine extract medium as previously described (van der Nest et al., 2008).

AFLP and BSA analysis

DNA was isolated from cultures (van der Nest et al., 2008) and stored at -20 °C. The AFLP procedure described by De Vos et al. (2007) using a 20 primer pairs was followed and AFLP fragments were visualized using the 4200 LI-COR® automated DNA sequencer as described by Myburg et al. (2001). To ensure that the AFLP profiles used in this study were reproducible, we repeated the AFLP procedure using DNA isolated from eight individuals. AFLP fragments were scored as present (coded as 'A') or absent (coded as 'H') using QUANTAR Version 1.0 (KeyGene Products B.V., The Netherlands). Each fragment that segregated in the progeny was treated as an independent genetic locus. As previously proposed (Bagley et al., 2001), we ensured that our scoring of the polymorphic bands segregating in the progeny was repeatable, by excluding bands with low intensity, bands with very high and low molecular weight and bands that were inordinately close to each other and thus complicating their accurate scoring. Bands were also rescored manually several times to ensure that they had been scored correctly. The *mat* and *het* alleles that segregated in the mapping population were identified in a previous study using hyphal morphology and DNA-based assays (van der Nest et al., 2008). It is possible that additional *het* loci exist in *A. areolatum*, but we could only identify two *het* loci segregating in the mapping population. The two *mat* and the two *het* loci were each treated as 4 markers segregating in the progeny.

BSA was used to identify additional AFLP markers that were closely linked to any of the *mat* or *het* loci. For this purpose 8 AFLP template pools consisting of equal amounts of DNA from 15 different progeny sharing unique *mat* or *het* alleles were subjected to AFLP analysis. Templates 1, 2, 3 and 4 contained DNA from progeny sharing the *mat-A1*, *mat-A2*, *mat-B1* and *mat-B2* alleles, respectively. Templates 5, 6, 7 and 8 contained DNA from progeny sharing the *het-A1*,

het-A2, *het-B1* and *het-B2* alleles, respectively. Thirty one AFLP primer pairs were tested on the 8 pools to identify possible markers linked to the loci of interest. Four primer pairs that generated fragments potentially linked to any of the *mat* or *het* loci were chosen for analysis in the entire mapping population. These fragments were scored as described above and included during map construction.

Framework map construction

Joinmap® 3.0 (Van Ooijen and Voorrips, 2001) was used for map construction and for graphical representation of the linkage groups. This program uses likelihood of odds (LOD) scores of recombination frequencies to assemble pairwise marker associations and then constructs maps of these groupings using a modified squares method, in which the squares of the LOD scores are used as weights (Van Ooijen and Voorrips, 2001). The Kosambi mapping function (Kosambi, 1944) was used to convert recombination fractions into map distances. Since it was not possible to distinguish between the parental genotypes that generated the original basidiocarp or heterokaryon, the data were coded as HAP, *i.e.*, haploid originating from a diploid parent with unknown linkage phase. Initial linkage groups were determined based on a LOD threshold value between 2.0 and 10.0 and a recombination ratio upper threshold of 0.45 in the pairwise comparison. The LOD scores used by JoinMap are based on χ^2 tests for independence of segregation and markers with high χ^2-contribution to a linkage group were excluded from the analysis as they could have resulted in a poor fit and a significant disturbance of map order across the linkage group (Staelens et al., 2008). All the markers, including those showing segregation distortion ($\alpha = 0.05$), were included and evaluated during linkage map construction.

The total genome length of the framework map was estimated using the Hulbert estimate, $E(G) = n(n-1)X/K$, where n is the number of loci, X is the maximum map distance between locus pairs above a minimum LOD value for linkage grouping (Z), and K is the number of locus pairs above Z (Hulbert et al., 1988). The linkage threshold of LOD 3.0 (Z) was used to estimate genome length as the mapping set was separated into different linkage groups at this threshold. For a Z-value of 3, both X and K were obtained from the list of values generated by the 'big Lods' command of the program MAPMAKER Macintosh V2.0 (Lander et al., 1987). Theoretical genome coverage was estimated using the formula, $C = 1\text{-}e^{-2dn/L}$, where C is the proportion of the genome within d cM (centimorgan) of a marker, L is the estimated genome length and n is the

number of markers (Remington et al., 1999).

Marker distribution and haplotype analysis

Marker distribution between different linkage groups was evaluated by comparing the actual marker density with what would be expected under a Poisson distribution (Remington et al., 1999). For this purpose, each linkage group had a length $Gi = Mi + 2s$, where Mi is the map distance between terminal markers of the i_{th} linkage group, and s is the average marker spacing calculated by dividing the summed length of all maps by the number of marker intervals. Where the underlying marker density was the same for all linkage groups, the number of markers (mi) in the $_{ith}$ linkage group would be a sample from a Poisson distribution with parameter, $\lambda_i = mG_i/\Sigma iG_i$, where m is the total number of markers. Here, the null hypothesis requires that there is equal marker density in each of the linkage groups (Remington et al., 1999).

The number of crossovers per linkage group per individual was estimated by visualizing the haplotypes of the individuals using the Graphical GenoTyping software (GGT) (Van Berloo, 1999) and counting the number of observed crossovers. Double-crossovers flanking a single marker-locus were not included in the estimate because their occurrence within short intervals could suggest genotyping errors or they could have resulted from gene conversion during local DNA repair (Shibata, 2001). The distribution of crossovers in the 10 major linkage groups were examined by performing a two-tailed test in Statistica Version 7.1 (www.statsoft.com) to determine whether the distribution of crossovers in the linkage groups follow a Poisson distribution.

Mycelial growth estimation and QTL identification

The mycelial growth rate of the 80 homokaryotic *A. areolatum* isolates used in this study was determined by taking a plug of mycelium from the edge of an actively growing culture on potato dextrose agar (Biolab, Johannesburg, South Africa) and placing these at the centres of 90 mm Petri dishes. After 7 days of incubation at 25 °C in the dark, the radial extension of each colony was measured along two perpendicular axes. Average colony diameter, standard deviation and analysis of variance (ANOVA) were determined using Statistica. Three repetitions per progeny were made with the mean mycelial growth based on 6 measurements being used for QTL analysis. Individual observed broad-sense heritability (H^2) which serves as an indication of the

extent to which mycelial growth of individuals is linked to a genotype, were determined using the equation $H^2 = \sigma^2_G/\sigma^2_p$ where σ^2_G= genotypic variance and σ^2_p = phenotypic variance (Falconer, 1989).

Map Manager QTX version b20 (Manly et al., 2001) was utilized to identify markers significantly associated with mycelial growth rate at 25 °C. Markers with segregation distortion were included in all of the analyses, using the Map Manager QTX "allow for segregation distortion" function. Significance levels for highly significant, significant and suggestive QTLs were determined with 1000 permutations using 1 cM steps. Simple interval mapping (SIM) was used to determine the likelihood for the presence of a segregating QTL for every 1 cM of the *A. areolatum* linkage map, while composite interval mapping (CIM) was used to establish the effect of QTL combinations. Likelihood ratio statistic (LRS) values were converted into LOD values by a direct transformation using the equation LRS = 4.6 X LOD (Liu, 1998). Primary QTLs were identified when SIM and CIM values coincided and exceeded the permuted test statistic thresholds for SIM, while secondary QTLs were identified when either the SIM or CIM scan exceeded the permuted SIM test statistic threshold (Thomas et al., 1998). Statistica was used to perform t-tests to determine if there were significant differences in mycelial growth of homokaryons that have different alleles at the loci associated with QTLs for mycelial growth.

RESULTS

AFLP and BSA analysis

AFLP analysis was performed on DNA of the *A. areolatum* parent heterokaryon, as well as the 80 selected homokaryons using 20 different primer combinations (Table 1). Of the 31 AFLP primer combinations evaluated for BSA, only 4 (Table 1) generated AFLP fragments that were potentially linked to recognition loci. The analysis of these on the entire mapping population revealed five markers that apparently co-segregated with the loci of interest. One of these AFLP markers (at14399) segregated with the *het-A* locus and one (ac16085) with the *het-B* locus. One AFLP marker (cc13153) segregated with *mat-A*, while two markers (ac10290 and ac16260) segregated with the *mat-B* locus. However, none of these markers co-segregated consistently with the various recognition loci in the progeny.

For each of the 24 primer combinations, an average of 10 polymorphic AFLP bands was identified, with a total of 245 polymorphic bands across all primer combinations (Table 1). The primer pair *Eco*RI(+tc) + *Mse*I(+aa) gave the largest number of polymorphic AFLP fragments (18), while the primer pairs *Eco*RI(+at) + *Mse*I(+ct) and *Eco*RI(+ac) + *Mse*I(+cc) gave the smallest number of polymorphic AFLP fragments (3) (Table 1). Identical profiles were generated when the AFLP procedure was repeated on DNA isolated from eight selected progeny, supporting previous views regarding the repeatability of AFLPs (Myburg et al., 2001).

Framework map construction

JoinMap® 3.0 generated a framework map consisting of 151 AFLP markers (including those identified using BSA) distributed over 10 major linkage groups with more than 7 markers (Fig. 1). Another 49 linked AFLP markers mapped to 15 minor linkage groups containing 2-6 loci. Of the segregating markers, 81.6 % mapped to the 10 major and 15 minor linkage groups, while 18.4 % (45) of the markers did not map to any of the linkage groups. The 10 major linkage groups ranged in size from 164 cM (linkage group LG1) to 65 cM (linkage group LG10). The four recognition loci (*mat-A* and *mat-B*; *het-A* and h*et-B*) mapped on separate linkage groups. As expected, the specific marker(s) identified using BSA was also closely linked to the respective recognition loci. The total observed length of the map when only including the 10 major linkage groups with 151 AFLP markers and the four recognition loci was 1046 cM with an average

distance between markers of 7.2 cM (Table 2). The largest mapped distance between markers was 26 cM for linkage group LG3. The total observed length of the map including the minor and major linkage groups with 204 markers was 1693 cM with an average distance between markers of 8.3 cM.

Genome length (Hulbert et al., 1988) was estimated as 2922.6 cM. Based on this estimate, the theoretical genome coverage was calculated where 67.2 % of the markers were ≤10 cM apart and 89.3 % of the markers were ≤20 cM apart (Table 2). Because the physical genome size of *A. areolatum* is unknown, the genome size (33.7 Mbp) of a related fungus, *H. annosum* (http://genome.jgi-psf.org), was used. Accordingly, the physical distance per unit of recombination was estimated as 32.2 kbp/cM for the major linkage groups and 19.9 kbp/cM for all of the linkage groups. With the physical distance per genetic distance estimated as 19.9 kbp/cM, marker at14399 would theoretically be positioned 119.4 kbp from locus *het-A*, and marker ac16085 would be positioned 119.4 kbp from locus *het-B*. Markers cc13153 and aa10340 would be positioned 99.5 kbp and 59.7 kbp, respectively from locus *mat-A*, while marker ac10290 would be positioned 119.4 kbp from locus *mat-B*. With the exception of aa10340 all these markers were identified using BSA.Marker distribution and haplotype analysis

χ^2-analysis indicated that 29.2 % of the AFLP markers (44 of the 151 markers) that were placed on the map, showed significant segregation distortion ($\alpha = 0.05$) as they did not segregate in a Mendelian fashion (Fig. 1). Despite the fact that segregation distortion can interfere with mapping (Hackett and Broadfoot, 2003), these markers were retained in the map as their removal would have significantly reduced the map coverage.

Markers with segregation distortion mapped evenly to all of the linkage groups of *A. areolatum*, with several of these markers clustering together in the same region of a specific linkage group (Fig. 1). Although the distorted markers mapped to several linkage groups, LG7 had an excess of markers (6 of 44) showing segregation distortion. While the recognition loci were positioned near markers displaying segregation distortion, the alleles present at the *mat* and *het* loci did not demonstrate significant ($\alpha = 0.05$) segregation distortion. Furthermore, it was not possible to associate segregation distortion to a specific parent, because the genotypes of the parental strains are not known.

The two-tailed tests showed that there were significant differences (at $\alpha = 0.05$) in marker

density in two of the 10 major linkage groups (Table 3). Linkage group LG1 had a greater number of markers, while linkage group LG7 had fewer markers than expected under a Poisson distribution where the null hypothesis is that the average marker spacing (7.2 cM) is the same for all linkage groups. There were 23 and 15 markers (λ_i) expected to be located on linkage groups LG1 and LG7, respectively. However, 35 and eight markers (m_i), respectively, were actually observed on these linkage groups. Linkage group LG1, therefore, has significantly more markers and it also contained a high number of markers displaying segregation distortion.

Haplotype analysis of the individual genotypes using GGT revealed no linkage distortion in any of the 10 major linkage groups identified for *A. areolatum*, with both the inferred parental genomes segregating in a 1:1 ratio. Haplotype analysis of the individual genotypes was also used to estimate the number of crossover events per linkage group per individual. There were, however, no significant differences (at $\alpha = 0.05$) in the number of crossovers in the 10 major linkage groups, with all of these groups following a distribution as expected under a Poisson model. The average number of crossover events per linkage group per individual was 1.06, with linkage group LG10 displaying the fewest crossovers (0.66) and linkage group LG1 displaying the most crossovers (1.90) (Table 4). The low number of observed crossovers was probably due to our underestimation of linkage group sizes, as this number is dependent on linkage group size and the linkage groups identified in this study probably do not cover full chromosomes.

Mycelial growth estimation and QTL identification

Mycelial growth rate of the *A. areolatum* homokaryotic progeny and their heterokaryotic parent were determined. The average mycelial growth rate of the mapping population was 58.8 mm/wk with a standard deviation of 17.3 mm/wk after incubation at 25 °C. The ANOVA showed that the average mycelial growth rate amongst the homokaryons differed significantly (Table 5). The distribution of mycelial growth rate was continuous at 25 °C, with 25 % of the fastest growing homokaryons having the same mycelial growth rate (70–80 mm/wk) as the parent. The frequency distribution of mycelial growth rate of the homokaryons was binomial, with two distinct peaks at growth rate classes 25-30 mm/wk and 70-75 mm/wk (Fig. 2). The broad-sense heritability (H^2) of mycelial growth rate was estimated as 0.98. Although the individual heritability of mycelial growth rate for the individual homokaryons used in this study was very high, it is similar to the individual heritability of mycelial growth in *H. annosum* (0.97) (Olsen,

2006). Olson (2006) suggested that this high value might be due to low environmental variation in the experiment.

Using SIM, a total of 7 putative QTLs associated with mycelial growth in *A. areolatum* were identified and located on linkage groups LG2, LG4 and LG5 (Fig. 1; Table 6). Based on 1000 permutations using 1 cM steps Map Manager QTX indicated that LOD scores between 2.4 and 4.1 represent significant QTLs, while LOD scores between 1.1 and 2.4 represent suggestive QTLs. Only the putative QTL positioned on LG2 in the same region as the *het-A* locus (*i.e.*, 0 cM from the *het-A* locus, explaining 16 % of the phenotypic variance) was significant (LOD>2.4). The other 6 putative QTLs were suggestive (LOD 1.1-2.4) and were positioned on linkage groups LG2, LG4 and LG5. Using CIM, only 6 putative QTLs associated with mycelial growth were detected. The second putative QTL on linkage group LG2 was not included because its LOD score was below the suggested significance level. However, the LOD values of two of the QTLs increased from suggestive to the significant level using CIM. These are the QTL positioned in the same region as the *mat-A* locus on linkage group LG5 (*i.e.*, 1 cM from the m*at-A* locus, explaining 14 % of the phenotypic variance) and the QTL positioned in the same genomic region as the AFLP marker tc10849 (*i.e.*, 3 cM from the tc10849 locus, explaining 11 % of the phenotypic variance). One of the suggestive QTLs was also positioned in the same genomic region as the *mat-B* locus (*i.e.*, 6 cM from the m*at-B* locus, explaining 6 % of the phenotypic variance). All of the putative QTLs detected with CIM, explained 76 % of the total mycelial growth variation.

The average growth for homokaryons with different alleles at their *het-A* and *mat-A* loci differed significantly (P< 0.05) (Table 5). Homokaryons with alleles *het-A2* and *mat-A1* generally grew faster, while homokaryons with alleles *het-A1* and *mat-A2* grew slower. The mean mycelial growth for homokaryons with different alleles at the *tc10849* locus also differed significantly (P< 0.05). Homokaryons that share the *tc10849-1* allele displayed higher average mycelial growth than homokaryons that share the *tc10849-2* allele. The average mycelial growth for homokaryons with different alleles at their *het-B* and *mat-B* loci did not differ significantly (P > 0.05).

No epistatic interactions between the QTLs or unlinked markers were detected using the "interactions" function in Map Manager QTX, thereby suggesting that these loci act

independently. However, we did detect the presence of digenic interactions that may affect mycelial growth by analyzing the effects of all possible pair wise allelic combinations (of the three markers associated with the significant QTLs) on mycelial growth (Table 5). There was a significant difference ($P < 0.05$) in the average mycelial growth of homokaryons that shared the fast growing alleles (*mat-A1*, *het-A2* and *tc10849-1)* in comparison to homokaryons that shared the alleles associated with slow mycelial growth (*mat-A2*, *het-A1* and *tc10849-2*). Homokaryons that shared the *mat-A1* and *hetA-2* alleles, the *mat-A1* and *tc10849-1* alleles or the *het-A2* and *tc10849-1* alleles grew faster, while homokaryons that shared the *mat-A2* and *hetA-1* alleles, the *mat-A2* and *tc10849-2* alleles or the *het-A1* and *tc10849-2* alleles grew more slowly. Thus, homokaryons that shared one of the alleles (*mat-A1*, *het-A2* or *tc10849-1*) associated with rapid growth and one of the alleles (*mat-A2, hetA-1* or *tc10849-2*) associated with slow growth displayed intermediate growth. Accordingly, homokaryons that shared the *mat-A1* and *het-A1* alleles, the *mat-A2* and *het-A2* alleles, the *mat-A1* and *tc10849-2* alleles, the *mat-A2* and *tc10849-1* alleles, the *het-A1* and *tc10849-1* alleles or the *het-A2* and *tc10849-2* alleles had intermediate growth.

DISCUSSION

A framework map for *A. areolatum*

Genetic linkage maps for homobasidiomycetes have been limited to economically important species such as *A. bisporus, P. ostreatus* and *H. annosum* (Callac, et al., 1997; Larraya, et al., 2000; Lind et al., 2005). This is because genetic studies for homobasidiomycetes are hindered by some species being unculturable or due to the inability of their spores to germinate *in vitro*. Others, including *A. areolatum*, rarely fruit in nature and do not readily produce fruiting bodies in the laboratory (van der Nest et al., 2008). In this study we present a genetic linkage map (Fig. 1) for *A. areolatum* based on segregation analysis of a population of 80 homokaryons isolated from a basidiocarp collected in the field. For this purpose, we used AFLP analysis, because it provides a rapid means to generate large numbers of markers, allowing us to identify on average 10 polymorphic bands per primer combination (Table 1).

The *A. areolatum* map generated in this study included 10 major (Fig. 1) and 15 minor linkage groups together spanning about 1693 cM. As a related homobasidiomycete, *H. annosum*, has 10 chromosomes (Lind et al., 2005), it is possible that *A. areolatum* also has 10 chromosomes, although further research is required to confirm this. Overall, however, the *A. areolatum* map compares well with those published for other fungi, as the average distance between markers (8.3 cM) is similar to that of *H. annosum* (6.0 cM), *F. subglutinans* (12.0 cM) and *P. ostreatus* (5.3 cM) (Larraya et al., 2000; Lind et al., 2005; De Vos et al., 2007). The physical distance per unit of recombination for *A. areolatum* (19.9 kbp/cM) is also comparable to those of *H. annosum* (11.1 kbp/cM) and *C. neoformans* (9.6 kbp/cM), although it is considerably lower than those of *P. ostreatus* (35.1 kbp/cM) and *C. cinerea* (27.9 kbp) (Larraya et al., 2000; Forche et al., 2000; Muraguchi et al., 2003; Lind et al., 2005). Nonetheless, our *A. areolatum* map is not saturated, as only one of the AFLP markers was positioned within 5 cM of a recognition locus. Future work will seek to place additional markers on this framework map to saturate it further.

Consistent with other homobasidiomycetes with tetrapolar mating systems (Larraya et al., 2000; Muraguchi et al., 2003), the *A. areolatum mat-A* and *mat-B* loci were positioned on separate linkage groups (Fig. 1). The two *A. areolatum het* loci, *het-A* and *het-B*, also appeared to be positioned on separate linkage groups, which is consistent with previous work demonstrating

that some of the different *het* loci in a particular species are unlinked (e.g., Kubisiak and Milgroom, 2006). The identification of markers linked to these loci and subsequent characterisation of the genes encoded at the recognition loci may be facilitated by approaches such as BSA and map-based cloning. Accordingly, we have found that BSA represents a feasible approach to identify genetic markers closely linked to the recognition loci of *A. areolatum*. It has also been suggested that a relationship between genetic and physical distance <70 kbp/cM (compared to our much lower 19.9 kbp/cM) is favourable for map-based cloning (Sicard et al., 2003). Therefore, despite the fact that the *A. areolatum* map is not yet saturated and possibly does not cover entire chromosomes, it provides the basis for detailed characterization of all the recognition loci of *A. areolatum* using positional cloning.

Association between recognition and fitness in *A. areolatum*

Mycelial growth in *A. areolatum* displayed a continuous distribution and, therefore, represents a quantitative trait, consistent with results obtained for other fungi (e.g., Lind et al., 2005; Olson, 2006). Even though mycelial growth is an apparently polygenic trait in *A. areolatum*, this property seems to be predominantly controlled by only one or a few genes, as is evident from the binomial frequency distribution of mycelial growth (Fig. 2) (Buertsmayr et al., 2002). Only three significant putative QTLs and three suggestive putative QTLs for mycelial growth were identified in this study, which confirms the presence of only a few genes with major effects and additional genes with minor effects on mycelial growth. Since the 6 putative QTLs explained 76 % of the total mycelial growth rate variation, it is likely that there are additional QTLs associated with mycelial growth in *A. areolatum* that were not detected. Non-detection of additional QTLs could be due to QTLs being inordinately small to be detected, as was found by Olsen (2006). There might also be additional loci not indicated because they were not expressed under the experimental conditions used, or the parents might not have been polymorphic for them.

Three of the four recognition loci of *A. areolatum* were located in or near the observed QTLs associated with mycelial growth rate (Fig. 1). The *het-A* and the *mat-A* loci were positioned in the same region as two of the putative significant QTLs associated with mycelial growth rate in culture, while the *mat-B* locus was positioned in the same region as one of the putative QTL associated with mycelial growth rate in culture. The association between recognition and mycelial growth rate was confirmed when the growth rate of progeny with different alleles at either their *mat-A* or *het-A* loci, differed significantly (Table 5). A similar association between

mycelial growth and sexual recognition has been observed in *A. bisporus*, *P. ostreatus, H. annosum* and *S. commune* (Simchen, 1966; Callac et al., 1997; Larraya et al., 2000; Olson, 2006). However, to the best of our knowledge, this is the first time that a link between mycelial growth and self/nonself recognition has been observed in fungi.

Genetic determinants of the evolution of the recognition loci

A large proportion of AFLP markers (29.2 %) displayed significant deviation from the expected Mendelian ratio of parental alleles segregating among the progeny (Fig. 1; Table 2). The concentration of AFLP markers displaying segregation distortion in particular regions suggests that these distortions are the result of biological (both pre- and post-fertilization) mechanisms and not due to chance events or scoring errors. For example, differences among progeny in spore survival, germination and vegetative growth may result in biased selection of more fit individuals for map construction, which in turn may result in markers displaying segregation distortion (e.g., Larraya et al., 2000; Lind et al., 2005).

All of the recognition loci (*het-A*, *mat-A*, *mat-B*) associated with growth rate QTLs in *A. areolatum* were positioned near markers or marker clusters showing segregation distortion (Fig. 1). It has been suggested that an association between mycelial growth rate and the *mat* loci in *P. ostreatus*, *H. annosum* and *C. neoformans* could potentially explain the segregation distortion displayed at the *mat* loci or the markers surrounding them (Larraya et al., 2001; Marra et al., 2004; Lind et al., 2005). In the *P. ostreatus* model system, it has been observed that faster-growing monokaryons belong to specific mating types (Larraya et al., 2001). A possible explanation for the association between mycelial growth and the recognition loci may lie in the fact that the evolutionary forces acting on these systems differ from those acting on the rest of the genome as balancing selection and suppressed recombination play a significant role in their evolution (e.g., Meyer and Thomson, 2001; Takebayashi et al., 2004; Uyenoyama, 2005).

Balancing selection that retains alleles at approximately equal proportions in populations may help to explain the association between the recognition loci and mycelial growth in *A. areolatum*. Larraya et al. (2001) also hypothesized that balancing selection acting on the recognition loci of *P. ostreatus* provides a possible explanation for the segregation distortion observed at the *mat* loci of this fungus. This is because balancing selection, which is thought to maintain the highly polymorphic multi-allelic nature of the recognition loci and the even distribution and long

persistence of alleles in populations (Meyer and Thomson, 2001), also results in the maintenance of potentially deleterious mutations in a population that would otherwise have been lost due to negative selection (Leppälä et al., 2008). Thus, balancing selection will prevent the loss of alleles associated with slow growth resulting in segregation distortion of these alleles. The presence of alleles for slow growth at the *het* loci, which are known to encode genes involved in housekeeping and other functions (Saupe, 2000), would therefore influence the fitness of individuals negatively. In the case of the *mat* loci, balancing selection could also affect genes that play no apparent role in mating but that have become entrapped at the *mat* loci (e.g., Uyenoyama 2005; Leppälä et al., 2008). This is especially as some of them encode proteins vital for growth such as ketopantoate reductase involved in energy metabolism and that is encoded at the homobasidiomycetes *mat-A* locus (James et al., 2004; Niculita-Hirzel et al., 2008). Therefore, it is likely that mycelial growth and fitness in *A. areolatum* is influenced by balancing selection acting on its recognition loci, or the genomic regions flanking these loci.

Suppressed recombination is a general feature of the recognition loci in eukaryotes where it is thought to limit potentially harmful recombination events such as vegetative self incompatibility or sexual self compatibility (e.g., Awadalla and Charlesworth, 1999; Callac et al., 1997; Meyer and Thomson, 2001; Uyenoyama, 2005; Menkis et al., 2008). For example, recombination is suppressed between the 25-kbp region spanning the *un-24* and *het-6* loci in *N. crassa*, as recombination at these loci may lead to vegetative self incompatibility (Smith et al., 2000). In fungi with tetrapolar mating systems where the *mat* loci consist of multiple subloci, recombination within subloci is suppressed to prevent self-compatibility, while recombination between different subloci is allowed for the generation of new mating type specificities (Lukens et al., 1996). Recombination is apparently also not suppressed in the genomic regions surrounding the homobasidiomycete *mat-A* locus, as there is a marked difference in nucleotide diversity between the *mat* loci and the surrounding regions (James et al., 2006). Recombination thus separates the *mat* loci that are under balancing selection from the surrounding regions that are under neutral selection (James et al., 2006). Our results suggest that recombination is also not suppressed at the genomic region surrounding the recognition loci of *A. areolatum*, as none of these loci are associated with an excess of markers as seen in other fungi (e.g., Kubisiak and Milgroom, 2006).

Even though recombination does not appear to be more suppressed at the recognition loci of

A. areolatum, the possibility that recombination in this fungus is suppressed over the entire genome cannot be excluded. For example, the average observed number of crossovers per linkage group (1.06) for *A. areolatum* is low, although it is dependent on linkage group size which, in our study, probably did not cover full chromosomes. Nevertheless, the average observed number of crossovers per linkage group in *A. areolatum* is similar to that of *P. ostreatus* (0.89), a fungus known to be affected by genome-wide suppressed recombination (Larraya et al., 2000). These values are much lower than the expected theoretical number of crossovers per linkage group for other fungi (e.g., 1.8 for *P. ostreatus*, 1.9 for *Fusarium verticillioides* and 1.4 for *F. graminearum*) that are not affected by genome-wide suppressed recombination (Larraya et al., 2000; Jurgenson et al., 2002). Notably, several of the *A. areolatum* linkage groups displayed less than one observed crossover (Table 4), which is less than the number required for proper chromosome disjunction during meioses (Larraya et al., 2000). It is speculated that genome-wide suppressed recombination may be an evolutionary adaptation for the maintenance of heterozygosity in fungi with homothallic and inbreeding life cycles (e.g., Callac et al., 1997). It is, therefore, conceivable that genome-wide suppressed recombination has a similar function in *A. areolatum* with its low overall genetic diversity. However, it is important to emphasise that additional research is required to determine the mode of reproduction of this fungus in nature (e.g., sexual *vs.* asexual and outbreeding *vs.* inbreeding), as well as to ascertain the level at which suppressed recombination occurs in the *A. areolatum* genome.

Conclusions

In this study, we were able to construct a genetic linkage map for *A. areolatum* and to identify potential chromosomal regions that harbour the genes involved in sexual and self recognition. With the aid of BSA, we were able to also identify markers closely linked to these genes as potential candidates for positional cloning. Although homobasidiomycete *mat* loci have previously been mapped and characterised (e.g., Larraya et al., 2000), to the best of our knowledge, this is the first time that any basidiomycete *het* loci have been mapped to specific regions in a genetic linkage map and where genetic markers have been identified close these loci. The results presented therefore, provide an excellent genetic basis for increasing our knowledge of the recognition systems in this unique model homobasidiomycete with its obligate mutualistic insect association.

This study represents an important step towards identifying the genetic factors influencing

fitness in *A. areolatum*. This emerges from our linkage map that enabled us to identify regions of the genome (QTLs) that contribute to the expression of growth rate as an indicator of homokaryon fitness. These factors probably have important implications for the epidemiology, evolution and population biology of the fungus, which in turn will influence the spread and control of the fungus/insect association. Although the link between growth rate/fitness and *mat* loci has been observed previously, to the best of our knowledge, this is the first time that an association between growth rate and vegetative incompatibility has been shown in fungi. Ultimately the findings presented here will lead to an improved understanding of the complex interactions that apparently exists between the systems governing recognition and fitness in this and other fungi.

REFERENCES

Awadalla, P., Charlesworth, D., 1999. Recombination and selection at Brassica self-incompatibility loci. Genetics. 152, 413-425.

Bagley, M.J., Anderson S.L., May, B., 2001. Choice of methodology for assessing genetic impacts of environmental stressors: polymorphism and reproducibility of RAPD and AFLP fingerprints. Ecotoxicology. 10, 239-244.

Buerstmayr, H., Lemmens, M., Hartl, L., Doldi, L., Steiner, B., Stierschneider, M., Ruckenbauer, P., 2002. Molecular mapping of QTLs for Fusarium head blight resistance in spring wheat. I. Resistance to fungal spread (Type II resistance). Theor. Appl. Genet. 104, 84-91.

Callac, P., Desmerger, C., Kerrigan, R.W., Imbernon, M., 1997. Conservation of genetic linkage with map expansion in distantly related crosses of *Agaricus bisporus*. FEMS Microbiol. Lett. 146, 235-240.

Casselton, L.A., 2002. Mate recognition in fungi. Heredity. 88, 142-147.

De Vos, L., Myburg, A.A., Wingfield, M.J., Desjardins, A.E., Gordon, T.R., Wingfield, B.D., 2007. Complete genetic linkage maps from an interspecific cross between *Fusarium circinatum* and *Fusarium subglutinans*. Fungal Genet. Biol. 44, 701-714.

Falconer, D., 1989. Introduction to quantitative genetics., 3rd edn. Longman Group Limited. London.

Forche, A., Xu, J., Vilgalys, R., Mitchell, T.G., 2000. Development and characterization of the genetic linkage map of *Cryptococcus neoformans* var. *neoformans* using amplified fragment length polymorphisms and other markers. Fungal Genet. Biol. 31, 189-203.

Glass, N.L., Jacobson, D.J., Shiu, P.K.T., 2000. The genetics of hyphal fusion and vegetative incompatibility in filamentous ascomycete fungi. Ann. Rev. Genetics. 34, 165-186.

Hackett, C.A., Broadfoot, L.B., 2003. Effects of genotyping errors, missing values and segregation distortion in molecular marker data on the construction of linkage maps. Heredity. 90, 33-38.

Hill, J.A., Otto, S.P., 2007. The role of pleiotropy in the maintenance of sex in yeast. Genetics. 75, 1419-1427.

Hulbert, S.H., Ilott, T.W., Legg, E.J., Lincoln, S.E., Lander, E.S., Michelmore, R.W., 1988. Genetic analysis of the fungus, *Bremia lactucae*, using restriction fragment length polymorphisms. Genetics. 120, 947-958.

James, T.Y., Liou, S-R., Vilgalys, R., 2004. The genetic structure and diversity of the A and B mating type genes from the tropical oyster mushroom, *Pleurotus djamor*. Fungal Genet. Biol. 41, 813-825.

James, T.Y., Srivilai, P., Kuës, U., Vilgalys, R., 2006. Evolution of the bipolar mating system of the mushroom *Coprinellus disseminatus* from its tetrapolar ancestors involves loss of mating-type-specific pheromone receptor function. Genetics. 172, 1877-1891.

Jurgenson, J.E., Zeller, K.A., Leslie, J.F., 2002. Expanding genetic map of *Gibberella moniliformis* (*Fusarium verticillioides*). Appl. Environ. Microbiol. 68, 1972-1979.

Kosambi, D.D., 1944. The estimation of map distances from recombination values. Ann. Eugenics. 12, 172-175.

Kubisiak, T.L., Milgroom, M.G., 2006. Markers linked to vegetative incompatibility (*vic*) genes and a region of height heterogeneity and reduced recombination near the mating type locus (MAT) in *Cryphonectria parasitica*. Fungal Genet. Biol. 43, 453-463.

Lander, E.S., Green, P., Abrahamson, J., Barlow, A., Daly, M.J., Lincoln, S.E., Newburg, L., 1987. MAPMAKER: an interactive computer package for constructing primary genetic linkage maps of experimental and natural populations. Genomics. 1, 174-181.

Larraya, L.M., Idareta, E., Arana, D., Ritter, E., Pisabarro, A., Ramirez, L., 2002. Quantitative trait loci controlling vegetative growth rate in the edible basidiomycete *Pleurotus ostreatus*. Appl. Environ. Microbiol. 68, 1109-1114.

Larraya, L.M., Pérez , G., Ritter, E., Pisabarro, A.G., Ramirez, L., 2000. A genetic linkage map of *Pleurotus ostreatus*. Appl. Environ. Microbiol. 66, 5290-5300.

Larraya, L.M., Pérez, G., Iribarren, I., Blanco, J.A., Alfonso, M., Pisabarro, A.G., Ramirez, L., 2001. Relationship between monokaryotic growth rate and mating type in the edible basidiomycete *Pleurotus ostreatus*. Appl. Environ. Microbiol. 67, 3385-3390.

Leppälä, J., Bechsgaard, J.S., Schierup, M.H., Savolainen, O., 2008. Transmission ratio distortion in *Arabidopsis lyrata*: effects of population divergence and the S-locus. Heredity. 100, 71-78.

Lind, M, Stenlid, J., Olson A., 2007. Genetics and QTL mapping of somatic incompatibility and intraspecific interactions in the basidiomycete *Heterobasidion annosum s.l.* Fungal Genet. Biol. 44, 1242-1251

Lind, M., Olson, A., Stenlid, J., 2005. An AFLP-marker based genetic linkage map of *Heterobasidion annosum* locating intersterility genes. Fungal Genet. Biol. 42, 519-527.

Liu, B., 1998. Statistical Genomics: Linkage, Mapping and QTL Analysis. CRC Press, Boca Raton, FL.

Lukens, L., Yicunt, H., May, G., 1996. Correlation of genetic and physical maps at the A mating-type locus of *Coprinus cinereus.* Genetics. 144, 1471-1477.

Marra, R.E., Huang, J.C., Fung, E. Nielsen K., Heitman, J, Vilgalys R., Mitchell T.G., 2004. A genetic linkage map of *Cryptococcus neoformans* variety *neoformans* serotype D (*Filobasidiella neoformans*). Genetics. 167, 619-631.

Manly, K.F., Cudmore, R.H., Meer, J.M., 2001. Map Manager QTX, cross-platform software for genetic mapping. Mamm. Genome. 12, 930-932.

Menkis, A., Jacobson, D.J., Gustafsson, T., Johannesson, H., 2008. The mating-type chromosome in the filamentous ascomycete *Neurospora tetrasperma* represents a model for early evolution of sex chromosomes. Plos Genetics. 4, e1000030.

Meyer, D., Thomsen, G., 2001. How selection shapes variation of the human major histocompatibility complex: A review. Ann. Hum. Genet. 65, 1-26.

Muraguchi, H., Ito, Y., Kamada, T., Yanagi, S.O., 2003. A linkage map of the basidiomycete *Coprinus cinereus* based on random amplified polymorphic DNAs and restriction fragment

length polymorphisms. Fungal Genet. Biol. 40, 93-102.

Myburg, A.A., Remington, D.L., O'Malley, D.M., Sederoff, R.R., Whetten, R.W., 2001. High-throughput AFLP analysis using infrared dye-labelled primers and an automated DNA sequencer. BioTechniques. 30, 348-357.

Nauta, M.J., Hoekstra, R.F., 1994. Evolution of vegetative incompatibility in filamentous ascomycetes. I. deterministic models. Evolution. 48, 979-995.

Niculita-Hirzel, H., Labbé, J., Kohler, A., La Tacon, F., Martin, F., Sanders, I.R., Kües, U., 2008. Gene organization of the mating type regions in the ectomycorrhizal fungus *Laccaria bicolor* reveals distinct evolution between the two mating type loci. New Phytol. 180, 329-342.

Olson,A., 2006. Genetic linkage between growth rate and the intersterility genes S and P in the basidiomycete *Heterobasidion annosum s.lat.* Mycol. Research. 110, 979-984.

Remington, D.L., Whetten R.W., Liu, B.H., O'Malley, D.M., 1999. Construction of an AFLP genetic map with nearly complete genome coverage in *Pinus taeda*. Theor. Appl. Genet. 98, 1279-1292.

Sicard, D., Legg, E., Brown, S., Babu, N.K., Ochoa, O., Sudarshana P., Michelmore, R.W., 2003. A genetic map of the lettuce downy mildew pathogen, *Bremia lactucae*, constructed from molecular markers and avirulence genes. Fungal Genet. Biol. 39, 16-30.

Shibata, T., 2001. Functions of homologous DNA recombination. RIKEN Review. 41, 21-23.

Simchen, G., 1966. Monokaryotic variation and haploid selection in *Schizophyllum commun*e. Heredity. 21, 241-263.

Slippers, B., Coutinho, T.A., Wingfield, B.D., Wingfield, M.J., 2003. A review of the genus *Amylostereum* and its association with woodwasps. SA J. Sci. 99, 70-74.

Saupe, S.J., 2000. Molecular genetics of heterokaryon incompatibility in filamentous ascomycetes. Micro. Mol. Biol. Rev. 64, 489-502.

Takebayashi, N., Newbigin, E., Uyenoyama, M.K., 2004. Maximum-likelihood estimation of rates of recombination within mating-type regions. Genetics. 167, 2097-2109.

Thomas, W.T.B., Baird E., Fuller, J.D., Lawrence, P., Young, G.R., Ramsay, L., Waugh, R., Powell, A.J., 1998. Identification of a QTL decreasing yield in barley linked to Mlo powdery mildew resistance. Mol. Breeding. 4, 381-393.

Uyenoyama, M.K., 2005. Evolution under tight linkage to mating type. New Phytol. 165, 63-70.

Van Berloo, R., 1999. GGT: software for the display of graphical genotypes, J. Hered. 90, 328-329.

Van der Nest, M.A., Slippers, B., Stenlid, J., Wilken, P.M., Vasaitis, R., Wingfield, M.J., Wingfield, B.D., 2008. Characterization of the systems governing sexual and self-recognition in the white rot homobasidiomycete *Amylostereum areolatum*. Curr. Genet. 53, 323-336.

Van Ooijen, J.W., Voorrips, R.E., 2001. JoinMap 3.0 software for the calculation of genetic linkage maps. Plant Research International, Wageningen, the Netherlands.

Vos, P., Hogers, R., Bleeker, M., Reijans, M., Van der Lee, T., Hornes, M., Frijters, A., Pot, J., Peleman, J., Kuiper M., Zabeau, M., 1995. AFLP: A new technique for DNA fingerprinting,

Nucleic Acids. Res. 23, 4407-4414.
Worral, J.J., 1997. Somatic incompatibility in basidiomycetes. Mycologia. 89, 24-36.

FIGURES

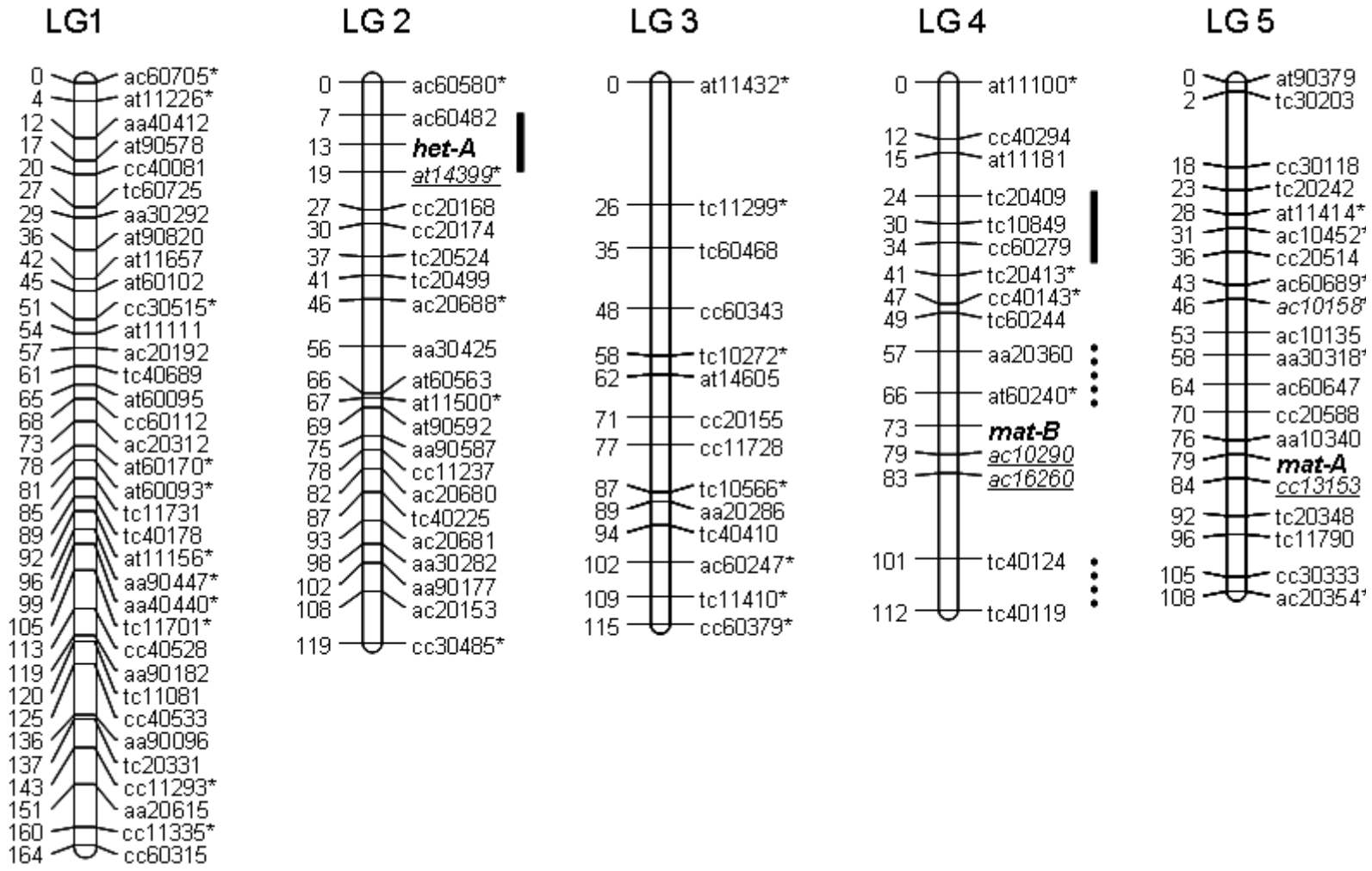

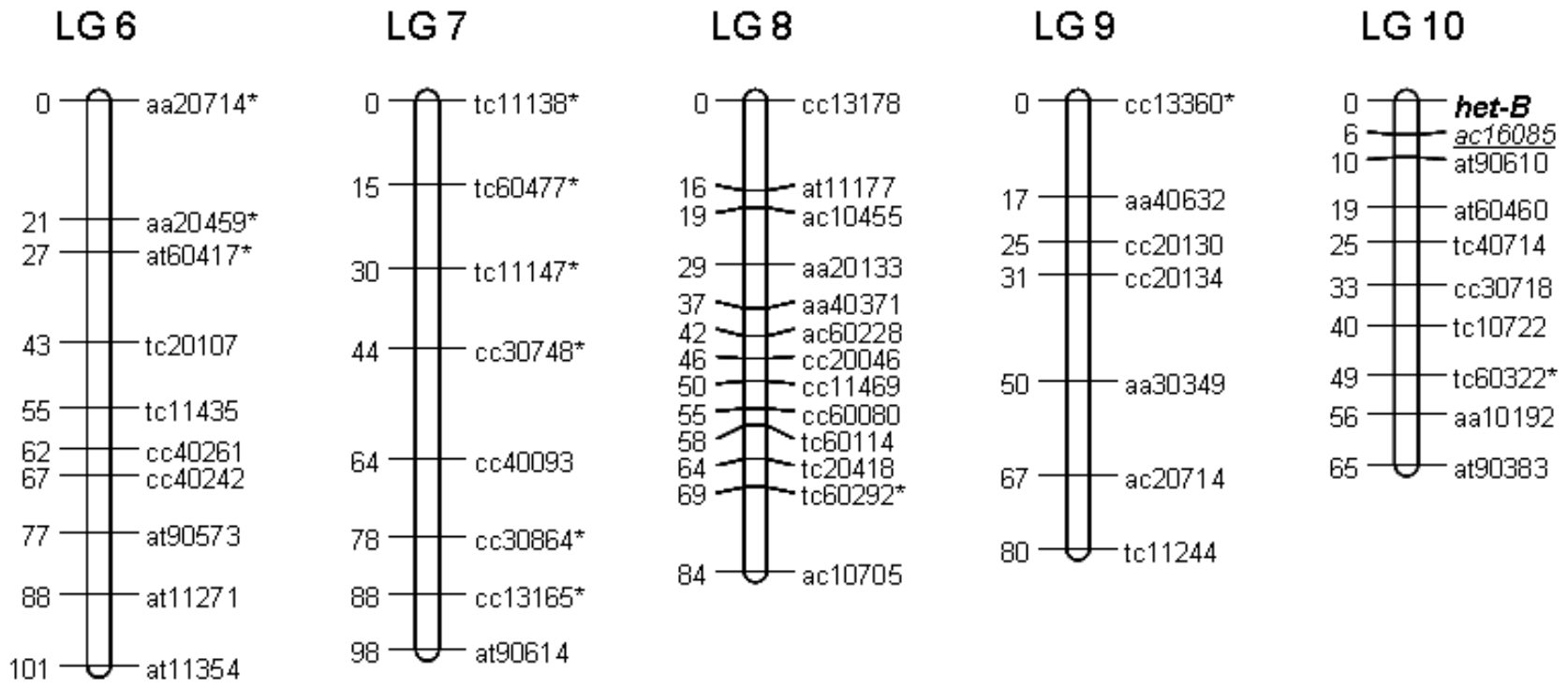

Figure 1. The AFLP genetic linkage map for *A. areolatum*. Linkage groups are numbered in declining size of the groups. The linkage distance (cM) between markers relative to the top marker is indicated on the left of each linkage group. The *het* and *mat* loci are indicated in bold, while markers identified with BSA are underlined. Markers showing segregation distortion are indicated with ∗. The position of putative significant QTLs is indicated with solid vertical lines, while the position of putative suggested QTLs are indicated with vertical dotted lines. Markers were named by indicating the *EcoRI* primer with two letters (Table 1), followed by two digits representing the *MseI* primer (Table 1) and then three digits that represent the size of the fragment in base pairs.

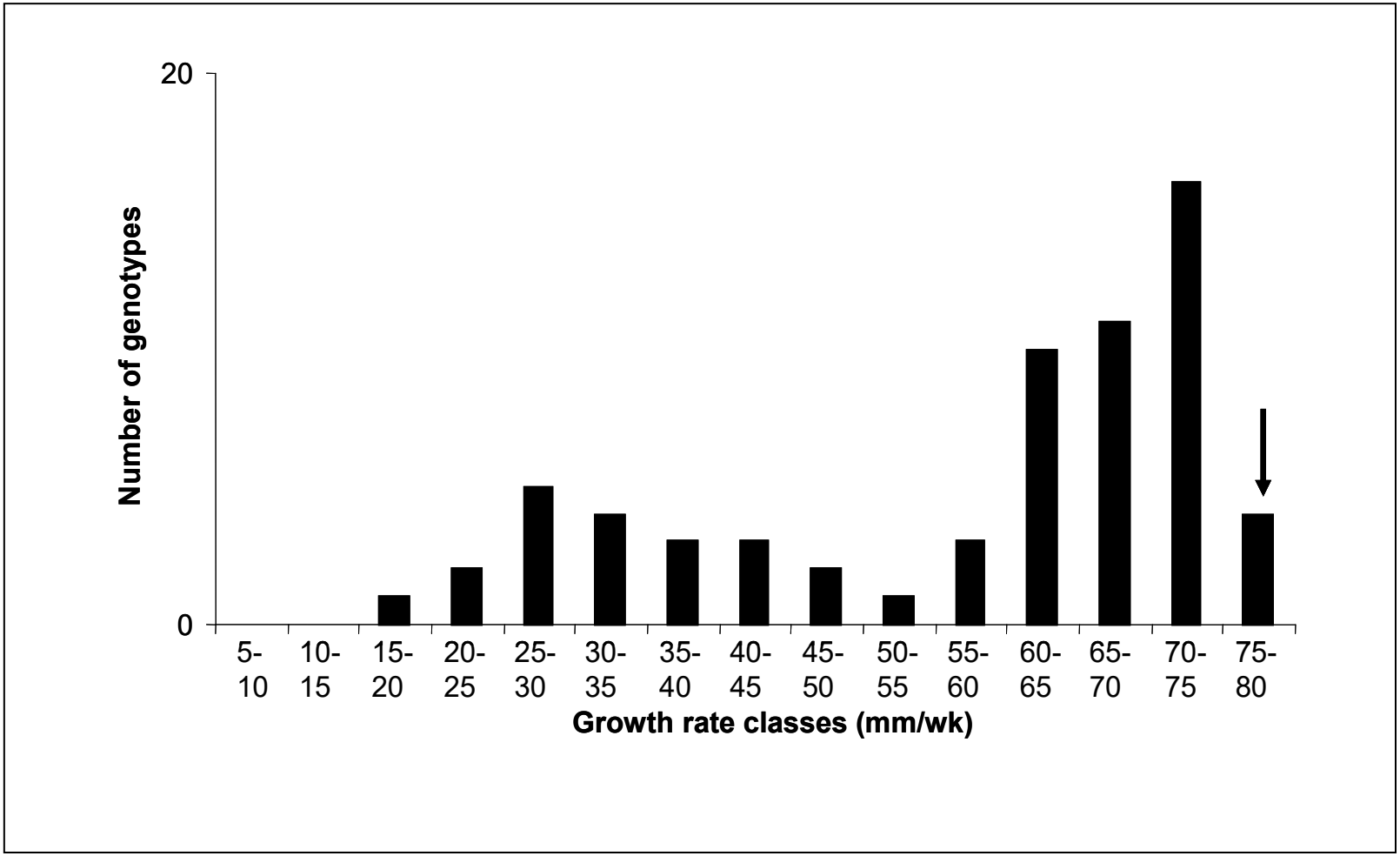

Figure 2. Frequency distribution of vegetative growth of the *A. areolatum* mapping population after incubation for 7 days at 25 °C. The growth class that the parent isolate belongs to is indicated with an arrow.

TABLES

Table 1. The number of monomorphic and polymorphic fragments per primer combination.

***Eco*RI Primer** [a]	***Mse*I Primer** [b]	**Monomorphic bands/primer**	**Polymorphic bands/primer**
E-AA	M-GC (11)	9	4
E-AA	M-AT (2)	20	11
E-AA	M-AG (3)	24	8
E-AA	M-AC (4)	19	11
E-AA	M-GA (9)	14	11
E-AC	M-AT (2)	10	10
E-AC	M-TT (6)	10	10
E-AT	M-TT (6)	17	13
E-AT	M-GC (11)	10	17
E-CC	M-AT (2)	18	11
E-CC	M-AC (4)	19	11
E-CC	M-TT (6)	10	12
E-CC	M-GC (11)	9	9
E-CT	M-TT (6)	8	14
E-CT	M-GC (11)	12	13
E-TC	M-AA (1)	16	18
E-TC	M-AT (2)	13	14
E-TC	M-AG (3)	15	11
E-TC	M-AC (4)	17	7
E-AT	M-CA (13)	19	10
BSA			
E-AT	M-CT (14)	8	3
E-CC	M-CA (13)	8	5
E-AC	M- GT(10)	18	9
E-AC	M-CC (16)	10	3

[a] The *Eco*RI adapter primer sequence without selective nucleotides was 5-gactgcgtaccaattc-3'.

[b] The *Mse*I adapter primer sequence without selective nucleotides was 5-gatgagtcctgagtaa-3'.

*Mse*I primer numbers are indicated in parentheses.

Table 2. Summary of map constructed using AFLP markers, mating type and vegetative compatibility information for a set of *Amylostereum areolatum* progeny.

Description	*Amylostereum areolatum* map
Markers	
Number of framework markers selected	200
Number of unlinked markers	45
Number of markers showing transmission ratio distortion[a]	44
Framework map	
Number of major linkage groups	10
Number of minor linkage groups	15
Average linkage group size (cM) [b]	112.9
Average marker spacing (cM) [c]	8.3
Observed map length (cM)	1693
Physical distance per unit of recombination	19.9 kb/cM
Estimate of genome length	
Using Hulbert estimate of genome length (cM) [e]	2922.6 cM
Framework map coverage[f]	
Map coverage (c = 100 %) at d = 20 cM	89.3 %
Map coverage(c = 100 %) at d = 10 cM	67.2 %

[a] Departure of markers from the expected 1:1 ratio (at the 5 % level of significance).

[b] Distance are in centimorgans (cM).

[c] Calculated by dividing the summed length of all the linkage groups by the number of marker intervals. The number of marker intervals was calculated by the number of linked markers minus the number of linkage groups.

[d] The genome size of *H. annosum* (33.7 Mb) (http://genome.jgi-psf.org/) was used to calculate the physical distance per unit of recombination.

[e] The total genome length of the framework map was estimated as describe by Hulbert *et a*l. (1988).

[f] The theoretical genome coverage was estimated according to Remington *et al*. (1999).

Table 3. Verification of random marker distribution using Poisson two-tailed P-test[a].

Linkage Group	Number of markers (m_i)	Map length (M_i)	Inferred map length (G_i)	Expected number of markers (λ_i)	Poisson two-tailed P-value[b]
LG 1	35	164	178.4	23.5	0.0059*
LG 2	22	119	133.4	16.4	0.0358
LG 3	14	115	129.4	16.9	0.0814
LG 4	16	112	126.4	16.5	0.0985
LG 5	20	108	122.4	19.9	0.0888
LG 6	10	101	115.4	15.0	0.0486
LG 7	8	98	112.4	14.6	0.0234*
LG 8	13	84	98.4	12.8	0.1098
LG 9	7	80	94.4	12.3	0.0385
LG 10	10	65	79.4	10.3	0.1246

[a] Poisson probability of having as many markers as the observed number of markers, m_i in the i_{th} linkage group under the null hypothesis that the average marker spacing (7.1 cM) is the same for all linkage groups.

[b] In a two-tailed test, a P-value of 0.025 corresponds to a significance level of 0.05. Linkage groups 1 and 7 (indicated with *) shown significant deviation from the Poisson distribution.

Table 4. Distribution of observed crossovers per linkage group.

Linkage Group	Number of markers	Map length (cM)	Average marker interval (cM)[a]	Number of crossover events[b]
LG 1	35	164	5.0	1.90
LG 2	22	119	5.4	1.40
LG 3	14	115	8.2	0.94
LG 4	16	112	7.0	1.12
LG 5	20	108	5.4	1.08
LG 6	10	101	10.1	0.99
LG 7	8	98	12.3	0.93
LG 8	13	84	6.5	0.69
LG 9	7	80	11.4	0.84
LG 10	10	65	6.5	0.66
Avg.	15.5	104.6	6.7	1.06

[a] The average marker spacing was calculated by dividing the summed length of all the linkage groups by the number of marker intervals, while the number of marker intervals represented the difference between the number of markers and the number of linkage groups.

[b] The number of crossover events per linkage group per individual was estimated by visualizing the haplotypes of the individuals using the GGT program and counting the number of crossovers observed.

Table 5. The average colony diameter of isolates harbouring specific alleles at the loci positioned near putative significant QTL associated mycelial growth.

Alleles[1]	Mean colony diameter (mm/wk)[2]	Standard deviation (mm/wk)
Allelic interactions		
het-A1	50.7 (a)	20.4
het-A2	66.6 (b)	11.3
het-B1	58.3 (a)	19.9
het-B2	59.4 (a)	16.3
mat-A1	64.2 (a)	16.5
mat-A2	52.5 (b)	19.1
mat-B1	56.6 (a)	19.6
mat-B2	61.4 (a)	16.4
tc10849-1	65.5 (a)	12.4
tc10849-2	50.6 (b)	19.7
Digenic interactions		
mat-A1, *het-A1*	57.5 (ab)	19.5
mat-A2, *het-A1*	43.8 (b)	19.0
mat-A1, *het-A2*	69.0 (a)	6.0
mat-A2, *het-A2*	60.7 (ab)	15.0
mat-A1, *tc10849-1*	69.4 (a)	11.4
mat-A1, *tc10849-2*	62.7 (ab)	15.8
mat-A2, *tc10849-1*	61.5 (ab)	15.8
mat-A2, *tc10849-2*	45.1 (b)	19.7
het-A1, *tc10849-1*	57.9 (ab)	18.3
het-A1, *tc10849-2*	46.3 (b)	9.2
het-A2, *tc10849-1*	71.1 (a)	4.2
het-A2, *tc10849-2*	61.1 (ab)	9.2

[1] To evaluate allelic and digenic interactions, the growth of isolates with specific alleles or allelic combinations were compared.

[2] For each comparison the average colony diameters that differ significantly ($P<0.05$) are indicated by different letters in parentheses.

Table 6. QTLs for mycelial growth detected in *Amylostereum areolatum* using simple interval mapping (SIM) and composite interval mapping (CIM).

Linkage group	Best flanking markers	LOD[a]	R^2 (%)[b]	Significant level[c]
SIM				
Linkage group 2	ac60482 & *het-A*	2.9	17	Significant
Linkage group 2	tc20524 & tc20499	2.0	12	Suggestive
Linkage group 4	tc10849	2.2	13	Suggestive
Linkage group 4	tc40124 &tc40119	1.7	10	Suggestive
Linkage group 4	at60240	1.3	8	Suggestive
Linkage group 5	cc20588, *mat-A* & cc13001	1.5	9	Suggestive
Linkage group 5	cc30333	1.6	10	Suggestive
CIM				
Linkage group 2	ac60482 & *het-A*	3.1	16	Significant
Linkage group 4	tc10849	2.7	11	Significant
Linkage group 4	tc40124 & tc40119	1.5	6	Suggestive
Linkage group 4	at60240	1.3	6	Suggestive
Linkage group 5	cc20588, *mat-A* & cc13001	2.8	14	Significant
Linkage group 5	cc30333	2.2	14	Suggestive

[a] LOD values were obtained by converting LRS scores using the following equation LRS = 4.6 X LOD (Liu, 1998).

[b] Explained percentage of phenotypic variance.

[c] Significance levels determined in Map manager QTX based on a 1000 permutation using 1 cM steps.

CHAPTER 5

Influence of symbiosis on the evolution and mode of reproduction of two white rot fungi

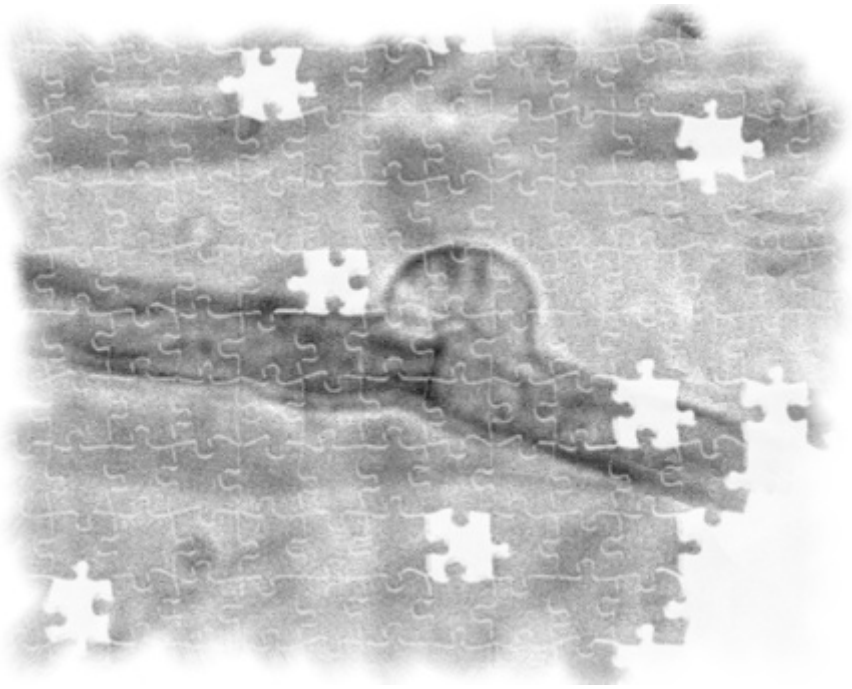

TABLE OF CONTENTS

ABSTRACT

Amylostereum areolatum exists in a tightly evolved symbiosis with the woodwasp *Sirex noctilio*. Similar to other symbionts, *A. areolatum* is characterised by predominantly asexual reproduction and is transmitted vertically. This fungus can also reproduce sexually and has a heterothallic and tetrapolar mating system. In fungi with such mating systems, the genes governing sexual recognition are present on two unlinked mating type (*mat*) loci. To establish whether symbiosis has influenced these genes in the fungal partner, we compared the DNA sequence information for the pheromone receptor gene *RAB1* encoded at the *mat-B* locus and two nuclear regions, *i.e.,* the eukaryotic translation elongation factor 1α gene and the ribosomal RNA internal transcribed spacer region. For comparative purposes the closely related species *A. chailletii* was included because it is less dependent on insects for dispersal and unlike *A. areolatum*, it more frequently reproduces sexually. Results showed that the *RAB1* gene sequences of *A. areolatum* and *A. chailletii* are highly polymorphic and diverse. Balancing selection and purifying selection, but not positive selection were implicated in their evolution. The results of the study also confirmed that *A. areolatum* and *A. chailletii* favour a mixed mode of reproduction, despite the costs associated with sexual reproduction.

INTRODUCTION

Most eukaryotic organisms reproduce sexually to generate offspring even though it is more costly than asexual reproduction (e.g., Barton and Charlesworth, 1998; Otto, 2003). This costly reproductive mode could be maintained because recombination acts to create advantageous genotypes necessary for adaptation to changing environments or because recombination acts to eliminate deleterious mutations (e.g., Zeyl and Bell, 1997; Taylor et al., 1999; Neiman et al., 2010). Both of these hypotheses are consistent with the fact that the absence of sexual reproduction decreases the overall fitness of an organism and could ultimately lead to extinction (Butlin, 2006; Paland and Lynch, 2006; Howe and Denver, 2008). An observation in fungi is that most asexually reproducing populations also retain some level of sexual reproduction, despite the cost of this mode of reproduction, thus generally favouring a system of mixed modes of reproduction (Taylor et al., 1999; Hsueh and Heitman, 2008).

Despite the advantages of mixed modes of sexual and asexual reproduction, this form of reproduction appears not to be feasible in all organisms. For example, the symbionts of insects mainly reproduce asexually and are transmitted from mother to offspring in a vertical fashion (e.g., Baumann and Moran, 1997; Kaltenpoth et al., 2010). Such a mode of reproduction and transmission ensures co-dependence between the symbiotic partners, but it could lead to a reduction in the genetic diversity of the symbiont and the occurrence of genetic bottlenecks (Rispe and Moran, 2000; Mira and Moran 2002). The effective lack of sexual recombination in the symbiont could lead to increased genetic drift, accumulation of mildly deleterious mutations, more rapid sequence evolution (excess of amino acid substitutions), a shift in nucleotide base composition due to mutational bias and genome erosion (Rispe and Moran 2000; Kaltenpoth et al., 2010). Nevertheless, several ancient lineages of asexually reproducing organisms still exist in successful symbiotic relationships (Welch and Meselson, 2001; Jany and Pawlowska, 2010). A well-known example, is found with the fungal symbionts (*Lepiota* spp.) that have co-evolved for more than 23 million years with their ant insect partners (Welch and Meselson, 2001; Jany and Pawlowska, 2010). In these relationships, it is thought that selection by the insect host may limit the accumulation of deleterious mutations in the symbiont (Kaltenpoth et al., 2010).

In this study, we considered the obligate symbiotic relationship between the white rot homobasidiomycete fungus *Amylostereum areolatum* and its hymenopteran insect partner *Sirex*

noctilio. This fungus is a saprotrophic wood-rotting basidiomycete that poses no real economic threat in its native environment. On the other hand, *A. areolatum* and its insect symbiont represent one of the most serious threats to pine-based forestry in countries where they have been introduced (Slippers et al., 2003; Hurley et al., 2007). In this relationship, the fungus is necessary for the development of the larvae, while the woodwasp effectively spreads the asexual spores and/or mycelium of the fungus (Vasiliauskas et al., 1998), thereby facilitating vertical transmission of *A. areolatum* to the offspring of the insect (Madden, 1981). The fungus can also reproduce sexually and has a tetrapolar mating system, where the genes governing sexual recognition are present on two unlinked mating type (*mat*) loci (*mat-A* and *mat-B*) (Boidin and Lanquetin, 1984; van der Nest et al., 2008). The *mat-A* locus harbours genes that encode homeodomain proteins (functional transcriptional factors), while the *mat-B* locus harbours genes that encode pheromones and pheromone receptors (Larraya et al., 2001; Kothe et al., 2003). Nonetheless, sexual fruitbodies of *A. areolatum* are rarely found in nature and usually only in the native range of the insect and fungus (Vasiliauskas and Stenlid, 1999; Slippers et al., 2003; Nielsen et al., 2009). The population biology of this fungus also suggests that, like other insect symbionts, *A. areolatum* relies almost exclusively on asexual reproduction in certain regions (Vasiliauskas et al., 1998; Vasiliauskas and Stenlid, 1999).

The evolutionary forces acting on the *mat* loci are thought to drive divergence between *mat* alleles, thus ensuring compatibility between individuals in a population (e.g., May et al., 1999; Devier et al., 2009). A form of balancing selection, known as negative frequency-dependent selection, probably acts to preserve the characteristically high allelic and nucleotide diversities at these loci (May et al., 1999; Ruggiero et al., 2008). This mechanism involves the selection for rare alleles, because individuals carrying rare *mat* alleles will be sexually compatible with a larger number of other individuals (May et al., 1999; Ruggiero et al., 2008). Diversity at the *mat* loci is also promoted by accelerated evolutionary rates, which is evident in the increased non-synonymous substitution rates in these regions (Vicoso et al., 2008; Devier et al., 2009). These high rates of substitution could be ascribed to suppressed recombination and/or positive selection, where the former prevents the loss of harmful mutations and the latter acts to maintain beneficial substitutions (Uyenoyama, 2005; Menkis et al., 2008; Vicoso et al., 2008).

The overall aim of this study was to investigate how the symbiotic relationship between *A. areolatum* and *S. noctilio* might have influenced the evolution of the genes governing sexual

recognition in the fungal partner. For comparison, we included the closely related species *A. chailletii* and *A. laevigatum*, which are both less dependent on Siricid woodwasps for dispersal and consequently reproduce sexually more frequently (Tabata and Abe, 1997; Vasiliauskas et al., 1998; Vasiliauskas and Stenlid, 1999; Slippers et al., 2001). Two specific questions were addressed: (i) Are the *mat* loci of the fungal symbiont more polymorphic than the rest of its genome and if so, is balancing selection maintaining diversity at these loci? (ii) Do the genes encoded at the *mat* loci display accelerated rates of evolution, and if so, could this be due to suppressed recombination and/or positive selection? To answer these questions we utilized the DNA sequence information for the pheromone receptor gene (*RAB1*) encoded at the *mat-B* locus, and two nuclear regions, *i.e.*, the eukaryotic translation elongation factor 1α (Tef-1α) gene and the ribosomal RNA (rRNA) internal transcribed spacer (ITS) region, which includes the spacers ITS1, ITS2 and the 5.8S rRNA gene.

MATERIALS AND METHODS

Fungal strains

Isolates of *A. areolatum* (CMW16848), *A. chailletii* (NAc3) and *A. laevigatum* (SeA16-04,1.11) were included to identify the pheromone receptor genes present in these species. Additionally, twenty-five isolates each of *A. areolatum* and *A. chailletii* obtained from various culture collections were also included (Supplementary Tables 1 and 2). These isolates were selected to represent the known diversity of these fungi and were collected from South Africa, Brazil, Argentina, Australia, New Zealand, United States of America, Canada, France, Sweden, United Kingdom, Switzerland, Denmark, Norway, Austria, Italy, Greece and Lithuania. Working cultures of the isolates were maintained on potato dextrose agar (PDA) (24 gL^{-1} of PDA, 1 gL^{-1} glucose, and 1 gL^{-1} yeast extract) (Biolab, Johannesburg, South Africa). All of the isolates used in this study are also maintained at 4 ºC in the culture collection of the Forestry and Agricultural Biotechnology Institute (FABI), University of Pretoria, Pretoria, South Africa. Genomic DNA was isolated from the isolates using the method described by Zhou *et al.* (2004).

PCR, cloning and nucleotide sequencing

In this study, the *RAB1* pheromone receptor gene (van der Nest et al., 2008) sequences for the three species included were utilized. Those for *A. areolatum* (CMW16848) were available from a previous study (van der Nest et al., 2008), while those for *A. chailletii* and *A. laevigatum* were identified using the degenerate primers (br1-F and br1-R) designed by James et al. (2004b). Polymerase chain reaction (PCR) was performed on an Eppendorf thermocycler (Eppendorf AG, Germany) using a reaction mixture containing 1 ng/µl DNA, 0.2 mM of each of the four dNTPs, 1.5 mM $MgCl_2$, 0.5 µM of each primer and 2.5 U FastStart *Taq* (Roche Diagnostics, Mannheim). Thermal cycling conditions consisted of an initial denaturation step at 94 °C for 2 min followed by 30 cycles of denaturation at 94 °C for 30 s, annealing at 50 °C for 30 s, extension at 72 °C for 30 s, and a final extension at 72 °C for 10 min. The resulting PCR products were purified using polyethylene glycol (PEG) precipitation (Steenkamp et al. 2006) and the purified PCR products were cloned using the pGEM-T Easy vector System I (Promega Corporation, Madison, USA).

The PCR products were cloned, in order to obtain haplotype phases of all sequences derived from the heterokaryotic isolates. The cloned products were amplified from individual colonies with plasmid-specific primers (Steenkamp et al., 2006), after which the PCR products were purified using PEG precipitation. The products were then sequenced with the plasmid-specific primers, Big Dye Cycle Sequencing kit version 3.1 (Perkin-Elmer, Warrington, UK) and an ABI3700 DNA analyzer (Applied Biosystems, Foster City, USA).

The resulting sequence files were analyzed with Chromas Lite 2.0 (Technelysium) and BioEdit version 7.0.2.5 (Hall, 1999) and compared to those in the protein database of the National Centre for Biotechnology Information (www.ncbi.nih.nlm.gov) using BLASTX. To obtain the upstream and downstream sequences of these fragments in *A. areolatum* and *A. chailletii*, nested PCR primers designed with Primer 3 (cgi v0.2) (http://www.genome.wi.mit.edu/genome _software/other/primer3.html) and PCR-based genome walking (Siebert et al., 1995) were used. The nested primers used for genome-walking included RAB1 (5'-ttatgaagcgggtcgctacaag-3'), RAB2 (5'-tacagccatgaccatctggaactt-3'), RAB3 (5'-cgtgtaccccaaggtcatct-3') and RAB4 (5'-ccgagtctcgacgtacaacc-3') for *A. areolatum* and RAB5 (5'-ccagacgtcgacctcacat-3') for *A. chailletii*. The remaining portion of the pheromone receptor gene for *A. chailletii* was obtained using a primer (RAB6, 5'- gccatgaccatttggaactt-3') based on the sequence of *A. areolatum*. All PCR products were cloned and sequenced as described above.

To identify unique *RAB1* alleles in *A. areolatum* and *A. chailletii*, we amplified and sequenced a portion of the *RAB1* gene for 25 isolates of each species by using primer set RABF+RABR (5'-ctggctacgtcctcgtc TA-3'and 5'-gtatgtagcggctggagttg-3', respectively). Thirteen isolates were then selected from each of the two species for further analysis. To amplify and sequence a larger portion of the *RAB1* gene, primer sets RAB1-470F+RAB1-1800R (van der Nest et al., 2008) and RAB7+RAB8 (5'-tggcctacgtcctcgtctat-3' and 5'-aggggttgtacgttgagacg-3', respectively) were used for *A. areolatum* and *A. chailletii*, respectively. For the 13 isolates of each species, portions of the two housekeeping loci, ITS and Tef-1α were also amplified and sequenced. For the ITS region of both species the primer set ITS1+ITS4 (White et al., 1990) was used. For Tef-1α, the primer set TEFac1+TEFac2 (5'-tcctggagaggaagacgaag-3' and 5'-gttcgaggctggtatctccc-3', respectively) was used for *A. chailletii* and primer set TEFaa1+TEFaa2 (5'-agacgtcctggagaggaagg-3' and 5'-ggtatctccaaggacggtca-3', respectively) for *A. areolatum*. These PCR products were purified, cloned and at least 5 clones per individual were sequenced, as

described above. To control for the possible presence of low frequency *RAB1* alleles and to verify our sequencing results for *A. areolatum*, PCR-RFLPs (restriction fragment length polymorphism) (van der Nest et al., 2008) were used. For this purpose, PCR products generated with primers RAB1-470F and RAB1-1800R for the 25 isolates of *A. areolatum* were digested with the enzyme *Eco*RV (Roche Diagnostics) and visualised with agarose gel (Roche Diagnostics) electrophoresis (Sambrook et al. 1989; van der Nest et al., 2008).

Positive selection acting on RAB1

The CODEML program in PAML version 3.14 package (Yang and Nielson, 2002) was used to determine whether the *RAB1* and Tef-1α loci displayed positive selection. To achieve this, MAFFT version 5.85 (http://align.bmr.kyushu-u.ac.jp/mafft/online/server/) (Katoh et al., 2002) was used to generate nucleotide alignments that included sequences for each of the 13 isolates of *A. areolatum* and *A. chailletii*, as well as those for closely related homobasidiomycetes obtained from GenBank. The accession numbers for Tef-1α were *C. cinerea* (AACS01000024), *Schizophyllum commune* (X94913.2), *Echinodontium tinctorium* (AY885157); *Laccaria bicolor* (XM001873179), *Ustilago hordei* (DQ352832); *Saccharomyces serevisae* (EU014692); *Cryptococcus gattii* (EF211806) and *Moniliophthora perniciosa* (AY916741). The accession numbers for *RAB1* were *C. cinerea* (XM00183436, XM00183434 and AY393907CC), *L. bicolor* (XM00188857), *Pholiota nameko* (AB201119), *Lentinula edodes* (EU827518) and *C Coprinellus disseminatus* (DQ056142). These datasets were then subjected to maximum likelihood (ML) analyses using PhyML version 3.0 software (Guindon and Gascuel, 2003) after employing jModeltest and the Akaike Information Criterion (AIC) to select the best-fit substitution models (Posada, 2008). ML analysis of both datasets utilized gamma correction (G) to account for among site rate variation, while the *RAB1* dataset also included a proportion of invariable sites (I). Analysis of the *RAB1* and Tef-1α datasets respectively employed the HKY (Hasegawa et al., 1987) and TrNef (Tamura and Nei, 1993; Posada, 2008) models of nucleotide substitution.

Positive selection was evaluated by computing ω across all the sites for each of the loci (Yang et al., 2000; Devier et al., 2009), where ω reflects the non-synonymous (*dN*)/synonymous (*d*S) substitution rate ratio (Yang and Nielson, 1998). To test for variation of selective pressures across the codons, goodness of fit was calculated for the different site-specific models proposed

by Yang et al. (2000). The null model (M0) assumes that all of the codons have the same selective pressure (*i.e,.* ω=0); the neutral model (M1a) assumes two categories of site, *i.e.*, conserved sites with ω estimated from the data ($\omega < 1$) and neutral sites ($\omega = 1$); and the selection model (M2a) considers an additional or third class of sites under positive selection ($\omega > 1$) (Yang et al., 2005). To account for the fact that only a few codons are likely to be subjected to positive selection ($\omega < 1$), a discrete model (M3) with three categories of site, which allows the ω ratio free to vary for every site, was also used. Models M7 and M8 were also compared, because these models may indicate positive selection when it is detected by the M1 and M2 comparison (Metzger and Thomas, 2010). The M7 model assumes a beta distribution of ω-values between 0 and 1 and it does not allow any sites under positive selection ($\omega > 1$). In contrast, the M8 model also assumes a beta distribution of ω-values between 0 and 1, but it allows another category of sites in which $\omega > 1$. Statistical significance was calculated with likelihood ratio tests (LRT), which entailed analysis of the χ^2 distribution of $2\Delta\ln$ (*i.e.*, twice the log likelihood difference between the two models) for the different models (Yang and Nielson, 1998), where the degrees of freedom were equal to the differences in number of parameters between the two models (Yang et al., 2000).

The rates of evolution of the *RAB1* and Tef-1α loci in *A. areolatum* and *A. chailletii* were compared to one another and to their close relatives, because increased rates of evolution have been observed in asexual lineages (Paland and Lynch, 2006; Howe and Denver, 2008). For this purpose, the same phylogenetic trees and datasets that were used for the site-specific models were applied. These trees and data were used to determine the rates of evolution (ω) along branches (Yang and Nielson, 1998) by making use of the branch-site model (Zhang et al., 2005) implemented in the CODEML. In these analyses, equilibrium codon frequencies calculated from the average nucleotide frequencies at third codon positions (CodonFreq =2) were used to compare the goodness of between the one-ratio and the two-ratio ML models. The one ratio ML model assumes that *A. areolatum* and *A. chailletii* have the same rate of evolution (*i.e.*, all of the branches have the same ω value, ω=0), while the two-ratio ML model assumes different rates of evolution (the branches have different ω-values, $\omega >$ or < than 1) (Johnson and Howard, 2007). The goodness of fit of the different models was compared by doing a LRT with the appropriate degrees of freedom (Yang and Nielson, 1998).

Trans-specific polymorphisms

To determine whether balancing selection acts on *RAB1* to maintain rare alleles over long evolutionary times (Vieira et al., 2008), a phylogenetic tree based on the amino acid sequences of the pheromone receptors present in *A. areolatum*, *A. chailletii*, *A. laevigatum* and sequences from other Basidiomycetes and Ascomycetes available in GenBank was constructed. Accession numbers for the pheromone receptors of other fungi were as follows: *C. cinerea* (AAO17255, CAA71964, CAA71963, AAF01419, AAQ96345, AAQ96344, CAA71962 and AAF01420); *S. commune* (Q92275, CAA62595, P56502, AAR99618, P78741 and AAD35087); *Pleurotus djamor* (AAS46748, AAP57506 and AAP57502; *Cryptococcus neoformans* (AAF71292 and AAN75156); *C. gatti* (AAV28793); *Ustilago maydis* (P31302 and P31303); *U. hordei* (Q99063 and AAD56044); *Pneumocystis carinii* (AAG38536); *Sporisorium reilianum* (CAI59749, CAI59755 and CAI59763); *S. cerevisae* (P06783); *Puccinia graminis* (PGTG195592.2, PGTG00333.2 and PGTG01392.2); *C. disseminates* (AAP57492, AAZ04776, AAZ14943 and AAY88882). The amino acid sequences were aligned using MAFFT and ML phylogenies were inferred with PHYML. ML analysis utilized the best-fit model parameters indicated by ProtTest 2.4 (Abascal et al., 2005) and included the LG model (Le and Gascuel, 2008) of amino acid substitution, a proportion of invariable sites and the observed amino acid frequencies. Branch support was determined using PHYML with the best-fit model and 1000 bootstrap replicates.

Suppressed recombination

Tests of neutrality

Several tests were performed to determine whether polymorphism patterns in the three regions of each species deviated from standard neutral models expected under random mating. These included Tajima's *D* (Tajima, 1989), Fu and Li's *D* and *F* (Fu and Li, 1993), Kelly's *ZnS* (Kelly, 1997), Fay and Wu's *H* (Fay and Wu, 2000), and the nucleotide diversity π (Nei and Li, 1979), al which were obtained using the software package DnaSP version 5. Linkage disequilibrium was estimated using Fisher's method as implemented in DnaSP. The software package GENEPOP version 4.0.10 (Raymond and Rousset, 1995) was used for estimating F statistics according to the method proposed by Weir and Cockerham (1984). Allele frequencies were calculated and departures from Hardy-Weinberg equilibrium were tested using GENEPOP. The mean observed

heterozygosity and the expected heterozygosity for Hardy-Weinberg equilibrium were calculated using Levene's correction for small samples. Heterozygote deficit and excess were estimated with the Score test (U test) available in GENEPOP, using 1000 Markov chain iterations (Rousset and Raymond 1995). The GENEPOP software was also used to calculate the HKA test (Hudson et al., 1987) to compare silent-to-divergence ratios and the MC test (McDonald and Kreitman, 1991) to compare diversity-to-divergence ratios at synonymous and non-synonymous sites.

Phylogenetic analysis

Phylogenetic analyses were performed to determine whether recombination had occurred between the three genes and among the *A. areolatum* and *A. chailletii* representatives included in this study. To establish if the three gene trees in this study were compatible, a sequence alignment for each locus was produced using MAFFT. These datasets were then subjected to ML analyses using PhyML version 3.0 software (Guindon and Gascuel, 2003) after employing jModeltest to select the best-fit model parameters (Posada, 2008). ML analysis of the *RAB1* dataset employed the HKY with I and G, the ITS dataset employed the TrNeF model, and the Tef-1α dataset employed the TrN model (Tamura and Nei, 1993). For each dataset, branch support was determined using the respective best-fit models and 1000 bootstrap replicates. To assess congruencies between the resulting gene trees, a strict consensus tree was computed using Mega software version 4.0.2 (Kumar et al., 2008). The partition homogeneity test using PAUP version 4.0b10 (Swofford, 2000) was used to examine the null hypothesis of recombination in *A. areolatum* and *A. chailletii* (Houbraken et al., 2008). Significance was assigned by comparing the summed tree length from the actual data to those from 100 artificial datasets.

RESULTS

PCR, cloning and nucleotide sequencing

It was possible to identify and characterize the complete pheromone receptor gene *RAB1* (1615 bp) in *A. areolatum* (Fig. 1; Supplementary Fig. 1). Comparison of the pheromone receptor present in this fungus with those present in other homobasidiomycetes (e.g., *C. cinerea*, *L. bicolor*, *S. commune*, *Phanerochaete chrysosporium, Pleurotus ostreatus* and *Postia placenta*) revealed that they all share the same organization (e.g., James et al., 2004a; Raudaskoski and Kothe, 2010). Typical for these proteins, the pheromone receptor in *A. areolatum* harbours the seven-transmembrane and extracellular and cytoplasmic loop domains. The *RAB1* gene also contains five introns, which are comparable with those reported for the pheromone receptors of *C. cinerea* that has four or five and *S. commune* that has three introns (Vaillancourt et al., 1997). Despite several attempts, it was not possible to obtain the entire pheromone receptor genes present in *A. chailletii* (1265 bp, Fig. 1) and *A. laevigatum* (724 bp) (Supplementary Fig. 1). This is because the variable nature of the genes controlling sexual recognition complicates primer design (James et al., 2004b).

The aligned datasets for *RAB1* of the 25 representative isolates of each of *A. areolatum* and *A. chailletii* were 186 nucleotides in length. Eight nucleotide polymorphisms were identified in the *A. areolatum* sequences, six of which were located in intron regions (Supplementary Table 1). Six nucleotide polymorphisms were identified in *A. chailletii*, of which 3 were located in intron regions (Supplementary Table 2). No indels (insertions or deletions) were detected in either of the two species.

For 13 of the 25 representative isolates of *A. areolatum* and *A. chailletii*, a larger portion of the *RAB1* gene, as well as a portion of Tef-1α (Supplementary Fig. 2) and ITS (Supplementary Fig. 3) were sequenced. The aligned datasets for ITS, Tef-1α and *RAB1* in the 13 representative isolates of each of *A. areolatum* and *A. chailletii* were respectively 606, 474 and 682 nucleotides long. Based on the sequence alignments, two types of Tef-1α were identified. Because the one type contained a premature stop, it was considered a pseudogene and not included in subsequent analyses. Among the representatives of *A. areolatum*, we identified 6, 1 and 12 nucleotide polymorphisms in the Tef-1α, ITS and *RAB1* sequences, respectively (Supplementary Table 3).

For the Tef-1α and *RAB1* sequences, 4 and 8 of these respective polymorphisms were located in intron regions. The *A. chialletti* sequences harboured 7, 5 and 7 single nucleotide polymorphisms for Tef-1α, ITS and *RAB1*, respectively (Supplementary Table 4). For both the Tef-1α and *RAB1* sequences, 4 of the single nucleotide polymorphism were located in intron regions. The aligned *A. chialletti* ITS and Tef-1α datasets each harboured a single indel, with the latter located in an intron. The *A. chialletti RAB1* alignment harboured two large indels (6 and 21 nucleotides in length) in intron regions. All of the identified polymorphisms in both species represent synonymous substitutions and no non-synonymous substitutions were detected.

Similar to other eukaryotic recognition loci (e.g., Uyenoyama, 2005; Menkis et al., 2008), the *A. areolatum* and *A. chailletii RAB1* π-values (0.004 and 0.02, respectively) were generally higher than the π-values for the housekeeping genes (Table 1). For example, the π-values for the ITS locus were much lower for both *A. areolatum* (0.0004) and *A. chailletii* (0.002). However, even though π-value of Tef-1α (0.006) for *A. chialletii* was much lower than that for *RAB1* of this species, the π value of Tef-1α (0.005) for *A. areolatum* was similar to the π-value of *RAB1* for this species.

Positive selection acting on RAB1

The phylogenetic trees constructed for PAML analysis are indicated in Figures 2A and 2B. Calculations under model M3 with variable selective pressures acting on the codons and models that assumes no selection (M0 and M1) provides a better fit for *RAB1* and Tef-1α (Table 2). For *RAB1* the log likelihood difference between M3 and M0 was 144.08 with a significant χ^2 distribution test result ($P < 0.001$), while the M3 and M1 was 137.28 with a significant χ^2 distribution test result ($P < 0.001$). For Tef-1α, the log likelihood difference between M3 and M0 was 32.12 with a significant χ^2 distribution test result ($P < 0.001$), while the M3 and M1 was 22.90 with a significant χ^2 distribution test result ($P < 0.001$). However, for *RAB1* and Tef-1α in *A. areolatum* and *A. chailletii* the log likelihood differences were 0 for M2 and M1, as well as for M8 and M7. The positive-selection models (M2 and M8), therefore, did not provide a better fit in comparison to models that assume no positive selection (M1 and M7).

Because the external branches of *A. areolatum* and *A. chailletii* are not associated with any non-synonymous substitutions ($\omega = 0$) for either *RAB1* or Tef-1α, it was not possible to compare the rate of evolution between these species. However, it was possible to determine whether non-

synonymous and synonymous substitutions accumulate at different rates in *A. areolatum* and *A. chailletii* in comparison to close relatives (Table 3). The log likelihood of the two models (different ω-values for *Amylostereum* spp. and close relatives) was 15.72 for *RAB1* with 8 degrees of freedom and 1.64 for Tef-1α with 6 degrees of freedom, no significant difference ($P > 0.05$) were thus detected between these two models for *RAB1* and Tef-1α.

Trans-specific polymorphisms

The *RAB1* ML phylogeny included sequences from other Basidiomycetes and Ascomycetes, as well as sequences of a large portion of a pheromone receptor in *A. chailletii* (1265 bp), *A. laevigatum* (724 bp), and the *RAB1.1*, *RAB1.2* and *RAB1.3* (1380 bp) alleles that were previously identified in *A. areolatum* (van der Nest et al., 2008). Similar to previous studies, all of the homobasidiomycete pheromone receptors grouped into two major clusters (Riquelme et al., 2005; James et al., 2006). The putative pheromone receptor of *A. laevigatum* formed part of a clade that contained hypothetical proteins from *C. cinereus*, *L. bicolor* and *P. placenta*, as well as the known pheromone receptors present *S. commune* (Bbr2) and *C. cinerea* (Rcb2.6) (Riquelme et al., 2005), which suggests that the sequenced *A. laevigatum* pheromone receptor have an origin separate from those for *A. areolatum* and *A. chailletii*. The putative pheromone receptors of the latter species appeared to be each other's closest neighbours and they grouped together with hypothetical proteins from *C. cinereus*, *P. placenta*, *L. bicolor*, and *P. nameko*.

Suppressed recombination

Tests of neutrality

The allelic and genotypic frequencies of the 13 selected *A. areolatum* and *A. chailletii* isolates are presented in Figures 4A and 4B. The number of alleles identified in the three genes (*RAB1*, ITS and Tef-1α) investigated in this study ranged from 2 to 6 for *A. areolatum* and 3 to 5 for *A. chialletti*. Although similar numbers of alleles were detected in the 13 selected *A. areolatum* and *A. chailletii* isolates for Tef-1α (6 and 5 alleles, respectively) and RAB1 (3 each), more than twice as many ITS alleles were detected in *A. chailletii* (5 alleles) than in *A. areolatum* (2 alleles). The three *RAB1* alleles *(RAB1.1*, *RAB1.2* and *RAB1.3*) that were previously identified (van der Nest et al., 2008) were detected in the 13 selected *A. areolatum* isolates (Supplementary Table 3), as well as in the 25 isolates obtained from different regions of the world

(Supplementary Table 1). However, sequences obtained from the 25 *A. chailletii* isolates (3 alleles), as well as sequences obtained for a larger portion of the *RAB1* gene for the 13 selected isolates (two additional alleles) revealed the presence of five pheromone receptor alleles in this species (Supplementary Tables 2 and 5). More *RAB1* alleles were therefore, also detected in *A. chailletii* (5 alleles) than in *A. areolatum* (3 alleles). Despite the fact that most alleles were quite common, some occurred at very low frequencies. Because *Eco*RV only cleaves *RAB1.3*, the PCR-RFLPs demonstrated that this rare allele in *A. areolatum* is also present in such low frequencies in the 25 isolates tested in this study. Only the *A. areolatum RAB1* alleles and the ITS alleles for both species deviated significantly from what is expected under the Hardy-Weinberg equilibrium (Table 1).

Among the *A. chailletii* individuals, respectively 9, 8 and 6 unique ITS, Tef-1α and *RAB1* genotypes (*i.e.*, multilocus genotypes based on the three loci) were identified. Among the *A. areolatum* isolates respectively 3, 7 and 3 ITS, Tef-1α and *RAB1* genotypes were identified (Fig. 4B). Compared to *A. areolatum*, the *A. chailletii* individuals thus represented more than twice the number of unique ITS (9 *vs*. 3) and *RAB1* (6 *vs*. 3) genotypes. *Amylostereum chailletii* also included more than four times as many genotypes that were represented by a single individual (*i.e.*, 6 *vs*. 1 ITS genotypes and 4 *vs*. 0 *RAB1* genotypes). Some of the genotypes were over-represented. For example, 76.92 % of the *A. areolatum* individuals shared the same ITS genotype and 53.84 % of the *A. chailletii* individuals shared a *RAB1* genotype (Fig. 4B). These over-represented genotypes were also homozygotic, with both nuclei of the heterokaryon having the same allelic state. The frequency of observed homozygotes was higher than expected, except for *RAB1* in *A. areolatum* (Table 1). There was also a significant deficiency in heterozygosity associated with the ITS of *A. areolatum* and *A. chailletii* (Table 1). The inbreeding coefficient (fixation index, F_{is}) was positive for all three genes for both the species (F_{is} ranging from 0.055 to 0.7692) (Table 1). Furthermore, the F_{is}-values were significant for ITS in *A. areolatum* and *A. chailletii* and for *RAB1* in *A. areolatum*, suggesting a significant reduction in heterozygozity probably due to preferential or non-random mating with relatives for both these species.

Although the values from Tajima's test were not significant for any of the genes in both the species, the values of the Fu and Li's tests were significant for the *A. areolatum RAB1* data and the Tef-1α data present in both *A. areolatum* and *A. chailletii*, thereby rejecting the hypothesis of neutrality (Table 4). All of these significant values were positive, due to the presence of several

common alleles at each locus (Akey et al., 2004; Tennessen and Blouin, 2008). The results for both the HKA and MK tests were not significant because of the lack of non-synonymous substitutions in *A. areolatum* and *A. chailletii* for the genes investigated in this study. Little evidence was found for linkage disequilibrium occurring in ITS of *A. areolatum* and *A. chailletii*, as well as for *RAB1* present in *A. chailletii*. However, the results for 10 comparisons in *A. chailletii* Tef-1α and 5 comparisons in Tef-1α and 22 comparisons in *RAB1* present in *A. areolatum* were significant. Furthermore, 16 of the 22 comparisons in *RAB1* of *A. areolatum* were clustered within a 85-bp region (from site 74-159, covering the region that includes intron 5 and transmembrane segment 5. Clustering of the pairs of polymorphic sites with significant linkage disequilibrium was, therefore, observed for *RAB1* in *A. areolatum* and Tef-1α in *A. chailletii*. Significant linkage disequilibrium was also observed between *RAB1* and Tef-1α present in *A. areolatum* ($P = 0.0072$) and *A. chailletii* ($P = 0.0019$) using DnaSP (P-values was obtained for each locus pair across all populations using Fisher's method).

Phylogenetic analysis

Two distinct clades were identified for all three the genes, with the one clade containing the *A. areolatum* isolates and the other *A. chailletii* isolates (Fig. 5A, 5B and 5C). Clonal lineages were observed between the three trees for both species. For example, the alleles of the *A. areolatum* isolates from the Southern Hemisphere grouped together for all three the genes (Fig. 5A, 5B and 5C). However, incongruencies were also observed among the *RAB1*, Tef-1α and ITS phylogenies where the same isolates did not group in the same clades for all three the genes (Fig. 5A, 5B and 5C). For example, the alleles of the *A. areolatum* isolates obtained from Southern Hemisphere countries grouped together with different isolates for each of the gene trees. No structure was evident in the strict consensus tree for both *A. areolatum* and *A. chailletii* (Fig. 5D). Isolates of *A. areolatum* and *A. chailletii* clearly separated into two distinct clades in the strict consensus tree indicating that no sexual recombination has occurred between isolates of these two species (Fig. 5D). The partition homogeneity test results indicated that recombination has occurred in *A. areolatum* and *A. chailletii*, as the sums of the tree length of the resampled data were longer than that of the observed data ($P < 0.001$).

DISCUSSION

The putative pheromone receptor gene encoded at the *mat-B* locus of *A. areolatum* was characterised by making use of degenerate PCR and genome walking. Based on sequence similarity, the *A. areolatum RAB1* gene appears to form part of a new sub-class of pheromone receptor genes that have not yet been characterized (Fig. 3), it only shares sequence similarity with hypothetical pheromone receptors of *C. cinerea* (Riquelme et al., 2005). Although we sequenced only part of the *RAB1* gene of *A. chailletii*, it also forms part of this new sub-class of pheromone receptor gene. The *RAB1* gene of *A. laevigatum* forms part of an existing sub-class that includes rcb2.6 of *C. cinerea* and hypothetical pheromone receptors from other homobasidiomycetes such as *S. commune* and *L. bicolor* (Riquelme et al., 2005; James et al., 2006).

Results of this study suggest that the genes controlling sexual recognition in *A. areolatum* and *A. chailletii* are more polymorphic and diverse than the rest of the genome, which is similar to what was previously found for other eukaryotes (e.g., May et al., 1999; James et al., 2001; Devier et al., 2009). Both *A. areolatum* and *A. chailletii* displayed nucleotide diversities for *RAB1* that are higher than the nucleotide diversities observed for their corresponding ITS and Tef-1α sequences (Table 1). The *A. areolatum* and *A. chailletii RAB1* nucleotide diversity values (π =0.004 and π=0.02, respectively) were generally lower and in some cases comparable to those reported for the pheromone receptor genes of other homobasidiomycetes. For example, the π-values for the pheromone receptors present in *C. disseminates* ranged between 0.005 and 0.371 (James et al., 2006), while the the π-values for the pheromone receptors present in *Serpula lacrymans* ranged between 0.048 and 0.062 (Engh et al., 2010). However, the differences between the nucleotide diversity of the pheromone receptor and housekeeping genes in *A. areolatum* and *A. chailletii* was smaller than those observed for *S. lacrymans* (Engh et al., 2010). The π-values of *RAB1* was 10 times higher than those for ITS in both *A. areolatum* and *A. chailletii*. In contrast, the difference between the pheromone receptor gene and ITS was generally about 100 times higher for *S. lacrymans* (Engh et al., 2010). In fact, the nucleotide diversities of all three of the regions investigated in this study are much lower (π-values ranging between 0.0004 and 0.006) than those observed for the nuclear genes of other fungi. For example, in the basidiomycete *Rhizoctonia solani* π-values ranged between 0.003 and 0.025

(Ciampi et al., 2009). Therefore, the nucleotide diversities of the examined *RAB1* gene in this study are generally lower than those reported for other fungi and the overall diversity of the housekeeping genes of *A. areolatum* and *A. chailletii* were also low. This is consistent with the observations in previous studies (e.g., Vasiliauskas et al., 1998; Vasiliauskas and Stenlid, 1999).

The genes present at the *mat-B* locus of *A. areolatum* and *A. chailletii* were multiallelic in having at least three alleles each (Fig. 2). This is similar to what is known for other fungi with a tetrapolar mating type system (e.g., Kothe et al., 2003; Riquelme et al., 2005). Evidence of trans-specific polymorphism among the pheromone receptor genes of the *Amylostereum* spp. studied was also detected in this study (Fig. 3). This is because the *A. laevigatum* pheromone receptor gene grouped separately from those identified for *A. chailletii* and *A. areolatum*, even though it were previously demonstrated that the *Amylostereum* spp. are each other's closest relatives (Slippers et al., 2000; Tabata et al., 2000). This suggests that these genes are more ancient than the species themselves, which is characteristic of trans-specific polymorphisms and balancing selection (Vieira et al., 2008; Devier et al., 2009). However, different from other sex-related genes (Civetta and Singh, 1998), we detected no evidence for positive selection acting on the *RAB1* genes of *A. areolatum* or *A. chailletii*. Instead, the ω-values for *RAB1* of *A. areolatum* and *A. chailletii* were significantly below 1, indicating that purifying selection has probably acted to eliminate most amino acid substitutions in these genes. This has also been suggested for *Microbotryum* spp., where purifying selection and not positive selection was implicated in the evolution of their pheromone receptors (Devier et al., 2009).

Further evidence of balancing selection acting on the *mat* loci of *A. areolatum* and *A. chailletii*, is that the *mat* alleles identified in this study occurred at roughly equal frequencies (Fig. 4). Balancing selection is known to keep the *mat* alleles distributed throughout the world at equal frequencies (James et al., 2001). However, in both fungi, the remaining *RAB1* alleles occurred at very low frequencies among the isolates originating from different regions of the world. Although, it is possible that these low-frequency alleles could have appeared recently through migration or mutation, it is also possible that they are associated with impaired-fitness factors (Larraya et al., 2001). Van der Nest et al. (2009) suggested previously that gene/s closely linked to the *mat* loci could contain mildly deleterious alleles, because such alleles would be retained in a population due to balancing selection. It is thus conceivable that *A. areolatum* and *A. chailletii* homokaryons carrying such deleterious pheromone receptor alleles will not be able

to out-compete other homokaryons, which in turn reduce the number of possible mating types (*i.e.*, functional *mat* alleles) in a population (Uyenoyama, 2003; Devier et al., 2009). This is important, because the number of *mat* alleles will influence the frequency of outcrossing (Hsueh and Heitman, 2008). Sexual reproduction in these fungi is thus dependent on the efficiency of balancing selection to maintain *mat* allele diversity despite their possible association with impaired-fitness factors.

Allelic diversity of eukaryotic recognition loci is subjected, not only to the effects of balancing selection, but also suppressed recombination (e.g., Uyenoyama, 2005; Menkis et al., 2008). However, no evidence of recombination was detected within the region of the pheromone receptor gene studied in *A. areolatum* and *A. chailletii*. This is consistent with the view that recombination between different subloci is allowed and necessary for the formation of new mating type specificities, while recombination within subloci is suppressed to prevent self-compatibility in fungi with tetrapolar mating systems (Lukens et al., 1996). The fact that reduced recombination at the *mat-B* locus was not detected is also consistent with the results of a previous study where a genetic linkage map was used to study the evolution of the *mat* loci of *A. areolatum* (van der Nest et al., 2009). Even though it was suggested that recombination is suppressed over the entire genome of *A. areolatum* (van der Nest et al., 2009), recombination was detected among the three loci examined in this study in *A. areolatum* and *A. chailletii*. These species were both characterized by unique multilocus genotypes among individuals and by incongruencies among the phylogenies inferred from the three loci studied (Fig. 5), which are due to the effects of recombination that has broken-up the association between alleles (Milgroom, 1996; Otto, 2003; Haag and Roze, 2007; Houbraken et al., 2008). However, these findings do not imply that suppressed recombination is not acting on the *mat* loci of *A. areolatum* and *A. chailletii* as the portion of the genome of the *mat-B* locus examined in this study was probably inordinately short to detect recombination over the entire locus. An analysis with the entire locus and the regions flanking it might reveal that recombination is reduced in or excluded from this region in these fungi to ensure the identity and diversity of these loci (e.g., Uyenoyama, 2005; Menkis et al., 2008).

In addition to balancing selection, positive selection and suppressed recombination, the patterns of polymorphism observed in this study may also reflect demographic processes *i.e.,* population dynamics (Johnson and Howard, 2007). This is consistent with the significantly

positive values obtained for Fu and Li's tests, which suggest that recent population bottlenecks and/or population subdivision can also partly explain the observed patterns of polymorphism (Akey et al., 2004; Tennessen and Blouin, 2008). Such bottlenecks and population subdivisions often occur in inbreeding and asexual organisms (Woolfit and Bromham, 2003; Glémin et al., 2006). It is thus possible that recent genetic bottlenecks and population subdivisions in *A. areolatum* and *A. chailletii* resulted from asexual reproduction and inbreeding. For example, inbreeding and/or asexuality in *A. areolatum* and *A. chailletii* could explain the low nucleotide diversity of the genes investigated in this study and the observed linkage disequilibrium between these genes, as such associations have previously been observed (Glémin et al., 2006; Haag and Roze, 2007; Haudry et al., 2008). Similar patterns of polymorphisms have also been observed in other symbionts of insects that reproduce mostly asexually with reduced levels of recombination and effective population sizes (Rispe and Moran, 2000; Mira and Moran 2002).

A predominantly asexual mode of reproduction will decrease the overall diversity of *A. areolatum* and *A. chailletii*. Consistent with this notion, dominant genotypic classes in both *A. areolatum* and *A. chailletii* were detected, which possibly indicate that well-adapted genotypes associated with the woodwasp had been spread successfully through asexual reproduction (Fig. 4). Also, the allelic and genotypic diversities associated with the three loci examined in *A. areolatum* were lower than those observed for *A. chailletii* (Table 1), which possibly reflect the fact that *A. areolatum*, with its more pronounced asexual mode of reproduction, has a closer relationship with the woodwasp than *A. chailletii* (Slippers et al., 2001; Vasiliauskas et al., 1998; Vasiliauskas and Stenlid, 1999). However, based on the results of this study, it is not possible to exclude the possibility that inbreeding may occur in *A. areolatum* and *A. chailletii.* In addition to detecting significant heterozygosity deficiencies in the ITS sequences of both fungi, significant F_{is}-values were also observed for *RAB1* in *A. areolatum* and ITS in *A. areolatum* and *A. chailletii*. The latter result suggests the presence of increased frequency of individuals that are homozygous for alleles identical by descent due to preferential (non-random) mating with relatives (Keller and Weller, 2002).

The populations of inbreeding or asexually reproducing organisms are typically associated with decreased fitness (Keller and Weller, 2002; Haag and Roze, 2007; Haudry et al., 2008; Howe and Denver, 2008). In this study, a potentially deleterious mutation in *A. areolatum* was observed where a nucleotide substitution in one of the Tef-1α alleles resulted in a change from

encoding a lysine to a stop codon, and translation of this variant would result in a truncated and potentially non-functional protein. To counter the effect of deleterious mutations, multi-copy genes are often employed (Welch and Meselson, 2001; Jany and Pawlowska, 2010). In both *A. areolatum* and *A. chailletii* two types of Tef-1α were identified in this study, which could be associated with opposing the effects of deleterious mutations. Asexuality is expected to lead to an increased rate of fixation of slightly deleterious mutations within endosymbiont lineages due to bottlenecks and population subdivision (Woolfit and Bromham, 2003), while inbreeding may decrease fitness due to increased homozygosity and genetic load (*i.e.*, inbreeding depression) (Keller and Weller, 2002; Haudry et al., 2008). It is thus possible that deleterious mutations might have arisen in *A. areolatum* and *A. chailletii* as a result of the reduced effective recombination and reduced effective population size (Butlin, 2006; Haag and Roze, 2007; Howe and Denver, 2008).

Collectively, the results of this study indicated that the genes encoded at the *mat* loci were more polymorphic than the rest of the genome of the fungi examined. This is similar to what is known for other fungi with tetrapolar mating systems (e.g., May et al., 1999; James et al., 2001; Devier et al., 2009). However, it appears that balancing selection and not positive selection retains the diversity of the pheromone receptors in *A. areolatum* and *A. chailletii*. Similar to other asexually reproducing fungi (Taylor et al., 1999; Hsueh and Heitman, 2008), these results also suggest that, despite the effective asexual spread of *A. areolatum* and *A. chailletii* by the woodwasp, these fungi favour a system of mixed modes of reproduction. However, results of this study also indicate that the association of the fungus with the woodwasp has influenced the evolution and biology of these fungi. This is because the nucleotide, allelic and genotypic diversities were lower for *A. areolatum* than those for *A. chailletti*, which is not as closely associated with its insect partner. This possibly reflects the population bottlenecks and subdivision that is associated with the effective spread of these fungi by the woodwasp and inbreeding. However, in order to more fully determine the influence of the woodwasp on the population structure of these fungi, it would be necessary to conduct a thorough population study, including larger numbers of isolates.

REFERENCES

Abascal, F., Zardoya, R., Posada, D., 2005. ProtTest: selection of best-fit models of protein evolution. Bioinformatics. 21, 2104-2105.

Akey, J.M., Eberle, M.A., Rieder, M.J., Carlson, C.S., Shriver, M.D., Nickerson, D.A., Kruglyak, L., 2004. Population history and natural selection shape patterns of genetic variation in 132 genes. Plos Biol. 2, e286.

Barton, N. H., Charlesworth, B., 1998. Why sex and recombination. Science. 281, 1986-1990.

Baumann, P., Moran, N.A., 1997. Non-cultivable microorganisms from symbiotic associations of insects and other hosts. Anton. Leeuw. Int. J. G. 72, 39-48.

Boidin, J., Lanquentin, P., 1984. Le genre *Amylostereum* (Basidiomycetes) intercompatibilités partielles entre espèces allopartriques. Bull. Soc. Mycol. Fr. 100, 211-236.

Butlin, R., 2006. Comment on "transitions to asexuality result in excess amino acid substitutions". Science. 313, 1389b.

Carbone, I., Anderson, J.B., Kohn, L.M., 1999. Patterns of descent in clonal lineages and their multilocus fingerprints are resolved with combined gene genealogies. Evolution. 53, 11-21.

Ciampi, M.B., Gale, L.R, de Macedo Lemos, E.G., Ceresini, P.C., 2009. Distinctively variable sequence-based nuclear DNA markers for multilocus phylogeography of the soybean- and rice-infecting fungal pathogen *Rhizoctonia solani* AG-1 IA. Genet. Mol. Biol. 32, 4, 840-846.

Civetta, A. R., Singh, S., 1998. Sex-related genes, directional sexual selection, and speciation. Mol. Biol. Evol. 15, 901-909.

Devier, B., Aguileta, G., Hood, M.E., Giraud, T., 2009. Ancient trans-specific polymorphism at pheromone receptor genes in Basidiomycetes. Genetics. 181, 209-223.

Engh, I.B., Skrede,I., Sætre, G.-P., Kauserud, H., 2010. High variability in a mating type linked region in the dry rot fungus *Serpula lacrymans* caused by frequency-dependent selection? BMC Genetics. 11, 64.

Fay, J.C., Wu, C.-I., 2000. Hitchhiking under positive Darwinian selection. Genetics, 155, 1405-1413.

Fu, Y.-X., Li, W.-H., 1993. Statistical tests of neutrality of mutations. Genetics, 133, 693-709.

Glémin, S., Bazin, E., Charlesworth, D., 2006. Impact of mating systems on patterns of sequence polymorphism in flowering plants. Proc. R. Soc. London. B. 273, 3011-3019.

Guindon, S., Gascuel, O., 2003. A simple, fast and accurate algorithm to estimate large phylogenies by maximum likelihood. Syst. Biol. 52, 696-704.

Haag, C.R., Roze, D., 2007. Genetic load in sexual and asexual diploids: segregation, dominance and genetic drift. Genetics. 176, 1663-1678.

Hall, T., 1999. BioEdit: A user-friendly biological sequence alignment editor and analysis program for Windows 95/98/NT. Nucl. Acid. S. Series. 41, 95-98.

Hasegawa, M., Kishino, H., Yano, T., 1985. Dating of human-ape splitting by a molecular clock of mitochondrial DNA. J. Mol. Evol. 22, 160-174.

Haudry, A., Cenci, A., Guilhaumon, C., Paux, E., Santoni, S., David, J., Glémin, S., 2008. Mating system and recombination affect molecular evolution in four *Triticeae* species. Genet. Res. Camb. 90, 97-109.

Houbraken, J., Varga, J., Rico-Munoz, E., Johnson, S., Samson, R.A., 2008. Sexual Reproduction as the Cause of Heat Resistance in the Food Spoilage Fungus *Byssochlamys spectabilis* (Anamorph *Paecilomyces variotii*). Appl. Environ. Microb. 74, 1613-1619.

Howe, D.K., Denver, D.R., 2008. Muller's ratchet and contemporary mutation in *Caenorhabditis briggsae* mitochondrial genome evolution. BMC Evol. Biol. 8, 62.

Hsueh, Y-P., Heitman, J., 2008. Orchestration of sexual reproduction and virulence by the fungal mating-type locus. Curr. Opin. Microbiol. 2008.

Hudson, R.R., Kreitman, M., Aguade, M., 1987. A test of neutral molecular evolution based on nucleotide data. Genetics. 116, 153-159.

Hurley, B.P., Slippers, B., Wingfield, M.J., 2007. A comparison of control results for the alien invasive woodwasp, *Sirex noctilio*, in the southern hemisphere. Agric. For. Entomol. 9, 159-171.

James, T.Y., Kües, U., Rehner S.A., Vilgalys, R., 2004a. Evolution of the gene encoding mitochondrial intermediate peptidase and its cosegregation with the A mating-type locus of mushroom fungi. Fungal Genet. Biol. 41, 381-390.

James, T.Y., Liou, S.-R., Vilgalys, R., 2004b. The genetic structure and diversity of the A and B mating type genes from the tropical oyster mushroom, *Pleurotus djamor*. Fungal Genet. Biol. 41, 813-825.

James, T.Y., Moncalvo, J-M., Li, S., Vilgalys, R., 2001. Polymorphism at the ribosomal DNA spacer and its relation to breeding structure of the widespread mushroom *Schizophyllum commune*. Genetics. 157, 149-161.

James, T.Y., Srivilai, P., Kües, U., Vilgalys, R., 2006. Evolution of the bipolar mating system of the mushroom *Coprinellus disseminatus* from its tetrapolar ancestors involves loss of mating-type-specific pheromone receptor function. Genetics. 172, 1877-1891.

Jany, J.-L., Pawlowska, T.E., 2010. Multinucleate spores contribute to evolutionary longevity of asexual Glomeromycota. Am. Nat. 175, 424-435.

Johnson, S.G., Howard, R.S., 2007. Contrasting patterns of synonymous and nonsynonymous sequence evolution in asexual and sexual fresh water snail lineages. Evolution. 61, 2728-2735.

Kaltenpoth, M., Goettler, W., Koehler, S., Strohm, E., 2010. Life cycle and population dynamics of a protective insect symbiont reveal severe bottlenecks during vertical transmission. Evol. Ecol. 24, 463-477.

Katoh, K., Misawa, K., Kuma, K., Miyata, T., 2002. MAFFT: a novel method for rapid multiple sequence alignment based on fast Fourier transform. Nucl. Acids Res. 30, 3059-3066.

Keller, L.F., Weller, D.M., 2002. Inbreeding effects in wild populations. Trends Ecol. Evol.17, 230-241.

Kelly, J.K., 1997. A test of neutrality based on interlocus associations. Genetics. 146, 1179-1206.

Kothe, E., Gola, S., Wendland, J., 2003. Evolution of multispecific mating-type alleles for pheromone perception in the homobasidiomycetes fungi. Curr. Genet. 42, 268-275.

Kumar, S., Dudley, J., Nei, M., Tamura, K., 2008. MEGA: A biologist-centric software for evolutionary analysis of DNA and protein sequences. Brief. Bioinform. 9, 299-306.

Larraya, L.M., Perez, G., Iribarren, I., Blanco, J.A., Alfonso, M., Pisabarro, A.G., Ramírez, L., 2001. Relationship between monokaryotic growth rate and mating type in the edible basidiomycetes *Pleurotus ostreatus*. Appl. Environ. Microb. 67, 3385-3390.

Le, S.Q., Gascuel, O., 2008. An improved general amino acid replacement matrix. Mol. Biol. Evol. 25, 1307-1320.

Lukens, L., Yicunt, H., May, G., 1996. Correlation of genetic and physical maps at the A mating-type locus of *Coprinus cinereus*. Genetics. 144, 1471-1477.

Madden, J.L., 1981. Egg and larval development in the woodwasp, *Sirex noctilio* F. Aust. J. Bot. 14, 25-30.

May, G.S., Badrane, H., Vekemans, X., 1999. The signature of balancing selection: Fungal mating compatibility gene evolution. Proc. Natl. Acad. Sci. USA. 96, 9172-9177.

McDonald, J.H., Kreitman, M., 1991. Adaptive protein evolution at the ADH locus in *Drosophila*. Nature. 351, 652-654.

Menkis, A., Jacobson, D.J., Gustafsson, T., Johannesson, H., 2008. The mating-type chromosome in the filamentous ascomycete *Neurospora tetrasperma* represents a model for early evolution of sex chromosome. Plos Genetics. 4, e1000030.

Metzger, K.J., Thomas, M.A., 2010. Evidence of positive selection at codon sites localized in extracellular domains of mammalian CC motif chemokine receptor proteins. BMC Evol. Biol. 10, 139.

Milgroom, M.G., 1996. Recombination and the multilocus structure of fungal populations. Annu. Rev. Phytopathol. 34, 457-477.

Mira, A., Moran, N.A., 2002. Estimating population size and transmission bottlenecks in maternally transmitted endosymbiotic bacteria. Microb. Ecol. 44, 137-143.

Nei, M., Li, W.-H., 1979. Mathematical model for studying genetic variation in terms of restriction endonucleases. Proc. Natl. Acad. Sci. USA. 76, 5269-5273.

Neiman, M., Hehman, G., Miller, J.T., Logsdon, J.M., Taylor, D.R., 2010. Accelerated mutation accumulation in asexual lineages of a freshwater snail. Mol. Biol. Evol. 27, 954-963.

Nielsen, C., Williams, D.W., Hajek, A.E., 2009. Putative source of the invasive *Sirex noctilio* fungal symbiont, *Amylostereum areolatum*, in the eastern United States and its association with native siricid woodwasps. Mycol. Res. 113, 1242 - 1253.

Otto, S.P., 2003. The Advantages of Segregation and the Evolution of Sex. Genetics 164: 1099-1118.

Paland, S., Lynch, M., 2006. Transitions to asexuality results in excess amino acid substitutions. Science. 311, 990-992.

Posada D., 2008. jModelTest: Phylogenetic Model Averaging. Mol. Biol.Evol. 25, 1253-1256.

Raudaskoski, M., Kothe, E., 2010. Basidiomycete mating type genes and pheromone signaling. Euk. Cell. 9, 847-859.

Raymond, M., Rousset, F., 1995. GENEPOP (version 1.2): Population genetics software for exact tests and ecumenicism. J. Hered. 86, 248 - 249.

Riquelme, M., Challen, M.P., Casselton, L.A., Brown, A.J., 2005. The origin of multiple *b* mating specificities in *Coprinus cinereus.* Genetics. 170, 1105-1119.

Rispe, C., Moran, N.A., 2000. Accumulation of deleterious mutations in endosymbionts: Muller's ratchet with two levels of selection. Am. Nat. 156, 425-441.

Rousset, F., Raymond, M., 1995. Testing Heterozygote Excess and Deficiency. Genetics. 140, 1413-1419.

Ruggiero, M.V., Jacquemin, B., Castric, V., Vekemans, X., 2008. Hitch-hiking to a locus under balancing selection: high sequence diversity and low pollution subdivion at the S-locus genomic region in *Arabidopsis halleri*. Genet. Res. Camb. 90, 37-46.

Sambrook, J., Fritsch, E.F., Maniatis, T., 1989. Molecular cloning: a laboratory manual. Cold Spring Harbour Laboratory Press, New York.

Siebert, P.D., Chenchik, A., Kellog, D.E., Lukyanov, K.A., Lukyanov, S.A. 1995. An improved PCR method for walking in uncloned genomic. DNA. Nucleic Acids Res. 23, 1087–1088.

Slippers, B., Coutinho, T.A., Wingfield, B.D., Wingfield, M.J., 2003. A review of the genus *Amylostereum* and its association with woodwasps. SA. J. Sci. 99, 70-74.

Slippers, B., Wingfield, M.J., Wingfield, B.D., Coutinho, T.A., 2000. Relationships among *Amylostereum* species associated with siricid woodwasps inferred from mitochondrial ribosomal DNA sequences. Mycologia. 92, 955-963.

Slippers, B., Wingfield, M.J., Wingfield, B.D., Coutinho, T.A., 2001. Population structure and possible origin of *Amylostereum areolatum* in South Africa. Plant. Pathol. 50, 206-210.

Steenkamp, E.T., Wright, J., Baldauf, S.L., 2006. The protistan origins of animals and fungi. Mol. Biol. Evol. 23, 93-106.

Swofford, D.L., 2000. PAUP*: phylogenetic analysis using parsimony (*and other methods), version 4.0b4a. Sinauer Associates, Sunderland, MA.

Tabata, M., Abe, Y., 1997. *Amylostereum laevigatum* associated with the Japanese horntail, *Urocerus japonicus.* Mycoscience. 38, 421-427.

Tabata, M., Harrington, T.C., Chen, W., Abe, Y., 2000. Molecular phylogeny of species in the genera *Amylostereum* and *Echinodontium*. Mycoscience. 41, 585-593.

Tajima, F., 1989. Statisticalmethod for testing the neutralmutation hypothesis by DNA polymorphism. Genetics. 123, 585–595.

Tamura, K., Nei, N., 1993. Estimation of the number of nucleotide substitutions in the control region of mitochondrial-DNA in humans and chimpanzees. Mol. Biol. Evol. 10, 512-526.

Taylor, J.W., Jacobson, D.J., Fisher, M.C., 1999. The evolution of asexual fungi: Reproduction, speciation and classification. Annu. Rev. Phytopathol. 37, 197-246.

Tennessen, J.A., Blouin, M.S., 2008. Balancing selection at a frog antimicrobial peptide locus: Fluctuating immune effector alleles? Mol. Biol. Evol. 25, 2669-2680.

Uyenoyama, M.K., 2003. Genealogy-dependent variation in viability among self-incompatibility genotypes. Theor. Popul. Biol. 63, 281-293.

Uyenoyama, M.K., 2005. Evolution under tight linkage to mating type. New Phytol. 165, 63-70.

Vaillancourt, L.J., Raudaskoski, M., Specht, C.A., Raper, C.A., 1997. Multiple genes encoding pheromones and pheromone receptor define the Bβ1 mating-type specificity in *Schizophyllum commune*. Genetics. 146, 541-551.

Van der Nest, M.A., Slippers, B., Stenlid, J., Wilken, P.M., Vasaitis, R., Wingfield M.J., Wingfield, B.D., 2008. Characterization of the systems governing sexual and self-recognition in the white rot homobasidiomycete *Amylostereum areolatum*. Curr. Genet. 53, 323-336.

Van der Nest, M.A., Slippers, B., Steenkamp, E. T., de Vos, L., van Zyl, K., Stenlid, J., Wingfield, M.J., Wingfield B.D., 2009. Genetic linkage map for *Amylostereum arolatum* reveals an association between vegetative growth and sexual and self recognition. Fungal Genet. Biol. 46, 632-641.

Vasiliauskas, R., Stenlid, J., 1999. Vegetative compatibility groups of *Amylostereum areolatum* and *A. chialletii* from Sweden and Lithuania. Mycol. Res. 103, 824-829.

Vasiliauskas, R., Stenlid, J., Thomsen, I.M., Vasiliauskas, R., Stenlid, J., Thomsen, I.M., 1998. Clonality and genetic variation in *Amylostereum areolatum* and *A. chailletii* from northern Europe. New. Phytol. 139, 751-758.

Vicoso, B., Haddrill, P.R., Charlesworth, B., 2008. A multispecies approach for comparing sequence evolution of X-linked and autosomal sites in *Drosophila*. Genet. Res. Camb. 90, 421-431.

Vieira, J., Fonseca, N.A., Santos, R.A.M., Habu, T., Tao, R., Vieira, C.P., 2008. The number, age, sharing and relatedness of S-locus. Genet. Res. Camb. 90, 17-26.

Welch, D.B.M., Meselson, M.S., 2001. Rates of nucleotide substitution in sexual and anciently asexual rotifers. Proc. Natl. Acad. Sci. USA. 98, 6720-6724.

Weir, B.S., Cockerham, C.C., 1984. Estimating F-statistics for the analysis of population structure. Evolution. 38, 1358-1370.

White, T.J., Bruns, T., Lee, S., Taylor, J., 1990. Amplification and direct sequencing of fungal ribosomal RNA genes for phylogenetics. In: PCR Protocols. A Guide to Methods and Applications (eds Innis MA, Gelfand DH, Sninsky JJ, White TJ), pp. 315-322. Academic Press, San Diego.

Woolfit, M., Bromham, L., 2003. Increased rates of sequence evolution in endosymbiontic bacteria and fungi with small effective population sizes. Mol. Biol. Evol. 20, 1545-1555.

Yang, Z., 2007. PAML 4: phylogenetic analysis by maximum likelihood. Mol. Biol. Evol. 24, 1586-1591.

Yang, Z., Nielson, R., 1998. Synonymous and non-synonymous rate variation in nuclear genes of mammals. J. Mol. Evol. 46, 409-418.

Yang, Z., Nielson, R., 2002. Codon-substitution models for detecting molecular adaptation at individual sites along specific lineages. Mol. Biol. Evol. 19, 908-917.

Yang, Z., Nielson, R., Goldman, N., Pedersen, A.M., 2000. Codon-substitution models for heterogeneneous selection pressure at amino acid sites. Genetics. 155, 431-449.

Yang, Z., Wong, W.S.W., Nielsen, R., 2005. Bayes empirical Bayes inference of amino acid sites under positive selection. Mol. Biol. Evol. 22, 1107-1118.

Zeyl, C., Bell, G., 1997. The advantage of sex in evolving yeast populations. Nature. 388, 465-468.

Zhai, W., Rasmus Nielsen, R., Slatkin, M., 2009. An Investigation of the Statistical Power of Neutrality Tests Based on Comparative and Population Genetic Data. Mol. Biol. Evol. 26, 273-283.

Zhang, J., Nielsen, R., Yang, Z., 2005. Evaluation of an improved branch-site likelihood method for detecting positive selection at the molecular level. Mol. Biol. Evol. 12, 2472-2479.

Zhou, X.D., De Beer, Z.W., Ahumada, R., Wingfield, B.D., Wingfield, M.J., 2004. Ophiostomatoid fungi associated with two pine-infesting bark beetles from Chile. Fungal Div. 15, 253-266.

FIGURES

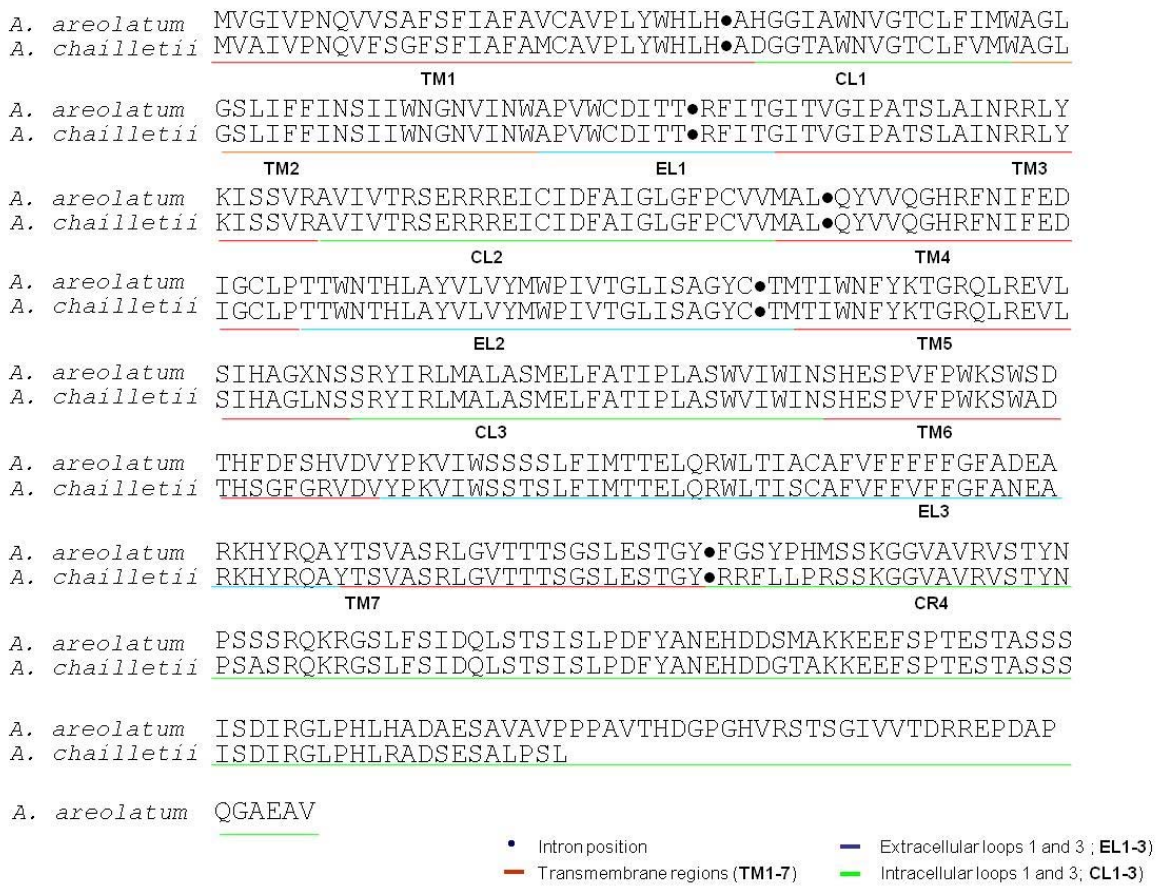

Figure 1. The amino acid sequences for part of the putative pheromone receptor, *RAB1*, present in *A. areolatum* and *A.chailletii.* Introns, transmembrane regions, and regions possibly corresponding to intra- and extracellular loops are indicated based on similarity to previously characterized homobasidiomycete pheromone receptor genes (Vaillancourt et al., 1997; James et al., 2004a; Raudaskoski and Kothe, 2010).

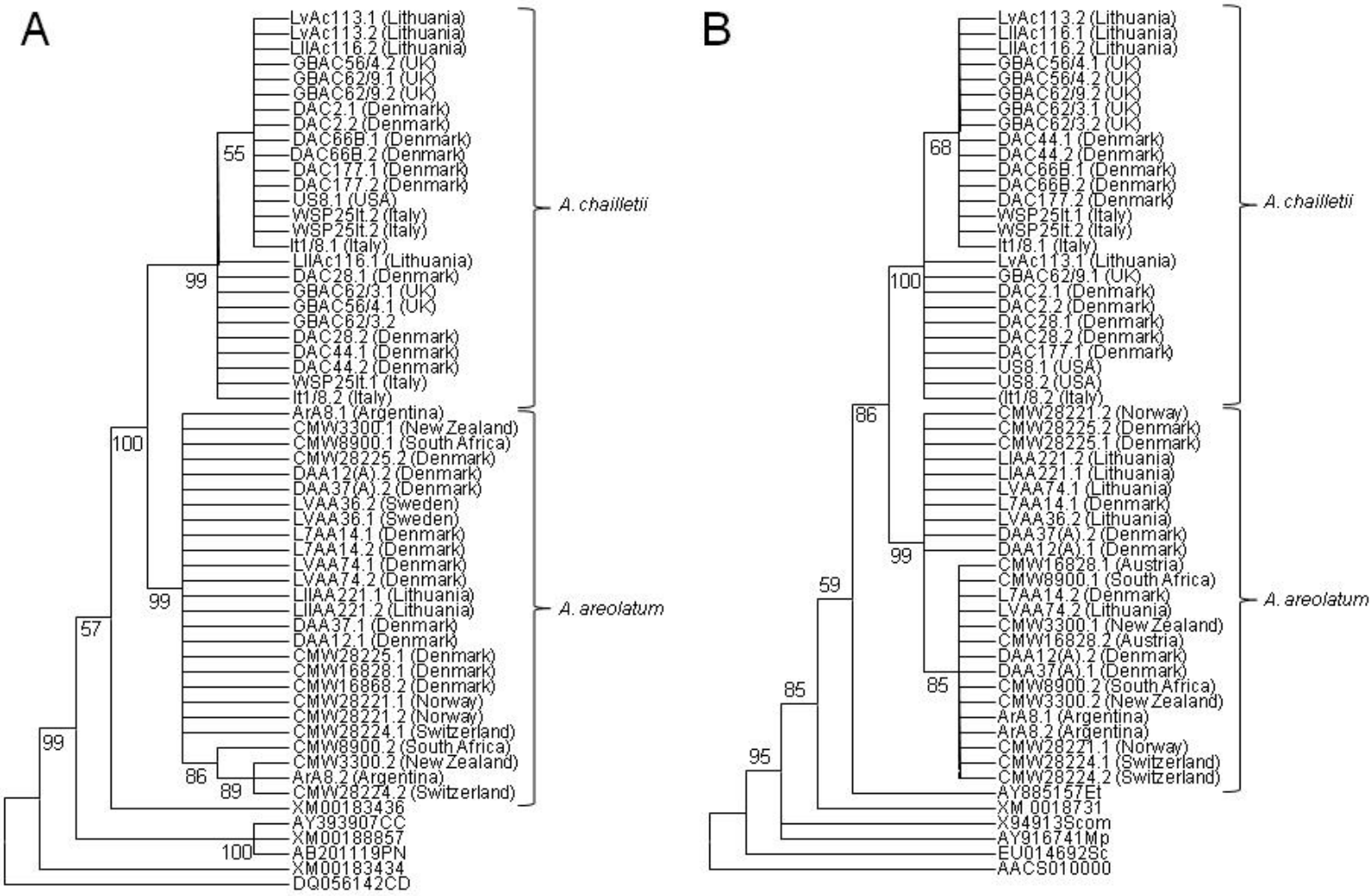

Figure 2. Maximum likelihood trees showing the evolutionary relationships between *A. areolatum* and *A. chailletii* and other fungi based on the pheromone receptors (A) and Tef-1α (B) sequences. Percentage bootstrap (100 replicates) values greater than 50% are shown below the tree branches. These trees were used in the CODEML analyses for detecting positive selection.

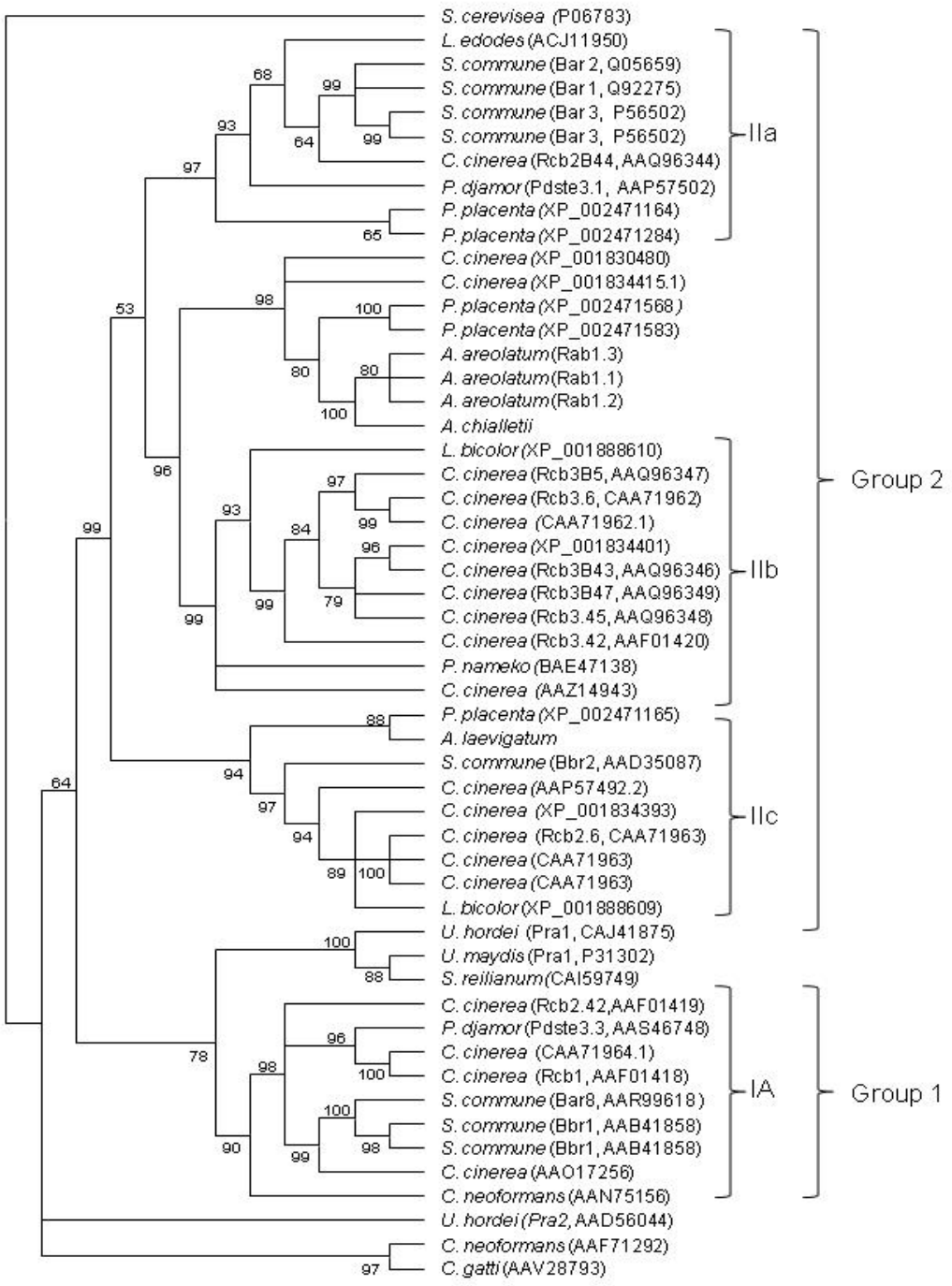

Figure 3. An amino acid-based maximum likelihood phylogeny of the pheromone receptors present in *A. areolatum*, *A. chailletii*, *A. laevigatum* and other Homobasidiomycetes. Percentage bootstrap (100 replicates) values greater than 50% are shown below the tree branches. The two main clusters of homobasidiomycete pheromone receptors are indicated as Groups 1 and 2 (James et al., 2006), while the groups that correspond to those identified for *C. cinerea* (Riquelme et al., 2005) are indicated with IA and IIa-c.

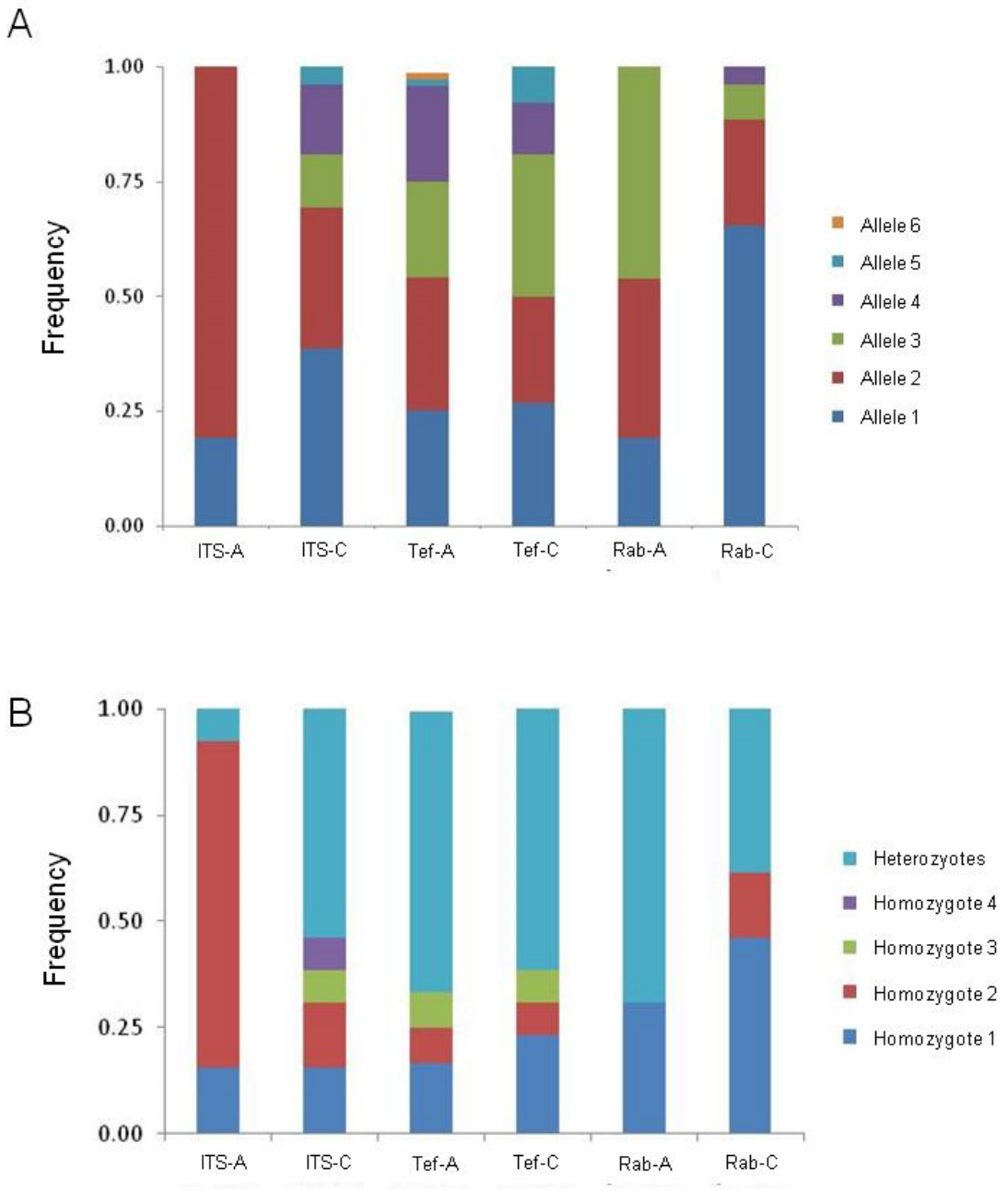

Figure 4. Stack histograms of allele frequencies (A) and genotype frequencies (B) at individual loci. ITS-A, ITS of *A. areolatum*; ITS-C, ITS of *A. chailletii*; Tef-A, Tef-1α of *A. areolatum*; Tef-C, Tef-1α of *A. chailletii*; Rab-A, *RAB1* of *A. areolatum*; Rab-C, *RAB1* of *A. chailletii*.

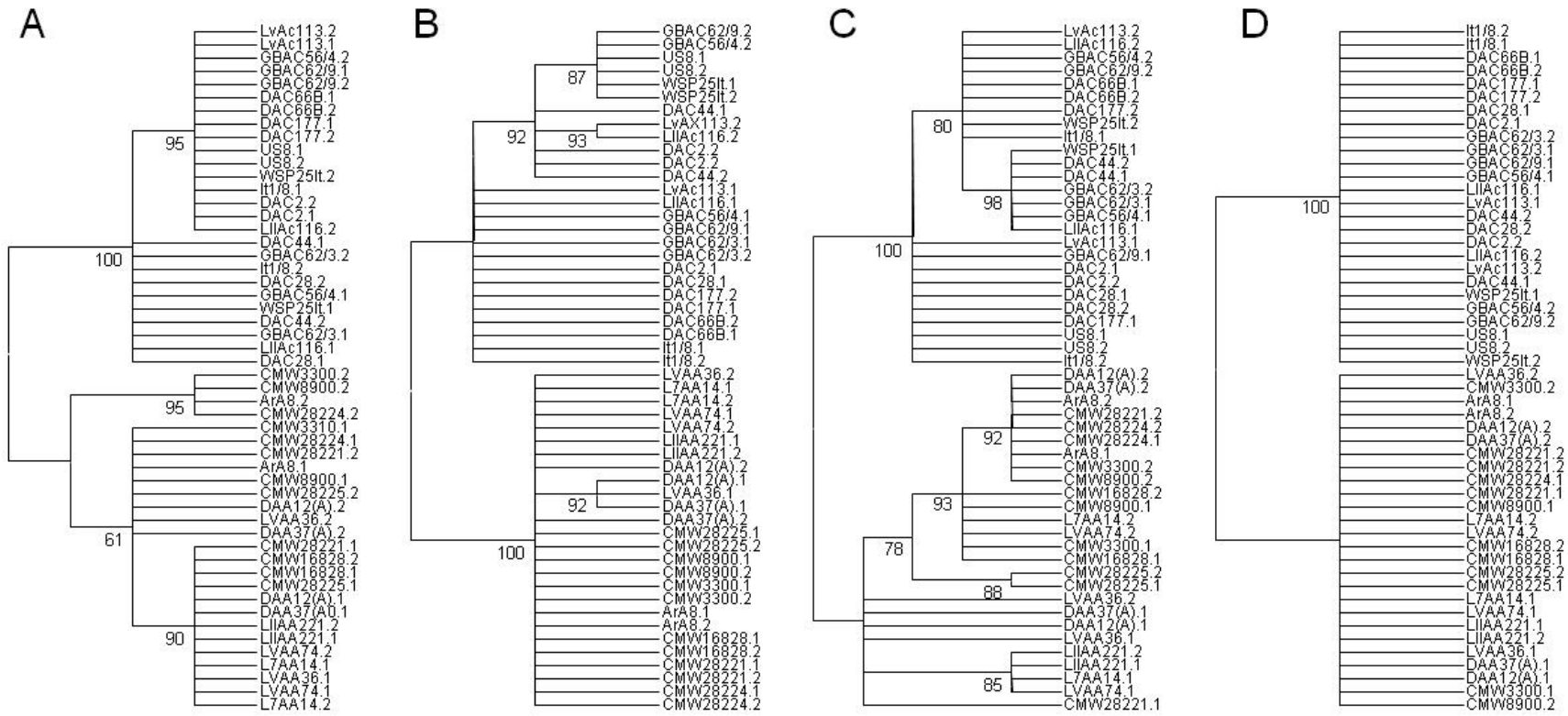

Figure 5. Maximum likelihood gene trees based on the *RAB1* (A), ITS (B) and Tef-1α (C) sequences for the isolates of *A. areolatum* and *A. chailletii* included in this study. The strict consensus (D) for the three trees was inferred in MEGA. For heterozygotic isolates, the alleles are indicated by the digits 1 or 2 following an isolate number. Percentage bootstrap (100 replicates) values greater than 50% are shown below the tree branches.

TABLES

Table 1. Heterozygosity tests[a] of the three genes present in the 13 heterokaryons each of *A. areolatum* and *A. chialletii*.

Locus	Species	A [b]	Π[c]	π_n/π_s[d]	Homozygotes[e]		Heterozygotes[f]		Heterozygote[g]		HWE[h]	F_{is}[1]
					H_o	H_e	H_o	H_e	deficit	excess		
ITS	*A. areolatum*	2	0.0004	-	12.0	8.80	1.0	4.2	0.03*	1.00	0.03*	0.769
	A. chialletii	5	0.0020	-	6.0	3.28	7.0	9.7	0.01*	0.99	0.05*	0.392
EF	*A. areolatum*	5	0.0050	0.00*	4.0	2.43	8.0	9.56	0.17	1.00	0.25	0.170
	A. chialletii	5	0.0060	0.00*	4.0	2.70	9.0	10.30	0.23	0.80	0.40	0.129
RAB1	*A. areolatum*	3	0.0042	0.00*	4.0	4.50	9.0	8.50	0.75	0.25	0.01*	0.487
	A. chialletii	4	0.0200	0.00*	7.0	6.08	6.0	6.90	0.37	0.84	0.68	0.055

[a] All estimates were determined with GENEPOP version 4. Significantly different values are indicated with an asterisk ($P<0.05$).

[b] Average number of alleles per locus.

[c] Mean number of pair-wise differences among sequences (Nei and Li, 1979).

[d] Ratio of non-synomous nucleotide variation to synonymous nucleotide variation.

[e] Observed homozygotes (H_o) and expected homozygotes (H_e).

[f] Observed heterozygotes (H_o) and expected heterozygotes (H_e).

[g] The results of global Hardy-Weinberg tests indicated significant heterozygote deficits ($p<0.05$).

[h] Population in Hardy-Weinberg disequilibrium ($p<0.05$).

[i] Fixation index (Weir and Cockerham, 1984).

Table 2. Likelihood scores and parameter estimates for the site-specific models (Yang et al., 2000) evaluated in this study.

Locus	Model [a]	*ln* Likelihood[b]	*dN*/*dS*[c]	Estimates of parameters[d]
RAB1	M0	-3972.27	0.016	ω_1=0.016
	M1 (neutral)	-3968.87	0.041	ω_0=0.018 F_0=0.98 ω_1=1 F_1=0.023
	M2 (selection)	-3968.87	0.041	ω_0=0.018 F_0=0.98 ω_1=1 F_1=0.023
	M3	-3900.23	0.016	ω_0=0.0 F_0=0.0 ω_1=0.002 F_1=0.30 ω_2=0.022 F_2=0.70
	M7 (β distribution)	-30902.72	0.018	*p=1.01 q=52.61 ω= 0.018*
	M8 (β + positive selection)	-30902.72	0.018	*p=1.01 q=52.61 ω= 0.018 ω1= 6.92 f1=0.0001*
	Average		0.025	
Tef-1α	M0	-1325.81	0.012	ω_1=0.012
	M1 (neutral)	-1321.20	0.021	ω_0=0.010 F_0=0.99 ω_1=1 F_1=0.01
	M2 (selection)	-1321.20	0.021	ω_0=0.01 F_0=0.98 ω_1=1 F_1=0.004
	M3	-1309.75	0.015	ω_0=0.0 F_0=0.67 ω_1=0.028 F_1=0.30 ω_2=0.230 F_2=0.02
	M7 (β distribution)	-1310.80	0.014	*p=0.170 q=10.164 ω= 0. 014*
	M8 (β + positive selection)	-1310.80	0.014	*p*=0.170 *q*=10.164 *ω*= 0.014 ω_1= 1 *f1*=0.0001
	Average		0.016	

[a] Site-specific models implemented in the CODEML program in PAML version 3.14 package (Yang and Nielson, 2002)

[b] Model likelihoods used for calculating statistical significance with likelihood ratio tests (LRT), which entailed analysis of the χ^2distribution of 2Δln (*i.e.*, twice the log likelihood difference between the two models) for the different models (Yang and Nielson, 1998).

[c] The non-synonymous (*dN*)/synonymous (*dS*) substitution rate ratio (Yang and Nielson, 1998).

[d] Parameters estimated for each model according to those proposed by Yang (2007).

Table 3. Likelihood ratio test (LRT) statistics for models of variable selective pressures among lineages.

Locus	Model[a]	*ln* Likelihood	2Δln[b]
Rab1	Model M0 (same dN/dS for all branches)	-3972.26	
	Model M1 (different dN/dS for each branches)	-3980.12	15.7
Tef-1α	Model M0 (same dN/dS for all branches)	-1325.82	
	Model M1 (different dN/dS for each branches)	-1326.64	1.64

[a] Branch-specific models (Zhang et al., 2005) implemented in the CODEML program in PAML version 3.14 package (Yang and Nielson, 2002).

[b] Twice the log likelihood difference between the two models (Yang and Nielson, 1998)

[c] The degrees of freedom were equal to the differences in number of parameters between the two models (Yang et al., 2000), which is one less than the number of branches in the phylogeny. There were 9 branches for Rab1 and 7 branches for Tef-1α.

Table 4. Population genetic parameters for the three genes present in *A. areolatum* and *A. chialletii*.

Locus	Species	ZnS [a]	Tajima's D [b]	Fu and Li's D [c]	Fu and Li's F [c]	Fay and Wu's Hn [d]
ITS	*A. areolatum*	n.a.	-0.311	0.612	0.415	0.451
	A. chialletii	0.158	-0.010	1.151	0.942	0.574
Tef-1α	*A. areolatum*	0.444	1.984	1.158	1.621*	-0.167
	A. chialletii	0.743	1.819	1.226	1.626*	0.298
RAB1	*A. areolatum*	0.609	-0.063	1.461*	1.192	-1.084
	A. chialletii	0.551	-0.755	-2.147	-2.017	-0.265

[a] Linkage disequilibrium statistic of Kelly (1997), tested if Zns is significantly high given S.

[b] Tajima's D, statistic of Tajima (1989).

[c] Fu and Li's D and F (Fu and Li, 1993).

[d] Fay and Wu's Hn (Fay and Wu, 2000).

* Significantly different (P<0.05).

SUPPLEMENTARY MATERIAL

Table 1. The nucleotide polymorphisms *RAB1* sequences in the 25 *A. areolatum* isolates.

Isolate number	Collector	Geographic origin	Nucleotide polymorphisms[a]							
			62	74	78	89	91	95	150	159
			*	*	*	*	*	*		
CMW16848	R. Vasaitis	Austria	C	T	G	C	G	T	A	A
			C	T	G	T	G	T	A	A
LIIAA5(LK)	R. Vasaitis	Lithuania	T	C	A	T	T	G	G	G
			T	C	A	T	T	G	G	G
LVAA36	R. Vasaitis	Sweden	C	T	G	C	G	T	A	A
			C	T	G	T	G	T	A	A
L7AA14	R. Vasaitis	Denmark	C	T	G	T	G	T	A	A
			C	T	G	T	G	T	A	A
LVAA74	R. Vasaitis	Lithuania	C	T	G	T	G	T	A	A
			C	T	G	T	G	T	A	A
LIIAA221	R. Vasaitis	Lithuania	C	T	G	T	G	T	A	A
			C	T	G	T	G	T	A	A
DAA12(A)	I. Thomsen	Denmark	C	T	G	C	G	T	A	A
			C	T	G	T	G	T	A	A
DAA37(A)	I. Thomsen	Denmark	C	T	G	C	G	T	A	A
			C	T	G	T	G	T	A	A
CMW28225	I. Thomsen	Denmark	C	T	G	C	G	T	A	A
			C	T	G	T	G	T	A	A
DAA547(B)	I. Thomsen	Denmark	C	T	G	C	G	T	A	A
			C	T	G	C	G	T	A	A
CMW4644	B. Slippers	Australia	C	T	G	T	G	T	A	A
			C	T	G	T	G	T	A	A
CMW8898	B. Slippers	Brazil	C	T	G	C	G	T	A	A
			C	T	G	T	G	T	A	A
CMW8900	B. Slippers	South Africa	T	C	A	T	T	G	G	G
			C	T	G	C	G	T	A	A
CMW3300	B. Slippers	New Zealand	T	C	A	T	T	G	G	G
			C	T	G	C	G	T	A	A
CMW3310	G.B. Rawlings	France	C	T	G	T	G	T	A	A
			C	T	G	T	G	T	A	A
ArA8	B. Slippers	Argentina	T	C	A	T	T	G	G	G
			C	T	G	C	G	T	A	A
CMW16828	B. Slippers	Austria	C	T	G	T	G	T	A	A
			C	T	G	T	G	T	A	A
At-II-28	B. Slippers	Austria	C	T	G	T	G	T	A	A
			C	T	G	T	G	T	A	A
CMW28221	H. Solheim	Norway	C	T	G	T	G	T	A	A
			C	T	G	C	G	T	A	A
DAA547B	H. Solheim	Norway	C	T	G	T	G	T	A	A
			C	T	G	T	G	T	A	A
CMW28223	O. Holgenrieder	Switzerland	T	C	A	T	T	G	G	G
			C	T	G	T	G	T	A	A
CMW28224	O. Holgenrieder	Switzerland	T	C	A	T	T	G	G	G
			C	T	G	C	G	T	A	A
AtII-18	B. Slippers	Austria	C	T	G	T	G	T	A	A
			C	T	G	T	G	T	A	A
At-23	B. Slippers	Austria	C	T	G	T	G	T	A	A
			C	T	G	T	G	T	A	A
AtIII-4	B. Slippers	Austria	C	T	G	C	G	T	A	A
			C	T	G	T	G	T	A	A

[a] Polymorphisms located in introns are indicated with asterisks.

Table 2. The nucleotide polymorphisms *RAB1* sequences in the 25 *A. chailletii* isolates.

Isolate number	Collector	Geographic origin	Nucleotide polymorphisms[a]					
			87	92	103	130	139	160
			*	*	*			
A.ch.536	R. Vasaitis	Sweden	C	T	C	C	T	C
			C	T	C	C	T	C
LvAc22C	R. Vasaitis	Lithuania	C	T	C	C	C	C
			C	T	C	C	C	C
LvAc113	R. Vasaitis	Lithuania	C	T	C	C	C	C
			C	T	C	C	C	C
LIIAc116	R. Vasaitis	Lithuania	C	T	C	C	C	C
			C	T	C	C	C	C
GBAC56.4	D. Redfern	UK	C	T	C	C	C	C
			C	T	C	C	C	C
GBAC62.11	D. Redfern	UK	C	T	C	C	T	C
			C	T	C	C	C	C
GBAC62.9	D. Redfern	UK	C	T	C	C	C	C
			C	T	C	C	C	C
GB AC62.3	D. Redfern	UK	C	T	C	C	T	C
			C	T	C	C	C	C
GBAC62	D. Redfern	UK	C	T	C	C	C	C
			C	T	C	C	C	C
DAC2	I. Thomsen	Denmark	C	T	C	C	C	C
			C	T	C	C	C	C
DAC7	I. Thomsen	Denmark	C	T	C	C	C	C
			C	T	C	C	C	C
DAC28	I. Thomsen	Denmark	C	T	C	C	C	C
			C	T	C	C	C	C
DAC35	I. Thomsen	Denmark	C	T	C	C	T	C
			C	T	C	C	C	C
DAC44	I. Thomsen	Denmark	C	T	C	C	C	C
			C	T	C	C	C	C
DAC66B	I. Thomsen	Denmark	C	T	C	C	C	C
			C	T	C	C	C	C
DAC66D	I. Thomsen	Denmark	C	T	C	C	T	C
			C	T	C	C	C	C
DAC78	I. Thomsen	Denmark	C	T	C	C	C	C
			C	T	C	C	C	C
DAC177	I. Thomsen	Denmark	C	T	C	C	C	C
			C	T	C	C	C	C
DAC1941	I. Thomsen	Denmark	C	T	C	C	T	C
			C	T	C	C	C	C
US1	H.H. Burdsall	US	A	C	G	T	C	T
			C	T	C	C	C	C
US8	H.H. Burdsall	US	A	C	G	T	C	T
			C	T	C	C	C	C
CMW3299	R.F. Cain	Canada	C	T	C	C	C	C
			C	T	C	C	C	C
GRWSP3	B. Slippers	Greece	C	T	C	C	C	C
			C	T	C	C	C	C
WSP25It	B. Slippers	Italy	C	T	C	C	C	C
			C	T	C	C	C	C
It1.8	B. Slippers	Italy	C	T	C	C	C	C
			C	T	C	C	C	C

[a] Polymorphisms located in introns are indicated with asterisks

Table 3. The nucleotide polymorphisms in the Tef-1α, ITS and RAB1 sequences in the 13 *A. areolatum* isolates.

Isolate number	Geographic origin	Nucleotide polymorphisms[a]																		
		ITS	Tef-1α type 1						*RAB1*											
		540	81	147	267	312	330	341	62	74	78	89	91	95	150	159	288	375	569	605
				*		*	*	*	*	*	*	*	*	*					*	*
LVAA36	Sweden	T	T	C	C	A	A	T	C	T	G	C	G	T	A	A	C	C	G	T
		T	T	C	C	A	A	T	C	T	G	T	G	T	A	A	C	C	G	T
L7AA14	Lithuania	C	T	C	C	G	A	T	C	T	G	T	G	T	A	A	C	C	G	T
		C	C	T	T	A	G	T	C	T	G	T	G	T	A	A	C	C	G	T
LVAA74	Lithuania	C	T	C	C	G	A	T	C	T	G	T	G	T	A	A	C	C	G	T
		C	C	T	T	A	G	T	C	T	G	T	G	T	A	A	C	C	G	T
LIIAA221	Lithuania	C	T	C	C	G	A	T	C	T	G	T	G	T	A	A	C	C	G	T
		C	T	C	C	G	A	T	C	T	G	T	G	T	A	A	C	C	G	T
DAA12(12)	Denmark	T	T	C	C	A	A	T	C	T	G	C	G	T	A	A	C	C	G	T
		C	C	T	T	A	G	C	C	T	G	T	G	T	A	A	C	C	G	T
DAA37(A)	Denmark	T	C	T	T	A	G	C	C	T	G	C	G	T	A	A	C	C	G	T
		T	T	C	C	A	A	T	C	T	G	T	G	T	A	A	C	C	G	T
CMW28225	Denmark	C	T	C	C	A	A	T	C	T	G	C	G	T	A	A	C	C	G	T
		C	T	C	C	A	A	T	C	T	G	T	G	T	A	A	C	C	G	T
CMW8900	South Africa	C	C	T	T	A	G	T	T	C	A	T	T	G	G	G	T	T	T	C
		C	C	T	T	A	G	C	C	T	G	C	G	T	A	A	C	C	G	T
CWM3300	New Zealand	C	C	T	T	A	G	T	T	C	A	T	T	G	G	G	T	T	T	C
		C	C	T	T	A	G	C	C	T	G	C	G	T	A	A	C	C	G	T
ArA8	Argentinia	C	C	T	T	A	G	C	T	C	A	T	T	G	G	G	T	T	T	C
		C	C	T	T	A	G	C	C	T	G	C	G	T	A	A	C	C	G	T
CMW16828	Austria	C	C	T	T	A	G	T	C	T	G	T	G	T	A	A	C	C	G	T
		C	C	T	C	A	G	T	C	T	G	T	G	T	A	A	C	C	G	T
CMW28221	Norway	C	C	T	T	A	G	C	C	T	G	T	G	T	A	A	C	C	G	T
		C	T	C	C	A	A	T	C	T	G	C	G	T	A	A	C	C	G	T
CMW28224	Switzerland	C	N	N	N	N	N	N	T	C	A	T	T	G	G	G	T	T	T	C
		C	N	N	N	N	N	N	C	T	G	C	G	T	A	A	C	C	G	T

[a] Polymorphisms located in introns are indicated with asterisks

Table 4. The nucleotide polymorphisms in the Tef-1α, ITS and RAB1 sequences in the 13 *A. chailletii* isolates.

Isolate number	Geographic origin	Nucleotide polymorphisms[a]																							
		ITS						Tef-1α								*RAB1*									
		97	144	193	220	504	512	129	135	162	325	343	358	486	498	87	92	103	130	160	261	595-600[b]	617-637[c]	646
								*	*		*	*				*	*	*				*	*	*
LvAc113	Lithuania	A	A	-	G	G	C	C	T	A	C	C	C	C	T	C	T	C	C	C	A	insert	-	A
		A	G	-	C	G	C	C	T	A	C	C	C	C	C	C	T	C	C	C	A	insert	-	A
LIIAc116	Lithuania	A	G	-	C	G	C	C	T	A	C	C	C	T	C	C	T	C	C	C	A	insert	-	A
		A	G	-	C	G	C	T	-	G	T	T	T	C	T	C	T	C	C	C	G	-	insert	G
GBAC56.4	UK	A	G	-	G	A	C	C	T	A	C	C	C	T	C	C	T	C	C	C	G	insert	insert	G
		A	A	A	G	G	C	T	-	G	T	T	T	T	C	C	T	C	C	C	A	insert	-	A
GBAC62.9	UK	A	G	-	G	A	C	C	T	A	C	C	C	C	T	C	T	C	C	C	A	insert	-	A
		A	A	A	G	G	C	C	T	A	C	C	C	C	C	C	T	C	C	C	A	insert	-	A
DAC2	Denmark	A	G	-	C	G	C	C	T	A	C	C	C	C	T	C	T	C	C	C	A	insert	-	A
		A	A	A	G	G	C	C	T	A	C	C	C	C	T	C	T	C	C	C	A	insert	-	A
DAC28	Denmark	A	G	-	C	G	C	C	T	A	C	C	C	C	T	C	T	C	C	C	G	-	insert	G
		A	A	-	G	G	C	C	T	A	C	C	C	C	T	C	T	C	C	C	G	insert	insert	G
DAC44	Denmark	G	G	-	G	A	T	T	-	G	T	T	T	T	C	C	T	C	C	C	G	insert	insert	G
		A	G	-	G	A	C	T	-	G	T	T	T	T	C	C	T	C	C	C	G	insert	insert	G
DAC66B	Denmark	A	A	-	G	G	C	C	T	A	C	C	C	T	C	C	T	C	C	C	A	insert	-	A
		A	A	-	G	G	C	C	T	A	C	C	C	T	C	C	T	C	C	C	A	insert	-	A
DAC177	Denmark	A	A	-	G	G	C	C	T	A	C	C	C	T	C	C	T	C	C	C	A	insert	-	A
		A	A	A	G	G	C	C	T	A	C	C	C	C	T	C	T	C	C	C	A	insert	-	A
US1	US	G	G	-	G	A	T	n	N	n	n	n	n	n	n	C	T	C	C	C	A	insert	-	A
		A	G	-	G	A	C	n	N	n	n	n	n	n	n	A	C	G	T	T	G	insert	-	A
US2	US	A	G	-	G	A	C	C	T	A	C	C	C	C	T	C	T	C	C	C	A	insert	-	A
		A	G	-	G	A	C	C	T	A	C	C	C	C	T	C	T	C	C	C	A	insert	-	A
WSP25It	Italy	A	G	-	G	A	C	C	T	A	C	C	C	T	C	C	T	C	C	C	A	insert	-	A
		A	G	-	G	A	C	T	-	G	T	T	T	T	C	C	T	C	C	C	G	insert	insert	G
It1.8	Italy	A	A	A	G	G	C	C	T	A	C	C	C	T	C	C	T	C	C	C	G	insert	insert	G
		A	A	A	G	G	C	C	T	A	C	C	C	C	T	C	T	C	C	C	A	insert	-	A

[a] Polymorphisms located in introns are indicated with asterisks. Deletions are indicated with hyphens and unknown bases with "n".

[b] insert sequence "CCGTTT"

[c] insert sequence "ATTCGGCTCCTACCCGCACAT"

A. areolatum (CMW19.12)

ATGGTCGGCATCGTACCCAACCAAGTCGTCTCcGCCTTCTCCTTCATTGCTTTCGCCGTGTGTGCGGTCCCATTGTATTGGCATCT
ACATGCTCACGGTGGGATAGCTTGGAACGTCGGCACCTGCTTGTTCATCATGTGGGCCGGGCTCGGATCCCTTATTTTCTTTATCA
ACTCCATCATCTGGAACGGGAATGTCATCAACTGGGCCCCAGTGTGGTGCGACATCACGACCCGCTTCATAACCGGCATCACCGTT
GGCAtCCCCGCCACCTCACTCGCCATCAACCGACGTCTGTACAAGATTTCGTCCGTGCGTGCGGTGATAGTCACACGGTCGGAAAG
GCGTAGGGAAATTTGCATCGATTTCGCGATTGGCCTCGGATTCCCATGCGTGGTCATGGCCCTTCAGTATGTCGTGCAGGGCCATC
GATTCAATATCTTTGAGGACATCGGATGCCTCCCCACCACCTGGAACACCCACCTGGCCTACGTCCTCGTCTACATGTGGCCAATC
GTGACGGGTCTCATCTCCGCGGGCTACTGCACCATGACCATCTGGAACTTCTACAAGACCGGTCGCCAGTTGCGCGAGGTCCTCTC
CATACACGCCGGCTCAACTCCAGCCGCTACATACGTCTCATGGCGCTCGCCTCCATGGAACTTTTCGCCACGATCCCGCTCGCGTC
CTGGGTGATATGGATCAACTCGCACGAGTCCCCTGTCTTCCCGTGGAAGTCTTGGTCGGACACCCATTTCGACTTCTCCCACGTGG
ACGTGTACCCCAAGGTCATCTGGTCATCATCGAGTCTGTTCATCATGACCACCGAACTCCAACGCTGGCTCACGATCGCCTGCGCC
TTCGTGTTTTTCTTCTTCTTTGGGTTCGCGGACGAGGCCAGGAAGCACTATCGCCAGGCGTATACGTCGGTTGCCAGCCGGCTCGG
CGTTACCACCACCTCCGGAAGCCTGGAGTCCACCGGgTaCGGCTCCTACCCGCACATGTCCTCCAAAGGCGGCGTCGCCGTCCGAG
TCTCGACGTACAACCCGTCGTCCTCGCGACAGAAGCGCGGCTCGCTCTTCTCCATCGACCAGCTCTCAACCTCGATCTCCCTACCC
GACTTTTACGCAAACGAGCACGACGACTCGATGGCGAAGAAGGAGGAGTTCTCGCCCACGGAGTCGACCGCTTCGTCATCAATCAG
CGATATTCGCGGGCTGCCGCATCTGCACGCGGACGCGGAGAGTGCGGTCGCGGTGCCCCCGCCCGCCGTGACTCATGATGGACCCG
GACATGTGAGGTCGACGTCTGGGATCGTGGTCACGGACAGGCGTGAGCCCGACGCGCCACAGGGCGCTGAAGCCGTGTAAACATCC
TTGTTCCCCCTCCCGCTCGCCTTCCATCGGATCCAACCTTTCCACACGCGCCACACCCCTTCCTTCAACTTCGCGCAACCCTGCTT
CTTTCATTACATCCCAGACTCAACAACACTAAAACCTCTACATGCGACATCCCTACCTTACACTCCTATTCGACCTTCACCTCTGC
ACCTTTGCCTACTTGTTTTGCCCACCCAGTGTATCACTACTCACACTCGCTCTCGGTCGCTCGATAC

A. chailletii (NAc3)

ATGGTTGCCATCGTCCCCAACCAGGTCTTCTCTGGCTTCTCCTTCATTGCCTTCGCAATGTGCGCGGTCCCATTGTATTGGCATCT
ACATGGTACGTAGCCTCTTCCTCTCTCGACTTCGTCGAGCTGACGGCGGGACAGCGTGGAACGTTGGCACTTGCCTGTTCGTCATG
TGGGCTGGGCTCGGATCCCTCATCTTCTTCATCAACTCCATCATCTGGAACGGGAACGTCATCAACTGGGCCCCGGTTTGGTGCGA
CATCAGTACGnnnTTGTGTGCTCTGCGTGTACTTGTCGCACGCTCATGCTTTTCTTGCAGCGACCCGCTTCATAACCGGCATCACC
GTCGGCATCCCCGCGACCTCCCTCGCCATCAACCGTCGTCTGTACAAGATCTCGTCCGTGCGAGCCGTCATCGTCACACGCTCGGA
AAGGCGCAGGGAAATTTGCATCGATTTCGCGATTGGGCTCGGATTCCCATGCGTGGTCATGGCCCTTCGTACGTAAAACATCGTGC
CTTCCAGGTTTTTTGGCTCACTTTTCTCGTAGAATACGTTGTGCAGGGCCATCGATTCAACATCTTTGAGGACATTGGGTGCCTTC
CGACTACCTGGAATACCCACCTGGCCTACGTCCTGGTCTATATGTGGCCAATTGTCACCGGCTTGATCTCTGCGGGCTACTGCAGT
GCGTTGTTCTTTCCCCCGCAATCTCCGCCATTCTCTGACCGCCCCCCTGCAGCCATGACCATTTGGAACTTCTACAAGACCGGACG
CCAACTGCGTGAAGTCCTCTCCATCCACGCCGGCCTCAACTCGAGCCGCTACATTCGCCTTATGGCCCTCGCCTCCATGGAGCTTT
TCGCGACGATCCCGCTCGCGTCCTGGGTGATATGGATCAACTCGCACGAGTCGCCCGTCTTCCCGTGGAAGTCCTGGGCGGACACG
CACTCCGGATTTGGGCGCGTGGACGTGTATCCGAAGGTCATCTGGTCGTCGACGAGCCTGTTCATCATGACGACCGAGCTCCAGCG
CTGGCTCACGATCTCGTGTGCCTTCGTGTTTTTCGTGTTCTTCGGTTTCGCCAACGAGGCCAGGAAGCACTACCGCCAGGCGTACA
CGTCCGTCGCCAGCAGGCTCGGCGTCACCACCACCTCCGGAAGCCTCGAGTCTACCGGGTACGTTTCCCTCTTCACCTCTATACCC
CCTCGCCTGAGCCTAACGCGCCGTTTCCTGCTACCTAGATCCTCCAAGGGCGGCGTCGCCGTCCGCGTCTCAACGTACAACCCCTC
GGCCTCGCGCCAAAAGCGCGGATCGCTCTTCTCCATCGACCAGCTCTCGACCTCGATCTCGCTCCCGGACTTCTACGCGAACGAGC
ACGACGACGGCACGGCGAAGAAGGAGGAGTTTTCGCCTACGGAATCCACCGCGTCCTCGTCGATCAGCGACATCCGCGGGCTGCCG
CATCTACGCGCCGACTCGGAGAGCGCGCTCCCGTCGCTGCC

A. laevigatum (SeA16-04,1.11)

TCAGCTGTCTCATACAATTCGTCGACGCGtTGGTCTGGCACAACAGCATCTTGAACGTCGCGCCTTCTACTGCGATATCGGTGAGT
AGCGTGCTTCAGCATTCGCTTACAGTTTCCTGAAGGAGGCCCACAGCGACGAAAATTCTTGTTGGCGCCTCCGTAGGCATTCCTGC
CTCGGGTCTCTGCATAAGCCGCCGCCTGTACAACATCAGTGCGGTTAAGGTGGTCTCTGTCACTCGCCGTGATGTACGTGTCCCAC
CAGCTCTCCCGACGGTGGCCCTGCTGACGCTCGCTCTTGCAGAAAATCAGGGCGATTATGTTCGACTGTGCGGTCGCTGTTCTTCT
CCCTCTTCTTGTGATGGCGCTGCGTGAGTCTCGTTTACACTGTCTCCCCGCTCTAGGCTGACCTTCCGCGGACGTAGACATCGTTG
TACAAGGACATAGGGCCAATATCTTGGAAGATGTCGGTTGTGTCGCGGTTATATTCAACACTGCTCCGGCGTACCCTCTGGTCTTT
ATGTGGCCGGCTCTCATCGGTTCTATCTCTTTCATCTATGCAGGTATGTCTTTTCAGCGTATTCCTGTTGTAACGACTCCCTGACG
CACCTTTCCTTTCGAAGCGTTGACGCTTCGTGCGTTCATGAAACATCGGGCGTCGTTCTTTGAGATCCTCTCTGGAACGTCAGCCT
CCCTTACAGCAAACCAATACCTACGTCTAATGGACCCTCGC

Figure 1. Nucleotide sequences of the pheromone receptor present in *Amylostereum areolatum, A. chailletii* and *A. laevigatum*.

A. areolatum (DAA12,A)

Type-A

GGTATCTCCAAGGACGGTCAGACTCGCGAGCACGCCCTCCTTGCGTTCACCCTCGGTGTTCGCCAGCTCATCGTCGC
TGTCAACAAGATGGACACCACGAAGGTGCGTTCTGTCTATCTGTCGATCTCGCTCGATGTTGACTTTATGTTCTTTA
TCCAGTGGAGCGAGGATCGTTTCAACGAAATCATCAAGGAGACGTCCACCTTCATCAAGAAGGTCGGCTACAACCCC
AAGGCCGTCGCTTTCGTTCCCATCTCAGGTTGGCACGGTGACAACATGTTGGAGGAGTCCCCCAAGTGAGTCACAAC
CTGCTCGACTCGTGCTCAACACCCCCTGATTCGTGCCGTACAGCATGCCGTGGTACAAGGGCTGGACCAAGGAGACC
AAGGCCGGTGTCGTCAAGGGCAAGACTCTCCTCGATGCTATCGACGCTATCGAGCCCCCAGCCGTCCCTCCGACAAG
CCTCTCCGCCTT

Type-B

GGTATCTCCAAGGACGGTCAGACTCGCGAGCACGCCCTCCTTGCGTTCACCCTCGGTGTTCGCCAGCTCATCGTCGC
TGTCAACAAGATGGACACCACGAAGGTGCGTTCTGTCTATCTGTCCATCTCGCTTGGTTCTGACATGCTATCTGTCC
AGTGGAGCGAGGATCGTTTCAACGAAATTATCAAGGAGACGTCCACCTTCATCAAGAAGGTTGGCTACAACCCCAAG
GCCGTCGCTTTCGTTCCCATCTCAGGCTGGCACGGCGACAACATGTTGGAGGAGTCCCCCAAGTGAGTCACAACCTG
ATCGACTCGTGCTCAACGCTCTCTAACTCGTGCCGTACAGCATGCCGTGGTGCAAGGGCTGGACCAAGGAGACCAAG
GCCGGTGTCGTCAAGGGAAAGACCCTCCTCGATGCTATCGACGCTATCGAGCCCCCACTCCGTCCCTCCGACAAGCC
TCTCCGCCT

A. chailletii (LvAc22C)

GGTATCTCCAAGGATGGCCAGACCCGCGAGCACGCCCTCCTTGCGTTCACCCTCGGTGTCCGCCAGCTCATCGTCGC
CGTTAACAAGATGGACACCACCAAGGTTAGTCTCGTTTATCTGATCTTGATTGATTTTGACCGTTTAATCAGTGGAG
CGAGGACCGCTTCAACGAAATCATCAAGGAGACGTCCACCTTCATCAAAAAGGTTGGCTACAACCCGAAGTCCGTCG
CGTTCGTTCCCATTTCCGGCTGGCACGGTGACAACATGTTGGAGGAGTCCCCCAAGTGAGTTATATGCGCATCTACC
TGCACCTAACACTGTCTGACCAGCGTCGTACAGCATGCCCTGGTACAAGGGCTGGACGAAGGAGACCAAGGCGGGTG
TCGTCAAGGGCAAGACTCTTCTCGATGCTATCGATGCTATCGAGCCCCCAGCCGTCCTTCCGACAAGCCCCTTCGTC
TT

Figure 2. Nucleotide sequences of Tef-1α present in *Amylostereum areolatum* and *A. chailletii*.

A. areolatum (L7AA14)

TCCTCCGCTTATTGATATGCTTAAGTTCAGCGGGTAGTCCCACCTGATCTGAGGTCAAGTTTCGATGAATTGTCCCG
AAGGACGGTTAGAAGCGAAAACCGCTACAGACAACCTTGGACGTAGACAATTATCACGCCGAGGCCACCTGGGCTTC
ACTAATGCATTTGAGAGGAGCGGACTTACGCCCGCAAGCCTCCAACTCCAAGCCCCGCGCTCCCGCAAAGGAGGCGG
AGTTGAGAAATTCACGACACTCAAACAGGTGTGCCCCTCGGAATACCAAGGGGCGCAAGGTGCGTTCAAAGATTCGA
TGATTCACTGAATTCTGCAATTCACATTACTTATCGCATTTCGCTGCGTTCTTCATCGATGCGAGAGCCAAGAGATC
CGTTGTTGAAAGTTGTATTAGATGCGCAACACGCAAAGACATTCTGAGACATACAAAGAGTGTATAAAATCGCGGGC
ACGGCAACCGAAGTCACCGCAGCCCACGCGGGAGTGCACAGGGTGTGTCGGAAAGAGCAAGGGCGAGCACTTGTCCC
GAAAGaCCAGCTACAACCCAAGCCTTCTGAATTCGATAATGATCCTTCCGCAGGTTCACCTACGGA

A. chailletii (LvAc22C)

TCCTCCGCTTATTGATATGCTTAAGTTCAGCGGGTAGTCCCACCTGATCTGAGGTCAAGTTTCGATGAATTGTCCCG
AGGGACGGTTAGAAGCGAAAACCGCAATAGACAACCTTGGACGTAGACAATTATCACGCCGAGGCCGCCTGGGCTTC
ACTAATGCATTTGAGAGGAGCGGACTTGCGCCCGCAAACCTCCAACTCCAAGCCCCGCTCTCCCGCAAAGGAGGCGG
AGTTGAGAAATTCACGACACTCAAACAGGTGTGCCCCTCGGAATACCAAGGGGCGCAAGGTGCGTTCAAAGATTCGA
TGATTCACTGAATTCTGCAATTCACATTACTTATCGCATTTCGCTGCGTTCTTCATCGATGCGAGAGCCAAGAGATC
CGTTGTTGAAAGTTGTATTAGATGCGCAACACGCAAAGACATTCTGAGACATACGAAGAGTGTATAAAATCGCGAGC
GCGACGACCGAGGTCATCGCAGCCCACGCGGGAGTGCACAAGGTGTGTCGGAAAGAGCAAGGGCGAGCACTTGTCCC
GAGGGACCAGCTACAACCCAAGCCTTCTGAATTCGATAATGATCCTTCCGCAGGTTCACCTACGGA

Figure 3. Nucleotide sequence of ITS present in *Amylostereum areolatum* and *A. chailletii*.

CHAPTER 6

Gene expression associated with vegetative incompatibility in *Amylostereum areolatum*

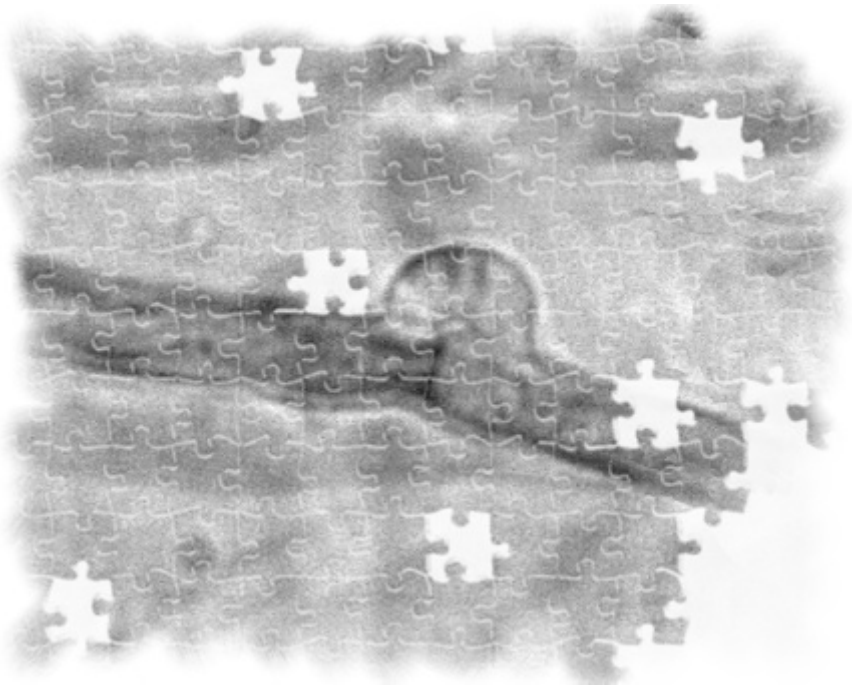

TABLE OF CONTENTS

ABSTRACT

Typical of filamentous fungi, the hyphae of genetically similar individuals of *Amylostereum areolatum* that share the same allelic specificities at their heterokaryon incompatibility (*het*) loci are able to fuse and intermingle. Interactions between individuals with different allelic specificities at their *het* loci result in cell death of the interacting hyphae, preventing hyphal fusion to persist. In this study, we used suppression subtractive hybridization (SSH) followed by pyrosequencing and quantitative reverse transcription PCR to identify genes that are selectively expressed when vegetatively incompatible *A. areolatum* individuals interact. The SSH library contained genes associated with various cellular processes, including cell-cell adhesion, stress and defence response, as well as cell death. Some of the transcripts identified encode putative proteins (e.g., laccase and tyrosine) that were previously implicated in vegetative incompatibility associated with stress and defence response. Qualitative assays confirmed the association of laccases during vegetative incompatibility in this fungus. Other transcripts encode putative proteins (e.g., ADP/ATP carrier protein and the ceramide synthase) known to be associated with programmed cell death (PCD), but have not previously been linked with vegetative incompatibility. Results of this study increase our knowledge about the processes underlying vegetative incompatibility in Basidiomycetes in general and *A. areolatum* in particular.

INTRODUCTION

Programmed cell death (PCD) in eukaryotes is a genetically controlled mechanism that requires the active participation of a cell in its own death (Gilchrist, 1998). This process plays various roles in tissue development and organization. For example, PCD eliminates cells between developing digits (e.g., fingers) in animals and it is involved in leaf senescence in plants (Gilchrist, 1998). PCD is also involved in eukaryotic non-self recognition, where suicide is triggered in infected plant and animal cells to prevent the spread of the infection to surrounding tissue (Greenberg and Yao, 2004; Hückelhoven, 2007). In fungi, PCD associated with non-self recognition or "PCD by incompatibility" limits vegetative hyphal fusion between genetically different individuals (Worral, 1997; Saupe, 2000; Glass and Kaneko, 2003). Although the exact biological function of PCD associated with the non-self recognition system in fungi is not yet clear, it was recently speculated that it may also be involved in pathogen recognition (Chevanne et al., 2010).

The non-self recognition system of filamentous fungi that determines vegetative hyphal fusion is controlled by genes encoded at the heterokaryon (*het*) or vegetative incompatibility (*vic*) loci. When genetically similar individuals that share the same allelic specificities at all of their *het* loci meet in nature, their hyphae will fuse and their cytoplasms intermingle (Worrall, 1997). However, if the interacting individuals are genetically dissimilar with different allelic specificities at some or all of their *het* loci, cell death of the interacting hyphae prevents unlike individuals from maintaining a functional connection and a zone of inhibition is formed between the two individuals (Worrall, 1997). Very little is known regarding the *het* loci of basidiomycetes, except that these fungi harbour fewer *het* loci than their ascomycete relatives (Worrall, 1999). At the DNA level, only a few *het* loci have been characterized in the model ascomycetes, *Neurospora crassa* and *Podospora anserina* (e.g., Kubisiak and Milgroom, 2006). However, the information obtained from these studies did not suggest any common function among the various *het* genes (Saupe, 2000). In some cases, the only apparent function of certain *het* gene products is to control non-self recognition (e.g., *het-6* in *N. crassa* and *het-D* and *het-E* loci in *P. anserina*), while other *het* gene products are also involved in additional cellular processes (e.g., the *mat* locus in *N. crassa* is also involved in mating and the *het-C* in *P. anserina* encodes a glycolipid transfer protein) (Saupe et al., 2000). Nevertheless, the fact that the *het-E*,

het-D and *het-R* genes of *P. anserina* encode homologues with a NACHT domain (named after known genes containing this domain, NAIP, CIIA, HET-E and TP1) suggests that PCD by incompatibility may be related to PCD in higher eukaryotes (Paoletti et al., 2007; Pinan-Lucarré et al., 2007; Chevanne et al., 2010). This is because proteins harbouring a NACHT domain belong to the STAND (signal transduction ATPases with numerous domains*)* class of NTPases (nucleoside triphosphate hydrolyses) that include various eukaryotic cell death proteins (Paoletti et al., 2007; Pinan-Lucarré et al., 2007).

In fungi, similar mechanisms appear to underlie PCD associated with vegetative incompatibility. This is because the interactions between individuals with different allelic specificities at their *het* loci all share the same morphological characteristics, which include the progressive shrinkage and fragmentation of the cytoplasm resulting in the formation of discrete remnants (Bursch, 2001; Marek et al., 2003). As these remnants resemble 'apoptotic bodies', it was first believed that PCD by incompatibility is similar to Type I PCD or apoptosis (Bursch, 2001; Marek et al., 2003). However, PCD by incompatibility is unlikely to be exactly the same as apoptosis (Marek et al., 2003) because the model fungi *N. crassa* and *Saccharomyces cerevisiae* lack important genes (e.g., caspases and Bcl-2/Bax) involved in apoptosis. An alternative hypothesis is that PCD by incompatibility is similar to Type II PCD or autophagy, where cells undergoing autophagy display morphological features such as vacuolization, cell lysis and chromatin condensation that are associated with vegetative incompatibility (Marek et al., 2003; Pinan-Lucarré et al., 2003; Pinan-Lucarré et al., 2007). Although it is possible that both types of cell death are involved in PCD by incompatibility, it has been suggested that autophagy is merely a consequence of PCD by incompatibility and does not represent an actual mechanism of PCD (Pinan-Lucarré et al., 2005).

Various approaches have been used to study the mechanisms that regulate vegetative incompatibility. One approach has been the use of mutations that suppress PCD by incompatibility (Glass and Kaneko, 2003; Dementhon et al., 2004). For example, a mutation in the *vib-1* (for *v*egetative *i*ncompatibility *b*lock) gene of *N. crassa* partly suppresses mating-type associated cell death, as well as *het-c/pin-c* induced cell death (Glass and Kaneko, 2003; Dementhon et al., 2004). This approach also led to the discovery of the *mod* (for *mod*ifier) genes in *P. anserina*, as mutations in *mod-C* suppresses *het-R/het-V* induced cell death (Loubradou and Turcq, 2000). Another approach has been the use of differentially expressed genes that are up-

regulated during vegetative incompatibility, which led to the discovery of the *idi* (for *i*nduced *d*uring *i*ncompatibility) genes induced during PCD by incompatibility in *P. anserina* (Bourges et al., 1998). PCR-based suppression subtractive hybridization (SSH) has also been used to study the genes involved in fungal-fungal interactions (Carpenter et al., 2005; Muthumeenakshi et al., 2007).

In this study, the non-self recognition system of the white rot fungus *Amylostereum areolatum*, which is an obligate symbiont of various *Sirex* woodwasps was considered (Slippers et al., 2003). Very little is known about the molecular genetics underlying the non-self recognition system of this fungus other than that it harbours at least two *het* loci (van der Nest et al., 2008; 2009). The aim was, therefore, to identify the mechanisms underlying vegetative incompatibility in *A. areolatum*. For this purpose, genes that are selectively expressed during vegetative incompatibility were identified using PCR-based SSH and 454-based pyrosequencing. Quantitative reverse transcription PCR (qRT-PCR) was employed to confirm up-regulation of selected transcripts and to compare the expression levels of these transcripts over time. Following the assignment of putative functions to the various up-regulated transcripts, the pathways and mechanisms involved in vegetative incompatibility were inferred. Staining assays were used to verify the role of laccase in vegetative incompatible interactions, as well better our understanding of PCD associated with this phenomenon.

MATERIALS AND METHODS

Fungal cultures and pairing reactions

The two heterokaryons of *A. areolatum* used in this study, CMW31512 (the result of a pairing between homokaryons CMW16848$_{12}$ X CMW16828$_{1}$) and CMW31513 (the result of a pairing between homokaryons CMW16848$_{41}$ X CMW16828$_{1}$), were previously synthesized and their vegetative compatibility groups determined based on hyphal morphology (van der Nest et al., 2008). One nucleus was thus common to the two heterokaryons, while the other nuclei were sib-related to each other. Working cultures of the isolates were maintained on potato dextrose agar (PDA) (24 gL^{-1} of PDA, 1 gL^{-1} glucose, and 1 gL^{-1} yeast extract) (Biolab, Johannesburg, South Africa) and all of the isolates used in this study are also maintained at 4 ºC in the culture

collection of the Forestry and Agricultural Biotechnology Institute (FABI), University of Pretoria, Pretoria, South Africa.

To allow for the identification of genes up-regulated during vegetative incompatibility and PCD associated with incompatibility in *A. areolatum*, a vegetatively incompatible interaction was compared with a "no pairing' reaction (*i.e.*, a heterokaryon that is not interacting with itself or another heterokaryon) (Fig. 1). By following this approach we hoped to identify not only those pathways and processes involved in the activation of PCD by incompatibility, but also those involved in other processes (e.g., hyphal fusion and recognition) that underlie self/non-self recognition in this fungus. For the incompatible interaction, heterokaryons CMW31512 and CMW31513 were paired by placing a mycelial plug (± 5 mm diameter) of each isolate, 3 cm apart in the middle of 9 cm Petri dish containing PDA. For the "no reaction", a single mycelial plug (± 5 mm diameter) of CMW31512 was placed at the centre of a 9 cm Petri dish containing PDA. For both the incompatible and the "no reaction", eight replicates were prepared and incubated in the dark at 25 ˚C. Three days after the establishment of hyphal contact between CMW31512 and CMW31513, mycelium of heterokaryon CMW31512 was harvested from the interaction site (Fig. 1) from all eight replicate plates and frozen in liquid nitrogen. To prevent cross-contamination with hyphae from heterokaryon CMW31513, mycelia were not harvested within 0.5 cm from the border between the interacting mycelia. At the same time, the mycelium of CMW31512 was harvested from the eight "no pairing" reactions and frozen in liquid nitrogen. A Zeiss Stereo microscope was used to determine when the hyphae had come into contact.

To verify the SSH results using real-time or quantitative reverse transcription PCR (qRT-PCR), the incompatible and the "no pairing" interactions were repeated as described above. In addition, for comparative purposes, a compatible reaction was induced by placing two mycelial plugs (± 5 mm diameter) of heterokaryon CMW31512 cm apart from each other on a 9 cm Petri dish containing PDA. At one, two and three days after hyphal contact, mycelium was harvested as described above for heterokaryon CMW31512, where the latter isolate was involved in a "no pairing", as well as the vegetatively compatible and incompatible interactions. To achieve a biological repeat for the qRT-PCRs, the mycelia from a duplicate set of interactions were also obtained.

Evans blue, Giemsa and α-naphthol staining

To establish if PCD is associated with vegetative incompatibility in *A. areolatum*, we employed Evans blue (Jacobson et al., 1998) and Giemsa (Hutchison et al., 2009) staining to compare compatible and incompatible interactions. As Evans blue only penetrate dead cells, we used it to compare the proportion of dead compartments between compatible and incompatible interactions. Evans blue staining does not allow differentiation between necrotic and apoptotic cell death (Chen and Dickman, 2005; Hutchison et al., 2009). We therefore employed Giemsa staining to determine if nuclear degradation, a trademark of apoptosis, occurs during vegetative incompatibility in *A. areolatum* (Hutchison et al., 2009). As it is well established that laccases are involved in fungal-fungal interactions (e.g., Iakovlev and Stenlid, 2000), the laccase activity associated with compatible and incompatible interactions was also compared using α-naphthol staining.

As before, for an incompatible interaction heterokaryons CMW31512 and CMW31513 were paired on PDA and for a "no reaction", a single mycelial plug of CMW31512 was grown on PDA. Three days after hyphal contact, segments of hyphae of the interaction zone (contact zone) were positioned on microscope slides after which the hyphae were stained with Evans blue (0.05 %; Sigma, St. Louis, MO) for 45 minutes at room temperature and washed with phosphate buffered saline (PBS) (Jacobson et al., 1998). A Zeiss Axiocam light microscope using Zeis software (Zeis, Germany) was then used to determine the proportion of dead compartments. Calculations were based on the mean of 10 replicates per sample per time point. The integrity of the nuclei between compatible and incompatible interactions were also examined by placing segments of hyphae of the interaction zone on a microscope slides and staining the hyphae with Giemsa stain (Sigma) according to manufactures recommendation. Thereafter, the stained hyphae were examined using the light microscope. Laccase activity was measured one month after hyphal contact by flooding mycelia with freshly prepared 1 % (wt/v) α-naphthol (Sigma) in 96 % ethanol and stained for 2 hours (Iakovlev and Stenlid, 2000). As laccase catalyses the oxidative polymerization of α-naphthol, the extracellular activity of this enzyme was assayed visually through the appearance of the purple coulored oxidative product.

RNA isolation and cDNA preparation

Total RNA was isolated from the frozen mycelia harvested from the incompatible and the "no pairing" reactions using TRIZOL Reagent (Invitrogen Life Technology). The quality and

quantity of the RNA samples were determined using the Nanodrop ND-1000 (Nanodrop Technologies, Wilmington, DE, USA) and agarose gel electrophoresis as previously described (Sambrook et al., 1989). Total RNA (A_{260}/A_{280}>1.8) isolated from the eight incompatible reaction plates and total RNA isolated from the eight "no pairing" interactions were combined, respectively. Messenger RNA (mRNA) was purified from the pooled total RNA using a commercially available kit (Purification of poly(A) mRNA Mini NucleoTrap®, Macherey-Nagel) following the manufacturer's recommendations. In all cases RNA was stored at -80 °C to maintain its integrity. Double-stranded cDNA was synthesized from the mRNA (4.0 µg) using the cDNA Synthesis System (Roche Diagnostics, Mannheim) following the manufacturer's recommendations using oligo$(dT)_{15}$ primer. The cDNA (10 µg) was purified using the MinElute PCR Purification Kit (Qiagen).

Preparation and sequencing of subtractive cDNA library

SSH (Diatchenko et al., 1996) was performed using the Clonetech (Palo Alto, CA) PCR Select-Subtraction cDNA kit. In principle, SSH was used to compare the mRNA transcripts between the "no pairing" and the vegetatively incompatible reactions and to obtain genes that are selectively expressed in the vegetatively incompatible reaction. The SSH library was constructed using the cDNA from the vegetatively incompatible reaction as Tester and those from the "no pairing" reaction as Driver. For this purpose cDNA from the Driver and the Tester was digested with *Rsa*I to generate short, blunt-ended double-strand cDNA. The digested cDNA was purified using the MinElute PCR Purification Kit, and the SSH Adaptors 1 or 2 ligated to the Tester cDNA. The Adaptor 1-ligated and the Adaptor 2-ligated Tester cDNAs were then separately hybridized to an excess of Driver cDNA at 68 ºC for 8h after denaturation at 98 ºC for 90 s. The two hybridization samples were mixed together without denaturation and hybridized at 68 ºC overnight with an excess of fresh denatured Driver cDNA. After diluting the resulting mixture in 200 µl buffer (Clonetech), two rounds of PCR was used to selectively amplify differentially expressed cDNA. The final PCR product (6 µg) was subjected to pyrosequencing using the Roche 454 GSFLX platform at Inqaba Biotech (Pretoria, Gauteng, South Africa). A single-lane sequencing run using one section of the PicoTitrePlate™ was performed. Sample preparation and analytical processing (e.g., base calling) were performed at Inqaba Biotech.

Evaluation of the subtraction efficiency

Subtraction efficiency was evaluated by comparing the relative amount of the constitutively expressed glycerol-3-phosphate dehydrogenase gene in subtracted cDNA and unsubtracted cDNA by PCR using the previously designed primers GpdF and GpdR (Neves et al., 2006). PCR were performed on an Eppendorf thermocycler (Eppendorf AG, Germany) using a reaction mixture containing 20 ng DNA, 0.2 mM of each of the four dNTPs, 1.5 mM $MgCl_2$, 0.5 µM of each primer and 2.5 U FastStart *Taq* (Roche Diagnostics, Mannheim). Thermal cycling conditions included an initial denaturation step at 94 °C for 2 min followed by 30 cycles of denaturation at 94 °C for 30 s, annealing at 50 °C for 30 s, extension at 72 °C for 30 s, and a final extension at 72 °C for 10 min. DNA was separated by electrophoresis on 2 % agarose (wt/v) gels (Roche Diagnostics, Mannheim), stained with ethidium bromide and visualized under ultraviolet light (Sambrook et al., 1989). Sizes of the amplicons were determined by comparison against a 100 base pair (bp) molecular weight marker (O'RangeRuler™ 100bp DNA ladder, Fermentas Life Science).

Sequence assembly and the identification of expressed genes

Individual sequence reads were aligned and assembled into contigs using Vector NTI Advance™ sequence analysis software (Invitrogen Life Technology). The basic local alignment search tool (BLAST, Altschul et al., 1990) implemented in BioEdit Version 7.0.9.0 (Hall, 1999) was used to identify and filter out sequences with similarity to known ribosomal RNA (rRNA) sequences (EU249344, AJ406498, AF506405, AF238456, AF454428) among the *A. areolatum* expressed sequence tags (ESTs). The remaining ESTs were annotated by web-based comparisons to the non redundant (nr) protein database of the National Center for Biotechnology Information (NCBI; http://www.ncbi.nlm.nih.gov) using translated blast searches (BLASTX) (Altschul et al., 1990). A scheme, similar to that used by Skinner et al. (2001), where ESTs were grouped as either highly significant in sequence similarity (E-value $<10^{-10}$), moderately significant in sequence similarity (E-value 10^{-9} to 10^{-4}), low significant sequence similarity (10^{-2} and 10^{-4}) or not significant in sequence similarity (E-values above 10^{-2}) was applied. ESTs with significant database matches were classified into functional categories based on Gene Ontology annotations (http://www.geneontology.org/).

Validation of SSH results

qRT-PCR was used to verify the up-regulation of the *A. areolatum* genes identified using SSH. In order to obtain information regarding the time course of the expression of the different EST sequences, total RNA was extracted from mycelium harvested from the compatible, incompatible and the "no reaction" at 1, 2 and 3 days after hyphal contact. Since high quality RNA is an essential requirement for qRT-PCR (Fleige et al., 2006), the extracted RNA was evaluated as described above and subjected to DNase I treatments (Invitrogen) following the supplier's protocols. For qRT-PCR, first-strand cDNA was synthesized using the DNase treated total RNA and random hexamer primers (First strand cDNA synthesis kit, Fermentas Life Science). This cDNA and specific primer pairs (Table 1), designed with Primer3 (http://bioinfo.ebc.ee/mprimer3/), were used to perform qRT-PCR with the SYBR Green I Master dye (Roche Diagnostics). Each PCR reaction (10 µL) contained SYBR Green Master Mix (5 µL) (Roche Diagnostics), 0.5 µl of each primer and 2 µL of 1:10 diluted first strand cDNA template. PCR amplification using a 384-well LightCycler 480 (Roche Diagnostics, Basel, Switzerland) was initiated at 95°C for 5 min followed by 45 cycles of 95°C for 5 s, 50°C for 5 s and 72°C for 20 s. After amplification, a melting curve analysis was run using the program for one cycle at 95°C for 30 s, 60°C for 30 s, and 95°C with 0-s hold in the step acquisition mode, followed by cooling at 40°C for 30 s. Biological repetitions (with RNAs from 2 independent cultures) for the incompatible, compatible and the "no pairing' interactions and technical repetitions for all the reactions were performed. PCR specificity and product detection was checked post-amplification by examining the temperature-dependent melting curves of the PCR products and a no-template control to confirm that there was no background contamination. To normalize the total amount of cDNA in each reaction, a portion of the 18S rRNA gene was co-amplified using the same cycling conditions described above and primers (Table 1) designed specifically for *A. areolatum*.

qRT-PCR is based on the number of cycles needed for amplification-generated fluorescence to reach a specific threshold of detection or the so-called Ct value. The Ct value for the 18S rRNA gene was used to normalize the Ct values for the selected targets. The delta-delta cycle threshold (ΔΔCT) method (Livak and Schnittgen, 2001) (Equation 1) was used to compare the relative expression between the different time intervals. Because this method assumes optimal

real time amplification efficiency (*i.e.*, a PCR efficiency $E = 2$ for the target and reference genes), another method (Equation 2) that implemented efficiency correction was also applied (Pfaffl, 2001). A standard curve was generated for each of the primer pairs by plotting Ct values against different template dilutions. The resulting data were analyzed for PCR efficiency correction using LightCycler 480 Relative Quantification Software (Roche Diagnostics) that used the slope of the standard curve to calculate the real time PCR efficiency (*E*). Un-paired Student's t tests were used for statistical assessments using Microsoft Excel 2007 software. Genes were considered as differentially expressed when the p-value associated with the F-value (Fisher-Snedecor) was <0.001, and when the mean ΔΔCT was ≤-0.6 or ≥0.6.

Equation 1.

$$\text{Relative expression} = 2^{-(\Delta Ct\ \text{sample} - \Delta Ct\ \text{control})}$$

Equation 2.

$$\text{Relative expression} = \frac{(E_{target})^{\ \Delta Ct\ \text{target (control - sample)}}}{(E_{reference})^{\ \Delta Ct\ \text{reference (control - sample)}}}$$

RESULTS

Evans blue, Giemsa and α-naphthol staining

The hyphae of compatible heterokaryons behaved as a single confluent mycelium, while a dark pigmented demarcation line was visible between incompatible heterokaryons (Fig. 2). It was suggested that increased levels of phenol oxidases (e.g., laccases) may cause this pigmentation, as phenol oxidases oxidise phenol substrates into melanin-like pigments (Iakovlev and Stenlid, 2000). Consistent with this idea, the α-naphthol staining (Fig. 2) demonstrated that the spatial localization of laccase activity differs between heterokaryons involved in vegetatively compatible and incompatible interactions. Laccase activity was higher in the interaction zone of heterokaryons involved in an incompatible interaction, but low or not detectable in other parts. In contrast, laccase activity was not localized to the interaction zone of heterokaryons involved in a compatible interaction. For the latter, all parts of the mycelia were homogeneously purple. This spatial distribution is similar to what have been observed in other fungal-fungal interactions of wood-decaying fungi (Li, 1981; Iakovlev and Stenlid, 2000).

The increased laccase activity at the interaction zone during fungal-fungal interactions has also been linked to the formation of melanin and free radicals that are likely to be associated with PCD (Rayner et al., 1994; Iakovlev and Stenlid, 2000). In fact, the sparse mycelium in the interaction zone is probably the result of cell death as the proportion of hyphae stained with Evans blue (Fig. 3) was almost twice as much for heterokaryons involved in an incompatible interaction (56.29 %) than for a compatible interaction (23.79 %). The Giemsa staining revealed that the hyphae of individuals involved in a compatible interactions displayed compact nuclei, while the hyphae of individuals involved in an incompatible interactions displayed diffuse nuclear staining (Fig. 3). This suggests that the chromatin of individuals involved in an incompatible interaction have degraded (Hutchison et al., 2009).

Generation and analysis of subtracted cDNAs

A SSH library was constructed for *A. areolatum* to identify genes selectively expressed during vegetative incompatibility. The fact that transcripts for the constitutively expressed gene glycerol-3-phosphate dehydrogenase was hardly detectable in the subtracted library compared to the unsubtracted sample, suggests that the SSH procedure indeed suppressed cDNA common to the "no pairing" and vegetatively incompatible reactions. Subjection of the subtracted cDNA library pyrosequencing generated 1.85 megabases (Mb) of sequence information that represented 8142 individual sequence reads. A large number of these individual sequence reads (6051, 74.3 %) represented rRNA sequences, suggesting that the mRNA purification was inefficient in removing rRNA. After removal of the rRNA sequences, the remaining sequence reads (2091, 25.7 %) could be assembled into 196 contigs (representing 1319 individual sequencing reads), while 764 represent singletons, indicating that a total of 960 ESTs were identified in this study.

BLASTX analyses using NCBI's nr protein database showed that 545 ESTs were similar to known database entries (Supplementary, Table 1). Of these, 418 (64 contigs and 354 singletons) were not significantly similar (E-values above 10^{-2}), while 127 (53 contigs and 74 singletons) were significantly similar (E-values below 10^{-2}). Of the 127 ESTs (53 contigs and 74 singletons) that were significantly similar to known database entries, 18 (11 contigs and 7 singletons) had low levels of similarity (E-values between 10^{-2} and 10^{-4}), 40 (13 contigs and 27 singletons) had moderately significant similarity (E-values between 10^{-5} and 10^{-10}) and 69 (29 contigs and 40 singletons) ESTs had highly significant similarity (E-values below 10-^{10}) to database entries. The remaining 415 ESTs (78 contigs and 337 singletons) identified in this study did not share similarity with any known sequence encoding either a known or a hypothetical protein in the nr database (Supplementary, Table 1), which highlights the lack of sequence information for fungi in general. In addition, many of the highly expressed ESTs (*i.e.*, those represented by contigs consisting of large numbers of sequence reads) were homologous to hypothetical proteins (e.g., Contig 75 with 100 sequencing reads), while some did not have any significant matches in the nr database (e.g., Contig 144 with 266 sequencing reads).

The identified ESTs that were significantly similar to known database entries were grouped into functional categories using the Gene Ontology website (http://www.geneontology.org/) (Fig. 4). The category with the highest representation in terms of the number of ESTs (19.0 %) is cell

death, which includes ESTs that share homology with genes previously implicated in the activation of cell death associated with oxidative stress (e.g., NADH-quinone oxidoreductase) (Fig. 4; Supplementary Table 1). This is followed by protein metabolism (15.0 %) and nucleic acid metabolism (14.0 %). The protein metabolism category is represented by various groups of genes, where protein degradation make up a substantial proportion (55.6 %) of this category, with the other two categories consisting of genes that showed significant similarity to ribosomal proteins (19.4 %) and translation factors (16.7 %). Genes involved in protein degradation that include a putative polyubiquitin, while genes involved in protein synthesis include a putative eukaryotic nascent polypeptide associate complex subunit alpha (alpha-nac) (Supplementary Table 1). The category containing genes associated with the cell defence and stress response also contains a high number of ESTs (12.0 %). A large proportion of the cell defence and stress category represents genes involved in a general stress response (71.4 %), followed by general defence response (21.4 %) and DNA repair (7.1 %). Cell defence and stress related genes identified in this study include phenoloxidases, a trehalose syntase, as well as the heat induced catalyse CAT1. Representative of the putative genes identified in this study that are known to be involved in hyphal fusion, the stress and defence response, as well as PCD are listed in Table 2.

Other abundant categories contain ESTs that showed significant similarity to proteins involved in transport (11.0 %), energy/carbon metabolism (10.0 %), cellular structure and organization (10.0 %), cell cycle and DNA processing (5.0 %), as well as proteins of which the function is not yet known (4.0 %). Various groups of genes are represented by the energy/carbon metabolism category, where genes involved in energy production have a high number of ESTs (60 %), while genes involved in sugar metabolism (8.0 %), amino acid metabolism (8.0 %), nitrogen metabolism (4.0 %) and lipid metabolism (4.0 %) were represented by fewer ESTs. Putative genes involved in cell metabolism and cellular transport included a major facilitator superfamily (Mfs) transporter/permease involved in sugar transport, a gamma-aminobutyrate receptor (GABA-gated ion channel) that transport the sugar GABBA and a sphingosine N-acyltransferase involved in ceramide synthesis.

Confirmation of SSH by qRT-PCR

The results of the qRT-PCRs on independent samples confirmed that the SSH library included transcripts that were selectively induced 3 days after the hyphae made contact (Fig. 5). All of the

11 randomly selected ESTs used for the qRT-PCR showed higher expression during a vegetatively incompatible reaction than during the "no reaction" 3 days after hyphal contact. Comparing the RNA levels of the selected up-regulated targets at three time points also made it possible to identify three expression patterns (designated as "hyphal fusion", "cell defence and stress response" and "cell death"). The "hyphal fusion" pattern is represented by the profiles for a putative mannoprotein, a putative MAPK (mitogen-activated protein kinase) and a putative mannose specific lectin-like protein flocculin, which are known to be involved in cell-cell adhesion (Guo et al., 2000). In all the instances, the targets were significantly up-regulated throughout the study. The expression profiles for a putative MAPK showed a decline in mRNA levels over the investigated time period. This suggests likely involvement of a MAPK signalling cascade early in vegetative incompatibility reactions, as well as confirming the important role that signalling plays in these reactions. The "cell defence and stress response" pattern is represented by the expression profiles for genes that may be directly (laccase and tyrosinase) or indirectly (Mfs transporter Mfs1.1, trehalose synthase and ubiquitin) associated with cell defence. Generally, the expression of these putative genes increased 2 days after hyphal contact. The "cell death" pattern is represented by the expression profiles for a putative ADP/ATP carrier protein, heterotrimeric protein phosphatase (P2A) and NADH-quinine oxidoreductase. In all three cases, a significant increase in RNA-levels was only observed 3 days after hyphal contact. Comparison of the RNA levels of the selected up-regulated targets during the compatible interaction at the three time points revealed that only the genes displaying the "adhesion" pattern were significantly up-regulated.

DISCUSSION

The results of this study substantially increased our understanding of the mechanisms underlying the events that lead to PCD associated with vegetative incompatibility in *A. areolatum*. Many of the putative genes identified here encode proteins potentially implicated in hyphal fusion, the stress and defence response, PCD, as well as proteins that are part of important signalling pathways that possibly regulate and coordinate these processes.

A large number of the putative genes also encoded proteins potentially involved in cellular processes associated with self/nonself recognition. These include genes that are apparently

involved in the production and transport of cellular components necessary for self/nonself recognition (Muthumeenakshi et al., 2007). Other genes appear to be unique to the vegetative incompatibility interaction, possibly associated with stress and PCD. For example, a number of genes, shown here for the first time to be involved in vegetative incompatibility, have previously been implicated in PCD in other eukaryotes. Taken together these findings suggest that *A. areolatum* utilizes the same mechanisms as other fungi to trigger PCD, and that this fungus employs the same proteins used by other fungi to mediate PCD. Results of this study, therefore, provide a sound framework for the identification and elucidation of the molecular mechanisms underlying self/nonself recognition in *A. areolatum* and other fungi. In the following section the findings of this study with respect to hyphal fusion, defence and stress, cell death and signalling are discussed in more detail.

Hyphal fusion

Various genes encoding proteins necessary for the generation and breakdown of cell walls were identified in this study. These included a putative UTP-glucose-1-phosphate uridylyltransferase involved in cell wall synthesis and various peptidases potentially involved in cell wall breakdown necessary for hyphal bridge formation (Pandey et al., 2004). One of the identified ESTs also encodes a putative monosaccharide permease that belongs to the mfs family of transporters that may be involved in the transport of various components necessary for the generation and breakdown of the cell wall (Muthumeenakshi et al., 2007). It is not surprising that these genes were up-regulated during vegetative incompatibility, because when two heterokaryons meet, their hyphae will anastomose, irrespective of whether they are compatible or incompatible (Worrall, 1997). During this process cell-cell attachment, production and targeting of cell wall degradation and synthesis enzymes to the attachment site and fusion of the plasma membrane are important (Pandey et al., 2004; Muthumeenakshi et al., 2007).

Cell-cell adhesion and recognition, which are processes central to hyphal fusion during vegetatively incompatible and compatible interactions, are probably mediated by glycoproteins in *A. areolatum.* Of the two putative glycoprotein-encoding ESTs identified in this study, one encodes a protein (mucin) from the FLO (flocculin) gene family, while the other encodes a mannoprotein. Both these proteins are thought to function as lectins to facilitate cell-cell adhesion by binding to cell surface carbohydrates (Fukazawa and Kagaya, 1997; Fichtner et al.,

2007; Douglas et al., 2007). In addition, the mannan moiety of mannoproteins also can bind to lectin (e.g., flocculins) to mediate cell-cell adhesion (Fukazawa and Kagaya, 1997). Although the exact nature of the putative proteinacious interactions involved in cell adhesion have not yet been fully characterized in fungi (Fukazawa and Kagaya, 1997), the SSH and qRT-PCR results presented here support the involvement of flocculin and mannoproteins in this process. The fact that transcripts for both these proteins were up-regulated during vegetative compatibility and incompatibility, confirms the idea that similar molecular mechanisms underlie hyphal fusion during these interactions.

Cell defence and stress response

The findings of this study suggest that vegetative incompatibility in *A. areolatum* is accompanied by an increase in cellular stress that includes an increase in reactive oxygen species (ROS), changes in pH and changes in redox potential. Several genes encoding putative proteins that alter cell redox potential and pH (e.g., vacuolar and plasma membrane H^+ATPases) and proteins involved in ROS production (e.g., 2-nitropropane dioxygenase) were identified in this study. Also, many genes identified here encoded proteins that are part of the electron transport complexes, for example a NADH-quinone oxidoreductase that froms part of complex I and a cytochrome c oxidase that froms part of complex III. The results thus suggest that the mitochondrial respiratory chain is central to ROS production during vegetative incompatibility in *A. areolatum*. Genes encoding proteins involved in ROS production (e.g., NADPH oxidase, glutaredoxin and cytochrome c) were also up-regulated during vegetative incompatibility in *P. anserina* (Hutchison et al., 2009). The involvement of ROS production in fungal-fungal interactions was accordingly also demonstrated in *Coniothyrium minitans* and *Sclerotinia sclerotiorum* (Gorlatova et al., 1998; Muthumeenakshi et al., 2007).

The qRT-PCR results presented here showed that the *A. areolatum* homologue of the NADH-quinone oxidoreductase was up-regulated during the incompatible interaction, which supports the notion that ROS production plays an integral part in the cell's response when it encounters a genetically different individual. This is despite the fact that an increase in ROS production and changes in redox potential and pH, which accompany incompatible vegetative interactions represent serious threats to cellular integrity (e.g., cause damage to DNA, lipids and proteins) (Kültz, 2005; Syntichaki et al., 2005; Dröse and Brandt, 2008).

The increase in cellular stress associated with vegetative incompatibility in *A. areolatum* may result in the activation of a cellular defence response. Evidence for the activation of a cellular defence response during vegetative incompatibility in *A. areolatum*, is that several of the identified ESTs encode proteins involved in ROS elimination (e.g., a putative heat induced catalyse CAT1) (Gucciardo et al., 2007) and proteins associated with the adaptation to stresses (e.g., putative mannoprotein and phenoloxidase for the adaptation to cell wall stress) (Iakovlev and Stenlid, 2000; Kültz, 2005). Several of the ESTs identified here also encode putative proteins involved in the sensing of stress (e.g., sensing of misfolded proteins such as the COP9 signalosome, CSN), the repair (e.g., DNA ligase and the aryl-alcohol dehydrogenase, AAD) (Horan et al., 2006) or the removal (e.g., the ubiquitin activation enzyme E1 and polyubiquitin) of damaged molecules and organelles. This suggests that the limitation of stress, repair of the damage caused by the stress and removal of damaged macromolecules are key aspects of vegetative incompatibility.

Further evidence of the activation of a cellular defence response during vegetative incompatibility in *A. areolatum* is that laccase is involved in vegetative incompatibility as indicated by the results of the staining experiments (Fig. 2). The laccase qualitative assays differed between vegetatively compatible and incompatible interactions. The qRT-PCR results also showed that the transcript encoding a putative laccase was strongly up-regulated in only vegetatively incompatibility interactions. Laccase was previously shown to play an important role in the defence response during fungal-fungal interactions (Iakovlev and Stenlid, 2000). Laccases in *A. areolatum* are thus likely to also eliminate ROS and free radicals during vegetative incompatibility (Iakovlev and Stenlid, 2000).

Results of this study further suggest that the sensing and signalling of nutrient stress may be involved in vegetative incompatibility in *A. areolatum*. This is comparable to what was found in *P. anserina,* where nutrient depletion and vegetative incompatibility illicit similar responses (Federovo et al., 2005; Pinan-Lucarré et al., 2003, 2007). Alterations of nutrient signalling pathways might also mediate the commitment of hyphae to enter PCD during incompatibility (Glass and Dementhon, 2004). In the present study, one of the *A. areolatum* ESTs encodes a putative nutrient-response GATA-type transcriptional factor involved in nitrogen starvation, while genes with promoter regions known to be targets for this type of transcriptional factor were also identified (e.g., a putative major facilitator superfamily, Mfs1.1) (Schmelzle et al., 2004;

Aro et al., 2005, Hewald et al., 2006). Mfs1.1 is also known to be involved in the cell defence response as it induces tyrosinase activity and melanin production (Zhao et al., 1999). The results of the qRT-PCR analysis in this study provided a similar link between the nutrient stress and defence responses with vegetative incompatibility for *A. areolatum*. The transcripts encoding the putative tyrosinase and Mfs1.1, as well as those encoding putative defence response components (*i.e.*, a laccase, polyubiquitin and a trehalose synthase) were strongly up-regulated only in the vegetatively incompatibility interactions. As the expression levels of these genes increased significantly only after two days post hyphal contact, their activation probably requires earlier responses, possibly involving the activation of signalling pathways.

Cell death

A characteristic of vegetative incompatibility is that PCD of the interacting hyphae prevents hyphal fusion to persist between unlike individuals (e.g., Worrall, 1997). The functional category with the highest number of *A. areolatum* sequence reads was the category containing putative proteins previously linked to PCD (Fig. 4). Also, the Evans blue staining results (Fig. 3) revealed that the proportion of dead cells of heterokaryons involved in an incompatible interaction are almost double than that for compatible interactions. Therefore, as previously shown in other fungi, PCD associated with vegetative incompatibility in *A. areolatum* also shares similarity with both Type I PCD (apoptosis) and Type II PCD (autophagy) in other eukaryotes (e.g., Marek et al., 2003; Hutchison et al., 2009).

Several genes identified in this study encoded proteins previously linked to autophagy. This included an EST that encoded a coatomer alpha-subunit that forms part of the subgroup of COPII (coatomer) proteins that are involved in autophagosome formation (Sato and Nakano, 2007). Other ESTs encode homologues of proteins (e.g., the sec10 secretory and SFT2 SNARE-like proteins) involved in the formation of the SNARE/NSF (*N*-ethylmaleimide-sensitive factor attached protein receptor, SNARE/*N*-ethylmaleimide-sensistive fusion protein, NSF1) responsible for the fusion of autophagosomes with the vacuole (Ishihara et al., 2001). ESTs whose inferred products may determine the levels of compounds such as phosphatidylinositol-3-phosphate (PtdIns-3-P) that regulate autophagy (Meijer and Codogno, 2004; Simonsen et al., 2004) were also present in the SSH library. Examples include the myotubularin related protein and casein kinase II that hydrolyse PtdIns-3-P, as well as the autophagy-linked FYVE (for Fab1,

YGLO23, Vps27, and EEA1) protein, Alfy, that binds to PtdIns-3-P (Meijer and Codogno, 2004; Simonsen et al., 2004). Genes encoding proteins that are known to be involved in autophagy were also up-regulated during vegetative incompatibility in *P. anserina* (Pinan-Lucarré et al., 2003). However, it is not possible to exclude the possibility that autophagy accompanying PCD by incompatibility in *A. areolatum* is triggered by the cellular defects that have arisen due to the toxic effect of the incompatibility of *het* gene interactions. An alternative explanation would be that autophagy is triggered in response to a signalling cascade that causes stress to the cell that is activated by the incompatibility of *het* gene interactions (Meijer and Codogno, 2004; Pinan-Lucarré et al., 2007).

It is possible that the induction of stress response during vegetative incompatibility in *A. areolatum* may result in the activation of PCD that resembles the Type I PCD (apoptosis) in other eukaryotes. Similar to what was observed during vegetative incompatibility in *P. anserina* (Hutchison et al., 2009), the Giemsa staining results indicated that the DNA of individuals involved in an incompatible interaction in *A. areolatum* has degraded, which is a hallmark of apoptosis. Several of the genes identified in this study also encoded putative proteins involved in the activation of PCD, as well as those involved in DNA and organellar integrity. For example, a homologue of the ubiquitin activation enzyme E1 implicated in the activation of DNA damage-associated cell death was identified (http://www.geneontology.org/; Fodorova et al., 2005). Another *A. areolatum* EST shares homology with the yeast ADP/ATP carrier (AAC) protein that is known to increase the permeability of the mitochondrial outer membrane and the consequent release of cytochrome c from the mitochondria thus triggering PCD (Pereira et al., 2007). This hypothesis is strengthened, as one of the genes up-regulated during vegetative incompatibility in *P. anserina* encoded a cytochrome c (Hutchison et al., 2009). The fact that laccase activity was limited to the interaction zones also suggests that the formation of melanin and free radicals are associated with the activation of PCD in *A. areolatum* (Rayner et al., 1994; Iakovlev and Stenlid, 2000).

It is possible that the activation of PCD by incompatibility in *A. areolatum* may involve mitochondrial perturbation associated with oxidative stress. It was also previously suggested that ROS and oxidative stress that has been implicated in apoptosis in mammals may play a role in PCD in *P. anserina* (Hutchison et al., 2009). This is possible because oxidative stress associated with incompatibility can cause the opening of non-specific high conductance permeability

transition pores during a process known as mitochondrial outer membrane transition (Orrenius et al., 2007). Indeed, one of the *A. areolatum* ESTs encodes a putative mitochondrial import inner membrane translocase subunit (Tim8), which protects mitochondria against stress-related protein aggregate formation, and that causes unselective channels in the mitochondria (Koehler et al., 2004). Under conditions of increased oxidative stress (e.g., due to the activity of ROS producers such as NADH-quinone oxidoreductase and cytochrome c oxidase identified in this study), more mitochondria are affected, up to a point where autophagy becomes inadequate to remove the damaged organelles and PCD is activated (Meijer and Codogno, 2004; Kiffin et al., 2006). It is thus likely that the cellular defects (e.g., damaged lipids, proteins, DNA and organelles) associated with vegetative incompatibility in *A. areolatum* are inordinately severe for autophagy to handle, ultimately leading to the triggering of PCD.

Consistent with the central role of PCD during vegetative incompatibility, the qRT-PCR results showed that all of the examined genes encoding homologues of known eukaryotic PCD related proteins were up-regulated in the vegetatively incompatible interactions only. Although ADP/ATP carrier (AAC) (Pereira et al., 2007) were up-regulated three days after hyphal contact, the gene encoding the NADH-quinone oxidoreductase was already up-regulated two days after hyphal contact. This supports the view that NADH-quinone oxidoreductase is involved in ROS production, that then results in DNA and organellar damage which in turn activates cascades (e.g., increase the permeability of the mitochondrial outer membrane) that trigger PCD during vegetative incompatible interactions in *A. areolatum*.

Signalling

Three types of signalling pathways appear to be central to the regulation and coordination of the cellular responses during vegetatively incompatible interactions in *A. areolatum*. These are the MAPK, cyclic adenosine monophosphate-dependent protein kinase A (RAS/cAMP-PKA) and the target of rapamycin (TOR) pathways (Omera et al., 1999; Schmelzle and Hall, 2000; Xu, 2000). Putative regulators for all three of these pathways were identified; e.g., the putative Ras GTPase-activating protein (Ras-GAP) NF1 that can inactivate small G-proteins (e.g., Ras, and Rho) to influence the RAS/cAMP-PKA and MAPK pathways (Schubert et al., 2006; Harispe et al., 2008), as well as the TOR pathway through cross-talk with the MAPK pathway (Sandsmark et al., 2007; Dunlop and Tee, 2009). Although, the involvement of TOR signalling in vegetative

incompatibility has been demonstrated previously in other fungi such as *P. anserina* (Federovo et al., 2005; Pinan-Lucarré et al., 2007), this study is the first to present a link between vegetative incompatibility and the cAMP-PKA and MAPK pathways have been demonstrated.

The MAPK, RAS/cAMP-PKA and TOR pathways probably regulate the events necessary for hyphal fusion during vegetative incompatibility in *A. areolatum*. For example, for *S. cerevisiae* it is known that all three of these pathways regulate the expression of flocculin (Verstrepen and Klis, 2006; Chen and Thorner, 2007) and for *Candida albicans* TOR is known to regulate cellular adhesion (Bastidas et al., 2009). The TOR and Rho/MAPK pathways also transfer signals to the CWI pathway to maintain cell wall integrity during morphogenesis (Levin, 2005). They could thus be involved in cell-cell adhesion during vegetatively incompatible and compatible interactions in *A. areolatum*. This is consistent with the presence of a putative *A. areolatum* MAPK that shares significant homology with MAPKs in *Magnaporthe grisea* (*Pmk1*) and *S. cerevisiae* (Mpk1/Slt2) where the latter is known to form part of the Rho/MAPK-dependent CWI pathway (Madrid et al., 2006). Two putative effectors of the Rho/MAPK-dependent CWI signalling pathway were also identified in this study. These are a putative formin (Faix and Grosses, 2006) and a putative myocardin-related transcription factor (MRTF), which activate the transcription of cytoskeleton/focal adhesion genes associated with the enhancement of stress fibres and focal adhesion formation (Levin, 2005; Morita et al., 2007).

The MAPK, RAS/cAMP-PKA and TOR pathways can also regulate and coordinate the defence and stress responses induced by vegetative incompatibility in *A. areolatum*. The putative MAPK (*Pmk1*) identified in this study shares homology with other members of the yeast extracellular signal-regulated kinase (YERK1) subfamily proteins associated with the defence response (Eliahu et al., 2007; Zeilinger and Omann, 2007). In *Trichoderma*, for example, a homologue of this kinase (*TmkA*) affects the mycoparasitism ability of the fungus as the kinase controls melanin biosynthesis and the expression enzymes for degrading the cell walls of the host fungus (Cho et al., 2007; Eliahu et al., 2007; Zeilinger and Omann, 2007). These pathways are also involved in sensing extracellular cues (e.g., nutrient sensing) and the response to these cues (Xu, 2000; Leberer et al., 2001). In *C. albicans* the MAPK, TOR and cAMP-PKA signalling pathways mediate nutrient starvation-induced morphogenesis from budding yeast to a polarized filamentous growth that were implicated in regulating virulence and pathogenicity (Xu, 2000; Leberer et al., 2001) and they also mediate CWI signalling to maintain cell wall integrity during

stress (Levin, 2005; Tsao et al., 2009). Therefore, it is likely that the MAPK pathway also regulates the defence response in *A. areolatum* during vegetative incompatibility in *A. areolatum*.

The MAPK pathway associated with stress-induced cell death may be involved in the activation of PCD during vegetative incompatibility in *A. areolatum*. A homologue of mammalian TAO1 (thousand-and-one amino acids 1) protein, which belongs to the yeast Ste20 protein kinase family (*i.e.*, part of the MAPK pathway) and has been implicated as potential apoptotic mediators in filamentous fungi (Fedorova et al., 2005), was identified in this study. It was shown previously that the activation of microtubule affinity-regulating kinase-activating kinase (MARKK), a homologue of TAO1, causes severe changes in the cytoskeleton thus impairing cellular functions (Dixit et al., 2008). Therefore, the TAO1 homolog of *A. areolatum* may be involved in the dynamic organization of the cytoskeleton to mediate PCD during incompatible interactions. Such cytoskeletal alterations mediated by MAPKs typically signals PCD during self-incompatibility (SI) in plants and PCD in animals (Bosch et al., 2008).

Results of this study suggest that ceramide represents an important component of PCD by incompatibility in *A. areolatum*. One of the sequences identified here encodes a putative spingosine-N-acyltrantransferase (a ceramide synthase) known to be involved in the *de novo* synthesis of ceramide, while another EST encodes a putative heterotrimeric protein phosphatase 2A (PP2A) that potentially represents a target of the ceramide pathway (Kolesnick and Krönke, 1998). It has also previously been suggested that sphingomyelin-ceramide signaling may mediate PCD during vegetative incompatibility (Andrieu-Abadie et al., 2001). Since, mitochondrial permeability transition represents a committed step in ceramide signalling of PCD (Andrieu-Abadie et al., 2001; Kolesnick and Krönke, 1998), it is possible that ceramide signalling and mitochondrial perturbation may represent a committed step in the induction of PCD by incompatibility in *A. areolatum*. This is similar to what has been observed in plants and animals (Gilchrist, 1998).

The notion that a MAPK pathway is involved in the early signalling in *A. areolatum* during cell-cell interactions was confirmed by the qRT-PCR results. The putative MAPK identified here was already up-regulated a day after hyphal contact in both the vegetatively incompatible and compatible interactions, perhaps coordinating and regulating processes involved in hyphal

fusion. However, the fact that the expression of this transcript was up-regulated more strongly in the incompatible interaction, suggests that it regulates and coordinates key processes necessary to cope with various stresses associated with non-self recognition. ESTs potentially involved in the activation of PCD in response to an increase mitochondrial permeability transition *i.e.*, the ADP/ATP carrier protein and ceramide signalling *i.e.*, PP2A were also significantly up-regulated, but only three days post hyphal contact in the vegetatively incompatible interactions. This is consistent with that the stresses associated with MPT trigger a cascade that activates PCD associated with incompatibility in *A. areolatum*.

Conclusions

Based on the results of this study, we propose a model of events that may occur during a vegetatively incompatible interaction in *A. areolatum* (Fig. 6). Hyphal fusion represents a key process associated with both vegetatively incompatible and compatible interactions. Several genes encoding putative proteins (e.g., glycosyltranferase, formin, casein kinase II, mannoprotein, flocculin and odd oz protein) involved in cell-cell adhesion as an initial step involved in hyphal fusion were identified. It is possible that cell-cell adhesion and recognition may partly be facilitated by lectin-mediated adhesion in *A. areolatum*, as a putative mannoprotein and a mannose specific lectin-like protein flocculin were selectively expressed during incompatible and compatible interactions. The MAPK, RAS/cAMP-PKA and TOR pathways are probably involved in regulating these events, as a putative MAPK, a snare-like protein involved in TOR signalling and a putative Ras-GAP that influence the RAS/cAMP-PKA and MAPK pathways were identified in this study. However, it is still not exactly clear which processes associated with vegetative incompatibility are influenced by these signalling pathways.

After hyphal fusion, the *het* gene incompatibility interaction activates a cascade (e.g., increase ROS, changes in pH and redox potential) that stress the cell (e.g., degradation of DNA, organelle damage, etc.) and trigger a stress response. Several genes encoding proteins (e.g., NADH-quinone oxidoreductase , cytochrome c oxidase and heat induced catalyse CAT1) associated with stress and the stress response were identified in this study. Again, the MAPK, RAS/cAMP-PKA and TOR pathways may regulate and coordinate the defence and stress responses induced by the *het* gene incompatibility products. Initially, the cell attempts to limit the damage, for example by autophagy that removes damaged organelles, DNA, etc. Several (COPII, sec10 secretory and the

autophagy-linked FYVE protein) genes previously linked with autophagy were identified in this study. It is possible that when the damage becomes inordinately severe, PCD is activated.

Apparently, the mitochondrial perturbation associated with oxidative stress plays an important role in the activation of PCD by incompatibility in *A. areolatum* and that mitochondrial outer membrane transition coupled with ceramide signalling represent a committed step in the activation of PCD. For example, a homologue of the yeast ADP/ATP carrier (AAC) protein was identified in this study that is known to increase the permeability of the mitochondrial outer membrane and the consequent release of cytochrome c from the mitochondria thus triggering PCD. One of the ESTs identified in this study encodes a putative a ceramide synthase, thus strengthening the hypthosis that ceramide signalling plays a role in vegetative incompatibility in *A. areolatum*. Following this proposed model, the pathways and processes associated with vegetative incompatibility are interlinked. This is reflected in the fact that some proteins are involved in multiple processes, and that certain pathways are also involved in processes other than vegetative incompatibility.

SSH combined with pyrosequencing were used in this study to identify a large number of genes differentially expressed during vegetative incompatiblity in *A. areolatum*. The PCR-based SSH method provided a powerful approach to identify selectively expressed genes, allowing for the detection of numerous potentially rare transcripts and low abundance genes that would otherwise be difficult to identify (Liu et al., 2007; Huang et al., 2007; Morissette et al., 2008). Using SSH, 91 unique proteins were identified, despite the fact that more than 50 % of the pyrosequencing reads were represented by ribosomal RNA regions. Combining of pyrosequencing and SSH, overcomes the major drawback of SSH, namely the overrepresentation of certain genes in clone libraries. This approach is also less labour intensive and time consuming than traditional cloning and sequencing of selected clones (Liu et al., 2007; Huang et al., 2007). Some authors suggest that SSH does not always exclude all non-differentially expressed genes (e.g., Huang et al., 2007), but qRT-PCR showed that all 11 of the selected genes in this study were up-regulated during vegetative incompatibility. These results support the conclusion that the majority of the sequences identified in this study play a role in vegetative incompatibility. To determine the roles played by the differentially expressed genes during vegetative incompatibility, further functional experiments (e.g., by gene knockout) will be needed

REFERENCES

Altschul, S.F., Gish, W., Miller, W., Myers, E.W., Lipman, D.J., 1990. Basic local alignment search tool. J. Mol. Biol. 215, 403-410.

Andrieu-Abadie, N., Gouazė, V., Salvayre, R., Levade, T., 2001. Ceramide in apoptosis signaling: Relationship with oxidative stress. Free Radical Biol. Med. 3, 717-728.

Aro, N., Pakula, T., Pentilä, M., 2005. Transcriptional regulation of plant cell wall degradation by filamentous fungi. FEMS Microbiol. Rev. 29, 719-739.

Bastidas, R.J., Heitman, H., Cardenas, M.E., 2009. The protein kinase TOR1 regulates adhesin gene expression in *Candida albicans*. PLoS Path. 5, e1000294.

Bosch, M., Poulter, N.S., Vatovec, S., Franklin-Tong, V.E., 2008. Initiation of programmed cell death in self-incompatibility: Role for cytoskeleton modifications and several caspase-like activities. Mol. Plant. 1, 879-887.

Bourges, N.G., Groppi, A., Barreau, C., Clave, C., Begueret, J., 1998. Regulation of gene expression during the vegetative incompatibility reaction in *Podospora anserina:* Characterization of three induced genes. Genet. 150, 633-641.

Bursch, W., 2001. The autophagosomal-lysosomal compartment in programmed cell death. Cell Death Diff. 8, 569-581.

Carpenter, M.A., Stewart, A., Ridgway, H.J., 2005. Identification of novel *Trichoderma hamatum* genes expressed during mycoparasitism using subtractive hybridisation. FEMS Microbiol. Lett. 251, 105-112.

Chen, C., Dickman, M.B., 2005. Proline suppresses apoptosis in the fungal pathogen *Colletotrichum trifolii*. Proc. Natl. Acad. Sci. U.S.A. 102, 3459-3464.

Chevanne, D., Saupe, S.J., Clavé, C., Paoletti, M., 2010. WD-repeat instability and diversification of the *Podospora anserina hnwd* non-self recognition gene family. BMC Evol. Biol. 10, 134.

Chen, R.E., Thorner, J., 2007. Function and regulation in MAPK signaling pathways: Lessons learned from the Yeast the *Saccharomyces cereviciae*. Biochim Biophys Acta. 177, 1311-1340.

Cho, Y., Cramer, R.A., Kim, K-H., Davis, J., Mitchell, T.K., Figuli, P., Pryor, B.M., Lemasters, E., Lawrence, C.B., 2007. The *Fus3/Kss1* MAP kinase homolog *Amk1* regulates the expression of genes encoding hydrolytic enzymes in *Alternaria brassicicola*. Fungal Genet. Biol. 44, 543-553.

Dementhon, K., Saupe, S.J., Clavé, C., 2004. Characterization of IDI-4, a bZIP transcription factor inducing autophagy and cell death in the fungus *Podospora anserina.* Mol. Microbiol. 53, 1625-1640.

Diatchenko, L., Lau, Y.F., Campbell, A.P., Chenchik, A., Moquadam, F., Huang, B., Lukyanov, S., Lukyanov, K., Gurskaya, N., Sverdlov, E.D., Siebert, P.D., 1996. Suppression subtractive hybridization: A method for generating differentially regulated or tissue-specific cDNA probes and libraries. Proc. Natl. Acad. Sci. U.S.A. 93, 6025-6030.

Dixit, R., Ross, J.L., Goldman, Y.E., Holzbaur, E.L.F., 2008. Differential regulation of dynein and kinesin motor proteins by Tau. Science. 319, 1086-1089.

Douglas, L.M., Li, L., Yang, Y., Dranginis, A.M., 2007. Expression and characterization of the flocculin Flo11/Muc1, a *Saccharomyces cerevisiae* mannoprotein with homotypic properties of adhesion. Euk. Cell. 6, 2214-2221.

Dröse, S., Brandt, U., 2008. The mechanism of mitochondrial superoxide production by the cytochrome *bc*1 complex. J. Biol. Chem. 283, 21649-21654.

Dunlop, E.A., Tee, A.R., 2009. Mammalian target of rapamycin complex 1: Signalling inputs, substrates and feedback mechanisms. Cell. Signal. 21, 827-835.

Eliahu, N., Igbaria, A., Rose, M.S., Horwitz, B.A., Lev, S., 2007. Melanin biosynthesis in the maize pathogen *Cochliobolus heterostrophus* depends on two MAP kinases, Chk1 and Mps1, and the transcriptional factor Cmr1. Euk. Cell. 6, 421-429.

Faix, J., Grosses, R., 2006. Staying in shape with formins. Dev. Cell. 10, 693 - 706.

Fang, X., Willis, R.C., Siano, M.A., Quinto-Pozos, M., Conrad, Richard, C., 2003. Automated high-throughput mRNA selection from eukaryotic Total RNA. J. Assoc. Lab. Autom. 8, 51-54.

Fedorova, N.D., Badger, J.H., Robson, G.D., Wortman, J.R., Nierman, W.C., 2005. Comparative analysis of programmed cell death pathways in filamentous fungi. BMC Genomics. 6, 1-14.

Fichtner, L., Schulze, F., Braus, G.H., 2007. Differential Flo8p-dependent regulation of FLO1 and FLO11 for cell-cell and cell-substrate adherence of *S. cerevisiae* S288c. Mol. Microbiol. 66, 1276-1289.

Fleige, S., Walf, V., Huch, S., Prgomet, C., Sehm, J., Pfaffl, M.W., 2006. Comparison of relative mRNA quantification models and the impact of RNA integrity in quantitative real-time RT-PCR. Biotechnol. Lett. 28, 1601-1613.

Fukazawa, Y., Kagaya, K., 1997. Molecular bases of adhesion of *Candida albicans.* J. Med. Vet. Mycol. 35, 87-99.

Gilchrist, D.G., 1998. Programmed cell death in plant diseases: The purpose and promise of cellular suicide. Annu. Rev. Phytopathol. 36, 393-414.

Glass, N.L., Dementhon, K., 2006. Non-self recognition and programmed cell death in filamentous fungi. Curr. Opin. Microbiol. 9, 553-558.

Glass, N.L., Kaneko, I., 2003. Fatal attraction: Nonself-recognition and heterokaryon incompatibility in filamentous fungi. Euk. Cell. 2, 1-8.

Gorlatova, N., Tchorzewski, M., Kurihara, T., Soda, K., Esaki, N., 1998. Purification, characterization, and mechanism of flavin mononucleotide-dependent 2-nitropropane dioxygenase from *Neurospora crassa*. Appl. Envir. Microbiol. 64, 1029-1033.

Greenberg, J.T., Yao, N., 2004. The role and regulation of programmed cell death in plant-pathogen interactions. Cell. Microbiol. 6, 201-211.

Gucciardo, S., Wisniewski, J-P., Brewin, N.J., Bornemann, S., 2007. A germin-like protein with superoxide dismutase activity in pea nodules with high protein sequence identity to a putative rhicadhesis receptor. J. Exper. Bot. 58, 1161-1171.

Guo, B., Styles, C.A., Feng, Q., Fink, G.R., 2000. A *Saccharomyces* gene family involved in invasive growth, cell-cell adhesion, and mating. Proc. Natl. Acad. Sci. USA. 97, 12158-12163.

Hall, T.A., 1999. Bioedit: A user-friendly biological sequence alignment editor and analysis program for Windows 95/98/NT, Nuc. Acids Symp. Ser. 41, 95-98.

Harispe, L., Portela, C., Scazzocchio, C., Pefialva, M.A., Gorfinkiel, L., 2008. Ras GTPase-activating protein regulation of actin cytoskeleton and hyphal polarity in *Aspergillus nidulans*. Euk. Cell. 7, 141-153.

Hewald, S., Linne, U., Scherer, M., Marahiel, M.A., Kämper, J., Bölker, M., 2006. Identification of a gene cluster for biosynthesis of mannosylerythritol lipids in the basidiomycetous fungus *Ustilago maydis*. Appl. Envir. Microbiol. 72, 5469-5477.

Horan, S., Bourges, I., Meunier, B., 2006. Transcriptional response to nitrosative stress in *Saccharomyces cerevisiae*. Yeast. 23, 519-535.

Huang, X., Li, Y., Niu, Q., Zhang, K., 2007. Suppression Subtractive Hybridization (SSH) and its modifications in microbiological research. Appl. Microbiol. Biotechnol. 76, 753-760.

Hückelhoven, R., 2007. Cell wall-associated mechanisms of disease resistance and susceptibility. Annu. Rev. Phytopathol. 45, 101-127.

Hutchison, E., Brown, S., Tian, C., Glass, N.L., 2009. Transcriptional profiling and functional analysis of heterokaryon incompatibility in *Neurospora crassa* reveals that ROS, but not metacaspases, are associated with programmed cell death. Microbiol. Papers.155, 3957-3970.

Iakovlev, A., Stenlid, J., 2000. Spatiotemporal patterns of laccase activity in interacting mycelia of wood-decaying basidiomycete fungi. Microb. Ecol. 39, 236-245.

Ishihara, N., Hamasaki, M., Yokota, S., Suzuki, K., Kamada, Y., Kihara, A., Yoshimori, T., Noda, T., Ohsumi, Y., 2001. Autophagosome requires specific early sec proteins for its formation and NSF/SNARE for vacuolar fusion. Mol. Biol. Cell. 12, 3690-3702.

Jacobson, D.J., Beurkens, K., Klomparens, K.L., 1998. Microscopic and ultrastructural examination of vegetative incompatibility in partial diploids heterozygous at *het* loci in *Neurospora crassa*. Fungal Genet. Biol. 23, 45-56.

Kiffin, R., Bandyopadhyay, U., Cuervo, A.M., 2006. Oxidative stress and autophagy. Antioxid. Redox Signal. 8, 152-162.

Koehler, C.M., 2004. New developments in mitochondrial assembly. Annu. Rev. Cell Dev. Biol. 20, 309-335.

Kolesnick, R.N., Krönke, M., 1998. Regulation of ceramide production and apoptosis. Annu. Rev. Physiol. 60, 643-665.

Kubisiak, T.L., Milgroom, M.G., 2006. Markers linked to vegetative incompatibility (*vic*) genes and a region of height heterogeneity and reduced recombination near the mating type locus (*MAT*) in *Cryphonectria parasitica*. Fungal Genet. Biol. 43, 453-463.

Kültz, D., 2005. Molecular and evolutionary basis of the cellular stress response. Annu. Rev. Physiol. 2005. 67, 225-57.

Leberer, E., Harcus, D., Dignard, D., Johnson, L., Ushinsky, S., Thomas, D.Y., Schröppel K., 2001. Ras links cellular morphogenesis to virulence by regulation of the MAP kinase and cAMP signalling pathways in the pathogenic fungus *Candida albicans*. Mol. Microbiol. 42, 673-687.

Levin, D.E., 2005. Cell wall integrity signaling in *Saccharomyces cerevisiae*. Microbiol. Mol. Biol. Rev. 69, 262-291.

Li, C.Y., 1981. Phenoloxidase and peroxidase activities in zone lines of *Phellinus weirii*. Mycologia. 73, 811-821.

Liu, H., Xi, L., Zhang, J., Li, X., Liu, X., Lu, C., Sun, J., 2007. Identifying differentially expressed genes in the dimorphic fungus *Penicillium marneffei* by suppression subtractive hybridization. FEMS Microbiol. Lett. 270, 97-103.

Livak, K.J., Schmittgen, T.D., 2001. Analysis of relative gene expression data using real-time quantitative PCR and the $2^{(-\Delta\Delta Ct)}$ method. Methods. 25, 402-408.

Loubradou, G., Turcq, B., 2000. Vegetative incompatibility in filamentous fungi: A roundabout way of understanding the phenomenon. Res. Microbiol. 151, 239-245.

Madrid, M., Soto, T., Khong, H.K., Franco, A., Vicente, J., Pėrez, P., Gacto, M., Cansado, J., 2006. Stress-induced response, localization, and regulation of the Pmk1 cell integrity pathway in *Schizosaccharomyces pombe*. J. Biol. Chem. 281, 2033-2043.

Mathias, S., Penna, L.A., Kolesnick, R.N., 1998. Signal transduction of stress via ceramide. Biochem. J. 335, 465-480.

Matsuyama, S., Xu, Q., Velours, J., Reed, J.C., 1998. The mitochondrial F0F1-ATPase proton pump is required for function of the proapoptotic protein bax in yeast and mammalian cells. Mol. Cell. 1, 327-336.

Marek, S.M., Wu, J., Glass, N.L., Gilchrist, D.G., Bostock, R.M., 2003. Nuclear DNA degradation during heterokaryon incompatibility in *Neurospora crassa.* Fungal Genet. Biol. 40, 126-137.

Meijer, A.J., Codogno, P., 2004. Regulation and role of autophagy in mammalian cells. Int. J. Biochem. Cell Biol. 36, 2445-2462.

Morissette, D.C., Dauch, A., Beech, R., Masson, L., Brousseau, R., Jabaji, S., 2008. Hare isolation of mycoparasitic-related transcripts by SSH during interaction of the mycoparasite *Stachybotrys elegans* with its host *Rhizoctonia solani*. Curr. Genet. 53, 67-80.

Morita, T., Mayanagi, T., Sobue, K., 2007. Reorganization of the actin cytoskeleton via transcriptional regulation of cytoskeletal/focal adhesion genes by myocardin-related transcription factors (MRTFs/MAL/MKLs). Exp. Cell Res. 313, 3432-3445.

Muthumeenakshi, S., Sreenivasaprasad, S., Rogers, C.W., Challen, M.P., Whipps, J.M., 2007. Analysis of cDNA transcripts from *Coniothyrium minitans* reveals a diverse array of genes involved in key processes during sclerotial mycoparasitism. Fungal Genet. Biol. 44, 1262-1284.

Neves, L., Lages, F., Lucas, C., 2004. New insights on glycerol transport in *Saccharomyces cerevisiae.* FEBS Lett. 565, 160-162.

Omero, C., Binbar, J., Rocha-Ramirez, V., Herrera-Estrella, A., Chet, I., Horwitz, B.A., 1999. G protein activators and cAMP promote mycoparasitic behaviour in *Trichoderma harzianum.* Mycol. Res. 103, 1637-1642.

Orrenius, S., Gogvadze, V., Zhivotovsky, B., 2007. Mitochondrial oxidative stress: Implications for cell death. Annu. Rev. Pharmacol. Toxicol. 47, 143-183.

Pandey, A., Roca, M.G., Read, N.D., Glass, N.L., 2004. Role of a mitogen-activated protein kinase pathway during conidial germination and hyphal fusion in *Neurospora crassa*. Euk. Cell. 3, 348-358.

Paoletti, M., Saupe, S.J., Clavé, C., 2007. Genesis of a fungal non-self recognition repertoire. Plos One. 3: e283.

Pereira, C., Camougrand, N., Manon, S., Sousa, M.J., Córte-Real, M., 2007. ADP/ATP carrier is required for mitochondrial outer membrane permeabilization and cytochrome c release in yeast apoptosis. Mol. Microbiol. 66, 571-582.

Pfaffl, M.W., 2001. A new mathematical model for relative quantification in real time RT-PCR. Nucl. Acid R. 29, 2002-2007.

Pinan-Lucarré, B., Balguerie, A., Clavé, C., 2005. Accelerated cell death in *Podospora* autophagy mutants. Euk. Cell. 4, 1765-1774.

Pinan-Lucarré, B., Paoletti, M., Dementhon, K., Coulary-Salin, B., Clave, C., 2003. Autophagy is induced during cell death by incompatibility and is essential for differentiation in the filamentous fungus *Podospora anserina.* Mol. Microbiol. 47, 321-333.

Pinan-Lucarré, B., Paoletti, M., Clavé, C., 2007. Cell death by incompatibility in the fungus *Podospora*. Sem. Cancer Biol. 17, 101-111.

Raha, S., Robinson, B.H., 2001. Mitochondria, oxygen free radicals, and apoptosis. Am. J. Med. Genet. (Semin. Med. Genet.). 106, 62-70.

Rayner, A.D.M., Griffith, G.S., Wildman, H.G., 1994. Differential insulation and the generation of mycelial patterns. In: Gow NAR, Gadd, G.M. (eds) Shape and form in plants and fungi. Academic Press, Londen, pp. 291-310.

Sambrook, J., Fritsch, E.F., Maniatis, T., 1989. Molecular cloning: A laboratory manual. 2nd ed. Cold Spring Harbor Laboratory Press, Cold Spring Harbor, NY, U.S.A.

Sandsmark, D.K., Zhang, H., Hegedus, B., Pelletier, C.L., Weber, J.D., Gutmann, D.H., 2007. Nucleophosmin mediates mammalian target of rapamycin-dependent actin cytoskeleton dynamics and proliferation in neurofibromin-deficient astrocytes. Cancer Res. 67, 4790-4799.

Sato, K., Nakano, A., 2007. Mechanisms of COPII vesicle formation and protein sorting. FEBS Lett. 581, 2076-2082.

Saupe, S.J., 2000. Molecular genetics of heterokaryon incompatibility in filamentous ascomycetes. Micro. Mol. Biol Rev. 64, 489-502.

Schmelzle, T., Beck, T., Martin, D.E., Hall, M.N., 2004. Activation of the RAS/Cyclic AMP pathway suppresses a TOR deficiency in yeast. Mol. Cell. Biol. 24, 338-351.

Schmelzle, T., Hall, M.N., 2000. TOR, a central controller of cell growth. Cell. 103, 253-262.

Schubert, D., Raudaskoski, M., Knabe, N., Kothe, E., 2006. Ras GTPase-activating protein GAP1 of the homobasidiomycete *Schizophyllum commune* regulates hyphal growth orientation and sexual development. Euk. Cell. 5, 683-695.

Simonsen, A., Birkeland, H.C.G., Gillooly, D.J., Mizushima, N., Kuma, A., Yoshimori, T., Slagsvold, T., Brech, A., Stenmark, H., 2004. Alfy, a novel FYVE-domain-containing protein associated with protein granules and autophagic membranes. J. Cell Sci. 117, 4239-4251.

Skinner, W., Keon, J., Hargreaves, J., 2001. Gene information for fungal plant pathogens from expressed sequences. Curr. Opin. Microbiol. 4, 381-386.

Slippers, B., Coutinho, T.A., Wingfield, B.D., Wingfield, M.J., 2003. A review of the genus *Amylostereum* and its association with woodwasps. SA J. Sci. 99, 70-74.

Syntichaki, P., Samara, C., Tavernarakis, N., 2005. The vacuolar H+-ATPase mediates intracellular acidification required for neurodegeneration in *C. elegants*. Curr. Biol. 15, 1249-1254.

Tsao, C.-C., Chen, Y.-T., Lan, C.-Y., 2009. A small G protein Rhb1 and a GTPase-activating protein Tsc2 involved in nitrogen starvation-induced morphogenesis and cell wall integrity of *Candida albicans*. Fungal Genet. Biol. 46, 126-136.

Van der Nest, M.A., Slippers, B., Stenlid, J., Wilken, P.M., Vasaitis, R., Wingfield, M.J., Wingfield, B.D., 2008. Characterization of the systems governing sexual and self-recognition in the white rot Agaricomycete *Amylostereum areolatum*. Curr. Genet. 53, 323-336.

Van der Nest, M.A., Slippers, B., Steenkamp, E.T., De Vos, L., Van Zyl, K., Stenlid, J., Vasaitis, R., Wingfield, M.J., Wingfield, B.D., 2009. Genetic linkage map for *Amylostereum arolatum* reveals an association between vegetative growth and sexual and self recognition Fungal Genet. Biol. 46, 632-641.

Vercesi, A.E., Kowaltowski, A.J., Grijalba, M.T., Meinicke, A.R., Castilho, R.F., 1997. The role of reactive oxygen species in mitochondrial permeability transition. Bioscience Reports.17, 43-52.

Verstrepen, K.J., Klis, F.M., 2006. Flocculation, adhesion and biofilm formation in yeasts. Mol. Microbiol. 60, 5-15.

Worral, J.J., 1997. Somatic incompatibility in basidiomycetes. Mycol. 89, 24-36.

Xu, J.-R., 2000. MAP Kinases in fungal pathogens. Fungal Genet. Biol. 31, 137-152.

Zeilinger, S., Omann, M., 2007. *Trichoderma* biocontrol: Signal transduction pathways involved in host sensing and mycoparasitism. Gene Reg. Syst. Biol. 1, 227-234.

Zhao, X., Wakamatsu, Y., Shibahara, M., Nomura, N., Geltinger, C., Nakahara, T., Murata, T., Yokoyama, K.K., 1999. Mannosylerythritol lipid is a potent inducer of apoptosis and differentiation of mouse melanoma cells in culture. Cancer Res. 59, 482-486.

FIGURES

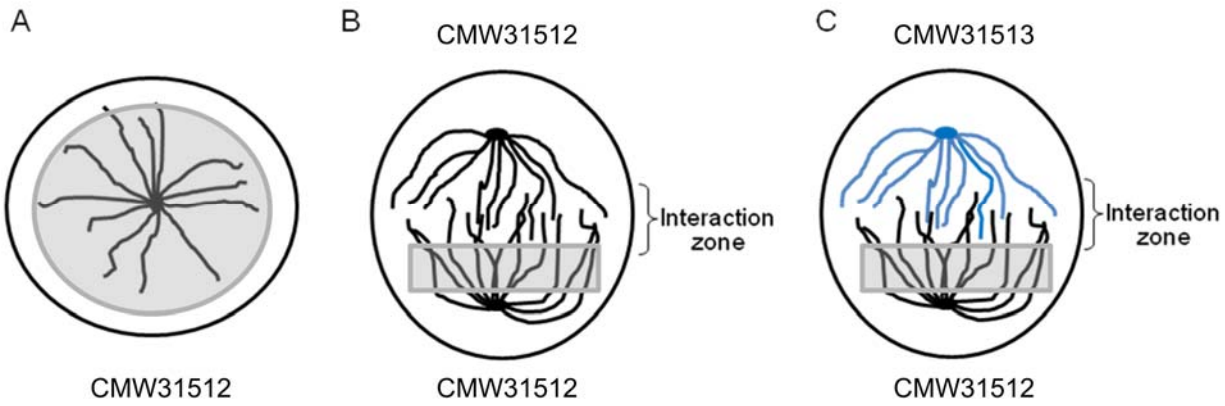

Figure 1. Mycelia were harvested from heterokaryon CMW31512 involved in a "no reaction" (A). Mycelia were also harvested from the interaction site (indicated with highlighted area) from heterokaryon CMW31512 involved in a vegetative compatibility (B) and a vegetative incompatible (C) reaction 3 days after hyphal contact. To prevent contamination of CMW31513 RNA, mycelia were harvested more than 0.5 cM from the interaction zone. The "no reaction" (A) was used as a driver, while the vegetative incompatible (C) reaction was used as the tester for subtractive hybridization (SSH) cDNA library construction.

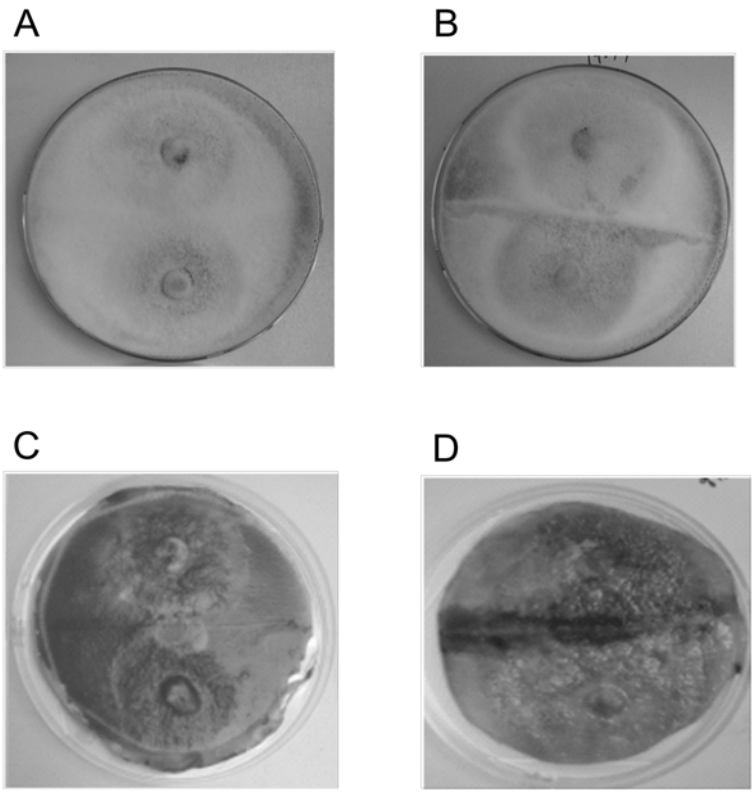

Figure 2. Macroscopic characteristic of a compatible and an incompatible interaction, as well as a comparison of laccase activity in a compatible *vs.* an incompatible interaction. The hyphae of compatible heterokaryons behaved as one confluent mycelium (**A**), while a demarcation line was visible between incompatible heterokaryons (**B**). Compatible interactions were characterized by the non-localization of laccase activity as indicated by a-naphtol-assays that stained entire plates purple (**C**). Strongly vegetative incompatible interactions were characterized by the localization of laccase activity as indicated by a-naphtol-assays that stained only the interacting zone purple (**D**).

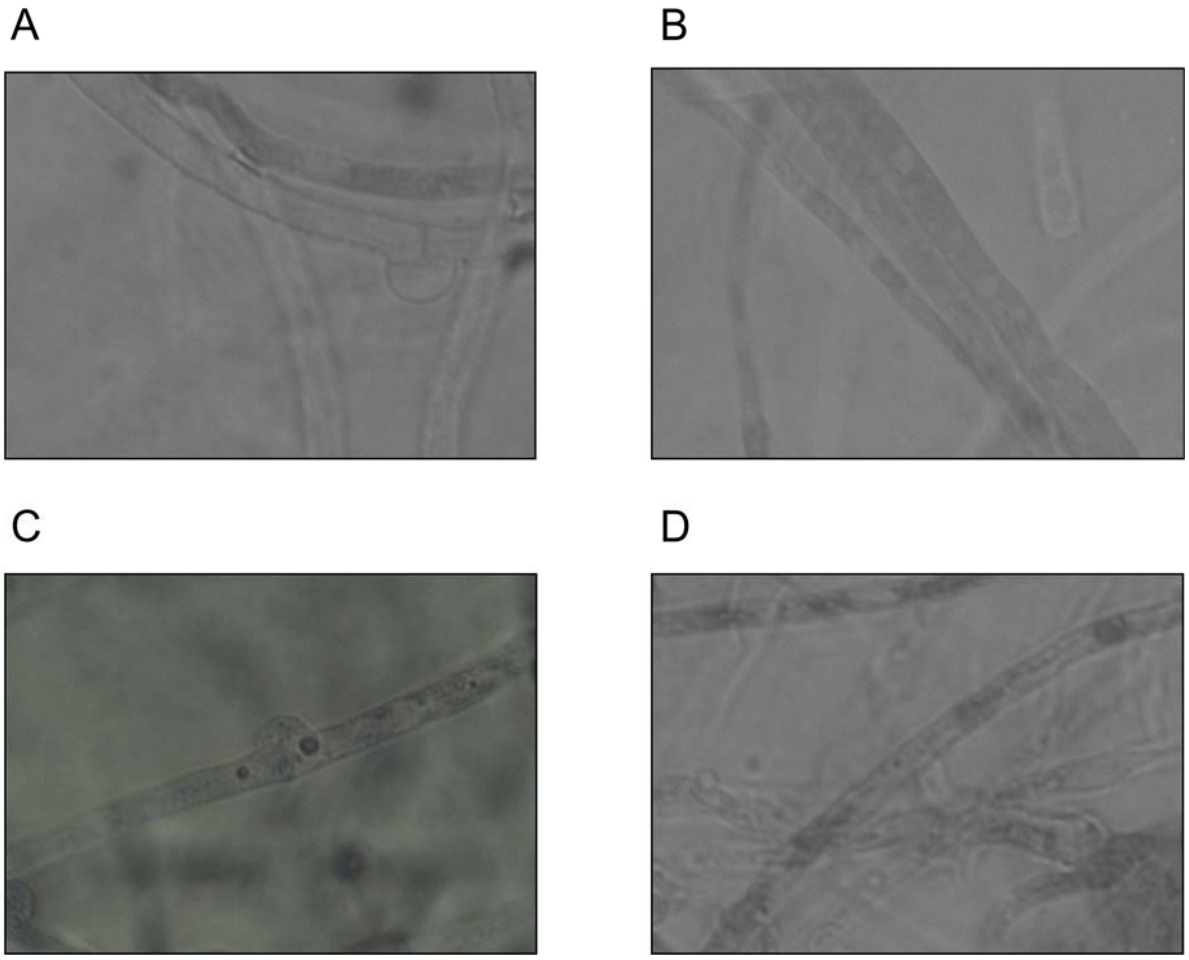

Figure 3. Microscopic characteristic of compatible and incompatible interactions. A smaller proportion of hyphae of heterokaryons involved in a compatible interaction were stained with Evans blue (**A**), than the proportion of hyphae of heterokaryons involved in a compatible interaction (**B**). The nuclei of heterokaryons involved in a compatible interaction stained with Giemsa stain was compacted (**C**), while the nuclei of heterokaryons involved in a compatible interaction stained with Giemsa stain was diffused (**D**).

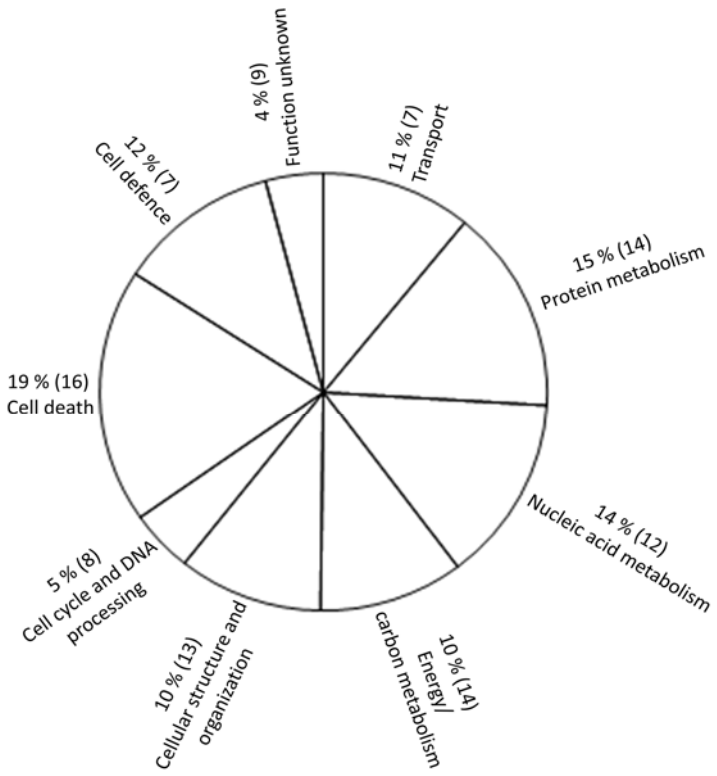

Figure 4. Distribution of the putative functions of the identified contigs and singletons as a percentage of the total number (indicated in brackets) and the ESTs as a percentage of the total number that comprise the contigs in that category. Functional categories were identified using Gene Ontology annotations (http://www.geneontology.org/).

.

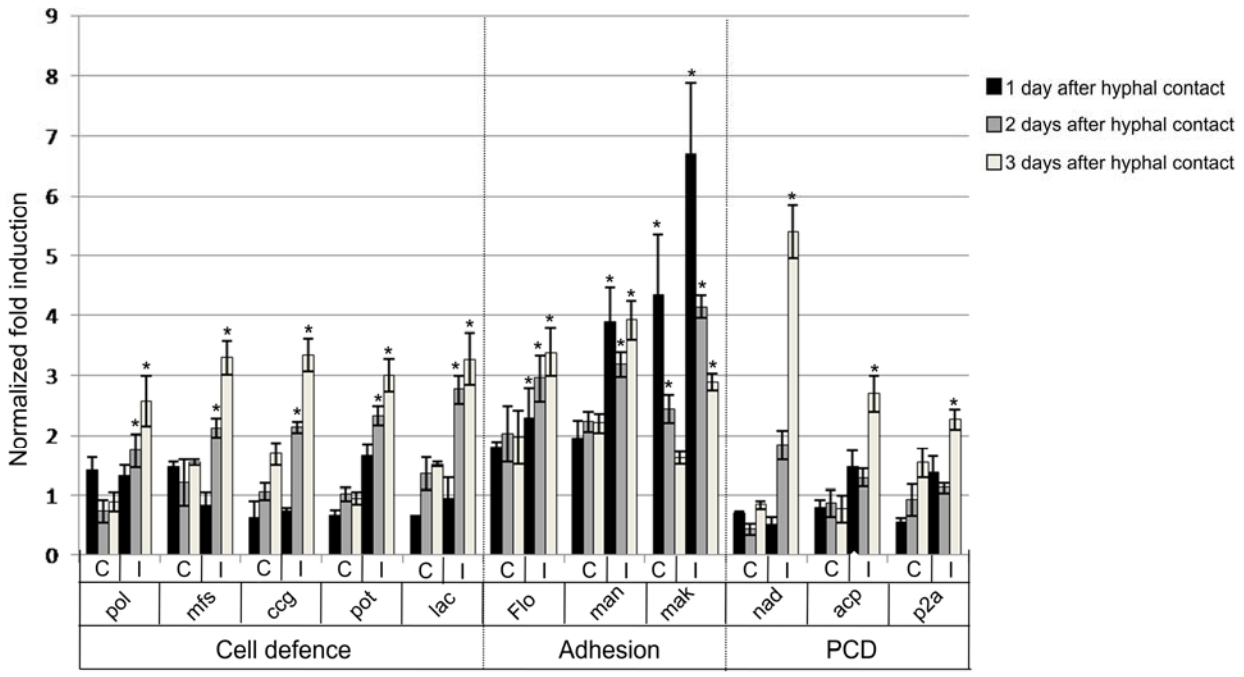

Figure 5. Comparison of gene expression during vegetative incompatibility at different time intervals. Data are compared by one-way analysis of variance. Gene expressions during vegetative incompatibility are expressed as the ratio to the average expression of the control group (no reaction) as determined using the method that implemented efficiency correction (Pfaffl 2001). Error bars denote SDs. C indicate compatible reactions, while I indicate incompatible reactions. Pol, polyubiquitin; Mfs, Mfs1.1; Ccg, trehalose synthase (clock control gene); Pot, polyphenol oxydease (tyrosinase); Lac, laccase; Flo, flocculin; Man, mannoprotein; Mak, map kinase; NAD, NADH-quinone oxidoreductase; ACP, ADP/ATP carrier protein; P2A, heterotrimeric protein phosphatase 2A.

Figure 6. Proposed model for a vegetatively incompatible interaction in *A. areolatum*. It is still not exactly clear which processes associated with vegetative incompatibility are influenced by the MAPK, cAMP-PKA and TOR signalling pathways (indicated by the dotted line).

TABLES

Table 1. List of the primers used for real-time quantitative qRT-PCR.

Putative function	Primer	Sequence 5'to 3'	%PCR efficiency [a]
18S	18S-F 18S-R	ACT GAC AGA GCC AGC GAG TT GTA CAA AGG GCA GGG ACG TA	95
Laccase	LAC-F LAC-R	GGC AGG TAC GCA TTC TTG AT CCG CTC GTC CCT ACT TAC AT	98
Flocullin	FLO-F FLO-R	CAA TGG ACG ATA TGC TGA CG CGA CTC GTA GGG GTC ATA GC	98
ADP/ATP carrier protein	ACP-F ACP-R	CAA GAA GAC CCT CGC TTC TG CAA GAA GGA TGC GAA GAA GG	100
Phosphatase 2A	P2A-F P2A-R	GTA CCA ACC CAA CCT TGA CG TCG GAT CCT TCT TGT CGA AC	96
Polyubiquitin	POL-F POL-R	GGG CAG GTA CAG TCT CCT CA GGA CCA GCA ACG TCT CAT TT	100
MAP kinase	MAK-F MAK-R	CAT CCT TGC TGA GAT GCT GA TGG GGA ACG AAG AGA GAG AA	99
Mannoprotein	MAN-F MAN-R	GTA CTT GGA CGG GCA GTT GT GAG GTA CTC GTC CGC CTT C	100
Mfs1.1	MFS-F MFS-R	TAG GGA ACT GCG TCG CTA TC ACC GGC CCC AGA ACT ATA TC	97
Polyphenol oxidase (tyrosinase)	POT-F POT-R	TCA CCC TCT CTC CTT CTC CA GTA GGT GAT GCG GGA GGT AA	85
Trehalose synthase	CCG-F CCG-R	CGA GGT ACA GGT CGA ACA GA AAC TCA AAG ATT GCC CTC CA	85
NADH quinone oxidoreductase	NAD-F NAD-R	CAA GGA GAA ATA CCC CAT CC GAC GAA AAT TCC AGC GAA CT	87

[a] The efficiency of PCRs was determined the LightCycler 480 Relative Quantification Software (Roche Diagnostics).

Table 2. Some of the genes that were up-regulated during vegetative incompatible interactions associated with hyphal anastomosis, stress and defence response, PCD and signalling in *A. areolatum*.

Contig information		BLAST information[a]				Gene Ontology[b]
Size (bp)	**Number of reads**	**Annotation**	**Species**	**GenBank accession no.**	***e*-value**	**Functional category**
			HYPHAL ANASTNOMOSIS			
264	1	UTP-glucose-1-phosphate uridylyltransferase	*Aedes aegypti*	XP_001651137.1	1e-04	Protein amino acid glycosylation, GO:0006486
243	2	Major Facilitator Superfamily (Mfs) transport monocarboxylase	*Neosartorya fischer*	XP_001258699.1	1e-13	Carbohydrate metabolic process, GO:0006810
437 210	7 2	Mucin (*Trichomonas vaginalis*) Mucin 5, subtypes A and C and Flocculin	*Mus musculus* *Saccharomyces cerevisiae*	XP_001330599.1 NP_034974.1 ABS87372.1	0.027 1e-02 2e-02	Cell adhesion, GO:0007155 Cell adhesion, GO:0007155 Cell-cell adhesion, GO:0016337
210	2	Mannoprotein	*Filobasidiella neoformans*	ABB48433.1	0.075	Agglutination during conjugation with cellular fusion, GO:0000752
			STRESS AND DEFENCE RESPONSE			
430	3	Cytochrome c oxidase subunit III	*Russula rosacea,*	AAD02916.1	4e-44	Mitochondrial electron transport, GO:0022900
259	1	2-Nitropropane dioxygenase	*Filobasidiella neoformans*	XP_572051.1	6e-18	Nitrogen compound metabolic process, GO:0006807
276	1	Vacuolar protein ATPases	*Aedes aegypti*	XP_001657344.1	8e-14	Proton transport, GO:0015992
239	2	Plasma membrane H+-transporting ATPase	*Laccaria bicolour*	XP_001885558.1	3e-18	Proton transport, GO:0015992
203	2	Heat induce catalyse (CAT1)	*Pleurotus sajor-caju,*	AF286097_1	2e-18	Oxygen and reactive oxygen species metabolic process, GO:0006800
261	1	Phenoloxidase (laccase)	*Pleurotus ostreatus*	CAR48257.1	7e-22	Defence response, GO:0006952
167	1	Phenoloxidase (tyrosinase)	*Agaricus bisporus*	CAA59432.1	3e-05	Defence response, GO:0006952
113	1	COP9 signalosome complex subunit 7	*Aedes aegypti*	XP_001649790.1	4e-06	Regulation of proteasomal ubiquitin-dependent protein catabolic process, GO:0032434
240	2	Aryl-alcohol dehydrogenase (AAD)	*Filobasidiella neoforman*	XP_567886.1	5e-06	Autophagy response to toxin, GO:0006914
254 254	2 2	DNA ligase 4	*Laccaria bicolour*	XP_001874645 XP_001874645	4e-07 8e-15	DNA ligation during DNA recombination and repair, GO:0051103 DNA ligation during DNA recombination and repair, GO:0051103
251	2	Trehalose synthase	*Grifola frondosa*	BAA31349.1	1e-32	Response to desiccation, GO:0009269

448	12	Gata-binding protein 4	*Nasonia vitripennis*	XP_001607828	2e-19	Regulation of transcription, GO:0006355
394 256	15 1	Polyubiquitin	*Sclerotinia sclerotiorum*	XP_001598085.1 XP_001598085.1	1e-43 6e-36	Ubiquitin-dependent protein catabolic process, GO:0016567 Ubiquitin-dependent protein catabolic process, GO:0016567
249 263	1 1	NAD binding dehydrogenase family protein	*Schizosaccharomyces pombe*	NP_593960.1 NP_596018.1	6e-10 6e-18	Cellular response to stress, GO:0033554 Cellular response to stress, GO:0033554
216	20	Mfs1.1 (Major Facilitator Superfamily)	*Coprinus cinereus*	AAF01426.1	6e-07	Transport, GO:0006810; Response to cAMP, GO:0051591
PROGRAM CELL DEATH						
252	1	Coatomer alpha-subunit	*Apis mellifera*	XP_623198.1	4e-35	Intra-Golgi vesicle-mediated transport, GO:0006891
248	1	SFT2 like protein (snare like protein)	*Ostreococcus tauri*	CAL51925.1	3e-10	Golgi to endosome transport, GO:0006895
244	1	Sec10 secretory protein	*Aedes aegypti*	XP_001650302.1	6e-18	Vesicle fusion during extra-cellular transport, GO:0006906
278	5	Myotubularin related protein	*Apis mellifera*	XP_623157.1	4e-09	Protein amino acid dephosphorylation, GO:0006470
264	2	Casein kinase II (alpha subunit)	*Aspergillus fumigatus*	XP_747287.1	2e-17	Flocculation, GO:0000501
260	1	Autophagy-linked FYVE protein (ALFY)	*Homo sapiens*	AAN15137.1	6e-05	Unknown
275 286	4 4	NADH-quinone oxidoreductase	*Gloeophyllum trabeum*	AAQ24589.1 AAQ24589.1	9e-27 7e-20	Induction of apoptosis, GO:0043065
298	2	Cytochrome c oxidase subunit II	*Tilletia indica*	YP_001492844.1	2e-06	Mitochondrial electron transport, GO:0006123
430	3	Cytochrome c oxidase subunit III	*Russula rosacea*	AAD02916.1	4e-44	Mitochondrial electron transport, GO:0022900
236	1	Ubiquitin activating enzyme E1	*Coccidioides immitis*	XP_001246521.1	1e-11	Cell death, GO:0008219
249	1	Mitochondrial import inner membrane translocase subunit 8 (Tim8)	*Arabidopsis thaliana*	NP_199894.1	6e-07	Mediates import and insertion of mitochondrial membrane proteins, GO:0008565
322	3	ADP/ATP carrier protein (AAC)	*Neosartorya fischeri*	XP_001265129.1	8e-41	ADT:ATP transport, GO:0015866
251	1	Serine/theorine-protein kinase (TAO1)	*Culex quinquefasciatus*	XP_001864007.1	4e-08	Defence response, GO:0006952
SIGNALLING						
267	1	Formin 3	*Tribolium castaneum*	XP_970252.2	3e-13	Establishment or maintenance of cell polarity, GO:0007163
258	1	MAP kinase *(Pmk1)*	*Magnaporthe grisea*	AAC49521.2	3e-22	Signal transduction during conjugation with cellular fusion, GO:0000750
260	1	Myocardin related transcriptional	*Tribolium castaneum*	XP_973061.2	9e-06	Actin cytoskeleton organization,

		factor				GO:0030036
262	1	Ceramide synthase (Sphingosine N-acyltransferase)	*Cryptococcus neoformans*	XP571121.1	9e-17	Ceramide biosynthetic process, GO:0046513
268	1	Similar to Serine/threonine protein phosphatase 2A (P2A)	*Botryotinia fuckeliana*	XP_001553716.1	0.86	Cell cycle arrest, GO:0007050
307	2	Nascent polypeptide associate complex subunit alpha	*Melampsora medusae*	NP_001040365.1	8e-09	Translation, GO:0006412

[a] Database similarity identified using BLASTX (Altschul et al., 1990).

[b] Functional categories identified using Gene Ontology annotations (http://www.geneontology.org/).

SUPPLEMENTARY MATERIAL

Table 1. Genes that were up-regulated during vegetatively incompatible interactions in *A. areolatum* 3 days after hyphal contact.

CONTIG INFORMATION			BLASTX INFORMATION [a]			GENE ONTOLOGY	
Contig number[b]	**Size (bp)**	**Read identity**	**Annotation**	**GenBank accession no.**	**E-value**	**Functional category[c]**	***Het* related function and reference[d]**
TRANSPORT							
-	248	003025_2651_0882	Membrane protein in ER to Golgi (SFT2 like protein) (snare like protein) (*Ostreococcus tauri*)	CAL51925.1	3e-10	Golgi to endosome transport, GO:0006895	TOR signalling, autophagy and stress response (Singh and Tyers, 2009)
-	249	002899_2739_2307	Mitochondrial import inner membrane translocase subunit 8 (Tim8) (*Arabidopsis thaliana*)	NP_199894.1	6e-07	Mediates import and insertion of mitochondrial membrane proteins, GO:0008565	PCD (Lohret et al., 1997; Paschen et al., 2000)
-	252	001256_2710_0660	Coatomer alpha-subunit (*Apis mellifera*)	XP_623198.1	4e-35	Intra-Golgi vesicle-mediated transport, GO:0006891	Autophagy (Ishihara et al., 2001)
-	244	001740_2728_0448	Sec10 secretory protein (*Aedes aegypti*)	XP_001650302.1	6e-18	Vesicle fusion during extra-cellular transport, GO:0006906	Autophagy (Ishihara et al., 2001)
Contig 69	218	001107_2736_0895; 014033_2736_0898	Gamma-aminobutyrate receptor a beta subunit 1, 2 and 3 (GABA-gated ion channel) (*Apis mellifera*)	NP_001103251.1	6e-04	Chloride transport, GO:0006821; Gamma-aminobutyrate signaling, GO:0007214	Stress response (Martijena et al., 1997)
Contig 3	216	013828_2739_2074; 000058_2665_1344; 000162_2677_3263; 003874_2623_1316; 011666_2657_3404; 014016_2646_0876; 013911_2626_2345; 013281_2683_2104; 002811_2612_3414; 001678_2659_2267; 001294_2657_1329; 000946_2681_2106; 000717_2739_2071; 000684_2692_2044; 000575_2654_2503; 000532_2648_0878; 000453_2628_2347;	Mfs1.1 (Major Facilitator Superfamily) (*Coprinus cinereus*)	AAF01426.1	6e-07	Transport, GO:0006810; Response to cAMP, GO:0051591	Signalling (Hewald et al., 2006)

		000128_2628_1380; 000117_2685_0962; 014098_2668_1344					
METABOLISM							
PROTEIN SYNTHESIS							
Contig 143	307	006001_2718_2352; 003825_2639_2296	Nascent polypeptide associate complex subunit alpha (*Melampsora medusae*)	NP_001040365.1	8e-09	Translation, GO:0006412	PCD (Hotokezaka et al., 2009)
-	125	004034_2708_0348	Zinc finger protein (*Apis mellifera*)	XP_001121352.1	9e-06	rRNA metabolic process, GO:0016072; ribosome biogenesis, GO:0042254	Stress response (Davletova et al., 2005)
-	270	000400_2685_0374	UTP14 small nuclear ribonucleoprotein (*Gallus gallus*)	XP_420142.2	5e-12	Maturation of SSU-rRNA, GO:0030490	
Contig 154	229 102	006803_2736_2199; 000301_2679_0316; 011610_2666_3087; 010808_2704_3570	Elongation factor 3 (*Cryptococcus neoformans*) Elongation factor 3 (*Cryptococcus neoformans*)	XP_570261.1 XP_570261.1	1e-17 2e-04 1-32	Translational elongation, GO:0006414	Stress response (Begley et al., 2007)
Contig 132	274	005229_2731_0348; 006355_2737_0924; 007666_2731_3111; 007516_2605_0729; 008494_2695_1428; 002712_2689_1076	Translation initiation factor (eIF1) SUI1 (*Aspergillus niger*)	XP_001270644.1	1e-11	Ribosome biogenesis, GO:0042254	Stress response (Ptushkina et al., 2004)
Contig 156	169	007106_2645_1094; 010806_2624_1601	40S ribosomal protein S23 (*Cryptococcus neoformans*)	XP_572112.1	4e-23	Translation, GO:0006412	Defence response (Morissette et al., 2008)
-	256	004732_2627_0870	WD-repeat containing protein (Dip2/UTP12 small nuclear ribonucleoprotein) (*Cryptococcus neoformans*)	XP_568060.1	2e-11	rRNA processing, GO:0000462	
PROTEIN DEGRADATION							
Contig 170	328	009400_2631_3429; 004629_2635_1235	L-amino-acid amidase (*Pseudomonas syringae*)	YP_276357.1	2e-10	Metabolic process, GO:0008152	
Contig 12	394	006412_2657_0926; 006716_2729_2155; 000686_2670_0661; 002167_2688_1503; 000182_2732_0374; 011550_2677_0930; 004747_2667_0851; 006870_2660_0902;	Polyubiquitin (*Sclerotinia sclerotiorum*)	XP_001598085.1	1e-43	Ubiquitin-dependent protein catabolic process, GO:0016567	Stress and defence response (Hanna et al., 2007)

-	256	008183_2700_0708; 000569_2637_1178; 013622_2693_3368; 001305_2695_3370; 001242_2736_2627; 014409_2635_1176; 002917_2692_0725	Polyubiquitin (*Sclerotinia sclerotiorum*)	XP_001598085.1	6e-36		
-	113	012419_2722_1099	COP9 signalosome complex subunit 7 (*Aedes aegypti*)	XP_001649790.1	4e-06	Regulation of proteasomal ubiquitin-dependent protein catabolic process, GO:0032434	PCD (da Silva et al., 2007)
-	258	003136_2729_0989	Peptidase (*Nasonia vitripennis*)	XP_001599321.1	3e-08	Protein metabolism, GO:0044248	Defence response (Williams et al., 2003)
-	250	008487_2628_2094	Peptidase MM2 (glycoprotease) (*Medicago truncatula*)	ABD33122.2	4e-05	Proteolysis, GO:0006508	Cell adhesion (Yeo et al., 1994)
NUCLEIC ACID METABOLISM							
NUCLEIC ACID DEGRADATION							
-	185	000619_2713_1533	Exonuclease 1 (*Culex quinquefasciatus*)	XP_001843211.1	8e-10	Nucleobase, nucleoside, nucleotide and nucleic acid metabolic process, GO:0006139	Defence response (Nimonkara et al., 2008)
TRANSCRIPTIONAL FACTOR							
-	242	002817_2622_0602	Winged helix transcriptional factors (*Tribolium castaneum*)	NP_524542.1	5e-28	Regulation of transcription, GO:0000122	Stress response (Zinke et al., 2002)
Contig 120	448	004143_2650_1139; 001664_2728_0347; 001151_2657_2094; 001722_2619_0568; 001786_2673_1129; 002932_2693_0747; 002924_2690_0844; 001947_2727_0397; 001348_2717_0941; 006225_2653_2964; 001231_2610_3045; 001418_2636_1848	Gata-binding protein 4; zinc finger DNA binding domain (*Nasonia vitripennis*)	XP_001607828	2e-19	Regulation of transcription, GO:0006355	Stress response (Hardwick et al., 1999)
Contig 135	251 239	008687_2648_3683; 005500_2639_0379; 000523_2653_0357	Gag-like zinc-finger protein (*Drosophila mercatorum*) Gag-like zinc-finger protein (*Drosophila mercatorum*)	AAB94026.1 ABB94026.1	9e-05 3e-13	Nucleic acid metabolism, GO:0045449	
Contig 150	409	006513_2681_3214;	Histone H2B.1	XP_001832379.1	1e-13	Nucleic acid	PCD (Ahn et al., 2005)

		010191_2635_2232; 008381_2692_3244; 009137_2650_1841; 006483_2745_2706	(*Coprinopsis cinerea*)			metabolism, GO:0006334	
TRANSPOSABLE ELEMENTS							
Contig 78	373	014244_2705_0426; 001515_2707_0428; 001095_2723_3125; 006553_2734_1683; 000715_2631_0613; 003224_2724_0803	Reverse transcriptase (*Drosophila neotestacea*)	AAA30338.1	2e-23	Nucleic metabolism, GO:0006278	
Contig 187	292	012717_2595_0299; 005775_2720_3056; 006076_2598_0387	Reverse transcriptase (*Drosophila neotestacea*)	AAF75684.1	8e-07	Nucleic metabolism, GO:0006278	
-	258	000476_2633_0339;	Reverse transcriptase (*Drosophila mercatorum*)	AAB94027.1	5e-16	Nucleic metabolism, GO:0006278	
-	239	010851_2700_2553	LreO3 reverse transcriptase (*Danio rerio*)	XP_697813.3	8e-10	Nucleic metabolism, GO:0006278	
ENERGY/CARBON METABOLISM							
AMINO ACID							
Contig 22	261	000373_2620_0496; 012825_2622_0498	Decarboxylase group II (*Nasonia vitripennis*)	XP_001604406.1	3e-07	Metabolism, GO:0006519	Stress response (Akiyama and Jin, 2007)
SUGAR/GLYCOLYSIS							
Contig 28	243	000421_2722_0327; 004479_2646_1639	Major Facilitator Superfamily (Mfs) transport monocarboxylase (permease) (*Neosartorya fischeri*)	XP_001258699.1	1e-13	Carbohydrate metabolic process, GO:0006810	Stress response (Hahn et al., 2006)
NITROGEN							
-	259	011503_2612_1988	2-Nitropropane dioxygenase (NPD) (*Cryptococcus neoformans*)	XP_572051.1	6e-18	(Nitrogen compound metabolic process, GO:0006807	Stress response (Dowd et al., 2004)
LIPID/FATTY ACID/STEROL							
-	255	000725_2722_0448	Low-density lipoprotein receptor (*Bombyx mori*)	NP_001116809.1	4e-13	Lipid metabolic process, GO:0006629	
CARBON METABOLISM							
Contig 186	340	012350_2744_2132; 006724_2668_1843; 004213_2667_0835; 004420_2650_1233	Hydroxymethylglutaryl-CoA synthase (*Cryptococcus neoformans*)	XP_569805.1	3e-23	Isopentenyl diphosphate biosynthetic process, GO:0019287	
ENERGY/TCA CYCLE							
Contig 136	298	005527_2740_2768; 011750_2691_2374	Cytochrome c oxidase subunit II (COX2) (*Tilletia indica*)	YP_001492844.1	2e-06	Mitochondrial electron transport, GO:0006123	Stress response and PCD (Hsu et al., 2008)
-	276	000770_2671_0491	Vacuolar protein ATPases (*Aedes*	XP_001657344.1	8e-14	Proton transport,	Stress response and

			aegypti)			GO:0015992	PCD (Byun et al., 2007)
Contig 83	239	001745_2639_1424; 003731_2660_2125	Plasma membrane H+-transporting ATPase (*Laccaria bicolour*)	XP_001885558.1	3e-18	Proton transport, GO:0015992	Stress response and PCD (Piper et al., 1997)
Contig 102	322	002701_2683_0887; 003253_2643_1076; 005701_2735_2790	ADP/ATP carrier protein (*Neosartorya fischeri*)	XP_001265129.1	8e-41	ADT:ATP transport, GO:0015866	PCD (Vercesi et al., 1997)
Contig 122	265	010703_2610_3504; 004230_2652_1209	ATP synthase subunit 4 (*Ajellomyces capsulatus*)	XP_001542657.1	3e-12	Proton transport, GO:0015992	PCD (Crompton, 1999)
Contig 177	244	010461_2644_1664; 002671_2708_1386	Aldo/keto reductase protein (*Arabidopsis thaliana*)	NP_176267.3	1e-06	Carbohydrate metabolic process, GO:0005975	Defence response (Jin and Penning, 2007)
-	283	007217_2669_1772	Apocytochrome b (*Schizophyllum commune*)	NP_150121.1	8e-28	Mitochondrial respiratory chain complex III, GO:0005750 :	PCD (Kroemer et al., 1998)
-	262	007568_2720_1307	Sphingosine N-acyltransferase (*Cryptococcus neoformans*)	XP571121.1	9e-17	Ceramide biosynthetic process, GO:0046513	PCD (Mathias et al., 1997)
Contig 181	430	010784_2689_3799; 012978_2702_2933; 009665_2674_2912	Cytochrome c oxidase subunit III (*Russula rosacea*)	AAD02916.1	4e-44	Mitochondrial electron transport, GO:0022900	Stress response and PCD (Chandel et al., 2000)
CELLULAR STRUCTURE AND ORGANIZATION							
-	233	000704_2620_0557	Odd oz protein (Teneurin) (*Nasonia vitripennis*)	XP_001605548.1	6e-34	Cell adhesion (Regulation of cell shape), GO:0007155	Cell adhesion (Ben-Zur et al., 2000)
Contig 8	78	000150_2709_1332; 014530_2709_1335	Glycosyltransferase (*Haemophilus influenzae*)	NP-438427.1	7e-05	Cell wall biosynthesis (Glycoprotein biosynthesis), GO:0008150	Cell adhesion (Hewald et al., 2006)
-	260	005789_2699_1674	Myocardin related transcriptional factor (*Tribolium castaneum*)	XP_973061.2	9e-06	Actin cytoskeleton organization, GO:0030036	Stress response (Parmacek, 2007)
-	221	006923_2686_1598	Metaxin (*Apis mellifera*)	XP_393141.2	9e-33	Outer mitochondrial membrane organization, GO:0007008	Stress response (Zhang et al., 2008)
-	267	003753_2718_1771	Formin 3 (*Tribolium castaneum*)	XP_970252.2	3e-13	Establishment or maintenance of cell polarity, GO:0007163	Cell dhesion (Gomez et al., 2007)
Contig 140	239	005830_2654_3396; 008527_2641_1018; 008573_2732_1757; 009542_2741_1783	WD-repeat protein (RiB40) (*Cryptococcus neoformans*)	XP_568060.1	4e-04	Mycelium development, GO:0043581	
Contig 149	264	006351_2741_1574; 012135_2627_1781	Casein kinase II (alpha subunit) (*Aspergillus fumigatus*)	XP_747287.1	2e-17	Flocculation, GO:0000501	Cell adhesion (Chaar et al., 2006)
Contig 81	210	001725_2685_0869; 003769_2665_3387	Mannoprotein (*Filobasidiella neoformans*)	ABB48433.1	0.075	Agglutination during conjugation with	Cell adhesion (Fukazawa and Kagaya,

						cellular fusion, GO:0000752	1997)
-	258	012398_2686_1472	MAP kinase (mitogen-activated protein) (*Phycomyces blakesleeanus*)	ABB77843.1	4e-23	Signal transduction during conjugation with cellular fusion, GO:0000750	Signalling (Xu, 2000)
Contig 24 Contig 168 & 171	230 437	000383_2693_0314; 000767_2716_0549 006990_2706_2271; 009524_2708_1493; 014610_2606_3077; 009182_2686_2661; 009491_2736_1926	Mucin (*Trichomonas vaginalis*) Mucin 5, subtypes A and C (*Mus musculus*) also Flocculin (*Saccharomyces cerevisiae*)	XP_001330599.1 NP_034974.1 ABS87372.1	0.027 1e-02 2e-02	Cell adhesion, GO:0007155 Cell adhesion, GO:0007155 Cell-cell adhesion, GO:0016337	Cell adhesion (Verstrepen and Klis, 2006)
CELL CYCLE & DNA PROCESSING							
-	268	013349_2602_0722	Hypothetical protein similar to Serine/threonine protein phosphatase 2A regulatory B-subunit (*Botryotinia fuckeliana*)	XP_001553716.1	0.86	Cell cycle arrest, GO:0007050	Stress and defence response (Erental et al., 2007)
-	179	000658_2602_0448	Encore protein (*Nasonia vitripennis*)	XP_001607517.1	5e-09	Mitosis, GO:0007067	
-	262	005069_2663_1860	GTP-binding protein (RAN GTPase; Spi1) (*Coprinopsis cinerea*)	XP_001833111.1	6e-36	Cell mitotic cycle, GO:0007346	
Contig 124	278	000129_2726_0368; 004260_2687_1682; 004391_2709_0397; 001265_2657_0378; 000133_2685_0345	Myotubularin related protein 2 (*Apis mellifera*)	XP_623157.1	4e-09	Protein amino acid dephosphorylation, GO:0006470	Autophagy (Lorenzo et al., 2005)
-	199	005588_2598_0337	Enhancer of polycomb (*Apis mellifera*)	XP_001606623.1	5e-10	Establishment or maintenance of chromatin architecture, GO:0006325	
-	257	000937_2704_0657	Similar to RNA-binding protein EWS (Ewing sarcoma breakpoint region 1) (*Canis familiaris*)	XP_857966.1	4e-06	Mitosis, GO:0007067	
-	257	011410_2622_2662	Histone 3 (*Laccaria bicolour*)	XP_001873642.1	6e-36	Chromatin assembly or disassembly, GO:0006333	
CELL DEFENCE							
-	254	011280_2618_3291;	DNA ligase 4	XP_001874645	4e-07	DNA ligation during	Stress response (Ma et

			(*Laccaria bicolour*)			DNA recombination and repair, GO:0051103	al., 2005)
	254	004498_2643_2165	DNA ligase 4 (*Laccaria bicolor*)	XP_001874645	8e-15		
-	278	002516_2658_3158	Neurofibromin 1 (*Nasonia vitripennis*)	XP_001602698.1	2e-22	Response to stress, GO:0006950	Cell defence (Tong et al., 2007)
Contig 95	203	002284_2630_2426; 003603_2710_0950	Heat induce catalyse (peroxisomal catalyse, CAT1) (*Pleurotus sajor-caju*)	AF286097_1	2e-18	Oxygen and reactive oxygen species metabolic process, GO:0006800	Cell defence (Wang et al., 2007)
Contig 96	251	002315_2710_3783; 007216_2703_2825	Trehalose synthase (clock control gene) (*Grifola frondosa*)	BAA31349.1	1e-32	Response to desiccation, GO:0009269	Cell defence (Tao et al., 2008)
-	264	010656_2632_3545	UDP-glucose pyrophosphorylase (UTP-glucose-1-phosphate uridylyltransferase) (*Aedes aegypti*)	XP_001651137.1	1e-04	Response to salt stress, GO:0009651	Stress response (Yan et al., 2005)
-	251	009112_2714_1304	Serine/theorine-protein kinase (TAO1) (*Culex quinquefasciatus*)	XP_001864007.1	4e-08	Defence response, GO:0006952	Cell defence (Johne et al., 2008)
-	259	012330_2646_1826;	Short chain dehydrogenase (*Schizosaccharomyces pombe*)	NP_587784.1	4e-07	Cellular response to stress, GO:0033554	Cell defence (Belyaeva et al., 2008)
-	208	011627_2691_0365	Short chain dehydrogenase (*Aedes aegypti*)	XP_001651898.1	4e-04		
Contig 103	354	002734_2705_1026; 008297_2663_2382; 008056_2627_2575; 008949_2637_1205; 009249_2660_2731; 011019_2634_3581; 010935_2614_2799; 011577_2711_2737; 011691_2689_2915	Heat-shock protein (Hsp30) (*Pichia stipitis*)	XP_001384623.2	0.009	Stress response, GO:0006950	Cell defence and stress response (Piper et al., 1997)
-	261	009044_2743_3237	Phenoloxidase (laccase) (*Pleurotus ostreatus*)	CAR48257.1	7e-22	Defence response, GO:0006952	Cell defence (Iakovlev and Stenlid, 2000)
-	249	001247_2660_1005	Importin alpha subunit (*Cryptococcus neoformans*)	XP_570493.1	0.002	Response to stress, GO:0033554; Regulate cell cell cycle, GO:0000087	PCD (Faustino et al., 2008)
Contig 19	357	000285_2603_0341; 014020_2605_0343; 011354_2682_0602	T-cell receptor beta chain (*Brugia malayi*)	XP_001900795.1	5e-04	Cellular defence response, GO:0006968	
-	167	005379_2717_0698	Phenoloxidase (tyrosinase) (*Agaricus bisporus*)	CAA59432.1	3e-05	Defence response, GO:0006952	Cell defence (Score et al., 1997)
-	249	004562_2706_0605;	NAD binding dehydrogenase	NP_593960.1	6e-10	Cellular response to	

-	263	009404_2679_3082	family protein (*Schizosaccharomyces pombe*) NAD binding dehydrogenase family protein (*Schizosaccharomyces pombe*)	NP_596018.1	6e-18	stress, GO:0033554	
CELL DEATH							
Contig 67	476	010855_2690_3434; 010240_2620_0268; 001094_2731_0351; 009704_2683_2835; 009480_2622_1895; 007598_2736_2179; 009913_2636_2280; 011423_2610_1007; 005344_2619_1363;	Elongation factor 1-alpha (EEF1A1) (*Schizophyllum commune*)	CAA64399.1	8e-31	Anti-apoptosis, GO:0006916	PCD (Borradaile et al., 2006)
Contig 113	317	003728_2739_1996; 004648_2627_2524; 012754_2727_3188; 003661_2697_3374; 008943_2618_3316; 006974_2636_3492; 009085_2707_0893; 007089_2663_0790; 009424_2727_2357; 004660_2725_3493; 004902_2704_0925; 010296_2613_1532; 007116_2678_2350; 010532_2649_1922; 010560_2736_2556; 004689_2740_2016; 010401_2640_3288; 005676_2665_2715; 014600_2663_2713; 002635_2724_1076; 003247_2662_2362; 010002_2659_3543	Elongation factor -1 alpha (*Hebeloma cylindrosporum*)	AAQ90154.1	8e-07		
Contig 173	240	011988_2615_2744; 009959_2691_1668	Aryl-alcohol dehydrogenase (*Cryptococcus neoformans*)	XP_567886.1	5e-06	Autophagy response to toxin, GO:0006914	Stress response (Matsuzaki et al., 2008)
-	236	003782_2639_1145	Ubiquitin activating enzyme E1 (*Coccidioides immitis*)	XP_001246521.1	1e-11	Cell death, GO:0008219	PCD (Egger et al., 2007)
Contig 123	275	013325_2609_0756; 012386_2717_2142;	NADH-quinone oxidoreductase (*Gloeophyllum trabeum*)	AAQ24589.1	9e-27	Induction of apoptosis, GO:0043065	PCD (Gong et al., 2007)

Contig 130	286	004259_2715_2144; 011174_2637_1381; 004855_2740_2143; 014641_2738_2141; 008143_2716_1029; 002003_2645_2148	NADH-quinone oxidoreductase (*Gloeophyllum trabeum*)	AAQ24589.1	7e-20		
Contig 185	269	011340_2736_3002; 012032_2734_3561	Cap binding protein (eIF4E) (*Agaricus bisporus*)	AAM89495.1	7e-19	Autophagic cell death, GO:0048102	PCD (Othumpangat et al., 2005; Jacobson et al., 2006)
	240	000423_2648_2006	Activin receptor type 1 Saxophone protein (*Nasonia vitripennis*)	XP_001603482.1	7e-30	Regulation of apoptosis, GO:0043066	PCD (van der Zee et al., 2008)
FUNCTION UNKOWN							
Contig 114	167	003745_2664_2279; 007414_2667_2725; 013651_2665_2727	GTP-binding protein EngA (*Erythrobacter* sp.)	ZP_01864806.1	1e-15	Unkown	
Contig 121	305	013870_2665_1067; 009794_2676_2306; 004169_2616_2665; 010300_2638_0663; 004597_2671_0714	Extracellular serine-rich protein (*Aspergillus fumigatus*)	XP_754260.1	0.003	Unknown	
-	261	010819_2723_2213	SET domain proteins (protein lysine methyltransferase enzymes) (*Ustilago maydis*)	XP_758615.1	9e-06	Unknown	
-	267	006447_2703_3406	Phospatidylglycerol/phospatidylin ositol transfer protein (pg/pi/tp) (*Saccharomyces cerevisiae*)	EDV08324.1	5e-11	Unknown	Signalling (Li et a., 2000)
-	264	009937_2625_2693	Serine/threonine rich protein (*Aspergillus fumigatus*)	EDP55498.1	3e-05	Unknown	
-	273	012809_2620_2063	Spherulin-1A (*Physarum polycephalum*)	P09350	8e-13	Unknown	
-	291	001374_2657_0892	THiJ/PfpI family protein (*Pyrenophora tritici-repentis*)	XP_001935291.1	6e-13	Unknown	
	273	007556_2674_0876	Pro41 (*Sordaria macrospore*)	CAL68654.1	0.045	Unknown	
-	229	001009_2627_0342	Retrovirus-related Pol polyprotein (*Bradysia coprophila*)	Q03277	8e-09	Unknown	
-	260	002460_2629_0533	WD-repeat & FYVE domain (ALFY - autophagy-linked FYVE protein) (*Homo sapiens*)	AAN15137.1	6e-05	Unknown	Autophagy (Simonsen et al., 2004)

[a] Database similarity identified using BLASTX (Altschul et al., 1990).

[b] Sequences represented by single reads are indicated with hyphens.

[c] Functional categories identified using Gene Ontology annotations (http://www.geneontology.org/).

[d] Respective references are include in list on the next page.

REFERENCES INCLUDED IN SUPPLEMENTARY TABLE 1

Ahn, S.-H., Cheung, W.L., Hsu, J.-Y., Diaz, R.L., Smith, M.M., Allis, C.D., 2005. Sterile 20 kinase phosphorylates histone H2B at serine 10 during hydrogen peroxide-induced apoptosis in *S. cerevisiae.* Cell. 120, 25-36.

Akiyama, T., Jin, S., 2007. Molecular cloning and characterization of an arginine decarboxylase gene up-regulated by chilling stress in rice seedlings. J. Plant Phys. 164, 645-654.

Begley, U., Dyavaiah, M., Patil, A., Rooney, J.P., DiRenzo, D., Young, C.M., Conklin, D.S., Zitomer, R.S., Begley, T.J., 2007. Trm9-catalyzed tRNA modifications link translation to the DNA damage response. Mol. Cell. 28, 860-870.

Belyaeva, O.V., Korkina, O.V., Stetsenko, A.V., Kedishvili, N.Y., 2008. Human retinol dehydrogenase 13 (RDH13) is a mitochondrial short-chain dehydrogenase/reductase with a retinaldehyde reductase activity. FEBS J. 275, 138-147.

Ben-Zur, T., Feige, E., Motro, B., Wides, R., 2000. The mammalian Odz gene family: Homologs of a *Drosophila* pair-rule gene with expression implying distinct yet overlapping developmental roles. Dev. Biol. 217, 107-120.

Borradaile, N.M., Buhman, K.K., Listenberger, L.L., Magee, C.J., Morimoto, E.T.A., Ory, D.S., Schaffer, J.E., 2006. A critical role for Eukaryotic Elongation Factor 1A-1 in lipotoxic cell death. Mol. Biol. Cell. 17, 770-778.

Byun, Y.J., Lee, S-B., Kima, D.J., Lee, H.O., Sona, M.J., Yang, C.W., Sungd, K-W., Kima, H-S., Kwon, O-J., Kima, I-K., Jeong, S-W., 2007. Protective effects of vacuolar H+-ATPase c on hydrogen peroxide-induced cell death in C6 glioma cells. Neurosci. L. 425, 183-187.

Chaar, Z., O' Reilly, P., Gelman, I., Sabourin, L.A., 2006. V-Src-dependent down-regulation of the Ste20-like Kinase SLK by casein kinase II. J. Biol. Chem. 281, 28193-28199.

Chandel, N.S., McClintock, D.S., Feliciano, C.E., Wood, T.M., Melendez, J.A., Rodriguez, A.M., Schumacker, P.T., 2000. Reactive oxygen species generated at mitochondrial complex III stabilize hypoxia-inducible factor-1α during hypoxia a mechanism of O_2 sensing. J. Biol. Chem. 275, 25130-25138.

Crompton, M., 1999. The mitochondrial permeability transition pore and its role in cell death. Biochem. J. 341, 233-249.

da Silva, C.,J., Miranda, Y., Leonard, N., Ulevitch, R.J., 2007. The subunit CSN6 of the COP9 signalosome is cleaved during apoptosis. J. Biol. Chem. 282, 12557-12565.

Davletova, S., Schlauch, K., Coutu, J., Mittler, R., 2005. The Zinc-Finger Protein Zat12 plays a central role in reactive oxygen and abiotic stress signaling in *Arabidopsis*. Plant Physiol. 139, 847-856.

Dowd, C., Wilson, I., W., McFadden, H., 2004. Gene expression profile changes in cotton root and hypocotyl tissues in response to infection with *Fusarium oxysporum* f. sp. *Vasinfectum.* Mol. Plant-Microbe Interact. 17, 654-667.

Egger, L., Madden, D.T., Rhême, C., Rao, R.V., Bredesen, D.E., 2007. Endoplasmic reticulum stress-induced cell death mediated by the proteasome. Cell Death Diff. 14, 1172-1180.

Erental, A., Harel, A., Yarden, O., 2007. Type 2A Phosphoprotein phosphatase is required for asexual development and pathogenesis of *Sclerotinia sclerotiorum.* Mol. Plant-Microbe Interact. 20, 944-954.

Faustino, R.S., Cheung, P., Richard, M.N., Dibrov, E., Kneesch, A.L., Deniset, J.F., Chahine, M.N., Lee, K., Blackwood, D., Pierce, G.N., 2008. Ceramide regulation of nuclear protein import. J. Lipid Res. 49, 654-662.

Fukazawa, Y., Kagaya, K., 1997. Molecular bases of adhesion of *Candida albicans.* J. Med. Vet. Mycol. 35, 87-99.

Gomez, T.S., Kumar, K., Medeiros, R.B., Shimizu, Y., Leibson, P.J., Billadeau, D.D., 2007. Formins regulate the actin-related protein 2/3 complex-independent polarization of the centrosome to the immunological synapse. Immunity. 26, 177-190.

Gong, X., Kole, L., Iskander, K., Jaiswal, A.K., 2007. NRH:Quinone Oxidoreductase 2 and NAD(P)H:Quinone Oxidoreductase 1 protect tumor suppressor p53 against 20S Proteasomal degradation leading to stabilization and activation of p53. Cancer Res. 67, 5380-5388.

Hahn, J.-S., Neef, D.W., Thiele, D.J., 2006. A stress regulatory network for co-ordinated activation of proteasome expression mediated by yeast heat shock transcription factor. Mol. Microbiol. 60, 240-251.

Hanna, J., Meides, A., Zhang, D.P., Finley, D., 2007. A ubiquitin stress response induces altered proteasome composition. Cell. 129, 747-759.

Hardwick, J.S., Kuruvilla, F.G., Tong, J.K., Shamji, A.F., Schreiber, S. L., 1999. Rapamycin-modulated transcription defines the subset of nutrient-sensitive signaling pathways directly controlled by the Tor proteins. Proc. Natl. Acad. Sci. U.S.A. 96, 14866-14870.

Hewald, S., Linne, U., Scherer, M., Marahiel, M.A., Kämper, J., Bölker, M., 2006. Identification of a gene cluster for biosynthesis of mannosylerythritol lipids in the basidiomycetous fungus *Ustilago maydis* Appl. Envir. Microbiol. 72, 5469-5477.

Hotokezaka, Y., van Leyen, K., Lo, E.H., Beatrix, B., Katayama, I., Jin, G., Nakamura, T., 2009. α-NAC depletion as an initiator of ER stress-induced apoptosis in hypoxia. Cell Death Diff. 16, 1505-1514.

Hsu, Y.C., Chou, T.Y., Wang, C.F., Chen, D., Su, C.L., Hu, R.T., 2008. Rat liver ischemia/reperfusion induced proinflammatory mediator and antioxidant expressions analyzed by gene chips and real-time polymerase chain reactions. Transplant. P. 40, 2156-2158.

Iakovlev, A., Stenlid, J., 2000. Spatiotemporal patterns of laccase activity in interacting mycelia of wood-decaying basidiomycete fungi. Microb. Ecol. 39, 236-245**.**

Ishihara, N., Hamasaki, M., Yokota, S., Suzuki, K., Kamada, Y., Kihara, A., Yoshimori, T., Noda, T., Ohsumi. Y., 2001. Autophagosome requires specific early sec proteins for its formation and NSF/SNARE for vacuolar fusion. Mol. Biol. Cell. 12, 3690-3702.

Jacobson, B.A., Alter, M.D., Kratzke, M.G., Frizelle, S.P., Zhang, Y., Peterson, M.S., Avdulov, S., Mohorn, R.P., Whitson, B.A., Bitterman, P.B., Polunovsky, V.A., Kratzke, R.A., 2006. Repression of cap-dependent translation attenuates the transformed phenotype in non-small cell lung cancer both In vitro and In vivo. Cancer Res. 66, 4256-4262.

Jin, Y., Penning, T.M., 2007. Aldo-keto reductases and bioactivation/detoxication. Annu. Rev. Pharmacol. Toxicol. 47, 263-92.

Johne, C., Matenia, D., Li, X.-Y., Timm, T., Balusamy, K., Mandelkow, E.-M., 2008. Spred1 and TESK1—Two new interaction partners of the kinase MARKK/TAO1 that link the microtubule and actin cytoskeleton. Mol. Biol. Cell. 19, 1391-1403.

Kroemer, G., Dallaporta, B., Resche-Rigon, M., 1998. The mitochondrial death/life regulator in apoptosis and necrosis. Annu. Rev. Physiol. 60, 619-42.

Li, X., Xie, Z., Bankaitis, V.A., 2000. Phosphatidylinositol/phosphatidylcholine transfer proteins in yeast. Biochimica et Biophysica Acta. 1486, 55-71.

Lohret, T.A., Jensen, R.E., Kinnally, K.W., 1997. Tim23, a protein import component of the mitochondrial inner membrane, is required for normal activity of the multiple conductance channel. MCC. J. Cell Biol. 137, 377-386.

Lorenzo, O., Urbé, S., Clague, M.J., 2005. Analysis of phosphoinositide binding domain properties within the myotubularin-related protein MTMR3. J. Cell Sci. 118, 2005-2012.

Ma, Y., Haihui, L., Schwarz, K., Lieber, M.R., 2005. Repair of double-strand DNA breaks by the human non-homologous DNA end joining pathway: The Iterative processing model. Cell Cycle. 4, 1193-1200.

Martijena, I.D., Tapia, M., Molina, V.A., 1996. Altered behavioural and neurochemical response to stress in benzodiazepine-withdrawn rats. Brain Res. 712, 239-244.

Mathias, S., Penna, L.A., Kolesnick, R.N., 1998. Signal transduction of stress via ceramide. Biochem. J. 335, 465-480.

Matsuyama, S., Xu, Q., Velours, J., Reed, J.C., 1998. The mitochondrial F0F1-ATPase proton pump is required for function of the proapoptotic protein Bax in yeast and mammalian cells. Mol. Cell. 1, 327-336.

Matsuzaki, F., Shimizu, M., Wariishi, H., 2008. Proteomic and metabolomic analyses of the white-rot fungus *Phanerochaete chrysosporium* exposed to exogenous benzoic acid. J. Proteome Res. 7, 2342-2350.

Morissette, D.C., Dauch, A., Beech, R., Masson, L., Brousseau, R., Jabaji-Hare, S., 2008. Isolation of mycoparasitic-related transcripts by SSH during interaction of the mycoparasite *Stachybotrys elegans* with its host *Rhizoctonia solani*. Curr. Genet. 53, 67-80.

Nimonkara, A.V., Özsoya, A.Z., Genschelb, J., Modrichb, P., Kowalczykowskia, S.C., 2008. Human exonuclease 1 and BLM helicase interact to resect DNA and initiate DNA repair. Proc. Natl. Acad. Sci. U.S.A. 105, 16906-16911.

Othumpangat, S., Kashon, M., Joseph, P., Sodium arsenite-induced inhibition of eukaryotic translation initiation factor 4E (eIF4E) results in cytotoxicity and cell death. Mol. Cell. Biochem. 279, 123-131, 2005.

Parmacek, M.S., 2007. Myocardin-Related Transcription Factors Critical Coactivators Regulating Cardiovascular Development and Adaptation. Circul. Res. DOI: 10.1161/01.RES.0000259563.61091.e8

Paschen, S.A., Rothbauer, U., Káldi, K., Bauer, M.F., Neupert, W., Brunner, M., 2000. The role of the TIM8-13 complex in the import of Tim23 into mitochondria. EMBO J. 19, 6392-6400.

Piper, P.W., Ortiz-Calderon, C., Holyoak, C., Coote, P., Cole, M., 1997. Hsp30, the integral plasma membrane heat shock protein of *Saccharomycescere visiae*, is a stress-inducibleregu lator of plasma membrane H^+-ATPase. Cell Stress Chap. 2, 12-24.

Ptushkina, M., Malys, N., McCarthy, J.E.G., 2004. eIF4E isoform 2 in *Schizosaccharomyces pombe* is a novel stress-response factor. EMBO Report. 5, 311-316.

Score, A.J., Palfreyman, J.W., White, N.A., 1997. Extracellular phenoloxidase and peroxidase enzyme production during interspecific fungal interactions. Int. Biodeterior. Biodegrad. 39, 225-233.

Simonsen, A., Birkeland, H.C.G., Gillooly, D.J., Mizushima, N., Kuma, A., Yoshimori, T., Slagsvold, T., Brech, A., Stenmark, A., 2004. Alfy, a novel FYVE-domain-containing protein associated with protein granules and autophagic membranes. J. Cell Sci. 117, 4239-4250.

Singh, J., Tyers, M., 2009. A Rab escort protein integrates the secretion system with TOR signalling and ribosome biogenesis. Genes Dev. 23, 1944-1958.

Tao, D., Mu, Y., Fu, F.-L., Li, W.-C., 2008. Transformation of maize with trehalose synthase gene cloned from *Saccharomyces cerevisiae*. Biotechnol. 7, 258-265.

Tong, J.J., Schriner, S.E., McCleary, D., Day, B.J., Wallace, D.C., 2007. Life extension through neurofibromin mitochondrial regulation and antioxidant therapy for neurofibromatosis-1 in *Drosophila melanogaster.* Nature Genet. 39, 476 - 485.

Van der Zee, M., Nunes da Fonseca, R., Roth, S., 2008. TGFβ signaling in Tribolium: Vertebrate-like components in a beetle. Dev. Genes Evol. 218, 203-213.

Vercesi, A.E., Kowaltowski, A.J., Grijalba, M.T., Meinicke, A.R., Castilho, R.F., 1997. The role of reactive oxygen species in mitochondrial permeability transition. Biosci. Rep. 17, 43-52.

Verstrepen, K.J., Klis, F.M., 2006. Flocculation, adhesion and biofilm formation in yeasts. Mol. Microbiol. 60, 5-15.

Wang, N., Yoshida, Y., Hasunuma, K., 2007. Catalase-1 (CAT-1) and nucleoside diphosphate kinase-1 (NDK-1) play an important role in protecting conidial viability under light stress in *Neurospora crassa.* Mol. Genet. Genomics. 278, 235-242.

Williams, J., Clarkson, J.M., Mills, P.R., Cooper, R.M., 2003. Saprotrophic and mycoparasitic components of aggressiveness of *trichoderma harzianum* groups toward the commercial mushroom *Agaricus bisporus.* Appl. Envir. Microbiol. 69, 4192-4199.

Xu, J.-R., 2000. MAP Kinases in fungal pathogens. Fungal Genet. Biol. 31, 137-152.

Yan, S., Tang, Z., Sum, W., Sun, W., 2005. Proteomic analysis of salt stress-responsive proteins in rice root. Proteomics. 5, 235-244.

Yeo, E.L., Sheppard, J-A.I., Feuerstein, I.A., 1994. Role of P-selectin and leukocyte activation in polymorphonuclear cell adhesion to surface adherent activated platelets under physiologic shear conditions (an injury vessel wall model). Blood. 83, 2498-2507.

Zhang, J., Liem, D.A., Mueller, M., Wang, Y., Zong, C., Deng, N., Vondriska, T.M., Korge, P., Drews, O, MacLellan, W.R., Honda, H., Weiss, J.N., Apweiler, R., Ping, P., 2008. Altered,

proteome biology of cardiac mitochondria under stress conditions. J. Proteome Res. 7, 2204-2214.

Zinke, I., Schütz, C.S., Katzenberger, J.D., Bauer, M., Pankratz, M.J., 2002. Nutrient control of gene expression in *Drosophila*: microarray analysis of starvation and sugar-dependent response. EMBO J. 21, 6162-6173.